Section 1

INTRODUCTION

1.1 BACKGROUND

The rapidly expanding applications of composites in the recent past have provided much optimism for the future of our technology. Although man-made composites have existed for thousands of years, the high technology of composites has evolved in the aerospace industry only in the last twenty years. Filament-wound pressure vessels using glass fibers were the first strength critical application for modern composites. After these, boron filaments were developed in the 1960's, which started many US Air Force programs to promote aircraft structures made of composites. The F-111 horizontal stabilizer was the first flight-worthy composite component.

Production of a composite stabilizer for the F-14 in the early 1970's was another major milestone. That was followed by the composite stabilator for the F-15, and composite rudder and stabilizer for the F-16. In the early 1980's, the Boeing 767 used nearly two tons of composite materials in its floor beams and all of its control surfaces. The USSR giant transport, Antonov 124, has a total of 5500 kg of composite materials, of which 2500 kg are graphite composites. The all-composite fin box of the Airbus Industrie A310-300 is an impressive structure in its simplicity. Nearly all emerging aircraft use composites extensively: examples include nearly every fighter aircraft in Europe, and the US. A new generation of commercial aircraft such as the Airbus 320-340, McDonnell-Douglas MD-11, and Boeing 777 also have more extensive use of composite materials than ever before.

In 1986, an all-composite airplane that set a world record in nonstop flight around the world was the Voyager, designed and built by Burt Rutan and his coworkers. The plane was ultra light as expected. However, it also showed amazing toughness and resilience against many stormy encounters. For the 1992 America's Cup challenge, all-composite hull, keel, and mast were included in the new International America's Cup Class. Composite materials in other highly visible applications include racing car bodies which have been found to provide more safety to the drivers, and longer-lasting rigidity than an older material like aluminum. Such high visibility is an important ingredient for the growth and acceptance of composite materials as viable engineering materials.

The high technology of composites has spurred applications outside the aerospace industry. Sporting goods are a major outlet for composite materials. Hundreds of tons of graphite composites were used for tennis and squash rackets and golf shafts each year since 1983. The popularity of composite golf shafts were so popular that a shortage of carbon fibers was precipitated in the mid 1990’s. These high performance equipment and composites have become synonymous. The performance of tennis rackets is so impressive in terms of the speed of the balls that talk of banning these composites rackets for professional players has surfaced. Other applications of composites include bicycles, oars for rowing, and other equipment where weight, stiffness, and strength are important.

Areas of future growth may come from ground transportation such as high-speed trains, and subway cars. Benefit of the light weight can be translated into energy savings, and cost of track. Shipping containers can also be made of composite materials. Surface ships are now being made of composite materials, but they are made in most cases by wet layup. Pre-impregnated composite tapes provide significantly improved properties at only a modest increase in cost.

Rehabilitation of civil engineering structures susceptible to corrosion and fatigue have been reinforced by composites such as an over wrapping of columns. This reinforcement can also improve seismic resistance of the structures.

Usage of composites can be greatly enhanced if the cost is lowered, and design more precise. For some applications composites are accepted as much as those in aircraft and sporting goods. Satellites, for example, are nearly all composites. For other applications, like those in transportation and civil engineering, composites are not readily accepted. Thus, lower cost, better design must be further reinforced by more data and certification. These steps must be addressed systematically, and take time. In this book, we would like to address primarily the design issue, which is intimately related to the cost of materials and processing.

1.2 DEMAND AND USAGE OF COMPOSITE MATERIALS

According to a report by K. Fujisawa of Toray, the demand for graphite fiber in 1989 is shown in the figure below by regions. In each column that represents an region, it is further divided into sporting, industrial, and aerospace applications.

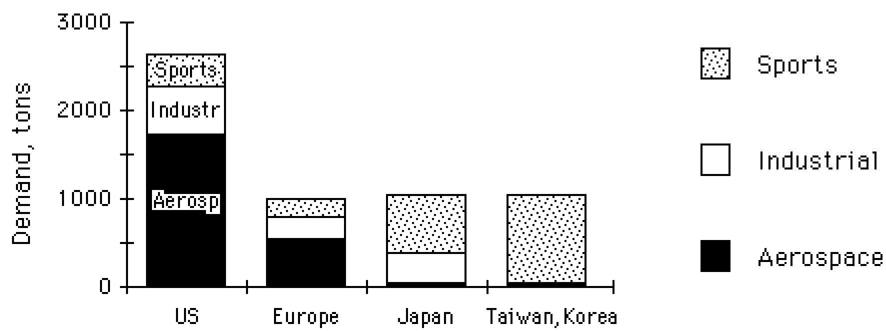

FIGURE 1.1 DEMAND OF GRAPHITE FIBERS BY REGIONS AND APPLICATIONS IN 1989

The total and percentage demand by area is shown in the figure below. The demand from the US is nearly one half of the total world demand; whereas the other three regions are evenly divided.

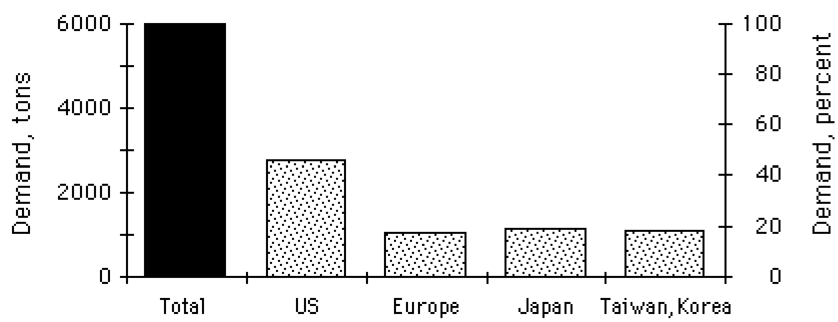

FIGURE 1.2 TOTAL AND PERCENTAGE DEMAND OF GRAPHITE FIBERS BY REGIONS

While the data represented the situation in the late 1980's, it remained the same for most of the 1990's. New developments include the emergence of China as a supplier and user of composites and that of the low-cost carbon fibers and prepregs in the late 1990's. Cost of carbon fibers have come steadily down due to the use of large tows pioneered by Zoltek. In 1999, carbon prepreg of sporting goods grade is at US$14 per pound. It is becoming more cost effective than glass composites in many applications.

1.3 DESIGNING WITH COMPOSITES

Designing with any material is often more art than science. Composites design is no exception and there is much information to learn. Universities prefer teaching analysis to design. Books on analysis outnumber those on design by a wide margin. Research topics have rarely been design-oriented. However, products are made with or without a rational design. Netting analysis is still considered useful for design. The carpet plots still remain in many design manuals. These approaches reflect the lack of respect for the interaction effect of combined stresses.

Design limit is often based on some uniaxial strain level; one level for laminates without holes, and a reduced level for those with holes or for damage tolerance. This approach does not do justice to composite materials because the contribution of plies to laminates is ignored. Nonetheless major aerospace companies continue to use artificially defined design allowables.

Workers in numerous emerging composite materials, such as metal-matrix composites, ceramic composites, molecular composites, and carbon-carbon composites, have been preoccupied with their particular problems, and have resorted to oversimplified models of shear lag, pull out, and their version of the netting analysis. These are typical practices in the US industry which are not always rationally developed. In fact, most of them are misleading if not wrong. They are still in use because the practices are simple.

Fortunately, the polymer-matrix composites are so strong that they have been reliable and competitive in spite of the less-than-perfect design practice. Our desire is to use as much calculation as possible for designing with composites. For this reason, netting analysis, carpet plots, and uniaxial strain limits are not used. Rationality is as important as practicality. We must have both if we are to succeed. We cannot afford to penalize composites by using the wrong design. By the same token we should not limit the extraordinary properties of composite materials by using outmoded tools. As we see it, the basic issue in designing with composites is to learn to use the directionally dependent properties. The scalar approach for the design of isotropic materials is acceptable because stiffness and strength can each be represented by one parameter; i.e., the Young's modulus and the uniaxial strength. Poisson's ratio can be assumed to remain constant at 0.3. Strength under combined stresses based on the von Mises or Tresca criterion does not deviate significantly from the uniaxial tensile or pure shear strength.

But for composites, the number of constants increase to four for the stiffness and at least five for the strength of an on-axis unidirectional ply. In a thick multidirectional laminate, the stiffness constants can be as many as 21, and the strength is five times the number of ply groups. We must use matrix in place of scalar operations. This is the challenge in working with anisotropic materials. Netting analysis, carpet plots, and the limit or maximum strain criterion ignore the effects of combined stresses, and do not use matrix algebra. Such approaches are at least 25 years out of date.

It is a common practice to limit the design of laminates to balanced (orthotropic), and symmetric construction. These restrictions are intended to simplify the design and manufacturing processes. A laminate may be designed to be balanced and symmetric before it is exposed to load and environments. When it is loaded beyond the first-ply-failure load, the laminate in its degraded form will become unbalanced and unsymmetric. When the laminate is exposed to unsymmetric temperature and moisture, the resulting deformation is also unsymmetric. It is therefore a fact of life that anisotropic and unsymmetric laminates are here to stay, and we must learn how they behave, and how they can be used as efficiently as possible.

How can we make our design conceptually simple and analytically consistent? This can be achieved by setting up a rational framework. An example is shown in Figure 1.3.

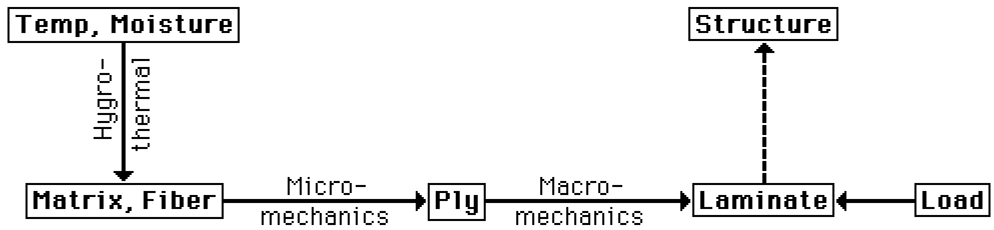

FIGURE 1.3 AN INTEGRATED FRAMEWORK FOR COMPOSITES DESIGN

Designing with composites require several additional factors which do not exist in conventional materials. Specifically, we need three bridges to link materials and environmental characteristics to the final stiffness and strength of a laminated composite. The bridges are: hygrothermal analysis and data, micromechanics, and macromechanics. The framework in Figure 1.4 is to minimize the number of variables and their functional dependency. We believe that a full-featured design process must consider all the variables.

1.4 OUR APPROACH

First, we want to expand Figure 1.3 to show key variables and their functional relations. Our approach is to use the simplest framework that still contains all the variables and connects them with the simplest relations. Then it becomes feasible to optimize composite laminates with all the features.

The most efficient configuration for stiffness and strength is the unidirectional composite. We will develop the method of the use of on- and off-axis unidirectional composites to carry combined loads. If the loads are such that unidirectional composites are inadequate and inefficient, we will go to bi-directional laminates. The process continues as we increase the ply angles to 3, 4 and higher. Obviously, the number of angles must be balanced between considerations of manufacturing and cost, and the requirement for stiffness and strength.

We take the highly directional composites as the upper bound of anisotropy; the quasi-isotropic laminate, the lower bound. The specific stiffness and strength of various composite materials and aluminum are compared in the following chart. Ranges of stiffness and strength are shown indicating the variability of properties by the degree of anisotropy. Note that the significant advantages of composite materials over aluminum. The challenge to designers is to use the opportunities offered by composites.

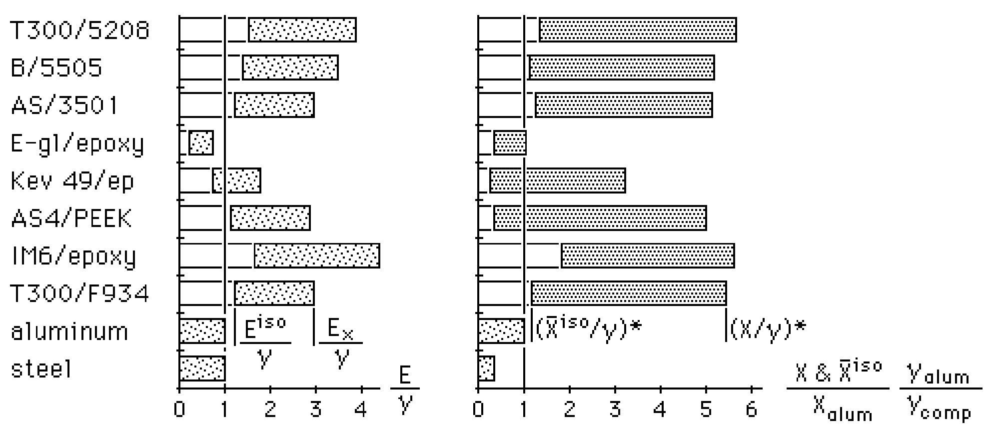

FIGURE 1.4 SPECIFIC STIFFNESS AND STRENGTH OF COMPOSITE MATERIALS VS ALUMINUM

We wish to emphasize designing composites on a consistent and rational basis. Thus, the salient features of composite materials can be fully exploited without the burden of unnecessary rules. The methodology described in this book represents the minimum required. Sufficient information has become available that designing with composite materials can be done as confidently as with conventional materials.

Matrix inversions are involved in the determination of laminate stiffness. It is impossible to anticipate the effects of simple operations such as adding and subtracting plies, and the rigid body rotation of a laminate. These effects can be systematically established and should not be surprises. Instead of guessing or using intuition we recommend calculation.

To enhance confidence in our design calculations, we make constant comparison of our optimum composite with the quasi-isotropic laminate of the same composite as a lower bound. This comparison is also important because the same calculation is needed to compare our laminate with isotropic materials like aluminum. We also make sure that calculations can be easily and accurately performed. The use of normalized variables for stresses and effective moduli makes quantitative results easy to understand. We see in the 1990's the personal computer or work station as the most effective tool to aid design. We have mentioned repeatedly that formulas must be simplified, and the number of design variables reduced. The use of micromechanics and repeated sub-laminates, for example, reduces the number of material and geometric variables. With simplification, many more design iterations can be effectively exercised than is possible with outmoded tools.

1.5 COVERAGE OF THIS BOOK

This book is written with the understanding that the reader is familiar with the basic principles of strength of materials. Many terms are defined here without derivations.

The simplest stress analysis of structures is the statically determinate case. The stress distribution is independent of material properties. Stresses are derived from equilibrium or the balance of forces. Examples shown below are the uniaxial tensile stress, and the membrane stresses in a pressure vessel. In both examples, stress is homogeneous; i.e., stress is uniform and does not vary from point to point. The same state of stress exists if the material is a composite. We only need to know the effective stiffness of the composite to calculate the resulting strain. The calculation of the effective stiffness under in-plane stresses is shown in Section 4. Thus for all statically determinate structures, many of which are listed in Roark's Formulas for Stresses and Strains, we can use the formulas as they are. We only need to use the effective elastic stiffness of the composites.

$$\sigma = \frac{P}{A} \qquad \epsilon = \frac{\sigma}{E} \qquad \sigma_2 = \frac{PD}{2h} \qquad \sigma_1 = \frac{PD}{4h}$$

FIGURE 1.5 EXAMPLES OF STATICALLY DETERMINATE STRUCTURES

In a composite laminate the effective stiffness for bending is different from that for in-plane. Only when the laminate is homogenized are the in-plane and flexural stiffnesses equal. The formulas for the flexural stiffness of a laminate can be found in Section 5, and can be used in the buckling of a strut, and the bending of a beam shown below. It is assumed that the laminate must by symmetric. If the laminate is unsymmetric, which is discussed in Section 6, in-plane and flexure deformations are coupled. Most of the formulas for statically determinate structures cannot be used by a direction substitution of the effective stiffness.

$$\sigma = \frac{P}{A} \qquad P_{cr} = \frac{\pi^2 EI}{l^2} \qquad\qquad \sigma = \frac{Mc}{I} \qquad \epsilon = \frac{\sigma}{E}$$

FIGURE 1.6 BUCKLING AND BENDING OF COMPOSITE BEAMS

For a general state of stress, elasticity theory calls for the solution of a partial differential equation with appropriate boundary conditions and the stress-strain relation of the material. For a two-dimensional state of stress, the equation of equilibrium in terms of stress function **F** is listed below for both orthotropic and isotropic materials. Stress distribution would be non-homogeneous; i.e., it varies from point to point like the stress around an opening in a plate. For orthotropic materials, stress is dependent on the materials coefficients such as **[a*]**, the compliance of the laminate. For isotropic materials, these coefficients are not independent, and can be canceled. Thus stress is the same for all isotropic materials. The stress concentration factor of an open hole is 3 for all isotropic materials.

$$\text{Stress function F:}\quad \sigma_x = \frac{\partial^2 F}{\partial y^2},\quad \sigma_y = \frac{\partial^2 F}{\partial x^2},\ \sigma_s = -\frac{\partial^2 F}{\partial x \partial y}$$

$$a^*_{22}\frac{\partial^4 F}{\partial x^4} + (2a^*_{12}+a^*_{66})\frac{\partial^4 F}{\partial x^2 \partial y^2} + a^*_{11}\frac{\partial^4 F}{\partial y^4} = 0,\ \text{For isotropy } \nabla^4 F = 0 \qquad (1.1)$$

For bending of a plate, the same difference exists between orthotropic and isotropic plates. The governing equations for plates are shown below. For orthotropic plates, components of flexural rigidity **[D]** are the coefficients of the displacement equation in **w**. The displacement surface will be different for different composite laminates. For isotropic plates, the coefficients in the governing equation are canceled. The displacement surface is the same for all isotropic materials.

$$D_{11}\frac{\partial^4 w}{\partial x^4} + 2(D_{12}+2D_{66})\frac{\partial^4 w}{\partial x^2 \partial y^2} + D_{22}\frac{\partial^4 w}{\partial y^4} = 0$$

$$\text{For isotropy } \nabla^4 w = 0 \qquad (1.2)$$

In this book we concentrate on the elastic constants and failure modes of composite laminates. We do not deal with the solutions of governing equations cited above. There are books dedicated specifically to this purpose; e.g., S. G. Lekhnitskii's *Anisotropic Plates*, J. M. Whitney's *Structural Analysis of Laminated Anisotropic Plates*, and others. Our book is concerned with the local behavior of a composite laminate, as opposed to the global behavior of a laminated composite structure.

There are many intermediate steps between the local and global scales. Designs for openings, bolted joints, effects of defects and damages, and their growth are all issues that must be solved. The approach which we recommend is to follow the micro- and macromechanics modeling described in this book. The approach defines the contributions of the constituents to the stiffness and strength of a composite laminate on a global level if the stress is homogeneous, or on a local or element level if the stress is non-homogeneous. Solutions of openings and bolted joints belong to the same boundary-value problem that is a matter of boundary conditions.

An alternative to the boundary-value problem is the empirical method. Thousands of tests have been performed on bolted joints, for example. Defects as a result of transverse impact to a laminate are also empirically defined, as is the loss of compressive strength. Design for damage tolerance is based more on philosophy than an analytically derived strategy. However, we advocate a different approach. Ideally, tests are for the purpose of measuring basic stiffness and strength of composite plies and laminates. Tests are also necessary to verify analytic predictions. Our book covers the basic models for the local behavior of a globally non-homogeneous state of stress. Without a solid understanding of the local behavior, it is not feasible to set up a boundary-value problem on a global level. We therefore think the subjects covered in this book are the best starting point for achieving predictability of the behavior of composite materials and structures.

Section 2

STRESS-STRAIN RELATIONS

Notation and symbols are the language for science and engineering. We should not only try to make them simple, but also internally consistent. Contacted notation is universally accepted as a shortcut, but the rules for contraction are not always followed faithfully. From generalized Hooke's law, we can simplify stress-strain relations for materials having increased symmetries, and reduce 3-dimensional laws to plane stress and plane strain. The permutation of indices provides a simple rule to generate symmetries of any rotation for stress, strain and elastic constants.

2.1 OUR NOTATIONS

We follow the notation and symbols used in the textbook: *Introduction to Composite Materials*, by S. W. Tsai and H. T. Hahn, Technomic, Lancaster, Pennsylvania 17604 (1985), and *Composites Design*, by S. W. Tsai, Think Composites (1988). We are bound by the following rules required by the contracted notation:

- Engineering shear strain and engineering twisting curvature are used. Their definitions in terms of displacements are:

  $$\text{Shear strain} = \epsilon_s = \frac{\partial u}{\partial y} + \frac{\partial v}{\partial x}, \ \text{Twisting curvature} = k_s = -\frac{2\partial^2 w}{\partial x \partial y} \Bigg] \tag{2.1}$$

  Note that the factor of 2 is added to the tensorial relation. Like the engineering shear strain, the twisting curvature here is an engineering rather than tensorial curvature. Our sign convention calls for a negative sign in this relation.

- Letter subscripts {x, y, z, q, r, s} designate the on-axis, material symmetry coordinates; numeric subscripts {1, 2, 3, 4, 5, 6} designate the off-axis material and laminate coordinates. The sequence is important for the permutation of indices to find the transformation equations of stress, strain, and elastic constants about different axes.

In addition, we use the following conventions:

- Engineering constants are defined from the components of the normalized compliance. Definitions are also given for the unsymmetric laminates. The coupling coefficients are normalized by columns, not by rows; Poisson's ratios and shear coupling coefficients are defined following the conventional matrix notation, and are different from other authors.

- We use normalized variables (those with *) for properties in addition to the absolute. Normalized properties are required in order to compare one property with another. Stiffness components, for example, are expressed in Pa.

- We use dimensionless variables whenever possible, in order to avoid concern with SI versus English units. We prefer to represent thickness by the number of plies instead of m or mm, and failure envelopes in strain space instead of stress space, and loss of stiffness or strength due to changes are expressed in ratios and non-dimensional quantities.

- Other symbols include:

  Asterisk [*] means a normalized variable.

  Prime ['] means compressive or negative.

- Superscript o means in-plane.

- Superscript f means flexural.

2.2 CONTRACTED NOTATION

Contracted notation is a simplification of the usual tensorial notation. Instead of having the same number of indices to match the rank of the tensor, such as having two indices for the second-rank tensor, and four for the fourth-rank, the contracted notation reduces the number of indices by one half. Single index is used for the second-rank tensors; double indices, for the fourth-rank. Contracted notation cannot be applied to the first-rank and other odd-rank tensors.

When contracted notation is used, engineering shear strain should be used, in place of the tensorial shear strain. Thus the factor of 2 must be properly and consistently applied. Twisting curvature in Equation 2.1 is of the engineering rather than the tensorial type. The components of the compliance must also be corrected in addition to the contraction of the indices. The numeric correction factors of 1, 2 and 4 must be applied in accordance with the relations in Table 2.9 (see page 2-5). Incorrectly or inconsistently applied correction factors can lead to unnecessarily complicated unsymmetric matrices, as well as uncertainty and confusion.

The contraction for the stress components is straightforward. No numeric correction is necessary. There are two systems of notations for the stress components; viz., the letter and numeric subscripts (see Table 2.1). The contraction of the normal stress components is natural and well accepted, but that of the shear stress is not universally followed. Our contraction of the numeric subscripts is more popular because it follows the same order of 1-2-3 if the plane of the shear stress is designated by the normal to the plane; e.g., the 2-3 plane by 1. This rule is consistent with the definition of the rotation tensor in solid and fluid mechanics, and is useful in the permutation of the indices shown in Figure 2.3 on page 2-7.

The contraction of the letter subscripts is arbitrary but consistent with the purpose of contraction. In this book we try not to mix single and double subscripts.

TABLE 2.1 CONTRACTION OF SUBSCRIPTS FOR STRESS AND STRAIN COMPONENTS

Subscripts	Normal	Shear	Normal	Shear
Regular letters	σ_{xx} σ_{yy} σ_{zz}	σ_{yz} σ_{zx} σ_{xy}	ϵ_{xx} ϵ_{yy} ϵ_{zz}	ϵ_{yz} ϵ_{zx} ϵ_{xy}
Regular numerals	σ_{11} σ_{22} σ_{33}	σ_{23} σ_{31} σ_{12}	ϵ_{11} ϵ_{22} ϵ_{33}	ϵ_{23} ϵ_{31} ϵ_{12}
Contracted numerals	σ_1 σ_2 σ_3	σ_4 σ_5 σ_6	ϵ_1 ϵ_2 ϵ_3	ϵ_4 ϵ_5 ϵ_6
Contracted letters	σ_x σ_y σ_z	σ_q σ_r σ_s	ϵ_x ϵ_y ϵ_z	ϵ_q ϵ_r ϵ_s

In Table 2.1 above, we use the engineering shear strains in the last two rows. Note the use of single letter designation for the shear components of stress and strain in order to be consistent in the contracted notation. Subscripts q, r, s are arbitrarily selected for the shear components. We do not recommend mixing single and double subscripts.

The contraction for the strain components needs a numeric correction factor of 2 for the shear components because engineering shear is used. The usual definition of the tensorial strain-displacement relation is shown in the equation below. Then the definition of engineering shear strains in terms of tensorial strains and displacements are also shown in the equation:

$$\left.\begin{array}{l}\text{Tensorial strains: } \epsilon_{ij} = \frac{1}{2}(u_{i,j}+u_{j,i}) : \epsilon_{11} = \frac{\partial u}{\partial x}, \ldots, \epsilon_{12} = \frac{1}{2}\left[\frac{\partial u}{\partial y} + \frac{\partial v}{\partial x}\right] \\ \text{Engineering shear strains:} \\ \quad \epsilon_4 = 2\epsilon_{23} = \frac{\partial v}{\partial z} + \frac{\partial w}{\partial y};\ \epsilon_5 = 2\epsilon_{31} = \frac{\partial w}{\partial x} + \frac{\partial u}{\partial z};\ \epsilon_6 = 2\epsilon_{12} = \frac{\partial u}{\partial y} + \frac{\partial v}{\partial x}\end{array}\right| \quad (2.2)$$

The same relations are valid if we use letter subscripts in place of the numeric subscripts.

2.3 CONTRACTED STIFFNESS

The stiffness matrix for the generalized Hooke's law in its uncontracted form is:

TABLE 2.2 GENERALIZED HOOKE'S LAW IN UNCONDENSED FORM

	ϵ_{11}	ϵ_{22}	ϵ_{33}	ϵ_{23}	ϵ_{32}	ϵ_{31}	ϵ_{13}	ϵ_{12}	ϵ_{21}
σ_{11}	C_{1111}	C_{1122}	C_{1133}	C_{1123}	C_{1132}	C_{1131}	C_{1113}	C_{1112}	C_{1121}
σ_{22}	C_{2211}	C_{2222}	C_{2233}	C_{2223}	C_{2232}	C_{2231}	C_{2213}	C_{2212}	C_{2221}
–									
–									
–									
σ_{21}	C_{2111}	C_{2122}	C_{2133}	C_{2123}	C_{2132}	C_{2131}	C_{2113}	C_{2112}	C_{2121}

Since both stress and strain are symmetric, the last table can be modified by factoring out the shear strain components as follows:

TABLE 2.3 GENERALIZED HOOKE'S LAW HAVING SYMMETRIC STRAINS

	ϵ_{11}	ϵ_{22}	ϵ_{33}	ϵ_{23}	ϵ_{31}	ϵ_{12}
σ_{11}	C_{1111}	C_{1122}	C_{1133}	$C_{1123} + C_{1132}$	$C_{1131} + C_{1113}$	$C_{1112} + C_{1121}$
σ_{22}	C_{2211}	C_{2222}	C_{2233}	$C_{2223} + C_{2232}$	$C_{2231} + C_{2213}$	$C_{2212} + C_{2221}$
–						
–						
–						
σ_{21}	C_{2111}	C_{2122}	C_{2133}	$C_{2123} + C_{2132}$	$C_{2131} + C_{2113}$	$C_{2112} + C_{2121}$

If we now introduce the engineering shear strain and the contracted notation for all the indices, we have:

TABLE 2.4 HOOKE'S LAW IN CONTRACTED STRESSES AND STRAINS

	ϵ_1	ϵ_2	ϵ_3	ϵ_4	ϵ_5	ϵ_6
σ_1	C_{11}	C_{12}	C_{13}	C_{14}	C_{15}	C_{16}
σ_2	C_{21}	C_{22}	C_{23}	C_{24}	C_{25}	C_{26}
-						
-						
-						
σ_6	C_{61}	C_{62}	C_{63}	C_{64}	C_{65}	C_{66}

Thus the indices for the stiffness components follow precisely those for the contraction of stress. No correction factor for the contraction is needed. This easy conversion from four to two indices is made possible by having:

- Symmetry of stress and strain,
- Symmetry of the stiffness matrix, and
- Use of engineering shear strain.

2.4 CONTRACTED COMPLIANCE

The generalized Hooke's law in terms of compliance is shown here. The first, the second, and the ninth rows for this uncondensed, uncontracted form of the generalized Hooke's law are:

TABLE 2.5 GENERALIZED HOOKE'S LAW HAVING SYMMETRIC STRAINS

	σ_{11}	σ_{22}	σ_{33}	σ_{23}	σ_{32}	σ_{31}	σ_{13}	σ_{12}	σ_{21}
ϵ_{11}	S_{1111}	S_{1122}	S_{1133}	S_{1123}	S_{1132}	S_{1131}	S_{1113}	S_{1112}	S_{1121}
ϵ_{22}	S_{2211}	S_{2222}	S_{2233}	S_{2223}	S_{2232}	S_{2231}	S_{2213}	S_{2212}	S_{2221}
-									
-									
-									
ϵ_{21}	S_{2111}	S_{2122}	S_{2133}	S_{2123}	S_{2132}	S_{2131}	S_{2113}	S_{2112}	S_{2121}

If we apply the symmetry of the stress components, we can factor out the shear stress components:

TABLE 2.6 GENERALIZED HOOKE'S LAW HAVING SYMMETRIC STRESSES

	σ_{11}	σ_{22}	σ_{33}	σ_{23}	σ_{31}	σ_{12}
ϵ_{11}	S_{1111}	S_{1122}	S_{1133}	$S_{1123}+S_{1132}$	$S_{1131}+S_{1113}$	$S_{1112}+S_{1121}$
ϵ_{22}	S_{2211}	S_{2222}	S_{2233}	$S_{2223}+S_{2232}$	$S_{2231}+S_{2213}$	$S_{2212}+S_{2221}$
-						
-						
-						
ϵ_{21}	S_{2111}	S_{2122}	S_{2133}	$S_{2123}+S_{2132}$	$S_{2131}+S_{2113}$	$S_{2112}+S_{2121}$

If we apply the contracted notation of stress and strain (with engineering shear), and retain the uncontracted compliance components we will have:

TABLE 2.7 HOOKE'S LAW HAVING CONTRACTED STRESSES AND STRAINS

	σ_1	σ_2	σ_3	σ_4	σ_5	σ_6
ϵ_1	S_{1111}	S_{1122}	S_{1133}	$S_{1123}+S_{1132}$	$S_{1131}+S_{1113}$	$S_{1112}+S_{1121}$
ϵ_2	S_{2211}	S_{2222}	S_{2233}	$S_{2223}+S_{2232}$	$S_{2231}+S_{2213}$	$S_{2212}+S_{2221}$
-						
-						
-						
$\epsilon_6/2$	S_{2111}	S_{2122}	S_{2133}	$S_{2123}+S_{2132}$	$S_{2131}+S_{2113}$	$S_{2112}+S_{2121}$

If we apply the contracted notation to the compliance matrix we need additional numeric corrections as follows:

$$\left.\begin{array}{l} S_{11} = S_{1111}, \ldots S_{12} = S_{1122}, \ldots \\ S_{14} = 2S_{1123}, S_{15} = 2S_{1131}, \ldots S_{61} = 2S_{1211}, \ldots \\ S_{44} = 4S_{2323}, S_{45} = 4S_{2331}, \ldots \end{array}\right] \tag{2.3}$$

The final compliance relations between stress and strain are as follows:

TABLE 2.8 GENERALIZED HOOKE'S LAW HAVING CONTRACTED COMPLIANCE

	σ_1	σ_2	σ_3	σ_4	σ_5	σ_6
ϵ_1	S_{11}	S_{12}	S_{13}	S_{14}	S_{15}	S_{16}
ϵ_2	S_{21}	S_{22}	S_{23}	S_{24}	S_{25}	S_{26}
-						
-						
-						
ϵ_6	S_{61}	S_{62}	S_{63}	S_{64}	S_{65}	S_{66}

Thus the contracted compliance matrix can be viewed as having four equal 3x3 sub-matrices. The correction factor is unity for the upper-left sub-matrix; 2, for the lower-left and the upper-right; and 4, for the lower-right; see the table below for the correction factors for the compliance matrix. These factors are necessary and are the results of the symmetry of stress and strain, the symmetry of the compliance matrix, and the use of engineering shear. In contrast to the compliance matrix, the stiffness matrix requires no correction factors between the contracted and uncontracted notations. This is also shown on the right of Table 2.9.

TABLE 2.9 CORRECTION FACTORS FOR COMPLIANCE AND STIFFNESS MATRICES

j \ i	1 2 3	4 5 6	1 2 3	4 5 6
1 2 3	$S_{ij} = S_{pqrs}$	$S_{ij} = 2S_{pqrs}$	$C_{ij} = C_{pqrs}$	$C_{ij} = C_{pqrs}$
4 5 6	$S_{ij} = 2S_{pqrs}$	$S_{ij} = 4S_{pqrs}$	$C_{ij} = C_{pqrs}$	$C_{ij} = C_{pqrs}$

If engineering shear is not used, a factor of 2 must be applied to the last three columns of the stiffness matrix in Equation 2.4, and the last three rows of the compliance matrix in Equation 2.5. These matrices are no longer symmetric. The rules governing the use of contracted notation is not always applied consistently in the literature. It is therefore prudent to establish the precise rules that an author may have employed.

A common incorrect application of the contraction rule in Equation 2.1 can lead to unsymmetric stiffness and compliance matrices, or the shear strain component carries a factor of 2. Examples are summarized in the next two equations below where necessary but confusing factors of 2 or 1/2 must be added:

$$\begin{Bmatrix} \sigma_1 \\ \sigma_2 \\ \sigma_6 \end{Bmatrix} = \begin{bmatrix} Q_{11} & Q_{12} & Q_{16} \\ Q_{21} & Q_{22} & Q_{26} \\ Q_{61} & Q_{62} & Q_{66} \end{bmatrix} \begin{Bmatrix} \epsilon_1 \\ \epsilon_2 \\ 2\epsilon_{12} \end{Bmatrix} = \begin{bmatrix} Q_{11} & Q_{12} & 2Q_{16} \\ Q_{21} & Q_{22} & 2Q_{26} \\ Q_{61} & Q_{62} & 2Q_{66} \end{bmatrix} \begin{Bmatrix} \epsilon_1 \\ \epsilon_2 \\ \epsilon_{12} \end{Bmatrix} \tag{2.4}$$

Factors of 2 must be added

$$\begin{Bmatrix} \epsilon_1 \\ \epsilon_2 \\ 2\epsilon_{12} \end{Bmatrix} = \begin{bmatrix} S_{11} & S_{12} & S_{16} \\ S_{21} & S_{22} & S_{26} \\ S_{61} & S_{62} & S_{66} \end{bmatrix} \begin{Bmatrix} \sigma_1 \\ \sigma_2 \\ \sigma_6 \end{Bmatrix} \qquad \begin{Bmatrix} \epsilon_1 \\ \epsilon_2 \\ \epsilon_{12} \end{Bmatrix} = \begin{bmatrix} S_{11} & S_{12} & S_{16} \\ S_{21} & S_{22} & S_{26} \\ \frac{S_{61}}{2} & \frac{S_{62}}{2} & \frac{S_{66}}{2} \end{bmatrix} \begin{Bmatrix} \sigma_1 \\ \sigma_2 \\ \sigma_6 \end{Bmatrix} \tag{2.5}$$

Factors of 2 or 1/2 must be added

2.5 THE GENERALIZED HOOKE'S LAW

The generalized Hooke's law is the linear stress-strain relation for an anisotropic material. It is derived from the existence of an elastic energy in the theory of elasticity. It is convenient to use the contracted notation described in the last section to represent anisotropic bodies. Several commonly encountered symmetries will be described in the following.

TRICLINIC SYMMETRY

There are 36 components or constants which completely describe this material. It has no material symmetry. This stiffness matrix, however, is symmetric from the energy consideration. Only 21 of the 36 constants are independent. Similarly, the compliance matrix of a triclinic material has 36 components, of which 21 are independent.

No symmetry

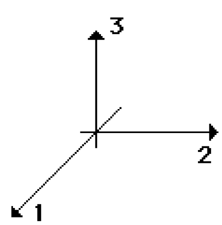

$$\begin{bmatrix} C_{11} & C_{12} & C_{13} & C_{14} & C_{15} & C_{16} \\ C_{21} & C_{22} & C_{23} & C_{24} & C_{25} & C_{26} \\ C_{31} & C_{32} & C_{33} & C_{34} & C_{35} & C_{36} \\ C_{41} & C_{42} & C_{43} & C_{44} & C_{45} & C_{46} \\ C_{51} & C_{52} & C_{53} & C_{54} & C_{55} & C_{56} \\ C_{61} & C_{62} & C_{63} & C_{64} & C_{65} & C_{66} \end{bmatrix} \qquad \begin{bmatrix} S_{11} & S_{12} & S_{13} & S_{14} & S_{15} & S_{16} \\ S_{21} & S_{22} & S_{23} & S_{24} & S_{25} & S_{26} \\ S_{31} & S_{32} & S_{33} & S_{34} & S_{35} & S_{36} \\ S_{41} & S_{42} & S_{43} & S_{44} & S_{45} & S_{46} \\ S_{51} & S_{52} & S_{53} & S_{54} & S_{55} & S_{56} \\ S_{61} & S_{62} & S_{63} & S_{64} & S_{65} & S_{66} \end{bmatrix}$$

FIGURE 2.1 STIFFNESS AND COMPLIANCE MATRICES OF A TRICLINIC MATERIAL

MONOCLINIC SYMMETRY
If any material symmetry exists, the number of constants will reduce. For example, if the plane of 1-2, 3 = 0, or z = 0 is a plane of symmetry, this is a monoclinic material. All constants associated with the positive 3- or z-axis must be the same as those with the negative 3- or z-axis. The Hooke's law in Figure 2.2 can be simplified for a material having a plane of symmetry; i.e., a monoclinic material. If the symmetry plane lies in the plane of 1-2, 3 = 0, or z = 0, the components in Figure 2.1 will be reduced to those in Figure 2.2 below.

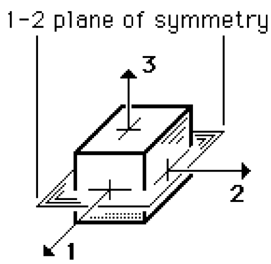

$$\begin{bmatrix} C_{11} & C_{12} & C_{13} & 0 & 0 & C_{16} \\ C_{21} & C_{22} & C_{23} & 0 & 0 & C_{26} \\ C_{31} & C_{32} & C_{33} & 0 & 0 & C_{36} \\ 0 & 0 & 0 & C_{44} & C_{45} & 0 \\ 0 & 0 & 0 & C_{54} & C_{55} & 0 \\ C_{61} & C_{62} & C_{63} & 0 & 0 & C_{66} \end{bmatrix} \quad \begin{bmatrix} S_{11} & S_{12} & S_{13} & 0 & 0 & S_{16} \\ S_{21} & S_{22} & S_{23} & 0 & 0 & S_{26} \\ S_{31} & S_{32} & S_{33} & 0 & 0 & S_{36} \\ 0 & 0 & 0 & S_{44} & S_{45} & 0 \\ 0 & 0 & 0 & S_{54} & S_{55} & 0 \\ S_{61} & S_{62} & S_{63} & 0 & 0 & S_{66} \end{bmatrix}$$

FIGURE 2.2 STIFFNESS AND COMPLIANCE MATRICES OF A MONOCLINIC MATERIAL (z = 0)

The 16 zero components are:

"14", "24", "34", "15", "25", "35", "46", "56"; and

their symmetric components "41", "42", "43", "51", "52", "53", "64", "65".

When expressed in this coordinate system there are 20 nonzero constants, of which 13 are independent.

If the plane of symmetry is in the plane of 2-3, 1 = 0, or x = 0, we only need to establish the permutation of the index by one; i.e., simply change 1 to 2, 2 to 3, 3 to 1; 4 to 5, 5 to 6, 6 to 4. The scheme of permutation is shown in the figure below. This scheme is a general rule for indices, and can be applied not only to stiffness and compliance matrices, but also to stress, strain and expansion coefficients.

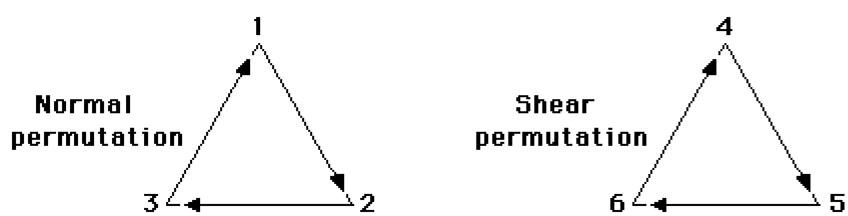

FIGURE 2.3 PERMUTATION SCHEME OF THE INDICES

If this permutation scheme is applied, the following 16 zero components will be:

"25", "35", "45", "26", "36", "16", "54", "64"; and

their symmetric components "52", "53", "54", "62", "63", "61", "45", "64".

If it is an arbitrary plane, the number of nonzero constants will increase up to 36. However, the independent constants remain 13 for all coordinate systems.

ORTHOTROPIC SYMMETRY

As the level of material symmetry increases, the number of independent constants continues to reduce. If we have symmetry in three orthogonal planes we have an orthotropic material. The number of independent constants is now 9. If the planes of symmetry coincides with the reference coordinate system, the nonzero components are 12; this is shown in Figure 2.4. If the symmetry planes are not coincident with the reference coordinates, the nonzero components can be those shown in Figure 2.1. If one of the symmetry planes coincide with the 3- or z-coordinate axis, the nonzero components will be those shown in Figure 2.2. The number of independent constants remains 9 for orthotropic materials irrespective of the orientation of the symmetry planes.

3 planes of symmetry

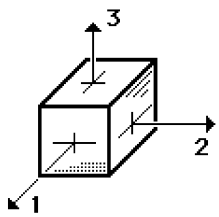

$$\begin{bmatrix} C_{11} & C_{12} & C_{13} & 0 & 0 & 0 \\ C_{21} & C_{22} & C_{23} & 0 & 0 & 0 \\ C_{31} & C_{32} & C_{33} & 0 & 0 & 0 \\ 0 & 0 & 0 & C_{44} & 0 & 0 \\ 0 & 0 & 0 & 0 & C_{55} & 0 \\ 0 & 0 & 0 & 0 & 0 & C_{66} \end{bmatrix} \quad \begin{bmatrix} S_{11} & S_{12} & S_{13} & 0 & 0 & 0 \\ S_{21} & S_{22} & S_{23} & 0 & 0 & 0 \\ S_{31} & S_{32} & S_{33} & 0 & 0 & 0 \\ 0 & 0 & 0 & S_{44} & 0 & 0 \\ 0 & 0 & 0 & 0 & S_{55} & 0 \\ 0 & 0 & 0 & 0 & 0 & S_{66} \end{bmatrix}$$

FIGURE 2.4 STIFFNESS AND COMPLIANCE MATRICES OF AN ORTHOTROPIC MATERIAL

TRANSVERSELY ISOTROPIC SYMMETRY

The next level of material symmetry is the transversely isotropic material, which has 5 independent constants. If the isotropic plane coincides with one of the planes of the coordinate system, the nonzero components are 12; this is shown in Figure 2.5. If the symmetry planes are not coincident with the reference coordinates, the nonzero components will be those shown in Figure 2.1. If one of the symmetry planes coincides with the 3- or z-coordinate axis, the nonzero components will be those shown in Figure 2.2 on page 2-6. The number of independent constants remain 5 for the transversely isotropic material irrespective of the orientation of the symmetry planes.

This is an important anisotropic material symmetry. It is frequently used to describe the elastic constants of anisotropic fibers, and unidirectional composites. The isotropic plane for both cases is normal to the axis of the fibers.

2-3 plane
isotropic symmetry

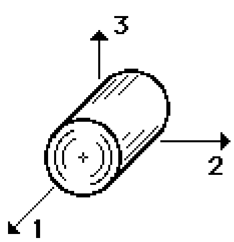

$$\begin{bmatrix} C_{11} & C_{12} & C_{12} & 0 & 0 & 0 \\ C_{21} & C_{22} & C_{23} & 0 & 0 & 0 \\ C_{21} & C_{32} & C_{22} & 0 & 0 & 0 \\ 0 & 0 & 0 & \frac{C_{22}-C_{23}}{2} & 0 & 0 \\ 0 & 0 & 0 & 0 & C_{66} & 0 \\ 0 & 0 & 0 & 0 & 0 & C_{66} \end{bmatrix} \quad \begin{bmatrix} S_{11} & S_{12} & S_{12} & 0 & 0 & 0 \\ S_{21} & S_{22} & S_{23} & 0 & 0 & 0 \\ S_{21} & S_{32} & S_{22} & 0 & 0 & 0 \\ 0 & 0 & 0 & \frac{S_{22}-S_{23}}{1/2} & 0 & 0 \\ 0 & 0 & 0 & 0 & S_{66} & 0 \\ 0 & 0 & 0 & 0 & 0 & S_{66} \end{bmatrix}$$

FIGURE 2.5 STIFFNESS MATRIX OF A TRANSVERSELY ISOTROPIC MATERIAL. NOTE THE DEPENDENCE OF SHEAR COMPONENT ON NORMAL COMPONENTS

Note that the number of independent constants are reduced from 3 to 2 because the 2-3 plane is isotropic. Thus the shear component "44" can be expressed in terms of the normal and Poisson's components, "22" and "23", respectively. Such relation is unique with isotropic materials. This can be derived from an equality between a combined stress or strain state of tension-compression and pure shear at an orientation 45 degree away from the combined normal components.

ISOTROPY

If a material is fully isotropic, the number of independent constants reduces from 5 to 2 This is shown in Figure 2.6. There are 12 nonzero constants, the same as in Figures 2.4 and 2.5. This is apparently the minimum number of nonzero constants regardless of material symmetry. All three shear components are expressed in terms of the normal components.

Complete symmetry

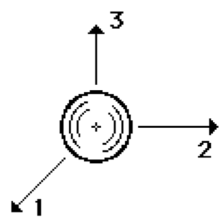

$$\begin{bmatrix} C_{11} & C_{12} & C_{12} & 0 & 0 & 0 \\ C_{21} & C_{11} & C_{12} & 0 & 0 & 0 \\ C_{21} & C_{21} & C_{11} & 0 & 0 & 0 \\ 0 & 0 & 0 & \frac{C_{11}-C_{12}}{2} & 0 & 0 \\ 0 & 0 & 0 & 0 & \frac{C_{11}-C_{12}}{2} & 0 \\ 0 & 0 & 0 & 0 & 0 & \frac{C_{11}-C_{12}}{2} \end{bmatrix} \quad \begin{bmatrix} S_{11} & S_{12} & S_{12} & 0 & 0 & 0 \\ S_{21} & S_{11} & S_{12} & 0 & 0 & 0 \\ S_{12} & S_{12} & S_{11} & 0 & 0 & 0 \\ 0 & 0 & 0 & \frac{S_{11}-S_{12}}{1/2} & 0 & 0 \\ 0 & 0 & 0 & 0 & \frac{S_{11}-S_{12}}{1/2} & 0 \\ 0 & 0 & 0 & 0 & 0 & \frac{S_{11}-S_{12}}{1/2} \end{bmatrix}$$

FIGURE 2.6 STIFFNESS MATRIX OF AN ISOTROPIC MATERIAL. ALL SHEAR COMPONENTS ARE RELATED TO HORMAL COMPONENTS

We have shown that the stiffness components are functions of material symmetries. The compliance components follow the same pattern of the nonzero and the number of independent components. They have the same appearance as the stiffness components in Figures 2.1-2 and 2.4-6. However, there is one exception; i.e., the equivalence of pure shear, and the combined tension and compression applied at a 45-degree orientation, which is shown in the figure above. The shear stiffness has a factor of 1/2 multiplying the difference between "11" and "12", and the shear compliance has the same factor dividing the difference.

The use of contracted notation reduces the number of indices, resulting in simpler mathematical expressions. But it must be applied consistently. We do not recommend mixing single and double indices such as using of single indices for the normal components and double indices for the shear. Furthermore, engineering shear strain is recommended for the contracted notation (Table 2.1 on page 2-2). While the contracted stiffness matrix is derived from the uncontracted without correction factors, the contracted compliance matrix requires correction factors of 1, 2 and 4 (Table 2.9 on page 2-5).

2.6 SUMMARY OF MATERIAL SYMMETRIES

We now present a summary of the Hooke's law in Table 2.10. The on-axis refers to the symmetry axes; the off-axis, the rotation about one of the reference axes; and the general, rotation about any axis.

TABLE 2.10 SUMMARY OF 3-DIMENSIONAL MATERIAL SYMMETRIES

Material Symmetry	Independent Constants	Nonzero: On-axis	Nonzero: Off-axis	Nonzero: General
Triclinic	21	36	36	36
Monoclinic	13	20	36	36
Orthotropic	9	12	20	36
Transversely Isotropic	5	12	20	36
Isotropic	2	12	12	12

The behavior of an anisotropic material depends not as much on the number of independent constants as on the nonzero components. For example, the on-axis orthotropic and the on-axis transversely isotropic materials behave the same qualitatively as an isotropic material. They all have 12 nonzero components, and are geometrically arranged like those in Figures 2.4, 2.5 and 2.6. For these materials, the shear and normal components of stress and strain are not coupled.

In Figure 2.7 we show graphically a summary of four most common material symmetries including isotropy. All components are of stiffness or compliance are shown relative to the principal axes 1, 2 and 3. The components associated to the isotropic plane for a transversely isotropic material are identified; so are the shear coupling components for a monoclinic material. In composite materials, we will use all these symmetries in two and three dimensional spaces.

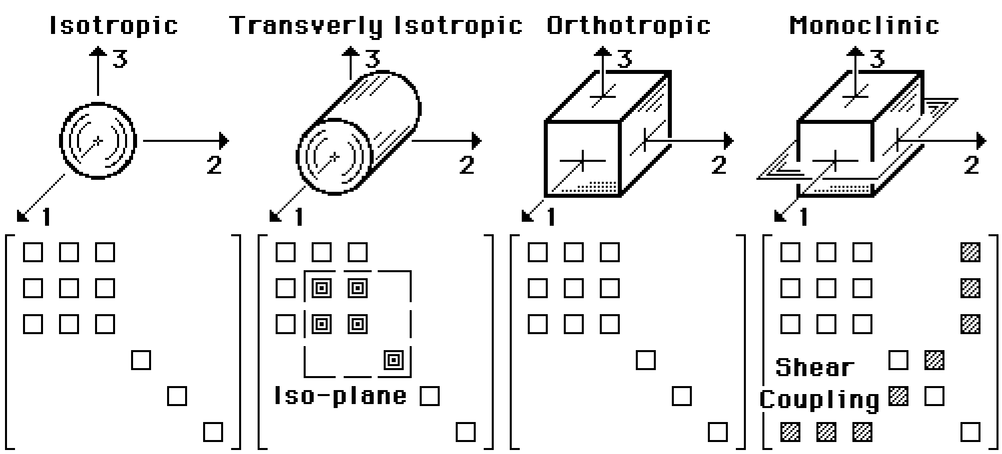

FIGURE 2.7 GRAPHICAL REPRESENTATIONS OF FOUR MATERIAL SYMMETRIES

When an orthotropic or transversely isotropic material rotates away from its symmetry axes about the 3- or z-axis, this off-axis orientation results in 20 nonzero components. Now shear coupling is present and this material will behave like a monoclinic material in its on-axis orientation. If the orthotropic or transversely isotropic material rotates about an axis other than the three reference axes, the nonzero components will be 36 and will behave like a triclinic material, shown in Figure 2.2 on page 2-3.

2.7 ENGINEERING CONSTANTS

The definitions of the Young's moduli of an anisotropic material follow those for isotropic materials subjected to uniaxial tensile or compressive tests. Using the stress-strain relation shown in Table 2.8, we can define Young's modulus in 1-direction by imposing a uniaxial test along the same axis, and repeat the same test along the 2- and 3-direction:

$$E_1 = \frac{\sigma_1}{\epsilon_1} = \frac{1}{S_{11}},\ E_2 = \frac{\sigma_2}{\epsilon_2} = \frac{1}{S_{22}},\ E_3 = \frac{\sigma_3}{\epsilon_3} = \frac{1}{S_{33}} \tag{2.6}$$

Shear moduli is derived from shear test and defined by using one or two subscripts:

$$E_4 = G_{23} = \frac{\sigma_4}{\epsilon_4} = \frac{1}{S_{44}},\ E_5 = G_{32} = \frac{\sigma_5}{\epsilon_5} = \frac{1}{S_{55}},\ E_6 = G_{12} = \frac{\sigma_6}{\epsilon_6} = \frac{1}{S_{66}} \tag{2.7}$$

We prefer the single subscript definition because it is consistent with the intent of the contracted notation.

The definitions of the Poisson and shear couplings are even less standardized and are, in fact, conflicting. We will show two definitions for a monoclinic material, in the following Tables 2.11 and 2.12. An off-axis orthotropic, and an off-axis transversely isotropic material have the same nonzero components as the monoclinic material.

In Table 2.11 each column is normalized by the same engineering constant derived from the diagonal term of the compliance matrix. Each off-diagonal term is multiplied and divided by the diagonal term, then engineering constants in Equations 2.6, 2.7 and 2.8 below are substituted. The results are shown in Table 2.11. We prefer this method of normalization because the interpretation of a simple uniaxial test can be readily made. Here we also follow the accepted convention of subscripts that the first subscript **i** refers to the row and the second subscript, the column. Mathematically, coupling component "12" means the stress or strain along the 1-axis as induced by an input in the 2-direction.

TABLE 2.11 COLUMN-NORMALIZED ENGINEERING CONSTANTS OF A MONOCLINIC MATERIAL

	σ_1	σ_2	σ_3	σ_4	σ_5	σ_6
ϵ_1	$1/E_1$	$-\nu_{12}/E_2$	$-\nu_{13}/E_3$	0	0	ν_{16}/E_6
ϵ_2	$-\nu_{21}/E_1$	$1/E_2$	$-\nu_{23}/E_3$	0	0	ν_{26}/E_6
ϵ_3	$-\nu_{31}/E_1$	$-\nu_{32}/E_2$	$1/E_3$	0	0	ν_{36}/E_6
ϵ_4	0	0	0	$1/E_4$	ν_{45}/E_5	0
ϵ_5	0	0	0	ν_{54}/E_4	$1/E_5$	0
ϵ_6	ν_{61}/E_1	ν_{62}/E_2	ν_{63}/E_3	0	0	$1/E_6$

Thus the definition of the coupling coefficients depends upon how the normalizing factor is applied. In Table 2.11 each column is normalized by the same Young's modulus or shear modulus. For the case of the longitudinal stiffness pointing along the 1-axis, the direction transverse to the fiber would be along the 2-axis, and the stiffness along the 1-axis would be considerably larger than that along the 2-axis:

$$\begin{aligned} \boldsymbol{\nu_{21}} &= \text{major or longitudinal Poisson's ratio} = \text{the larger ratio} = -\frac{S_{21}}{S_{11}} \\ \nu_{12} &= \text{minor or the smaller Poisson's ratio} = -\frac{S_{12}}{S_{22}} = \nu_{21}\frac{E_2}{E_1} \end{aligned} \tag{2.8}$$

But many if not most authors use the row nomrmalization for the definition of engineering constants. This is shown in Table 2.12 where each row is normalized by the same Young's modulus or shear modulus.

TABLE 2.12 ROW-NORMALIZED ENGINEERING CONSTANTS OF A MONOCLINIC MATERIAL

	σ_1	σ_2	σ_3	σ_4	σ_5	σ_6
ϵ_1	$1/E_1$	$-\nu_{12}/E_1$	$-\nu_{13}/E_1$	0	0	ν_{16}/E_1
ϵ_2	$-\nu_{21}/E_2$	$1/E_2$	$-\nu_{23}/E_2$	0	0	ν_{26}/E_2
ϵ_3	$-\nu_{31}/E_3$	$-\nu_{32}/E_3$	$1/E_3$	0	0	ν_{36}/E_3
ϵ_4	0	0	0	$1/E_4$	ν_{45}/E_4	0
ϵ_5	0	0	0	ν_{54}/E_5	$1/E_5$	0
ϵ_6	ν_{61}/E_6	ν_{62}/E_6	ν_{63}/E_6	0	0	$1/E_6$

The definitions for the coupling coefficients are defined exactly the opposite of those in Equation 2.8; where again we assume that the longitudinal direction is along the 1-axis.

$$\left.\begin{array}{l}\nu_{12} = \text{major or longitudinal Poisson's ratio} = \text{the larger ratio} = -\dfrac{S_{21}}{S_{11}} \\ \nu_{21} = \text{minor or the smaller Poisson's ratio} = -\dfrac{S_{12}}{S_{22}} = \nu_{12}\dfrac{E_2}{E_1}\end{array}\right] \tag{2.9}$$

As indicated earlier, we do not recommend the coupling coefficients by row normalization shown in Table 2.12. Unfortunately, many authors choose this normalization by rows even though it is less rational and consistent than by columns.

2.8 STIFFNESS IN TERMS OF ENGINEERING CONSTANTS

The expressions of **[C]** in terms of the engineering constants in the last section are lengthy because of the matrix inversion of the compliances. Such expressions for materials with orthotropic, transversely isotropic and isotropic symmetries can be found in the US Air Force Materials Laboratory report (AFML-TR-66-149, Part II): *Mechanics of Composite Materials*, by Stephen W. Tsai. For example, an orthotropic material in Figure 2.4 on page 2-7 can be expressed:

$$\left.\begin{array}{l}C_{11} = (1-\nu_{23}\nu_{32})VE_1,\ \ C_{22} = (1-\nu_{31}\nu_{13})VE_2,\ \ C_{33} = (1-\nu_{21}\nu_{12})VE_3 \\ C_{12} = (\nu_{12}+\nu_{13}\nu_{32})VE_1 = (\nu_{21}+\nu_{23}\nu_{31})VE_2 \\ C_{13} = (\nu_{13}+\nu_{12}\nu_{23})VE_1 = (\nu_{31}+\nu_{32}\nu_{21})VE_3 \\ C_{23} = (\nu_{23}+\nu_{21}\nu_{13})VE_2 = (\nu_{32}+\nu_{31}\nu_{12})VE_3 \\ C_{44} = G_{23},\ C_{55} = G_{31},\ C_{66} = G_{12} = E_6 \\ \text{where } V = \dfrac{1}{1-\nu_{12}\nu_{21}-\nu_{32}\nu_{23}-\nu_{13}\nu_{31}-2\nu_{21}\nu_{13}\nu_{32}}\end{array}\right] \tag{2.10}$$

All the engineering constants are defined in Table 2.11. A transversely isotropic material in Figure 2.5 on page 2-8 can be expressed:

$$\left.\begin{aligned}
&C_{11} = (1-\nu_{23}^2)VE_1,\ \ C_{22} = C_{33} = (1-\nu_{21}\nu_{12})VE_2 \\
&C_{12} = C_{13} = \nu_{12}(1+\nu_{23})VE_1 = \nu_{21}(1+\nu_{23})VE_2,\ \ C_{23} = (\nu_{23}+\nu_{21}\nu_{12})VE_2 \\
&C_{44} = (1-\nu_{23}-2\nu_{21}\nu_{12})VE_2/2,\ \ C_{55} = C_{66} = G_{12} = E_6 \\
&\text{where } V = \frac{1}{(1+\nu_{23})(1-\nu_{23}-2\nu_{21}\nu_{12})}
\end{aligned}\right] \tag{2.11}$$

For an isotropic material Equation 2.11 above can be further simplified:

$$\left.\begin{aligned}
&C_{11} = C_{22} = C_{33} = (1-\nu)VE,\ \ C_{23} = C_{31} = C_{12} = \nu VE \\
&C_{44} = C_{55} = C_{66} = G = E/2(1+\nu),\ \ \text{where } V = \frac{1}{(1+\nu)(1-2\nu)}
\end{aligned}\right] \tag{2.12}$$

These relations are relatively simple because shear coupling is absent in the matrix in Figures 2.4 to 2.6 starting on page 2-7. Similar closed-form expressions for a monoclinic material shown in Figure 2.2 would be nearly impossible because shear coupling terms are present. The inversion of this matrix is quite lengthy.

2.9 PLANE STRESS

This is a 2-dimensional idealization of a thin plate subjected to in-plane stresses. Most composite materials in use today can be modeled in a state of plane stress. The same assumption is used for the elementary theory of plates and shells made of isotropic materials. Thus the degree of confidence for assumed plane stress for thin composite plates should be the same as that for isotropic plates.

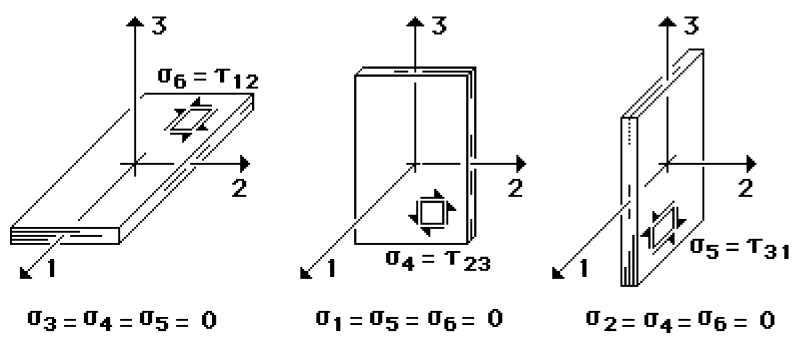

FIGURE 2.8 PLANE STRESS WITH THEIR PLANES COINCIDENT WITH THE SYMMETRY PLANES.

If the 1-2 plane is the plane of interest, the nonzero stress and strain components in this plane can be related by a specialized Hooke's law, as follows:

$$\{\boldsymbol{\varepsilon}\} = [\mathbf{S}]\{\boldsymbol{\sigma}\},\ \text{or}\ \boldsymbol{\varepsilon_i} = \mathbf{S_{ij}\sigma_j},\ \ i,j = 1, 2, 6 \tag{2.13}$$

where the compliance for plane stress has the same components as that for the 3-dimensional Hooke's law because stress components are specified. Because of Poisson or shear coupling the normal strain in the thickness or the 3 direction is not zero. From the specialized Hooke's law we can show:

$$\varepsilon_3 = S_{31}\sigma_1+S_{32}\sigma_2+S_{36}\sigma_6 \tag{2.14}$$

If the material is isotropic, the two Poisson couplings are equal and the shear coupling vanishes:

$$\varepsilon_3 = -\frac{\nu(\sigma_1+\sigma_2)}{E} \tag{2.15}$$

For plane stress in the 1-2 plane, the stresses in terms of the stiffness matrix are as follows:

$$\left.\begin{aligned}
\sigma_1 &= C_{11}\varepsilon_1+C_{12}\varepsilon_2+C_{13}\varepsilon_3+C_{16}\varepsilon_6\\
\sigma_2 &= C_{21}\varepsilon_1+C_{22}\varepsilon_2+C_{23}\varepsilon_3+C_{26}\varepsilon_6\\
\sigma_6 &= C_{61}\varepsilon_1+C_{62}\varepsilon_2+C_{63}\varepsilon_3+C_{66}\varepsilon_6\\
\sigma_3 &= C_{31}\varepsilon_1+C_{32}\varepsilon_2+C_{33}\varepsilon_3+C_{36}\varepsilon_6 = 0,\ \sigma_4 = \sigma_5 = 0
\end{aligned}\right] \tag{2.16}$$

We can eliminate the normal strain in the 3-direction as a dependent variable by solving the fourth line in Equation 2.16:

$$\varepsilon_3 = -\frac{C_{31}\varepsilon_1+C_{32}\varepsilon_2+C_{36}\varepsilon_6}{C_{33}} \tag{2.17}$$

By substituting Equation 2.17 into 2.16, we now have the stress-strain relation for plane stress in the 1-2 plane in terms of reduced stiffness:

$$\boldsymbol{\{\sigma\} = [Q]\{\varepsilon\}},\ \text{or}\ \boldsymbol{\sigma_i = Q_{ij}\sigma_j},\quad i,j = 1, 2, 6 \quad \text{where}\ \boldsymbol{Q_{ij}} = \frac{\boldsymbol{C_{ij}-C_{i3}C_{j3}}}{\boldsymbol{C_{33}}} \tag{2.18}$$

If the plane stress is in the 2-3, or the 1-3 plane, we will have the following relations, respectively. This is done following the same permutation of the indices, described in Figure 2.3 on page 2-7.

$$\left.\begin{aligned}
\{\sigma\} = [Q]\{\varepsilon\},\ \text{or}\ \sigma_i = Q_{ij}\varepsilon_j,\quad i,j &= 2,3,4 \quad \text{where}\quad Q_{ij} = C_{ij}-\frac{C_{i1}C_{j1}}{C_{11}}\\
&= 1,3,5 \quad \text{where}\quad Q_{ij} = C_{ij}-\frac{C_{i2}C_{j2}}{C_{22}}
\end{aligned}\right] \tag{2.19}$$

The three cases of plane stress that lie in the planes of symmetry are shown in Figure 2.8. Plane stress can exist on the symmetry planes only. If a material has no symmetry, the last two shear stresses in Equation 2.16 will not vanish. Then we cannot have plane stress.

The number of independent and nonzero constants for each symmetry is listed in Table 2.13 below.

TABLE 2.13 ELASTIC MODULI UNDER PLANE STRESS

Material Symmetry (independent constants)	Anisotropic(6) Off-orthotropic(4) Off-square symm(3)	On-orthotropic(4) On-square symm(3) Isotropic(2)
Nonzero Components	6	4
$Q_{11},Q_{22},Q_{12},Q_{66}$ $S_{11},S_{22},S_{12},S_{66}$	$\neq 0$	$\neq 0$
Q_{16},Q_{26} S_{16},S_{26}	$\neq 0$	$= 0$

The behavior of materials is controlled more by the number of nonzero constants than by the number of independent constants. For example, the nonzero constants will appear as coefficients of the equation of equilibrium of a plate. It does not matter if these nonzero coefficients are related or not. Thus for plane stress, the principal difference between the 6-constant material and the 4-constant material is the existence or absence of shear coupling.

The square symmetric material has equal stiffness on its symmetry axes, but unlike the isotropic material, the in-plane shear is independent, which gives 3 independent constants. A fabric with balanced weave is a square symmetric material.

Engineering constants are defined from the components of compliance. The coupling coefficients above are defined using the normalization by columns as in Table 2.11 on page 2-10, not by rows as in Table 2.12 on page 2-11.

$$\begin{aligned}
&E_1 = \frac{1}{S_{11}},\ E_2 = \frac{1}{S_{22}},\ E_6 = G_{12} = \frac{1}{S_{66}}, \\
&\nu_{21} = -\frac{S_{21}}{S_{11}},\ \nu_{12} = -\frac{S_{12}}{S_{22}} = \nu_{12}\frac{E_2}{E_1} \\
&\nu_{61} = \frac{S_{61}}{S_{11}},\ \nu_{16} = \frac{S_{16}}{S_{66}} = \nu_{61}\frac{E_6}{E_1},\ \nu_{62} = \frac{S_{62}}{S_{22}},\ \nu_{26} = \frac{S_{26}}{S_{66}} = \nu_{62}\frac{E_6}{E_1}
\end{aligned} \tag{2.20}$$

Finally, explicit relations between engineering constants and the stiffness components exist through the inversion of the compliance matrix. But these relations are simple only for the on-axis orthotropic material. Simple relations for anisotropic and off-axis orthotropic materials do not exist; i.e.,

$$\begin{aligned}
&Q_{11} \neq E_1/(1-\nu_{21}\nu_{12}),\ Q_{22} \neq E_2/(1-\nu_{21}\nu_{12}) \\
&Q_{12} \neq \nu_{21}Q_{11} \neq \nu_{12}Q_{22},\ Q_{66} \neq E_6 \neq G_{12}
\end{aligned} \tag{2.21}$$

In order to avoid confusion we designate the on-axis orthotropic constants by letter subscripts to distinguish them from numeric subscripts of the anisotropic and off-axis orthotropic constants:

$$Q_{xx} = \frac{E_x}{1-\nu_x\nu_y},\ Q_{yy} = \frac{E_y}{1-\nu_x\nu_y},\ Q_{xy} = \nu_x Q_{yy} = \nu_y Q_{xx},\ Q_{ss} = E_s \tag{2.22}$$

For the on-axis square symmetric material where the two Young's moduli are equal:

$$Q_{xx} = Q_{yy} = \frac{E_x}{1-\nu_x^2},\ Q_{xy} = \nu_x Q_{xx},\ Q_{ss} = E_s \tag{2.23}$$

The shear modulus for this material is independent, and is not dependent on the Young's modulus and Poisson's ratio, making this a 3-constant material. These constants are all defined relative to the symmetry axes. There are two sets of such axes, one 45 degrees from the other. For the isotropic material:

$$Q_{xx} = Q_{yy} = \frac{E}{1-\nu^2},\ Q_{xy} = \frac{\nu E}{1-\nu^2},\ Q_{ss} = \frac{E}{2(1+\nu)} \tag{2.24}$$

The basic differences between the square symmetric versus isotropic materials are: the 3 versus 2 independent constants, and that the engineering constants must be measured from the symmetry axes versus those from any axes, respectively. The subscripts in the engineering constants in Equation 2.22 are there to signify nonisotropic constants.

2.10 PLANE STRAIN

This is the other 2-dimensional state very analogous to the state of plane stress. This idealized state is applicable for structures having one very long dimension. For composite materials this situation exists, for example, for thick pressure vessels where the length of the cylinder is large in comparison with its diameter.

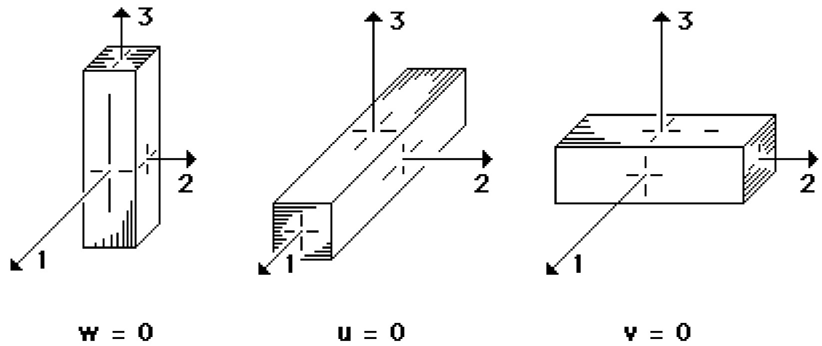

FIGURE 2.9 PLANE STRAIN IN THE PLANES OF ORTHOGONAL SYMMETRY

Since strain components are specified in plane strain, the stiffness components for 2-dimensional plane strain are the same as those for the 3-dimensional Hooke's law. Therefore, the stress and strain components in the 1-2 plane, for example, are related as follows:

$$\{\boldsymbol{\sigma}\} = [\mathbf{C}]\{\boldsymbol{\epsilon}\}, \text{ or } \boldsymbol{\sigma_i} = \mathbf{C_{ij}\epsilon_j}, \quad i,j = 1, 2, 6 \tag{2.25}$$

For materials other than the triclinic, 20-constants type, we can show that the stress component normal to the 1-2 plane can be determined:

$$\sigma_3 = C_{31}\epsilon_1 + C_{32}\epsilon_2 + C_{36}\epsilon_6 \tag{2.26}$$

The compliance components, however, must be modified for the plane strain state. This modification can be derived by substituting Equation 2.26 into the generalized Hooke's law to eliminate the out-of-plane normal stress (in the 3-direction) as an independent variable. This derivation is analogous to the reduced stiffness matrix for the plane stress case. Now we have the reduced compliance case for the plane strain. Assuming that the 1-2 plane is the plane strain, we have

$$\left.\begin{array}{l} \{\boldsymbol{\epsilon}\} = [\mathbf{R}]\{\boldsymbol{\sigma}\}, \text{ or } \boldsymbol{\epsilon_i} = \mathbf{R_{ij}\sigma_j}, \quad i,j = 1, 2, 6 \\ \quad \text{where } \mathbf{R_{ij}} = \dfrac{\mathbf{S_{ij} - S_{i3}S_{j3}}}{\mathbf{S_{33}}} = \text{reduced compliance for plane strain} \end{array}\right] \tag{2.27}$$

Like the case of plane stress, the reduced compliance matrix for plane strain for triclinic material symmetry is also beyond the scope of this section and thus is not obtained. We can derive the reduced compliance for plane strain in the other two symmetry axes, as shown in Figure 2.9 by the same permutation of indices described in Figure 2.3 on page 2-7 .

We can derive the engineering constants associated with plane strain the same as those with plane stress; e.g.,

$$E_1 = \frac{1}{R_{11}}, \ldots . \nu_{21} = -\frac{R_{21}}{R_{11}}, \ldots \tag{2.28}$$

The coupling coefficients are based on the normalization by columns as in Table 2.12. The relations between engineering constants and the stiffness components are not as straightforward because a matrix inversion is involved.

The independent and nonzero constants of anisotropic materials under plane strain, analogous to those in Table 2.13 for plane stress, are shown in Table 2.14.

TABLE 2.14 ELASTIC MODULI UNDER PLANE STRAIN

Material Symmetry (independent constants)	Anisotropic(6) Off-orthotropic(4) Off-square symm(3)	On-orthotropic(4) On-square symm(3) Isotropic(2)
Nonzero Components	6	4
$C_{11}, C_{22}, C_{12}, C_{66}$ $R_{11}, R_{22}, R_{12}, R_{66}$	$\neq 0$	$\neq 0$
C_{16}, C_{26} R_{16}, R_{26}	$\neq 0$	$= 0$

2.11 SAMPLE CALCULATIONS FOR ELASTIC MODULI

We can compute all the elastic constants from a given set of engineering constants. We take the following values for unidirectional CFRP laminate, T300/5208 (values for this and other composite materials can be found in Table 3.2 on page 3-12):

$$\left.\begin{aligned}
&E_x = 181 \text{ GPa}, E_y = 10.3 \text{ GPa}, \nu_x = 0.28, E_s = 7.17 \text{ GPa}\\
&\nu_y = \nu_x E_y/E_x = 0.28(10.3/181) = 0.0159\\
&Q_{xx} = E_x/(1-\nu_x\nu_y) = 181/(1-0.28x.0159) = 181.81 \text{ GPa}\\
&Q_{yy} = E_y/(1-\nu_x\nu_y) = 10.3/(1-0.28x.0159) = 10.346 \text{ GPa}\\
&Q_{xy} = \nu_x Q_{yy} = \nu_y Q_{xx} = 0.28 \times 10.346 = 2.897 \text{ GPa}\\
&Q_{ss} = E_s = 7.17 \text{ GPa}\\
&S_{xx} = 1/E_x = 1/181 = 5.52 \text{ TPa}^{-1}\\
&S_{yy} = 1/E_y = 1/10.3 = 97.09 \text{ TPa}^{-1}\\
&S_{xy} = -\nu_x/E_x = -\nu_y/E_y = -1.55 \text{ TPa}^{-1}\\
&S_{ss} = 1/E_s = 1/7.17 = 139.47 \text{ TPa}^{-1}
\end{aligned}\right] \qquad (2.29)$$

For the plane stress case, the compliance and stiffness matrices are the inverse of each other. Their product must produce a unity matrix; i.e.,

$$\mathbf{[Q] = [S]}^{-1} \qquad (2.30)$$

where the stiffness matrix is 3x3, with indices 1, 2 and 6.

In order to find the reduced compliance matrix and stiffness matrix of an on-axis transversely isotropic material, we will assume that the 2-3 plane is isotropic. If we further assume that the 1-2 plane is under plane strain, shown as the case on the left in Figure 2.9 on page 2-15, we need the following two additional components of the compliance matrix in order to complete Equation 2.27:

$$\left.\begin{aligned}
&S_{zz} = S_{yy} = 97.09 \text{ TPa}^{-1}, \text{ from } E_z = E_y\\
&\nu_{yz} = 0.5, \text{ from which } S_{yz} = -\nu_{yz}/E_y = -48.54 \text{ TPa}^{-1}
\end{aligned}\right] \qquad (2.31)$$

The transverse-transverse Poisson's ratio for this material was found to be approximately 0.5 by M. Knight, "Three-Dimensional Elastic Moduli of Graphite/Epoxy Composites," *Journal of Composite Materials,* Volume 16 (March 1982), p. 153. This Poisson's ratio was shown to be bounded between 0 and 1. The frequently assumed value of 0.3 is lower than that which Knight found.

From Equation 2.27, and letting 1 = x, 2 = y, 3 = z, we can compute the reduced compliance matrix for a plane strain in the 1-2 plane:

$$\left.\begin{aligned}
R_{xx} &= S_{xx}-S_{xz}^2/S_{zz} = 5.52-1.55^2/97.09 = 5.51\ \text{TPa}^{-1}\\
R_{yy} &= S_{yy}-S_{yz}^2/S_{zz} = 97.09-48.54^2/97.09 = 72.82\ \text{TPa}^{-1}\\
R_{xy} &= S_{xy}-S_{xz}S_{yz}/S_{zz} = -1.55-1.55\times 48.54/97.09 = -2.325\ \text{TPa}^{-1}\\
R_{ss} &= S_{ss} = 139.47\ \text{TPa}^{-1},\ \text{where } S_{zs} = S_{36} = 0
\end{aligned}\right] \qquad (2.32)$$

Reverting to numeric subscripts to conform to Figure 2.5, the following 3-dimensional stiffness matrix components can be computed from Equation 2.11:

$$\left.\begin{aligned}
V &= 1/(1+\nu_{23})(1-\nu_{23}-2\nu_{21}\nu_{12}) = 1/(1+0.5)(1-0.5-2\times 0.28\times 0.0159) = 1.36\\
C_{11} &= (1-\nu_{23}^2)VE_1 = (1-0.5^2)\times 1.36\times 181 = 184.6\ \text{GPa}\\
C_{22} &= C_{33} = (1-\nu_{21}\nu_{12})VE_2 = (1-0.28\times 0.0159)\times 1.36\times 10.3 = 13.94\ \text{GPa}\\
C_{12} &= C_{13} = \nu_{21}(1+\nu_{23})VE_2 = \nu_{12}(1+\nu_{23})VE_1 = 0.28\times(1+0.5)\times 1.36\times 10.3 = 5.88\ \text{GPa}\\
C_{23} &= (\nu_{23}+\nu_{21}\nu_{12})VE_2 = (0.5+0.28\times 0.0159)\times 1.36\times 10.3 = 7.06\ \text{GPa}\\
C_{44} &= (1-\nu_{23}-2\nu_{21}\nu_{12})VE_2/2 = (1-0.5-2\times 0.28\times 0.0159)\times 1.36\times 10.3/2 = 3.44\ \text{GPa}\\
C_{55} &= C_{66} = G_{12} = E_6 = 7.17\ \text{GPa}
\end{aligned}\right] \qquad (2.33)$$

For the plane strain case, the compliance and stiffness matrices are the inverse of each other. Their product must produce a unity matrix; i.e.,

$$\mathbf{[C] = [R]^{-1}} \qquad (2.34)$$

where the stiffness matrix is 3x3, with indices 1, 2 and 6.

2.12 STRESS AND STRAIN TRANSFORMATION EQUATIONS

Stress and strain at a point within a solid body are defined by how their components change with the reference coordinates. This coordinate-system dependence is of fundamental importance because laminate stress and strain and ply stress and strain can be explicitly related. One outstanding feature of composite materials is the highly directional or anisotropic property. It is often advantageous to rotate unidirectional or laminated composites to some arbitrary orientation. For example, applied loads to a structure are usually given in the laminate axes while failure criteria, for example, are usually applied to the stress or strain relative to the ply axes. The transformation equations allow us to move from one coordinate system to another.

The components of stress and strain change in accordance with specific transformation equations. The equations for stress are different from those for strain because we have elected to use the contracted notation which requires the use of engineering shear strain. The transformation equations in both the matrix and index notations are:

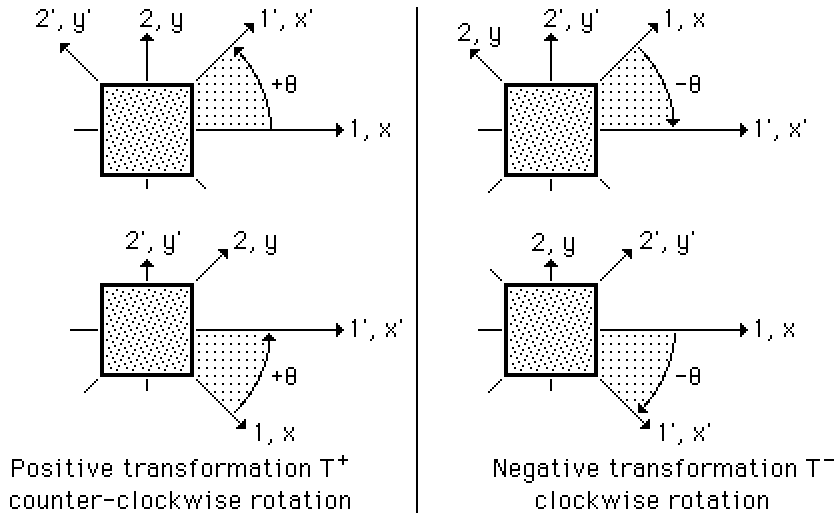

FIGURE 2.10 RELATION BETWEEN VARIOUS COORDINATES

Transformation relations for stress and strain are defined from tensor theory for second rank tensors. Such relations can also be derived from statics theory, such as the balance of forces and moments of a typical element subjected to normal and shear stresses. We can find such derivations in strength of materials books. Similarly, the transformation relations for strain can also be found in these books, and the relations are derivable from geometric relations before and after the element is deformed by normal and shear strains. Because of the use of engineering shear strain, the transformation equations for strain are different from those for stress. The difference is shown below:

$$\{\sigma'\} = [J]\{\sigma\} = [T^{+}]\{\sigma\} \qquad \{\sigma\} = [J]^{-1}\{\sigma'\} = [T^{-}]\{\sigma'\}$$

$$\{\varepsilon'\} = [J^{T}]^{-1}\{\varepsilon\} = [T^{+}]\{\varepsilon\} \qquad \{\varepsilon\} = [J^{T}]\{\varepsilon'\} = [T^{-}]\{\varepsilon'\}$$

$$\text{where } [J] = \begin{bmatrix} m^2 & n^2 & 2mn \\ n^2 & m^2 & -2mn \\ -mn & mn & m^2-n^2 \end{bmatrix} \qquad [J^{T}] = \begin{bmatrix} m^2 & n^2 & -mn \\ n^2 & m^2 & mn \\ 2mn & -2mn & m^2-n^2 \end{bmatrix}$$

$$[J]^{-1} = \begin{bmatrix} m^2 & n^2 & -2mn \\ n^2 & m^2 & 2mn \\ mn & -mn & m^2-n^2 \end{bmatrix} \qquad [J^{T}]^{-1} = \begin{bmatrix} m^2 & n^2 & mn \\ n^2 & m^2 & -mn \\ -2mn & 2mn & m^2-n^2 \end{bmatrix}$$

$$m = \cos\theta,\ n = \sin\theta \qquad (2.35)$$

The relations above are valid for all materials, isotropic and anisotropic. They are repeated in the following tables where specific transformations and figures are merged for easy identification.

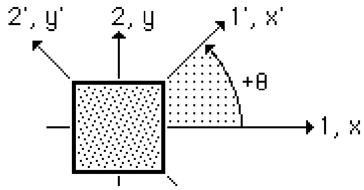

$$\begin{Bmatrix} \sigma_1' \\ \sigma_2' \\ \sigma_6' \end{Bmatrix} = \begin{bmatrix} m^2 & n^2 & 2mn \\ n^2 & m^2 & -2mn \\ -mn & mn & (m^2-n^2) \end{bmatrix} \begin{Bmatrix} \sigma_1 \\ \sigma_2 \\ \sigma_6 \end{Bmatrix}$$

Positive transformation T^+
counter-clockwise rotation

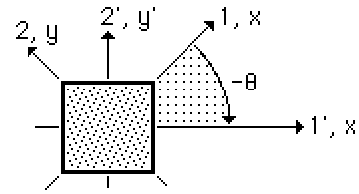

$$\begin{Bmatrix} \sigma_1' \\ \sigma_2' \\ \sigma_6' \end{Bmatrix} = \begin{bmatrix} m^2 & n^2 & -2mn \\ n^2 & m^2 & 2mn \\ mn & -mn & (m^2-n^2) \end{bmatrix} \begin{Bmatrix} \sigma_1 \\ \sigma_2 \\ \sigma_6 \end{Bmatrix}$$

Negative transformation T^-
clockwise rotation

FIGURE 2.11 STRESS TRANSFORMATION WITH POSITIVE AND NEGATIVE ROTATIONS

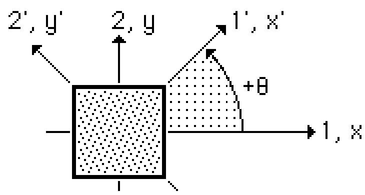

$$\begin{Bmatrix} \epsilon_1' \\ \epsilon_2' \\ \epsilon_6' \end{Bmatrix} = \begin{bmatrix} m^2 & n^2 & mn \\ n^2 & m^2 & -mn \\ -2mn & 2mn & (m^2-n^2) \end{bmatrix} \begin{Bmatrix} \epsilon_1 \\ \epsilon_2 \\ \epsilon_6 \end{Bmatrix}$$

Positive transformation T^+
counter-clockwise rotation

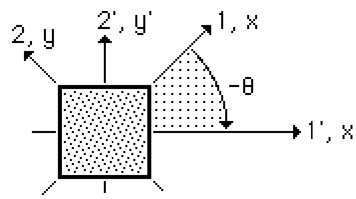

$$\begin{Bmatrix} \epsilon_1' \\ \epsilon_2' \\ \epsilon_6' \end{Bmatrix} = \begin{bmatrix} m^2 & n^2 & -mn \\ n^2 & m^2 & mn \\ 2mn & -2mn & (m^2-n^2) \end{bmatrix} \begin{Bmatrix} \epsilon_1 \\ \epsilon_2 \\ \epsilon_6 \end{Bmatrix}$$

Negative transformation T^-
clockwise rotation

FIGURE 2.12 STRAIN TRANSFORMATION WITH POSITIVE AND NEGATIVE ROTATIONS

For every state of stress, there is one particular orientation of the coordinate axes when the normal components reach extremum values and the shear vanish. The orientation and magnitude of the principal components are defined as follows:

TABLE 2.15 STRESS AND STRAIN TRANSFORMATION IN MOHR'S CIRCLES VARIABLES

	p	q	r	$\tan 2\theta_o$	R^2	Principal
Stress	$\frac{\sigma_1+\sigma_2}{2}$	$\frac{\sigma_1-\sigma_2}{2}$	σ_6	$\frac{2\sigma_6}{\sigma_1-\sigma_2}$	q^2+r^2	$p \pm R$
Strain	$\frac{\epsilon_1+\epsilon_2}{2}$	$\frac{\epsilon_1-\epsilon_2}{2}$	$\frac{\epsilon_6}{2}$	$\frac{\epsilon_6}{\epsilon_1-\epsilon_2}$	q^2+r^2	$p \pm R$

p = linear invariant, R = quadratic invariant

At 45 degrees from the principal axes, the shear reaches maximum and the normal components are equal.

The Mohr's circle representation of stress components and their variation with orientation is shown in Figure 2.13 below.

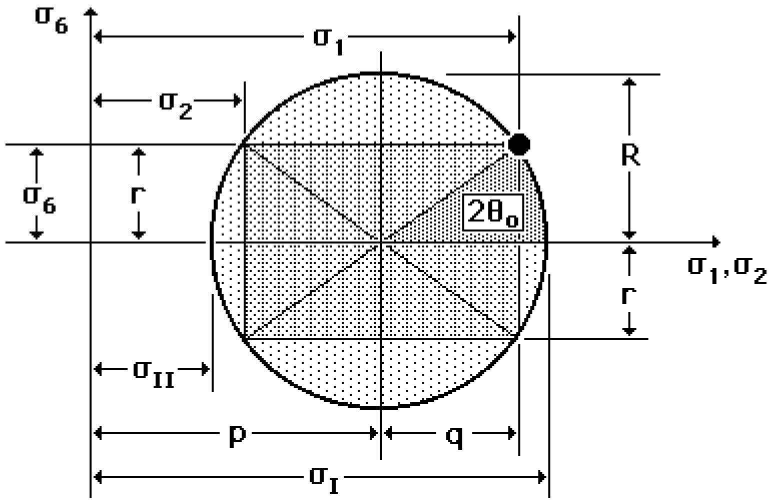

FIGURE 2.13 MOHR'S CIRCLE REPRESENTATION OF STRESS AND ITS PRINCIPAL COMPONENTS

The transformation of strain in Mohr's circle is shown in Figure 2.14 below. The vertical axis **r** is the tensorial shear strain which is one half the engineering shear strain.

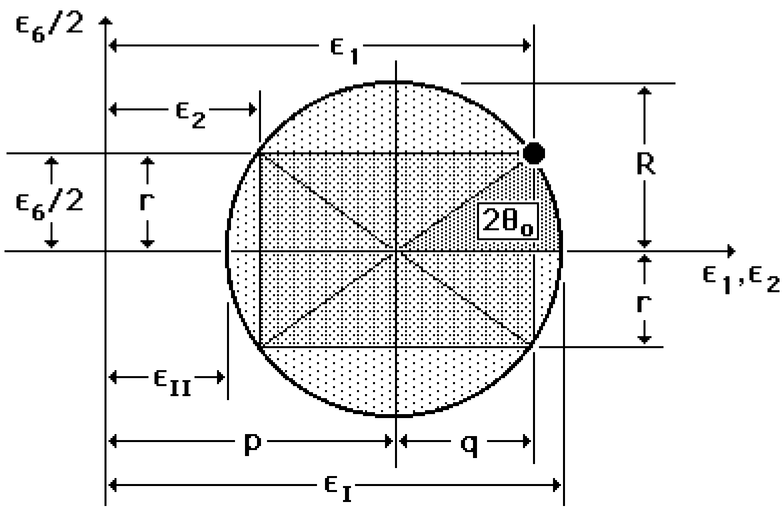

FIGURE 2.14 MOHR'S CIRCLE REPRESENTATION OF STRAIN AND ITS PRINCIPAL COMPONENTS; NOTE THAT ENGINEERING SHEAR STRAIN IS TWICE THE TENSORIAL SHEAR STRAIN

The Mohr's circle representation is important for failure envelopes. The rotation of a ply is equal to a rotation by a doubled angle in the Mohr's space. With such a simple relation, it is easy to generate failure envelopes of various ply angles by rigid body rotations.

Invariants are combinations of stress or strain components that remain constant under coordinate transformation. In a Mohr's circle, the location of the center **p** is a linear invariant. The radius of the circle **R** is a quadratic invariant. Invariants are useful for the design of composites. We can easily show that the following are also invariant:

$$
\begin{aligned}
&|\sigma^{mises}|^2 = |\sigma|^2 = \sigma_1^2 - \sigma_1\sigma_2 + \sigma_2^2 + 3\sigma_6^2 \\
&|\epsilon^{iso}|^2 = \frac{1+\nu^2}{E^2}\left[(\sigma^{mises})^2 + \frac{1-4\nu+\nu^2}{1+\nu^2}(\sigma_1\sigma_2 - \sigma_6^2)\right] \\
&|\epsilon|^2 = \epsilon_1^2 + \epsilon_2^2 + \frac{\epsilon_6^2}{2}
\end{aligned}
\qquad (2.36)
$$

The first is the von Mises invariant, which can be used as an effective stress or strength of a material under combined stresses. The second in Equation 2.36 is an effective strain that is also invariant. This can be used as a measure of deformation or susceptibility to deformation or buckling of a material under combined strains. It is better than using one of the normal strain components. The former is a scalar, and the latter is not. The difference is fundamental. We must design with invariants in order to arrive at an invariant design. If we do not use invariants, such as the maximum normal strain of a laminate, our design may depend on the choice of the coordinate system.

2.13 SAMPLE CALCULATIONS IN STRESS AND STRAIN

Sample 1: Given the following state of stress: {sigma} = {100, -30, 50}, (2.37)

find the transformed components and the principal and the maximum shear axes.

SOLUTION: Results shown in the following charts are obtained by substituting the values in Equation 2.37 into the first of Figure 2.11 on page 2-19.

Figure 2.15 below shows the variation of the stress components as a function of coordinate axes. The true essence of transformation is the principal axes, which, in this example, are analogous to the symmetry axes of the material.

From Table 2.15 on page 2-20, the phase angle based on the given stress components is:

$$\theta_0 = \frac{\arctan(r/q)}{2} = \frac{\arctan(2\text{x}50/130)}{2} = 18.8 \text{ degree} \qquad (2.38)$$

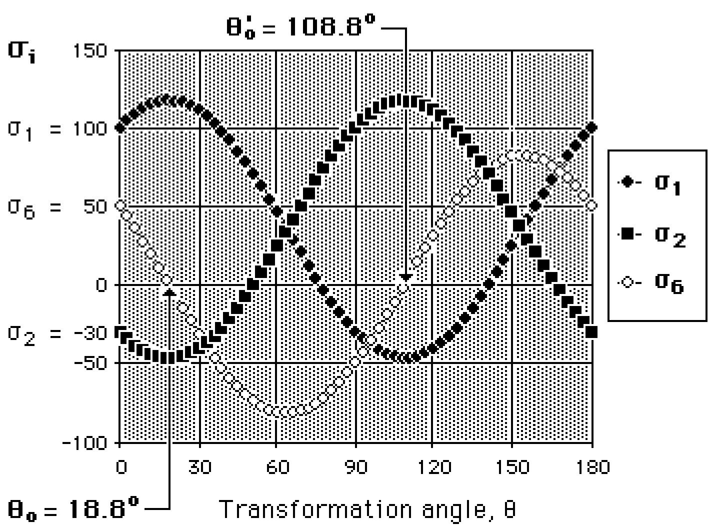

FIGURE 2.15 TRANSFORMED STRESS COMPONENTS OF EQUATION 2.37

The nature of stress transformation from the principal axes is graphically illustrated in Figure 2.16.

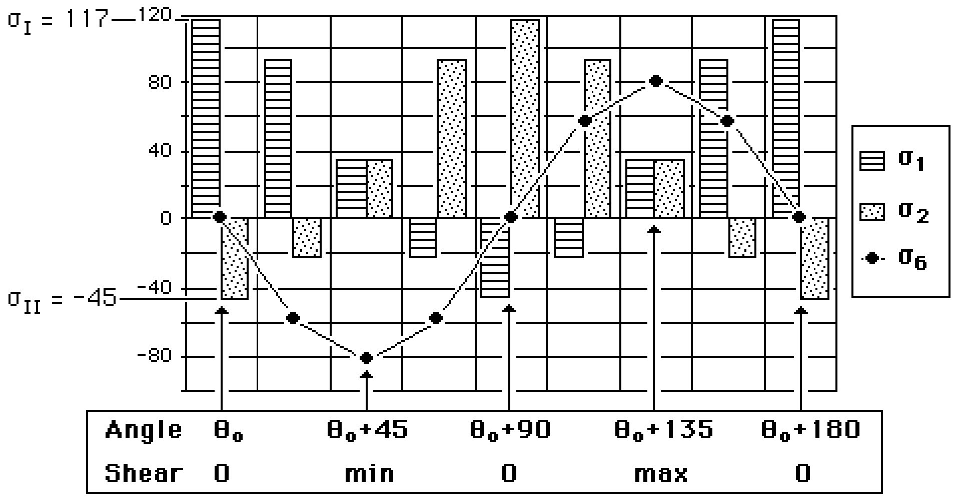

FIGURE 2.16 TRANSFORMED PRINCIPAL STRESS FROM THE PRINCIPAL AXES

Sample 2: Given the following state of principal stress: {sigma} = {117, -45, 0} (2.39)

find the transformed components, the average principal stresses, and the maximum shear.

SOLUTION: Results shown in the following charts are obtained by substituting the values in Equation 2.39 into the first of Figure 2.11 on page 2-19.

- The average principal stresses are (117-45)/2 = 36 at 45 degree transformation.
- The maximum shear stress is (117+45)/2 = 81 at the same transformed angle.

Sample 3: Given the following state of strain: {epsilon} = {100, -30, 50}, (2.40)

find the transformed components and the principal and maximum shear axes.

SOLUTION: Results shown in the charts above are obtained by substituting the values in Equation 2.40 into the first of Figure 2.12 on page 2-19.

From Table 2.15 on the same page, the phase angle based on the given strain in Equation 2.40 is:

$$\theta_0 = \frac{\arctan(r/q)}{2} = \frac{\arctan(50/130)}{2} = 10.5 \text{ degree} \qquad (2.41)$$

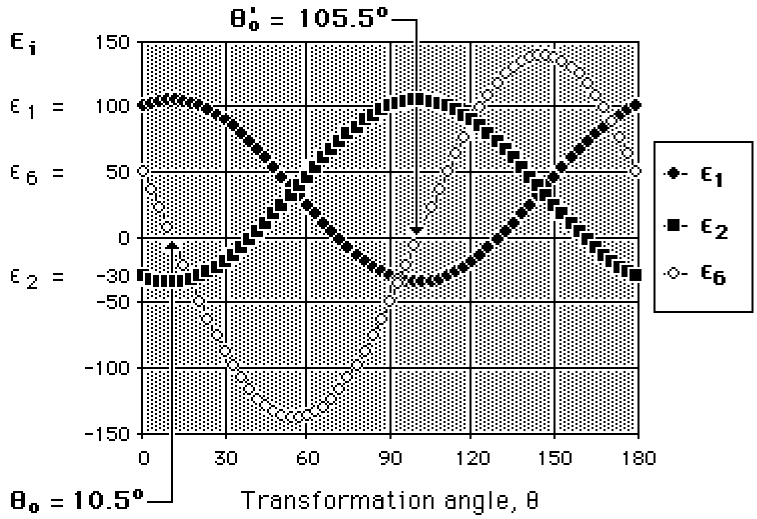

FIGURE 2.17 TRANSFORMED STRAINS FROM THE VALUES IN EQUATION 2.40

2.14 CONCLUSIONS

Generalized Hooke's law in three dimensions can be simplified by the presence of material symmetry and the chosen orientation of the reference coordinates. Material behavior, however, is dictated more by the number of nonzero components than by the number of independent constants. We strongly recommend that the intent of contracted notation be followed faithfully. Inconsistent use of this notation can lead to unnecessary confusion and complication. We must also be sure when we define the coupling coefficients. There are two commonly used definitions: one based on the normalization by columns, the other by rows. We prefer that of the columns because the conventional matrix rules of the off-diagonal terms are followed.

The stiffness and compliance matrices in the generalized Hooke's law for 3-dimensional stress and strain cannot be transferred directly to plane stress and plane strain. Modifications to the 3-dimensional state are necessary. The reduced stiffness for the plane stress case, and the reduced compliance for the plane strain case are examples of the modifications, and are summarized in Table 2.16 below.

The stress and strain transformations are simple algebraic equations. We want to emphasize the sign of the ply angle: it is positive if the new axis is reached by a counterclockwise rotation.

TABLE 2.16 SUMMARY OF 3- AND 2-DIMENSIONAL ELASTIC MODULI

Dimensions	3-Dimension	2-D Plane Stress	2-D Plane Strain
Stiffness	C_{ij}	Q_{ij}	C_{ij}
Compliance	S_{ij}	S_{ij}	R_{ij}

For anisotropic materials, principal stress or strain does not offer anything special in failure criteria. The invariants, however, are important for assessing the relative performance of composite laminates. We do not recommend the use of stress or strain components by themselves. One should rather use the invariants derived from them.

2.15 PROBLEMS

Prob. 2.1 **Fill in the nonzero components of the stiffness matrix of a monoclinic material having the 1-3 and 1-2 as planes of symmetry.**

TABLE 2.17 STIFFNESS MATRIX OF MONOCLINIC MATERIAL IN DIFFERENT PLANES OF SYMMETRY

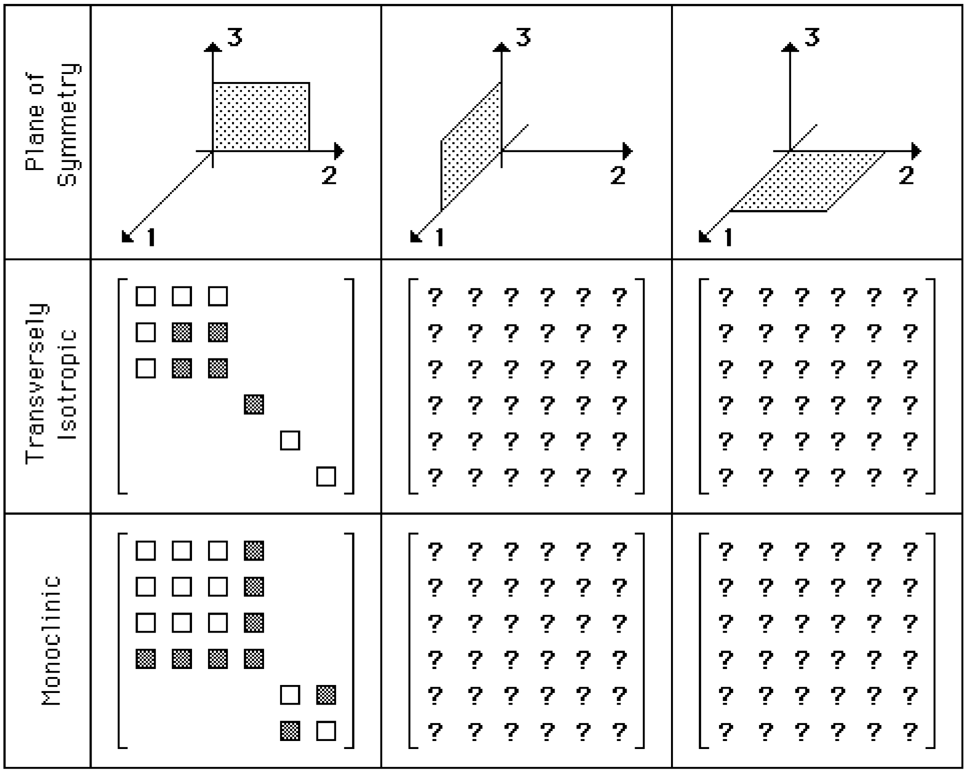

Prob. 2.2 **The 3 dimensional stress transformation about the 3-axis is shown in the figure below:**

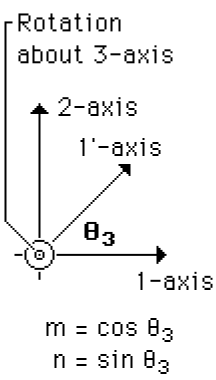

$$\begin{Bmatrix} \sigma_1' \\ \sigma_2' \\ \sigma_6' \\ \sigma_4' \\ \sigma_5' \\ \sigma_3' \end{Bmatrix} = \begin{bmatrix} m^2 & n^2 & 2mn & 0 & 0 & 0 \\ n^2 & m^2 & -2mn & 0 & 0 & 0 \\ -mn & mn & m^2-n^2 & 0 & 0 & 0 \\ 0 & 0 & 0 & m & -n & 0 \\ 0 & 0 & 0 & n & m & 0 \\ 0 & 0 & 0 & 0 & 0 & 1 \end{bmatrix} \begin{Bmatrix} \sigma_1 \\ \sigma_2 \\ \sigma_6 \\ \sigma_4 \\ \sigma_5 \\ \sigma_3 \end{Bmatrix}$$

FIGURE 2.18 STRESS TRANSFORMATION BY A ROTATION ABOUT THE 3-AXIS

What would be the values for a transformation about the 1- and 2-axis?

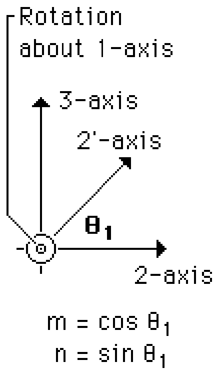

$$\begin{Bmatrix} \sigma_2' \\ \sigma_3' \\ \sigma_4' \\ \sigma_5' \\ \sigma_6' \\ \sigma_1' \end{Bmatrix} = \begin{bmatrix} ? & ? & ? & ? & ? & ? \\ ? & ? & ? & ? & ? & ? \\ ? & ? & ? & ? & ? & ? \\ ? & ? & ? & ? & ? & ? \\ ? & ? & ? & ? & ? & ? \\ ? & ? & ? & ? & ? & ? \end{bmatrix} \begin{Bmatrix} \sigma_2 \\ \sigma_3 \\ \sigma_4 \\ \sigma_5 \\ \sigma_6 \\ \sigma_1 \end{Bmatrix}$$

FIGURE 2.19 STRESS TRANSFORMATION BY A ROTATION ABOUT THE 1-AXIS

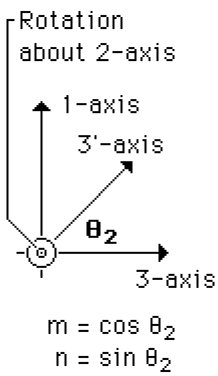

$$\begin{Bmatrix} \sigma_3' \\ \sigma_1' \\ \sigma_5' \\ \sigma_6' \\ \sigma_4' \\ \sigma_2' \end{Bmatrix} = \begin{bmatrix} ? & ? & ? & ? & ? & ? \\ ? & ? & ? & ? & ? & ? \\ ? & ? & ? & ? & ? & ? \\ ? & ? & ? & ? & ? & ? \\ ? & ? & ? & ? & ? & ? \\ ? & ? & ? & ? & ? & ? \end{bmatrix} \begin{Bmatrix} \sigma_3 \\ \sigma_1 \\ \sigma_5 \\ \sigma_6 \\ \sigma_4 \\ \sigma_2 \end{Bmatrix}$$

FIGURE 2.20 STRESS TRANSFORMATION BY A ROTATION ABOUT THE 2-AXIS

Prob. 2.3 **After the answers have been obtained in Figures 2.19 and 2.20, rearrange the stress and strain components in the same order as in Table 2.1, what would be the resulting stiffness matrices?**

Prob. 2.4 **Prove the relations between the normal and shear components on the isotropic, 2-3 plane in the stiffness and compliance matrices in Figure 2.5.**

Prob. 2.5 **Complete the missing 3-dimensional stiffness components for typical composite materials.**

TABLE 2.18 THREE-DIMENSIONAL STIFFNESS MATRIX OF TYPICAL COMPOSITES

Ply mat'l	T300/5208	B/55	AS/35	E-gl/ep	Kev/ep	AS/PK	IM6/ep	T3/F9
C_{xx}	184.62	?	?	?	?	?	?	?
$C_{yy} = C_{zz}$	13.94	?	?	?	?	?	?	?
C_{yz}	7.06	?	?	?	?	?	?	?
$C_{zx} = C_{xy}$	5.88	?	?	?	?	?	?	?
C_{qq}^*	3.44	?	?	?	?	?	?	?
$C_{rr} = C_{ss}$	7.17	5.59	7.10	4.14	2.30	5.10	8.40	4.55
C_{xx}/Q_{xx}	1.02	?	?	?	?	?	?	?
C_{yy}/Q_{yy}	1.34	?	?	?	?	?	?	?

*$C_{qq} = (C_{yy}-C_{yz})/2$. Subscript conversion: x = 1, y = 2, z = 3, q = 4, r = 5, s = 6

Section 3

PLY STIFFNESS

The elastic behavior of a unidirectional ply can be described in terms of the stiffness matrix, the compliance matrix, or a set of engineering constants. These moduli can be expressed in any arbitrary reference coordinate system by using appropriate transformation relations. Modulus values for representative composite materials are listed. The invariance of the transformed moduli, the quasi-isotropic constants, and the shear coupling are unique with composite materials, and can be utilized in design.

3.1 TRANSFORMATION OF STIFFNESS

The on-axis plane stress stiffness [Q] and compliance [S] of a unidirectional or fabric ply can be computed from the engineering constants as follows:

$$[Q] = \begin{bmatrix} \frac{E_x}{1-\nu_x\nu_y} & \frac{\nu_y E_x}{1-\nu_x\nu_y} & 0 \\ \frac{\nu_x E_y}{1-\nu_x\nu_y} & \frac{E_y}{1-\nu_x\nu_y} & 0 \\ 0 & 0 & E_s \end{bmatrix} \quad [S] = \begin{bmatrix} \frac{1}{E_x} & -\frac{\nu_y}{E_y} & 0 \\ -\frac{\nu_x}{E_x} & \frac{1}{E_y} & 0 \\ 0 & 0 & 1/E_s \end{bmatrix} \tag{3.1}$$

The off-axis stiffness matrix can be derived from the stress-strain relation in Equation 3.1, and stress and strain transformations in the last section:

$$\{\sigma\} = [Q]\{\varepsilon\} \quad [J]\{\sigma\} = [J][Q]\{\varepsilon\} \quad \{\sigma'\} = [J][Q][J^T]\{\varepsilon'\} \quad \{\sigma'\} = [Q']\{\varepsilon'\}$$
$$\text{Therefore } [Q'] = [J][Q][J^T] \tag{3.2}$$

This stiffness matrix transformation can go from the 1-axis to the 1'-axis, with the angle of rotation positive in the counter-clockwise direction. For composite materials, we adopt a system of designations such that the ply axes are the x-y axes, and the laminate axes, the 1-2 axes. This designation is arbitrary. Some authors use the 1-2 or L-T axes for the ply, and the x-y axes for the laminate. We use positive or negative angles as shown in Figure 3.1 below.

We wish to emphasize again the importance of keep consistent definition of angles. There are two directions: clockwise and counter-clockwise. For isotropic materials, properties of not directionally dependent. The response to a shear stress, for example, is the same whether it is positive or negative. Composites, on the other hand, behave completely differently if the sign of the shear stress is changes, or if it is applied to a positive or negative ply angle. Guesswork is right only 50 percent of the time. That is not good enough.

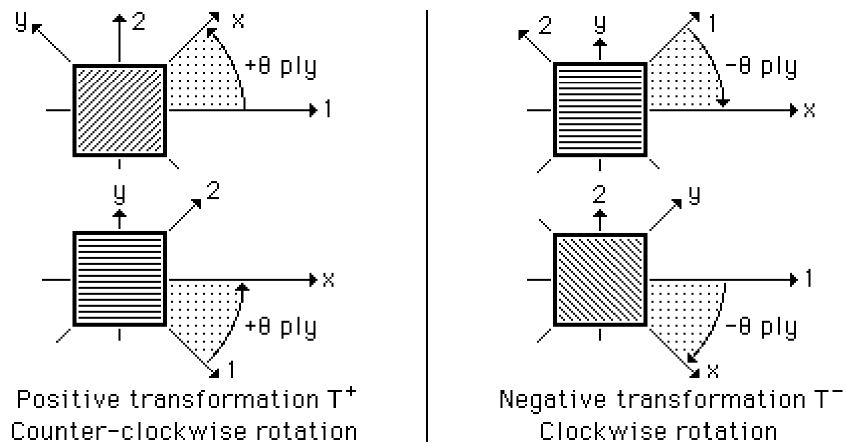

FIGURE 3.1 MATERIAL SYMMETRY AXES AND FIBER DIRECTIONS

Once the fiber orientations are defined, we can define the positive and negative transformations. In our notation, the transformation angle is in the same direction as the ply angle. Stress transformations from laminate to ply axes, and from ply to laminate axes are shown in Equation 3.3 below:

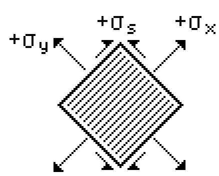

$$\begin{Bmatrix} \sigma_x \\ \sigma_y \\ \sigma_s \end{Bmatrix} = \begin{bmatrix} m^2 & n^2 & 2mn \\ n^2 & m^2 & -2mn \\ -mn & mn & (m^2-n^2) \end{bmatrix} \begin{Bmatrix} \sigma_1 \\ \sigma_2 \\ \sigma_6 \end{Bmatrix}$$

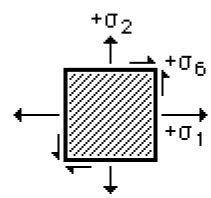

Positive transformation T^+ Counter-clockwise rotation

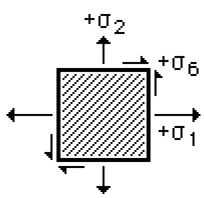

$$\begin{Bmatrix} \sigma_1 \\ \sigma_2 \\ \sigma_6 \end{Bmatrix} = \begin{bmatrix} m^2 & n^2 & -2mn \\ n^2 & m^2 & 2mn \\ mn & -mn & (m^2-n^2) \end{bmatrix} \begin{Bmatrix} \sigma_x \\ \sigma_y \\ \sigma_s \end{Bmatrix}$$

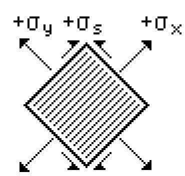

Negative transformation T^- Clockwise rotation (3.3)

The strain transformations are different from those for stress because engineering shear strain is used. A factor of 2 must be applied consistently. This is shown in Equation 3.4.

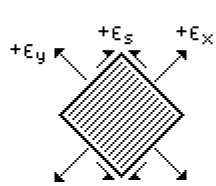

$$\begin{Bmatrix} \epsilon_x \\ \epsilon_y \\ \epsilon_s \end{Bmatrix} = \begin{bmatrix} m^2 & n^2 & mn \\ n^2 & m^2 & -mn \\ -2mn & 2mn & (m^2-n^2) \end{bmatrix} \begin{Bmatrix} \epsilon_1 \\ \epsilon_2 \\ \epsilon_6 \end{Bmatrix}$$

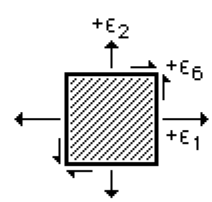

Positive transformation T^+ Counter-clockwise rotation

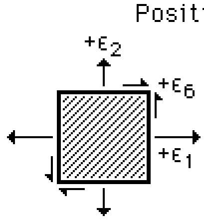

$$\begin{Bmatrix} \epsilon_1 \\ \epsilon_2 \\ \epsilon_6 \end{Bmatrix} = \begin{bmatrix} m^2 & n^2 & -mn \\ n^2 & m^2 & mn \\ 2mn & -2mn & (m^2-n^2) \end{bmatrix} \begin{Bmatrix} \epsilon_x \\ \epsilon_y \\ \epsilon_s \end{Bmatrix}$$

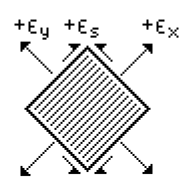

Negative transformation T^- Clockwise rotation (3.4)

The on- and off-axis stress-strain relations in terms of stiffness are listed below:

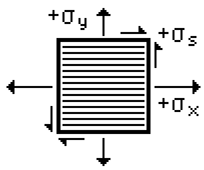

$$\begin{Bmatrix} \sigma_x \\ \sigma_y \\ \sigma_s \end{Bmatrix} = \begin{bmatrix} Q_{xx} & Q_{xy} & 0 \\ Q_{yx} & Q_{yy} & 0 \\ 0 & 0 & Q_{ss} \end{bmatrix} \begin{Bmatrix} \epsilon_x \\ \epsilon_y \\ \epsilon_s \end{Bmatrix}$$

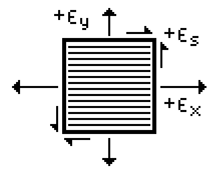

On-axis stress-strain relation

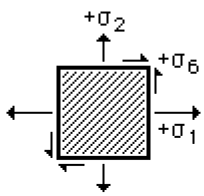

$$\begin{Bmatrix} \sigma_1 \\ \sigma_2 \\ \sigma_6 \end{Bmatrix} = \begin{bmatrix} Q_{11} & Q_{12} & Q_{16} \\ Q_{21} & Q_{22} & Q_{26} \\ Q_{61} & Q_{62} & Q_{66} \end{bmatrix} \begin{Bmatrix} \epsilon_1 \\ \epsilon_2 \\ \epsilon_6 \end{Bmatrix}$$

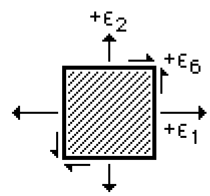

Off-axis stress-strain relation (3.5)

All stress and strain components are positive, which is intuitive for the normal components, but may not be self-evident for the shear component. We use the shear diagonal that goes through the first and third quadrants to designate the positive shear component. Another possibility is to define a positive shear as one that points to the positive direction on a positive surface.

Once we have mastered the stress and strain transformations and the stress-strain relation, we can derive the transformation of the stiffness and compliance matrices. The procedure goes from right to left in Figure 3.2 below:

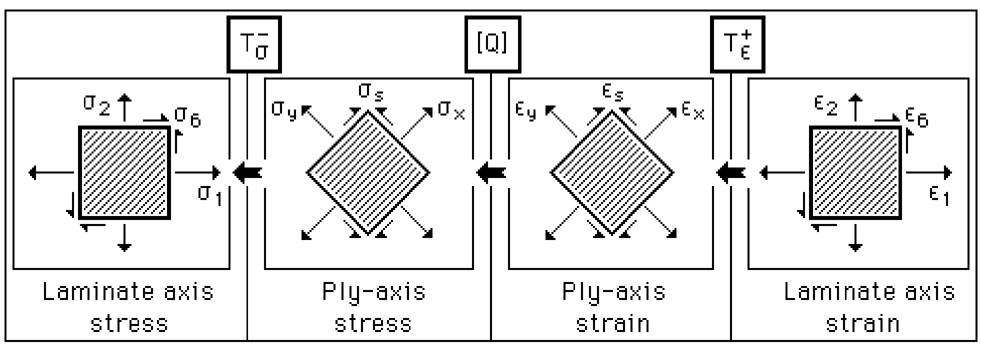

FIGURE 3.2 DERIVATION OF THE PLANE-STRESS STIFFNESS TRANSFORMATIONS

The actual relations of the transformation in the figure above are shown in detail in Figure 3.3 below.

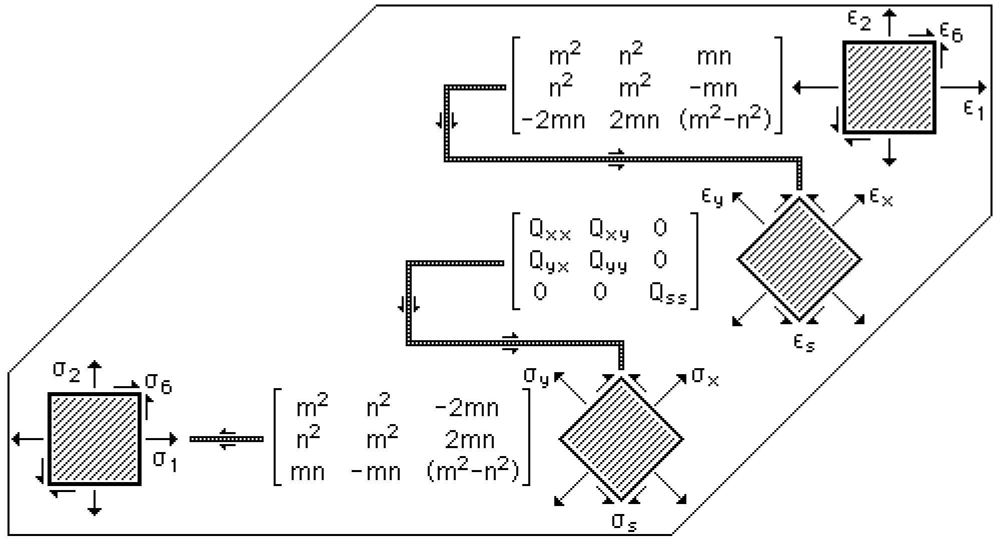

FIGURE 3.3 DETAILED DERIVATION OF THE PLANE-STRESS STIFFNESS TRANSFORMATIONS

The validity of the stiffness transformation relations depends on the transformation for stress and strain, and the linear stress-strain relation. As we have stated earlier, stress transformation depends on the balance of forces, which is a static equilibrium consideration. The transformation of strain is based purely on geometric relations. The linear stress-strain relation is assumed to remain valid. Since we make the same assumptions for the derivation of the transformation of the stiffness matrix, transformation should remain valid as a fundamental postulate in the mechanics of anisotropic solids.

The resulting transformation relations in Figure 3.3 lead to the matrix equation shown in Figure 3.4:

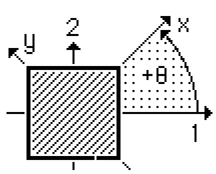

$$\begin{Bmatrix} Q_{11} \\ Q_{22} \\ Q_{12} \\ Q_{66} \\ Q_{16} \\ Q_{26} \end{Bmatrix} = \begin{bmatrix} m^4 & n^4 & 2m^2n^2 & 4m^2n^2 \\ n^4 & m^4 & 2m^2n^2 & 4m^2n^2 \\ m^2n^2 & m^2n^2 & m^4+n^4 & -4m^2n^2 \\ m^2n^2 & m^2n^2 & -2m^2n^2 & (m^2-n^2)^2 \\ m^3n & -mn^3 & mn^3-m^3n & 2(mn^3-m^3n) \\ mn^3 & -m^3n & m^3n-mn^3 & 2(m^3n-mn^3) \end{bmatrix} \begin{Bmatrix} Q_{xx} \\ Q_{yy} \\ Q_{xy} \\ Q_{ss} \end{Bmatrix}$$

FIGURE 3.4 TRANSFORMATION OF STIFFNESS MATRIX FOR POSITIVE ANGLES

The difference between the positive and negative transformations is that there are opposite signs in the shear coupling components because the odd power of a sine function is anti-symmetric.

If we look at the first line of the matrix equation in the figure above, the contribution to the "11" component comes from all four principal stiffnesses of an on-axis ply. Each part is multiplied by a fourth power of a trigonometric function, which are plotted in the figures below. The contribution of the on-axis stiffnesses to the off-axis ones are corrected by the fourth power functions, which in fact define a fourth-rank tensor.

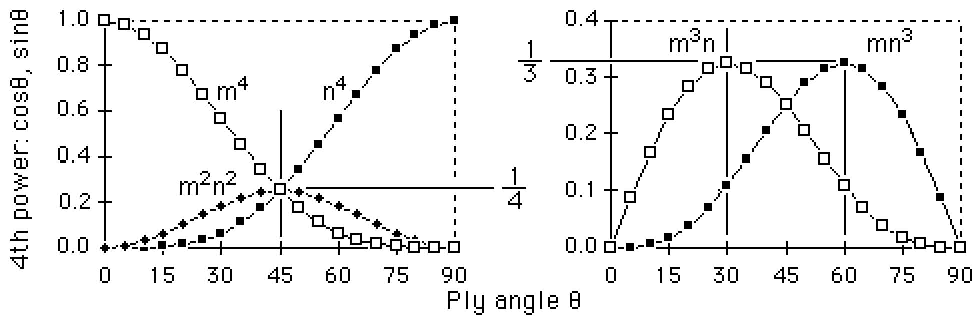

FIGURE 3.5 FOURTH POWER OF SINES AND COSINES THAT APPEAR IN THE TRANSFORMATION RELATIONS IN THE PREVIOUS FIGURE

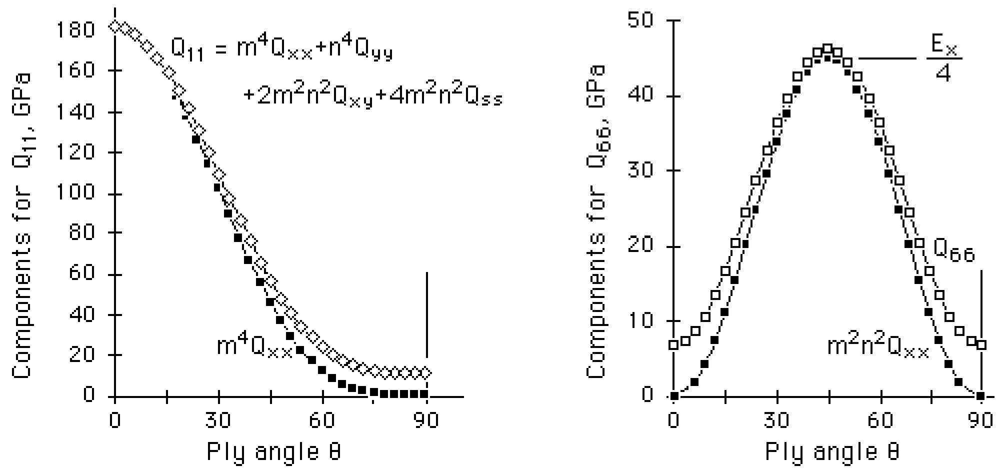

FIGURE 3.6 THE CONTRIBUTION OF LONGITUDINAL STIFFNESS TO THE "11" AND "66" STIFFNESS COMPONENTS (THE PLY MATERIAL IS T300/5208)

We show in the figure above the most significant contribution of "xx" component to the "11" and "66" components of the stiffness. The "xx" component is essentially the stiffness along the fiber direction. For the "11" component, on the left of the figure below, the "xx" contribution is most significant near the 0 degree ply angle; for the "66" component, near the 45 degrees. For example, the shear modulus at 45 degree is simply one fourth of the longitudinal modulus. For T300/5208, one quarter of 181 is about 45.25 GPa, with a 3 percent error from the exact value of 46.59 GPa. Shear coupling is approximately 1/3. That occurs at 30 degree, as shown in Figures 3.5 and 3.25.

3.2 TRANSFORMATION OF COMPLIANCE

We can similarly derive the transformation relations of the compliance matrix. This is done in nearly identical fashion as that with the stiffness in the last sub-section. The stress and strain transformations are the same, but the stress-strain relation in the ply axis is now in terms of compliance, as in Equation 3.6. The compliance transformation is different from the stiffness transformation because of the use of engineering shear strain.

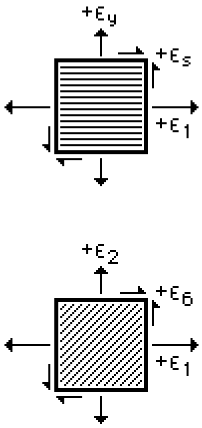

$$\begin{Bmatrix} \epsilon_x \\ \epsilon_y \\ \epsilon_s \end{Bmatrix} = \begin{bmatrix} S_{xx} & S_{xy} & 0 \\ S_{yx} & S_{yy} & 0 \\ 0 & 0 & S_{ss} \end{bmatrix} \begin{Bmatrix} \sigma_x \\ \sigma_y \\ \sigma_s \end{Bmatrix}$$

On-axis stress-strain relation

$$\begin{Bmatrix} \epsilon_1 \\ \epsilon_2 \\ \epsilon_6 \end{Bmatrix} = \begin{bmatrix} S_{11} & S_{12} & S_{16} \\ S_{21} & S_{22} & S_{26} \\ S_{61} & S_{62} & S_{66} \end{bmatrix} \begin{Bmatrix} \sigma_1 \\ \sigma_2 \\ \sigma_6 \end{Bmatrix}$$

Off-axis stress-strain relation

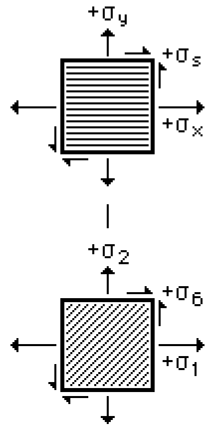

(3.6)

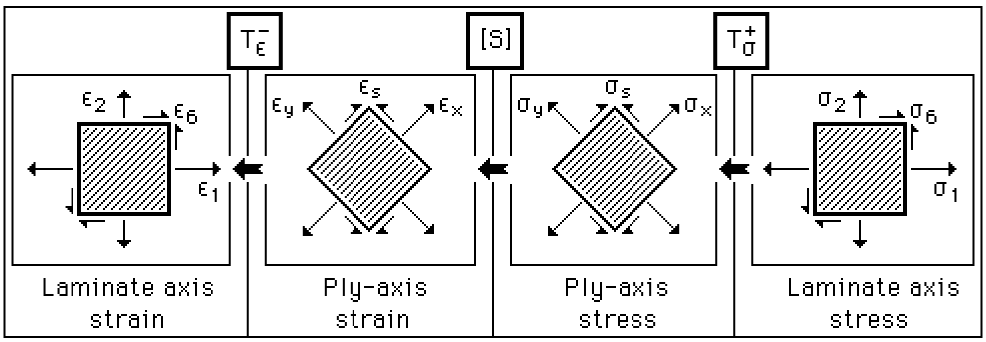

FIGURE 3.7 DERIVATION OF THE PLANE-STRESS COMPLIANCE TRANSFORMATIONS

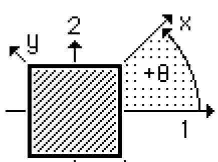

$$\begin{Bmatrix} S_{11} \\ S_{22} \\ S_{12} \\ S_{66} \\ S_{16} \\ S_{26} \end{Bmatrix} = \begin{bmatrix} m^4 & n^4 & 2m^2n^2 & m^2n^2 \\ n^4 & m^4 & 2m^2n^2 & m^2n^2 \\ m^2n^2 & m^2n^2 & m^4+n^4 & -m^2n^2 \\ 4m^2n^2 & 4m^2n^2 & -8m^2n^2 & (m^2-n^2)^2 \\ 2m^3n & -2mn^3 & 2(mn^3-m^3n) & mn^3-m^3n \\ 2mn^3 & -2m^3n & 2(m^3n-mn^3) & m^3n-mn^3 \end{bmatrix} \begin{Bmatrix} S_{xx} \\ S_{yy} \\ S_{xy} \\ S_{ss} \end{Bmatrix}$$

FIGURE 3.8 TRANSFORMATION OF COMPLIANCE MATRIX FOR POSITIVE ANGLES

3.3 TRANSFORMATION IN THREE DIMENSIONS

We have just shown the transformation in two dimensions; i.e., the plane-stress stiffness and compliance from the ply-axes to an arbitrary set of axes. Our formulation is such that the ply angle and the angle of transformation are equal. Some authors formulate their transformation relation such that the ply angle is the opposite of the transformation angle. The reader is reminded again of this fundamental difference among authors.

We now list the components of a three-dimensional orthotropic material which has 12 nonzero and 9 independent components. If the axis of transformation is a rotation about the 3- or z-axis, the resulting relations are shown in the next two figures below in a matrix multiplication table format.

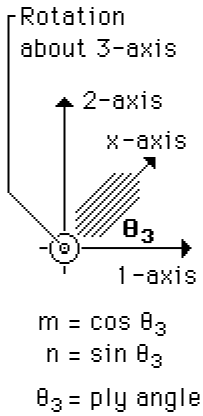

	$S_{xx}(C_{xx})$	$S_{yy}(C_{yy})$	$S_{xy}(C_{xy})$	$S_{ss}(4C_{ss})$
$S_{11}\,(C_{11})$	m^4	n^4	$2m^2n^2$	m^2n^2
$S_{22}\,(C_{22})$	n^4	m^4	$2m^2n^2$	m^2n^2
$S_{12}\,(C_{12})$	m^2n^2	m^2n^2	m^4+n^4	$-m^2n^2$
$S_{66}\,(4C_{66})$	$4m^2n^2$	$4m^2n^2$	$-8m^2n^2$	$(m^2-n^2)^2$
$S_{16}\,(2C_{16})$	$2m^3n$	$-2mn^3$	$2mn^3-2m^3n$	mn^3-m^3n
$S_{26}\,(2C_{26})$	$2mn^3$	$-2m^3n$	$2m^3n-2mn^3$	m^3n-mn^3

$S_{11} = m^4S_{xx}+n^4S_{yy}+2m^2n^2S_{xy}+m^2n^2S_{ss}$, $C_{11} = m^4C_{xx}+n^4C_{yy}+2m^2n^2C_{xy}+4m^2n^2C_{ss}$

FIGURE 3.9 THE IN-PLANE COMPONENTS OF THE 3-D TRANSFORMATION OF AN ORTHOTROPIC BODY ABOUT THE 3- OR Z-AXIS

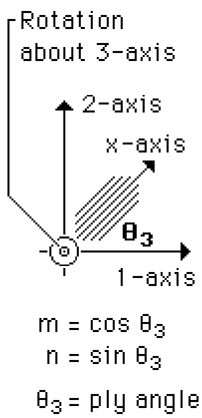

	$S_{xz}(C_{xz})$	$S_{yz}(C_{yz})$	$S_{qq}(C_{qq})$	$S_{rr}(C_{rr})$	$S_{zz}(C_{zz})$
$S_{13}\,(C_{13})$	m^2	n^2	0	0	0
$S_{23}\,(C_{23})$	n^2	m^2	0	0	0
$S_{36}\,(C_{36})$	mn	$-mn$	0	0	0
$S_{44}\,(C_{44})$	0	0	m^2	n^2	0
$S_{55}\,(C_{55})$	0	0	n^2	m^2	0
$S_{45}\,(C_{45})$	0	0	$-mn$	mn	0
$S_{33}\,(C_{33})$	0	0	0	0	1

FIGURE 3.10 THE OUT-OF-PLANE COMPONENTS OF THE 3-D TRANSFORMATION OF AN ORTHOTROPIC BODY ABOUT THE 3- OR Z-AXIS

In the first of the last two figures, the transformation relations of the in-plane components are identical to those of the 2-dimensional plane stress case, except that the 3-D stiffness is in **[C]**, and the 2-D case is in **[Q]**, the reduced stiffness. All relations of these components are driven by the 4th power of sine and cosine functions. The remaining components are the out-of-plane associated components which are driven by the second power, as shown in the second figure. These components are less affected by the transformation than those of the in-plane. Finally, the "33" component remains invariant under this transformation, or it is driven by the 0-th power. In the figure below, we show graphically the difference in the power functions in the transformation relations listed in the figure above.

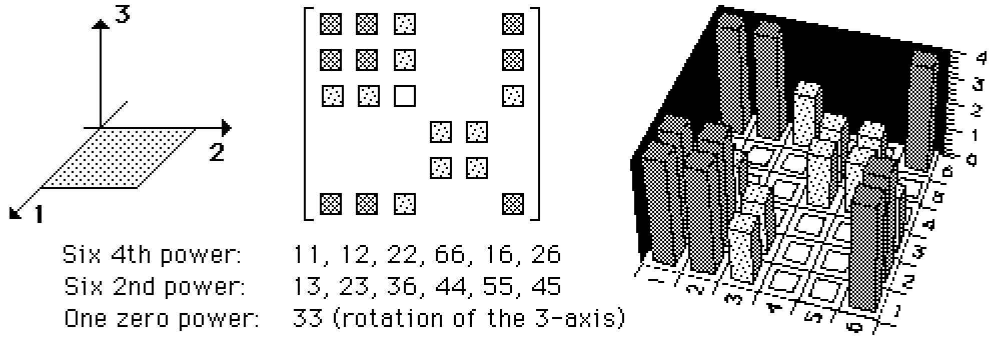

FIGURE 3.11 THREE POWER LEVELS OF THE STIFFNESS COMPONENTS OF TRANSFORMATION OF AN ORTHOTROPIC MATERIAL ABOUT THE 3-AXIS

3.4 MULTIPLE-ANGLE TRANSFORMATION

We introduce the following trigonometric identities to change the transformation relations above from the fourth powers of trigonometric functions to those in multiple angles.

$$m^4 = \frac{3+\cos 2\theta+\cos 4\theta}{8}, \quad m^3 n = \frac{2\sin 2\theta+\sin 4\theta}{8}$$
$$m^2 n^2 = \frac{1-\cos 4\theta}{8}, \quad mn^3 = \frac{2\sin 2\theta-\sin 4\theta}{8}, \quad n^4 = \frac{3-4\cos 2\theta+\cos 4\theta}{8} \qquad (3.7)$$

When we repackage the transformation relations by substituting these identities into those in Equation 3.4, we have a set of linear combinations of the principal stiffness listed in the table below:

TABLE 3.1 LINEAR COMBINATIONS OF ON-AXIS STIFFNESS MODULI

	Q_{xx}	Q_{yy}	Q_{xy}	Q_{ss}	Invariant?
$U_1 = U_4+2U_5$	3/8	3/8	1/4	1/2	Yes
U_2	1/2	-1/2	0	0	No
U_3	1/8	1/8	-1/4	-1/2	No
$U_4 = U_1-2U_5$	1/8	1/8	3/4	-1/2	Yes
$U_5 = (U_1-U_4)/2$	1/8	1/8	-1/4	1/2	Yes

Three of the combinations are invariant. There is a practical significance of invariance in design; i.e., regardless of laminate layup of multidirectional plies, the invariance remains constant. The non-invariant or cyclic combindations are responsible for the anisotropy of the ply material. By definition they are zero for isotropic materials, for which there are only two independent constants. One such indentity relation that would reduce the number of constants was cited in Figure 2.5 between shear modulus and Young's and Poisson's components.

Using these linear combinations Us and the multiple angles, we have a new set of transformation relations, shown in Figure 3.12. In this formulation, transformation relations are separated into two sets: materials in Us and geometry in trignometric functions of double and quadruple ply angles. This figure is different from Figure 3.4 where the trignometric functions are in the 4th power of ply angles. Multiple angles have certain advantages that they are easier to manipulate mathematically.

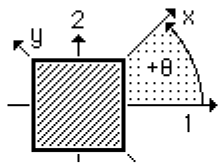

$$\begin{Bmatrix} Q_{11} \\ Q_{22} \\ Q_{12} \\ Q_{66} \\ Q_{16} \\ Q_{26} \end{Bmatrix} = \begin{bmatrix} U_1 & U_2 & U_3 & 0 & 0 \\ U_1 & -U_2 & U_3 & 0 & 0 \\ U_4 & 0 & -U_3 & 0 & 0 \\ U_5 & 0 & -U_3 & 0 & 0 \\ 0 & 0 & 0 & \frac{U_2}{2} & U_3 \\ 0 & 0 & 0 & \frac{U_2}{2} & -U_3 \end{bmatrix} \begin{Bmatrix} 1 \\ \cos 2\theta \\ \cos 4\theta \\ \sin 2\theta \\ \sin 4\theta \end{Bmatrix}$$

FIGURE 3.12 AN ALTERNATIVE PACKAGING OF TRANSFORMATION IN MULTIPLE ANGLES

We can also show the contribution of the three terms to the "11" component of the stiffness in the following figure. Components "11" and "22" in the multiple angle formulation consist of one invariant and two cyclic terms. The area under the transformed component remains constant. Thus the invariant term represents the total stiffness potential of an anisotropic material.

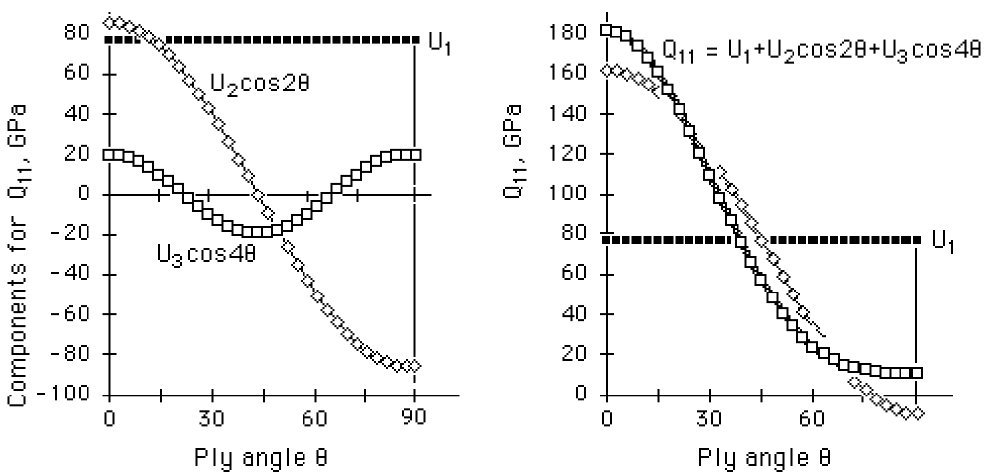

FIGURE 3.13 THE COMPONENTS AND THEIR SUM THAT MAKE UP THE "11" COMPONENT OF STIFFNESS IN THE MULTIPLE ANGLE FORMULATION

Two independent linear invariants shown in the figure above are shown in the figure below where the shaded areas above and below the invariant lines are equal. The cyclic terms cancel one another.

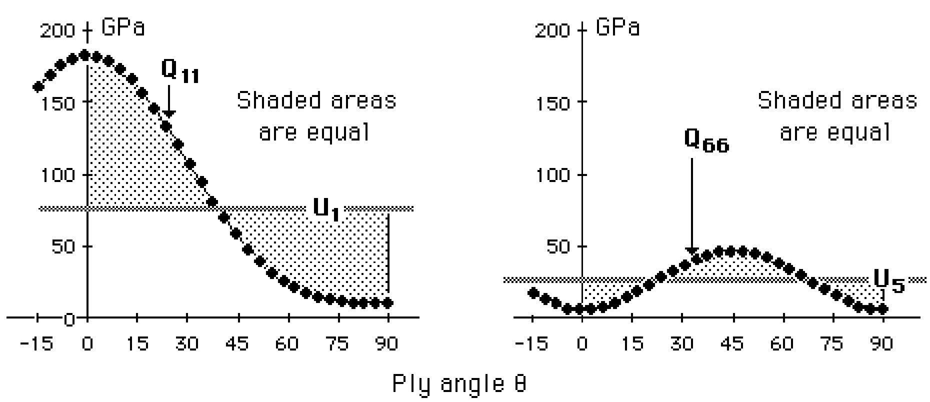

FIGURE 3.14 THE INVARIANTS OF THE "11" AND "66" COMPONENTS

If tensorial, in stead of engineering, shear strains are used, the stress-strain relation will appear in the following form, which is the same as Equation 2.5 on page 2-6. A factor of 2 must be multiplied for the stiffness matrix, and divided in the compliance matrix. With this factor of 2 added, both matrices are no longer symmetric.

$$\begin{Bmatrix} \sigma_1 \\ \sigma_2 \\ \sigma_6 \end{Bmatrix} = \begin{bmatrix} Q_{11} & Q_{12} & 2Q_{16} \\ Q_{21} & Q_{22} & 2Q_{26} \\ Q_{61} & Q_{62} & 2Q_{66} \end{bmatrix} \begin{Bmatrix} \epsilon_1 \\ \epsilon_2 \\ \epsilon_{12} \end{Bmatrix} \qquad \begin{Bmatrix} \epsilon_1 \\ \epsilon_2 \\ \epsilon_{12} \end{Bmatrix} = \begin{bmatrix} S_{11} & S_{12} & S_{16} \\ S_{21} & S_{22} & S_{26} \\ \frac{S_{61}}{2} & \frac{S_{62}}{2} & \frac{S_{66}}{2} \end{bmatrix} \begin{Bmatrix} \sigma_1 \\ \sigma_2 \\ \sigma_6 \end{Bmatrix} \tag{3.8}$$

The linear combinations of invariants are of course invariant. In the equation below, we show examples of Is in terms of Us. The trace of a matrix is the sum of its diagonal components, for which tensorial strains must be used. If engineering shear strains are used, a "trace" would be invariant only if the factor of 2 in the equation above is included.

$$\begin{aligned} I_1 &= Q_{xx}+Q_{yy}+2Q_{xy} = Q_{11}+Q_{22}+2Q_{12} = 2(U_1+U_4) \\ I_2 &= Q_{xx}+Q_{yy}+2Q_{ss} = Q_{11}+Q_{22}+2Q_{66} = 2(U_1+U_5) = \text{"trace" } [Q] \\ J_2 &= \text{"trace" } [S] = S_{xx}+S_{yy}+\frac{S_{ss}}{2} = S_{11}+S_{22}+\frac{S_{66}}{2} \end{aligned} \tag{3.9}$$

These linear combinations are invariant, and are shown in the figures below as the ply angle varies. While the components of [Q] and [S] change with ply angles, their sums remain constant.

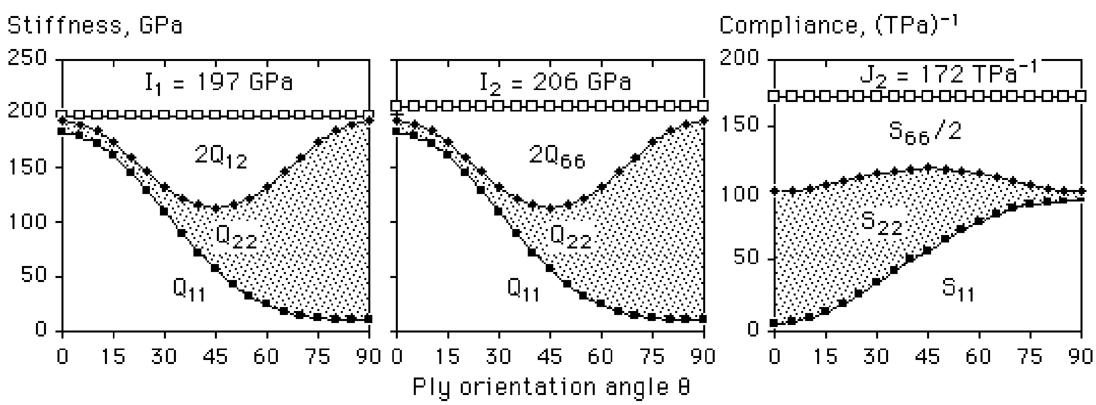

FIGURE 3.15 INVARIANTS OF STIFFNESS AND COMPLIANCE MATRICES OF A T300/5208

We will show later that the same combinations are invariant, and carry into the in-plane and flexural stiffnesses of laminates. When a ply material is selected, the invariants impose limits on the total stiffness potential of the multidirectional laminate made from this ply regardless of whether the loading is in-plane or flexural. To fully utilize directionality of composite materials, the increase in stiffness in one direction is at the expense of that in some other direction. This is an important concept in the design optimization of composite laminates. Also important for design is that the number of independent variables of a ply material is limited to two. Once two of the stiffness components are chosen, the remaining components are governed by the two invariants.

3.5 MATRIX INVERSION AND ENGINEERING CONSTANTS

The relation between the stiffness and compliance matrices is defined by a matrix inversion, shown in the equation below. There is nothing unique about this inversion except that all components of a matrix participate in the inversion process. It is not the reciprocal of each component by component. While we may have a good estimate of the stiffness matrix components as we vary the design parameters of a unidirectional ply, we cannot anticipate their impact on the compliance components before the inversion process is completed. To guess the result of an inversion by intuition is a dangerous business. That is why we emphasize calculation as the only reliable method.

$$\left.\begin{array}{ll} [S] = [Q]^{-1}, & |Q| = (Q_{11}Q_{22}-Q_{12}{}^2)Q_{66}+2Q_{12}Q_{26}Q_{16}-Q_{11}Q_{26}{}^2-Q_{22}Q_{16}{}^2 \\ S_{11} = (Q_{22}Q_{66}-Q_{26}{}^2)/|Q|, & S_{22} = (Q_{11}Q_{66}-Q_{16}{}^2)/|Q| \\ S_{12} = (-Q_{12}Q_{66}+Q_{16}Q_{26})/|Q|, & S_{66} = (Q_{11}Q_{22}-Q_{12}{}^2)/|Q| \\ S_{16} = (Q_{12}Q_{26}-Q_{22}Q_{16})/|Q|, & S_{26} = (Q_{12}Q_{16}-Q_{11}Q_{26})/|Q| \end{array}\right] \tag{3.10}$$

Engineering constants are defined from the compliance components listed in the equation below. These constants are either the reciprocals or ratios of compliance components, where guessing will be doubly hopeless. We have also listed the reciprocal relations of the coupling coefficients in the last line of the set of equations below. These relations, also shown in Equation 2.20, establish the magnitudes of coupling.

$$\left.\begin{array}{l} E_1 = 1/S_{11}, \quad E_2 = 1/S_{22}, \quad E_6 = G_1 = G_{12} = 1/S_{66} \\ \nu_{21} = -S_{21}/S_{11}, \quad \nu_{12} = -S_{12}/S_{22} \\ \nu_{61} = S_{61}/S_{11}, \quad \nu_{16} = S_{16}/S_{66}, \quad \nu_{62} = S_{62}/S_{22}, \quad \nu_{26} = S_{26}/S_{66} \\ \nu_{21}/\nu_{12} = S_{22}/S_{11} = E_1/E_2, \; \nu_{61}/\nu_{16} = S_{66}/S_{11} = E_1/E_6 = E_1/G_1 = E_1/G_{12} \end{array}\right] \tag{3.11}$$

The coupling constants are derived by using the same normalizing factor for each column of the compliance matrix. As explained in Section 2, we prefer this normalization by columns. Note that other authors may use the normalization by rows, which will lead to the following relations:

$$\nu_{12} = -S_{12}/S_{22}, \; \nu_{21} = -S_{21}/S_{11}, \quad \nu_{12}/\nu_{21} = S_{22}/S_{11} = E_1/E_2 \tag{3.12}$$

Although this system is popular, it is not rational; i.e., it is not consistent with the usual convention of the columns and the rows of a matrix.

In the figure below we show the difference between the stiffness components and the corresponding engineering constants between 0 and 45 degree ply orientation for T300/5208. When a ply angle is 0 or 90, there is practically no difference between them. However substantial difference between the two exist between 0 and 90 degree ply angles as a result of the matrix inversion of an off-axis orthotropic ply. Thus care must be exercised to distinguish the plane stress stiffness **[Q]**, and engineering constants.

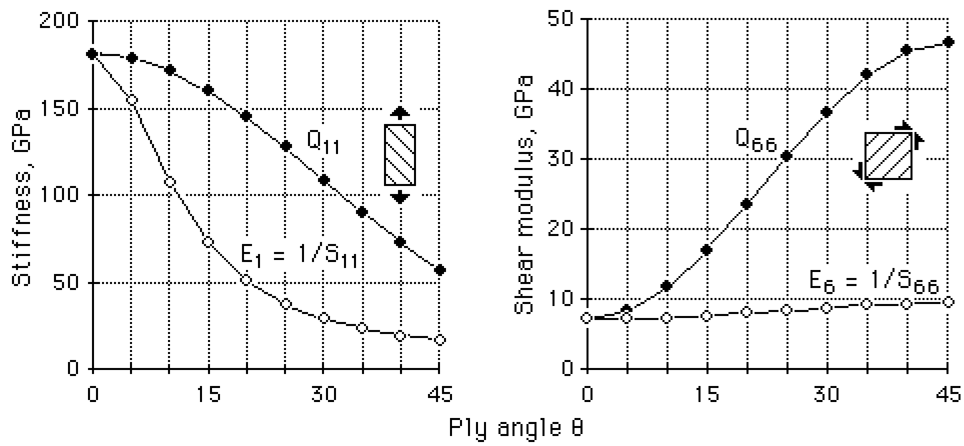

FIGURE 3.16 STIFFNESS COMPONENTS VS ENGINEERING CONSTANTS

3.6 ELASTIC CONSTANTS OF TYPICAL COMPOSITE PLIES

In Table 3.2 below, a variety of composite materials are listed. The first eight ply materials are unidirectional, the last two are fabric. These elastic constants are average values gathered from different sources. The data in the last three columns are statistically based; i.e., the B-allowable data (95 percent confidence interval having the minimum value for 90 percent of the population.)

TABLE 3.2 ELASTIC PROPERTIES OF VARIOUS COMPOSITE MATERIALS IN SI

Type	CFRP	BFRP	CFRP	GFRP	KFRP	CFRTP	CFRP	CFRP	CCRP	CCRP
Fiber/cloth	T300	B(4)	AS	E-glass	Kev 49	AS 4	IM6	T300	T300	T300
Matrix	N5208	N5505	H3501	epoxy	epoxy	PEEK	epoxy	Fbrt 934	Fbrt 934	Fbrt 934
Ply eng'g constants	and data					APC2		4-mil tp	13-mil c	7-mil c
Ex,GPa	181.0	204.0	138.0	38.6	76.0	134.0	203.0	148.0	74.0	66.0
Ey,GPa	10.30	18.50	8.96	8.27	5.50	8.90	11.20	9.65	74.00	66.00
nu/x	0.28	0.23	0.30	0.26	0.34	0.28	0.32	0.30	0.05	0.04
Es,GPa	7.17	5.59	7.10	4.14	2.30	5.10	8.40	4.55	4.55	4.10
v/f	0.70	0.50	0.66	0.45	0.60	0.66	0.66	0.60	0.60	0.60
Sp Gravity	1.60	2.00	1.60	1.80	1.46	1.60	1.60	1.50	1.50	1.50
ho,mm	0.125	0.125	0.125	0.125	0.125	0.125	0.125	0.100	0.325	0.175
[Q]^0,GPa										
Qxx	181.8	205.0	138.8	39.2	76.6	134.7	204.2	148.9	74.2	66.1
Qyy	10.35	18.59	9.01	8.39	5.55	8.95	11.26	9.71	74.19	66.13
Qxy	2.90	4.28	2.70	2.18	1.89	2.51	3.60	2.91	3.71	2.91
Qss	7.17	5.59	7.10	4.14	2.30	5.10	8.40	4.55	4.55	4.10
[S]^0,1/TPa										
Sxx	5.5	4.9	7.2	25.9	13.2	7.5	4.9	6.8	13.5	15.2
Syy	97.1	54.1	111.6	120.9	181.8	112.4	89.3	103.6	13.5	15.2
Sxy	-1.5	-1.1	-2.2	-6.7	-4.5	-2.1	-1.6	-2.0	-0.7	-0.7
Sss	139.5	178.9	140.8	241.5	434.8	196.1	119.0	219.8	219.8	243.

Transverse stiffnesses of composite plies having organic matrix materials average about 10 GPa , about three times the Young's modulus of the pure matrix. This is shown in Figure 3.17.

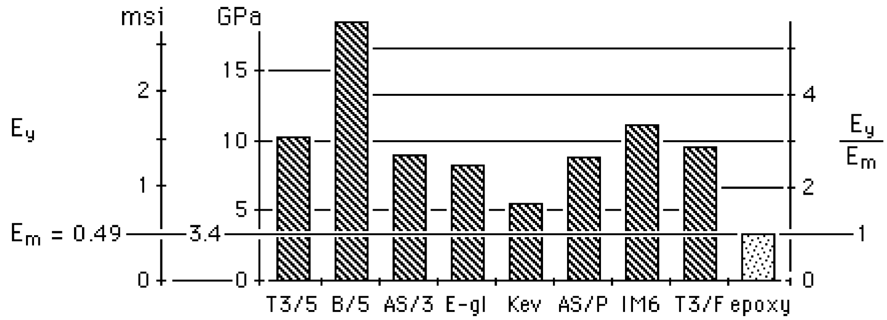

FIGURE 3.17 TRANSVERSE STIFFNESS OF VARIOUS EPOXY-BASED COMPOSITE PLIES

A common practice to equate transverse stiffness to that of pure matrix is not correct. The presence of fibers increases the stiffness by 300 percent. The resin is under complex stresses, and there is an interfacial bond of unknown nature. There cannot be a simple link between the resin and the transverse modulus of the ply. The contribution of fibers to the transverse stiffness is not insignificant as evidenced by a factor of 3 between the lowest from Kevlar fibers, and the highest from boron fibers.

Another unknown factor is the anisotropy of carbon and kevlar fibers. It is often assumed that the transverse stiffness of the fiber is lower than the longitudinal stiffness. We are not aware of any direct measurement of the transverse fiber stiffness. From the measured stiffness of [90] ply, the transverse fiber stiffness may be inferred. In fact, we will use this assumption in formulating micromechanic models in Section 7 of this book.

Longitudinal or major Poisson's ratios for various composite materials are shown in Figure 3.18 where the average value is nearly 0.3. These are measured values. We do not have a simple explanation other than the fact that all isotropic materials have the same Poisson's ratio of 0.3. Anisotropic materials can apparently be included in the same range for Poisson's ratios.

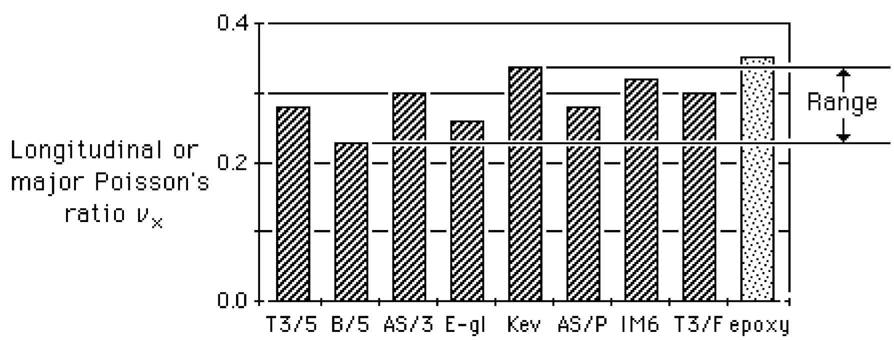

FIGURE 3.18 MAJOR POISSON'S RATIOS OF VARIOUS EPOXY-BASED COMPOSITE PLIES

The transverse or minor Poisson's ratio is small for various composite materials, and is difficult to measure experimentally. Usually we rely on the reciprocal relation to calculate the small value. These values are shown in Figure 3.19.

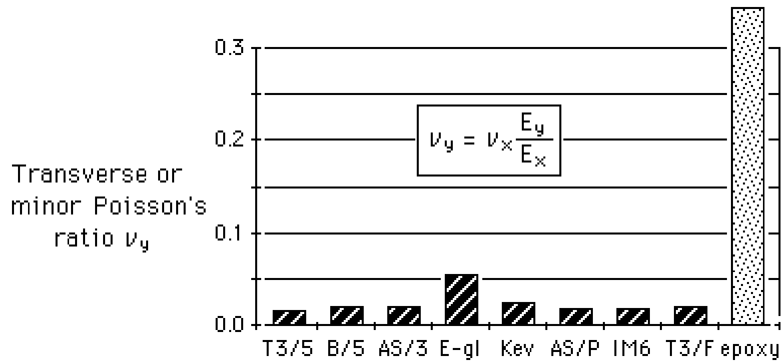

FIGURE 3.19 MINOR POISSON'S RATIOS OF VARIOUS EPOXY-BASED COMPOSITE PLIES

Finally, the relative magnitudes of the transverse and shear moduli of various composite plies are shown below, both in absolute and normalized values. Like isotropic materials, the transverse Young's modulus is higher than the longitudinal shear modulus for all composite materials listed in the table above.

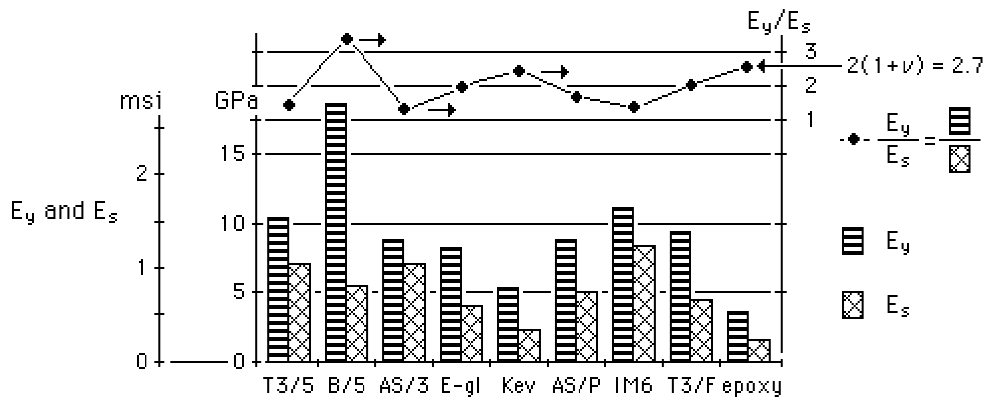

FIGURE 3.20 ABSOLUTE VALUES AND RATIOS OF TRANSVERSE STIFFNESS AND SHEAR MODULI OF VARIOUS EPOXY-BASED COMPOSITE PLIES

The purpose of singling out the moduli in the last three figures is to provide a basis for estimating the stiffness properties of new organic-matrix composite materials. Of the four principal elastic constants of a unidirectional ply, we would use rule of mixtures for the longitudinal stiffness, and use the average values of the last three figures for the remaining three constants:

- **Transverse modulus is three times the matrix modulus;**
- **Longitudinal Poisson's ratio is 0.3;**
- **Longitudinal shear modulus is one half of the transverse modulus.**

3.7 QUASI-ISOTROPIC CONSTANTS

As we have seen, associated with every anisotropic material are the invariants of coordinate transformation, from which quasi-isotropic constants can be derived. This is shown in Equation 3.13 below. These constants represent the lower bound performance of each composite. They are used as a guide in design to insure that, whatever ply angle orientations we may select for a given load, the laminate performance is at least equal to, if not better than, the quasi-isotropic laminate. These constants are invariant, and are better design parameters than the changing components of a stiffness matrix.

$$[Q]^{iso} = \begin{bmatrix} U_1 & U_4 & 0 \\ U_4 & U_1 & 0 \\ 0 & 0 & U_5 \end{bmatrix}, \quad [S]^{iso} = \begin{bmatrix} \frac{U_1}{D} & -\frac{U_4}{D} & 0 \\ -\frac{U_4}{D} & \frac{U_1}{D} & 0 \\ 0 & 0 & \frac{1}{U_5} \end{bmatrix}, \quad \left[\begin{array}{l} D = U_1^2 - U_4^2 \\ \nu^{iso} = \frac{U_4}{U_1}, \; G^{iso} = U_5 \\ E^{iso} = \frac{D}{U_1} \end{array} \right] \tag{3.13}$$

The quasi-isotropic constants can be used for a direct comparison with the conventional isotropic materials. Equally important is that many finite element programs are limited to isotropic materials. The use of quasi-isotropic constants of isotropic materials will provide the most conservative design.

TABLE 3.3 INVARIANTS AND QUASI-ISOTROPIC CONSTANTS OF VARIOUS COMPOSITE MATERIALS IN SI

Type	CFRP	BFRP	CFRP	GFRP	KFRP	CFRTP	CFRP	CFRP	CCRP	CCRP
Fiber/cloth	T300	B(4)	AS	E-glass	Kev 49	AS 4	IM6	T300	T300	T300
Matrix	N5208	N5505	H3501	epoxy	epoxy	PEEK	epoxy	Fbrt 934	Fbrt 934	Fbrt 934
						APC2		4-mil tp	13-mil c	7-mil c
Linear combinations of [Q],GPa										
U1*	76.37	87.70	59.66	20.45	32.44	57.04	85.88	62.47	58.84	52.37
U2	85.73	93.20	64.90	15.39	35.55	62.88	96.44	69.58	0.00	0.00
U3	19.71	24.08	14.25	3.33	8.65	14.78	21.83	16.82	15.34	13.75
U4*	22.61	28.36	16.96	5.51	10.54	17.28	25.43	19.73	19.05	16.66
U5*	26.88	29.67	21.35	7.47	10.95	19.88	30.23	21.37	19.89	17.85
* invariant										
Quasi-isotropic constants										
E,GPa	69.68	78.53	54.84	18.96	29.02	51.81	78.35	56.24	52.67	47.07
nu	0.30	0.32	0.28	0.27	0.32	0.30	0.30	0.32	0.32	0.32
G,GPa	26.88	29.67	21.35	7.47	10.95	19.88	30.23	21.37	19.89	17.8

The quasi-isotropic Young's modulus for various composite materials is shown in the figure below. These values are the lower bound or minimum performance that can be expected from composite materials, on an absolute and specific basis. These comparisons are ultra conservative, but form better bases than using the often accepted longitudinal stiffness. The latter basis is optimistic for any load other than uniaxial tension.

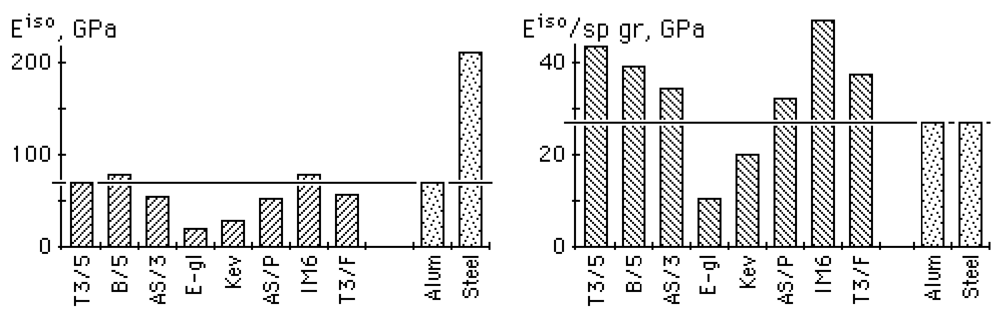

FIGURE 3.21 ABSOLUTE AND SPECIFIC QUASI-ISOTROPIC YOUNG'S MODULUS OF VARIOUS COMPOSITE MATERIALS AS COMPARED WITH ALUMINUM AND STEEL.

In the following figure we show the range of Young's modulus for various composite materials. The lower bound value is the quasi-isotropic Young's modulus; the upper bound, the longitudinal stiffness. As the directionality increases, the efficiency of composite materials should also increase. The advantage of composite materials is shown by the superior specific stiffness over both aluminum and steel by many factors. Learning to use directionality is a key step in composites design.

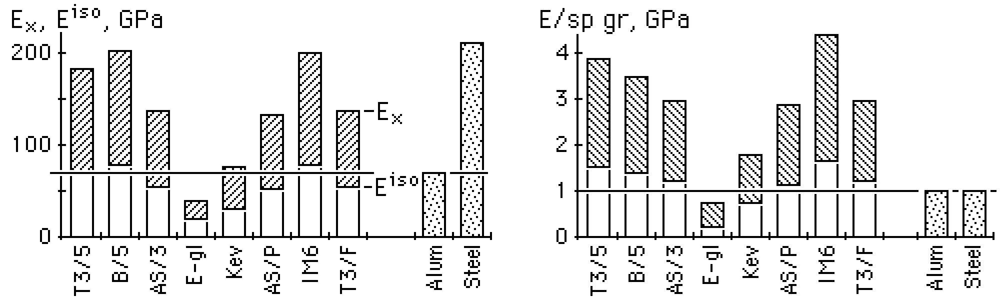

FIGURE 3.22 ABSOLUTE AND SPECIFIC QUASI-ISOTROPIC YOUNG'S MODULUS AND LONGITUDINAL STIFFNESS OF VARIOUS COMPOSITE MATERIALS COMPARED WITH ALUMINUM AND STEEL.

3.8 SAMPLE CALCULATIONS OF PLY ELASTIC CONSTANTS

As in the sample problems for plane stress in Section 2, we will use the same basic data for CFRP T300/5208 to calculate the off-axis stiffness of a [45] ply using two methods:

$$
\left.\begin{aligned}
&[Q] = \begin{bmatrix} 181.81 & 2.90 & 0 \\ 2.90 & 10.34 & 0 \\ 0 & 0 & 7.17 \end{bmatrix} \\
&\theta = 45°,\ m = n = 0.707,\ \bar{Q}_{11} = \frac{1}{4}(181.81+10.34+2\mathrm{x}2.90+4\mathrm{x}7.17) = 56.66 \text{ GPa} \\
&\qquad\qquad\qquad\qquad\qquad \bar{Q}_{26} = \frac{1}{4}(181.81-10.34) = 42.87 \text{ GPa}
\end{aligned}\right] \quad (3.14)
$$

For multiple-angle transformation listed in Table 3.1 and Figure 3.12, on pages 3-7 and 3-8 respectively, we first calculate the linear combinations of the plane stress stiffness, such as the U's, before we apply the transformation equations:

$$
\left.\begin{aligned}
&U_1 = \frac{3Q_{xx}+3Q_{yy}+2Q_{xy}+4Q_{ss}}{8} = \frac{3\mathrm{x}181.81+3\mathrm{x}10.34+2\mathrm{x}2.90+4\mathrm{x}7.17}{8} = 76.37 \text{ GPa} \\
&U_2 = \frac{181.81-10.34}{2} = 85.73 \text{ GPa},\ U_3 = 19.71,\ U_4 = 22.61,\ U_5 = 26.88 \text{ GPa} \\
&\text{When } \theta = 45\text{: } Q_{11} = U_1+U_2\cos 2\theta+U_3\cos 4\theta = 76.37+85.73\mathrm{x}0+19.71\mathrm{x}(-1) = 56.66 \text{ GPa} \\
&\qquad\qquad Q_{26} = \frac{U_2}{2}\sin 2\theta-U_3\sin 4\theta = 85.73/2-19.71\mathrm{x}0 = 42.87 \text{ GPa} = Q_{16} \\
&\qquad\qquad Q_{12} = 42.32 \text{ GPa},\ Q_{66} = 46.59 \text{ GPa}
\end{aligned}\right] \quad (3.15)
$$

We can calculate the quasi-isotropic constants which establish the minimum stiffness potential of anisotropic and orthotropic materials using Equation 3.13:

$$
\left.\begin{aligned}
&\nu^{iso} = \frac{U_4}{U_1} = \frac{22.61}{76.37} = 0.30,\ G^{iso} = U_5 = 26.88 \text{ GPa}, \\
&E^{iso} = U_1[1-(\nu^{iso})^2] = 76.37(1-0.30^2) = 69.68 \text{ GPa} \\
&[Q]^{iso} = \begin{bmatrix} 76.37 & 22.61 & 0 \\ 22.61 & 76.37 & 0 \\ 0 & 0 & 26.88 \end{bmatrix} \text{GPa},\ [S]^{iso} = \begin{bmatrix} 14.35 & -4.30 & 0 \\ -4.30 & 14.35 & 0 \\ 0 & 0 & 37.20 \end{bmatrix} \text{TPa}^{-1}
\end{aligned}\right] \quad (3.16)
$$

If we wish to calculate the compliance of the 45-degree T300/5208, we can invert the stiffness matrix in accordance with the formulas in Sub-Section 3.5 on page 3-10:

$$|Q| = (Q_{11}Q_{22}-Q_{12}^2)Q_{66}+2Q_{12}Q_{26}Q_{16}-Q_{11}Q_{26}^2-Q_{22}Q_{16}^2$$

$$= (56.66^2-42.32^2)\times 46.59+2\times(42.32-26.66)\times 42.87^2 = 1.3427\times 10^{30}(\text{Pa})^3$$

$$S_{11} = (Q_{22}Q_{66}-Q_{26}^2)/|Q| = (56.66\times 46.59-42.87^2)/|Q| = 59.75\ \text{TPa}^{-1} = S_{22}$$

$$S_{12} = (-Q_{12}Q_{66}+Q_{16}Q_{26})/|Q| = (-42.32\times 46.59+42.87^2)/|Q| = -9.99\ \text{TPa}^{-1}$$

$$S_{66} = (Q_{11}Q_{22}-Q_{12}^2)/|Q| = (56.66^2-42.32^2)/|Q| = 105.71\ \text{TPa}^{-1}$$

$$S_{16} = (Q_{12}Q_{26}-Q_{22}Q_{16})/|Q| = (42.32-56.66)\times 42.87/|Q| = -45.78\ \text{TPa}^{-1} = S_{26}$$

$$E_1 = 1/S_{11} = 1/59.75 = 16.74\ \text{GPa} = E_2,\ E_6 = 1/S_{66} = 1/105.71 = 9.46\ \text{GPa}$$

$$\nu_{21} = -S_{21}/S_{11} = 9.99/59.75 = 0.17 = \nu_{12}$$

$$\nu_{61} = S_{61}/S_{11} = -45.78/59.75 = -0.77 = \nu_{62}$$

$$\nu_{16} = S_{61}/S_{66} = -45.78/105.71 = -0.43 = \nu_{26}$$

$$[Q]^{(45)} = \begin{bmatrix} 56.66 & 42.32 & 42.87 \\ 42.32 & 56.66 & 42.87 \\ 42.87 & 42.87 & 46.59 \end{bmatrix} \text{GPa},\quad [S]^{(45)} = \begin{bmatrix} 59.75 & -9.99 & -45.78 \\ -9.99 & 59.75 & -45.78 \\ -45.78 & -45.78 & 105.71 \end{bmatrix} \text{TPa}^{-1} \tag{3.17}$$

The importance of the sample problems above is the numerous sets of constants that can represent the elasticity of a composite material. The relations among these sets are fixed and must be followed without deviation. There are no short cuts. We emphasize the stiffness components because in laminated plate theory, we take the average of the plane stress stiffness components rather than that of the corresponding compliance components. Plies are stacked together so they act as a unit. The laminate strain is assumed constant. That is why the laminate stiffness is composed of the ply stiffnesses. Stress is discontinuous and varies from ply to ply as the ply angle changes.

3.9 THE TRANSFORMED STIFFNESS OF TYPICAL COMPOSITES

We list in the table below the elastic moduli of a ply oriented at 45 degrees. The equality between the "11" and "22," and "16" and "26" are noted. By symmetry "1" and "2" are interchangeable.

TABLE 3.4 TRANSFORMED ELASTIC MODULI OF 45-DEGREE PLY ORIENTATION

Type	CFRP	BFRP	CFRP	GFRP	KFRP	CFRTP	CFRP	CFRP	CCRP	CCRP
Fiber/cloth	T300	B(4)	AS	E-glass	Kev 49	AS 4	IM6	T300	T300	T300
Matrix	N5208	N5505	H3501	epoxy	epoxy	PEEK	epoxy	Fbrt 934	Fbrt 934	Fbrt 934
[Q']^45,GPa						APC2		4-mil tp	13-mil c	7-mil c
11=22	56.66	63.62	45.41	17.12	23.79	42.26	64.06	45.65	43.50	38.62
12	42.32	52.44	31.21	8.84	19.19	32.06	47.26	36.55	34.40	30.42
66	46.59	53.76	35.60	10.80	19.60	34.66	52.05	38.19	35.24	31.61
16=26	42.87	46.60	32.45	7.69	17.77	31.44	48.22	34.79	0.00	0.00
[S']^45,1/TPa										
11=22	59.7	58.9	63.8	93.7	155.2	77.9	52.5	81.5	61.4	68.2
12	-10.0	-30.5	-6.6	-27.0	-62.2	-20.1	-7.0	-28.4	-48.5	-53.7
66	105.7	61.2	123.2	160.3	203.9	124.0	97.4	114.4	28.4	31.6
16=26	-45.8	-24.6	-52.2	-47.5	-84.3	-52.4	-42.2	-48.4	0.0	0.0
Eng'g constants at 45 degree										
E1=E2,GPa	16.74	16.98	15.66	10.67	6.44	12.83	19.04	12.27	16.30	14.6
E6,GPa	9.46	16.34	8.12	6.24	4.90	8.06	10.27	8.74	35.24	31.6
nu/21	0.17	0.52	0.10	0.29	0.40	0.26	0.13	0.35	0.79	0.79
nu/61	-0.77	-0.42	-0.82	-0.51	-0.54	-0.67	-0.80	-0.59	0.00	0.
nu/62	-0.43	-0.40	-0.42	-0.30	-0.41	-0.42	-0.43	-0.42	0.00	0.

In the following two figures we show the transformation of the "11" and "16" stiffness components of typical composites. The more pronounced the anisotropy, the greater the difference is between the two principal on-axis Young's moduli. The shear coupling component is also greater for a more highly anisotropic material. Boron/epoxy composite material shows the largest value for both the "11" and "16" components.

Aluminum is isotropic, and is therefore a horizontal line in this figure. The "11" components are even functions, having maximum values at the 0-degree axis, and minimum at 90-degree axis.

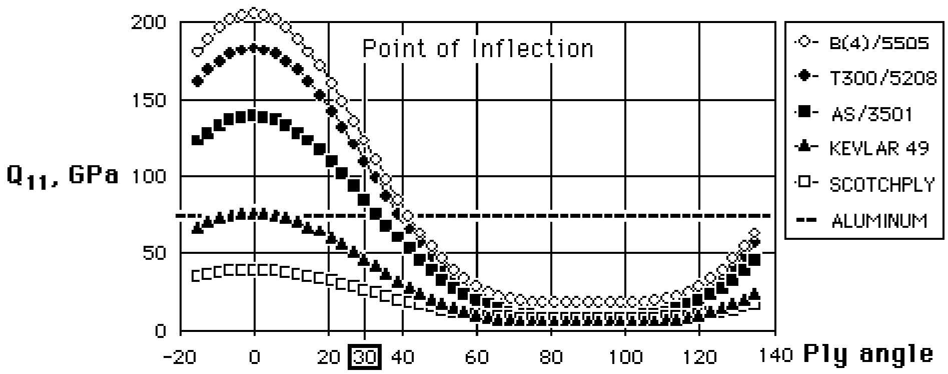

FIGURE 3.23 THE "11" STIFFNESS COMPONENT FOR VARIOUS COMPOSITES AND ALUMINUM . MAX AND MIN ARE REACHED AT 90 DEGREE INTERVALS. SHOWN ALSO IS THE POINT OF INFLECTION NEAR 30 DEGREE.

The "66" components are also even functions but is dominated by four times the ply angle. A maximum is reached at 45 degree precisely, and minimum at 0 and 90 degrees. Aluminum is isotropic and appears as a horizontal line.

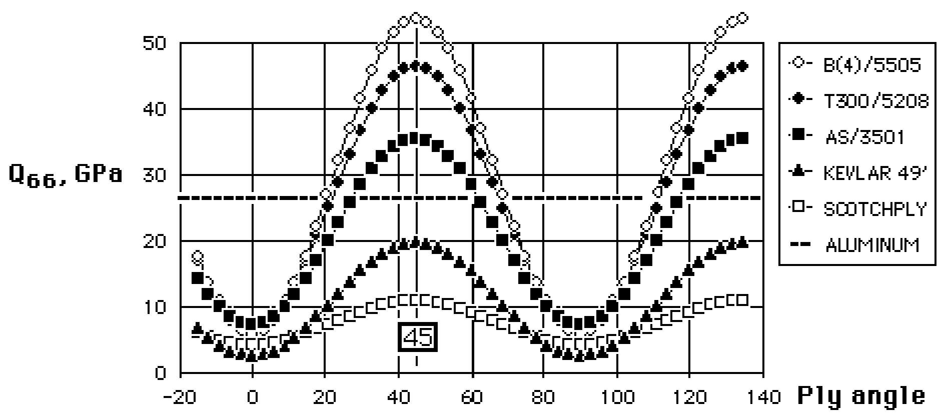

FIGURE 3.24 THE "66" STIFFNESS COMPONENT FOR VARIOUS COMPOSITES AND ALUMINUM. MAX AND MIN ARE REACHED AT INTERVALS OF 45 DEGREES.

The "16" and "26" are odd functions because the transformation relations have sine functions. This is unique with anisotropic materials. This coupling coefficient is zero for isotropic materials. The maximum is reached near 30 degrees as cited in Figure 3.5 earlier. Being odd, the value can be positive and negative depending on the ply angle.

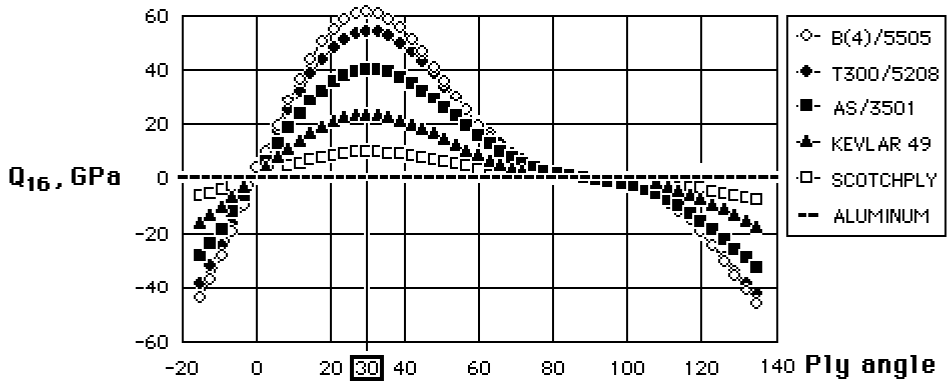

FIGURE 3.25 THE "16" STIFFNESS COMPONENT FOR VARIOUS COMPOSITES AND ALUMINUM . MAXIMUM IS REACHED AT 30 DEGREES.

The multiple angle formulation for the transformation relation has another useful feature. Differentiation and integration of the sine and cosine functions of multiple angles are simpler than powers of the same functions. The maxima, minima, and point of inflection of a transformed stiffness component are easily found by differentiating the functions of multiple angle like those in Figure 3.12 on page 3-8. By differentiating the "11" and "22" stiffness components, the resulting slopes are equal to the corresponding shear coupling components, as shown in the following equations:

$$\frac{\partial Q_{11}}{\partial \theta} = -2U_2\sin 2\theta - 4U_3\sin 4\theta = -4Q_{16},\ \frac{\partial Q_{22}}{\partial \theta} = 2U_2\sin 2\theta - 4U_3\sin 4\theta = 4Q_{26}$$

$$\text{Let: } \frac{\partial^2 Q_{11}}{\partial \theta^2} = \frac{\partial Q_{16}}{\partial \theta} = 0, \text{ we find point of inflection for } Q_{11}, \text{ and max } Q_{16} \tag{3.18}$$

When the second derivatives of the "11" stiffness component above are equal to zero, we can solve for the ply angle. At this angle, the normal component is a point of inflection, and the shear coupling "16" component reaches a maximum value. For T300/5208, the ply angle is approximately 30 degrees for the "11" stiffness components. In fact, this angle holds for all the other composites shown in Figures 3.23 and 3.25.

In the figure below we show the transformed stiffness constants of T300/5208. In the left graph, we compare the plane stress stiffness with the engineering constant. Note that the two have essentially identical values at 0 and 90 degrees, but differ significantly in intermediate angles. Also shown in this figure is the corresponding invariant which is the average value of the transformed "11" component. In the right graph, the shear moduli are compared. Again, the shear moduli at 0 and 90 are the same, but differ significantly in the intervening angles. The areas under the "66" shear component are equal to the corresponding shear invariant.

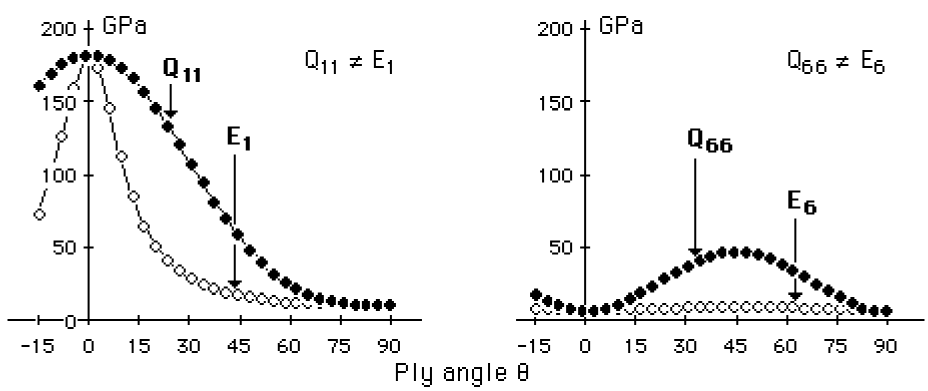

FIGURE 3.26 STIFFNESS CONSTANTS AS FUNCTIONS OF PLY ANGLE

We also show the Poisson and shear coupling coefficients in the next figure, respectively. For isotropic material, the shear coupling coefficient is identically zero. Note that the shear coupling is odd; i.e., anti-symmetric.

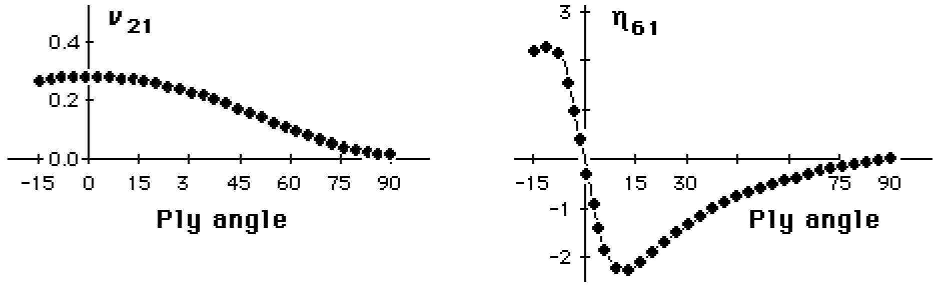

FIGURE 3.27 MAJOR POISSON'S RATIO AND SHEAR COUPLING COEFFICIENT AS FUNCTIONS OF PLY ANGLE

Another graphical representation of material anisotropy can be shown in polar plots of the "11" and "66" stiffness components, shown in Figure 3.28 below for T300/5208, and Figure 3.29 for E-glass/epoxy.

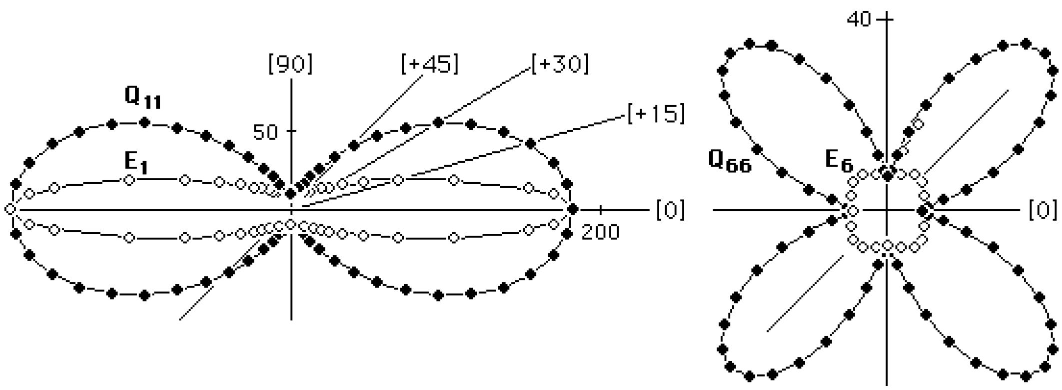

FIGURE 3.28 POLAR PLOT OF THE "11" AND "66" STIFFNESS COMPONENTS OF T300/5208

The "11" component has two lobes because it repeats itself every 180 degrees, or is a cosine function of doubled and quadrupled angles of ply orientation. The "66" component has four lobes because it repeats itself every 90 degrees, or is a cosine function of quadrupled angles of ply orientation. The multiple angle transformation relations in Equation 3.12 on page 3-8 show these functional relationships.

Analogous polar plots for E-glass/epoxy are shown in Figure 2.29 below.

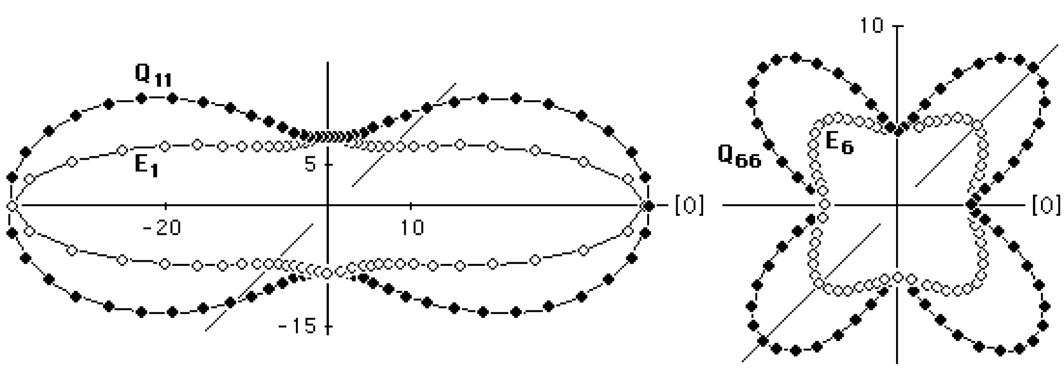

FIGURE 3.29 POLAR PLOT OF THE "11" AND "66" STIFFNESS COMPONENTS OF E-GLASS/EPOXY

The polar plots also show the difference between the stiffness components and the corresponding engineering constants. It should be pointed out that the scales of the last two figures are quite different.

The shear coupling coefficients can be used effectively in design that is unique to composite materials. The coupling behavior is shown in Equation 3.22 for simple load cases. Shear strain is induced by uniaxial stress; normal strain is induced by shear stress. Thus, under combined stresses, the induced strains can be entirely different from those in isotropic materials.

$$\text{Uniaxial tension: } \epsilon_1 = S_{11}\sigma_1,\ \epsilon_2 = S_{21}\sigma_2,\ \boldsymbol{\epsilon_6 = S_{61}\sigma_1 = \nu_{61}\epsilon_1}$$

$$\text{Pure shear: } \epsilon_6 = S_{66}\sigma_6,\ \epsilon_2 = S_{26}\sigma_6 = \nu_{26}\sigma_6,\ \boldsymbol{\epsilon_1 = S_{16}\sigma_6 = \nu_{16}\epsilon_6} \qquad (3.19)$$

In the figure below we show the value of the shear coupling coefficients for various composite materials. For positive 45 degree ply orientation the shear coupling is negative for all the composite materials listed.

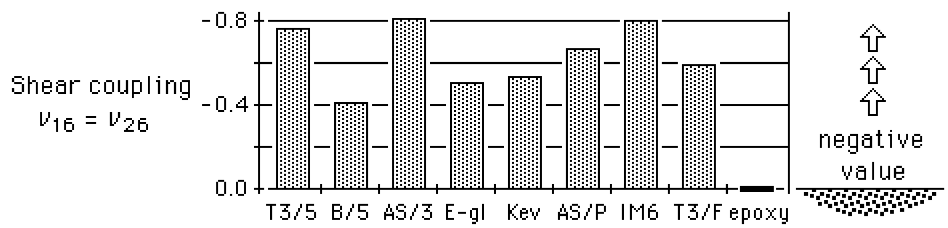

FIGURE 3.30 SHEAR COUPLING COEFFICIENTS OF [45] FOR VARIOUS COMPOSITE MATERIALS

Thus, under a uniaxial tensile stress, the induced shear strain would be negative; i.e., the shear diagonal would traverse between the second and the fourth quadrants. If the applied stress is uniaxial compression, the induced shear will be positive. If the ply angle is changed from [45] to [-45], the shear induced under uniaxial tension will be positive. No guessing should be necessary. If the sign conventions are followed faithfully, the resulting shear strain is easy to determine. Needless to say, shear is more difficult to determine than normal strains. For isotropic materials, the sign of shear strain is not important because material response is not sensitive to the sign. For composite materials, however, signs can be critical. That is why discipline, rather than guessing, is essential.

3.10 CONCLUSIONS

The key elastic properties of composite materials have been presented and discussed. The invariants are important because they define the limits of the elastic capability of a composite material. The transformed properties are exact and require no additional approximations beyond the basic assumptions of the mechanics of solids. The unidirectional plies are significantly different from isotropic materials. It is not accurate to compare the longitudinal Young's modulus with the Young's modulus of isotropic materials directly. The invariants should be used to represent composite materials. The shear coupling capability is unique to composite materials, and can be used as a design parameter in elastic tailoring. From the ply stiffness properties we can now examine the laminate properties.

3.11 PROBLEMS

Prob. 3.1 Derive the bulk modulus of various unidirectional composite material plies.

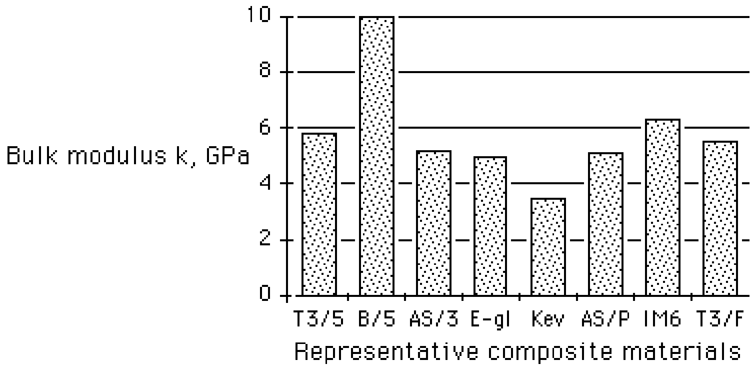

Prob. 3.2 Fill in appropriate transformation and stress-strain relations:

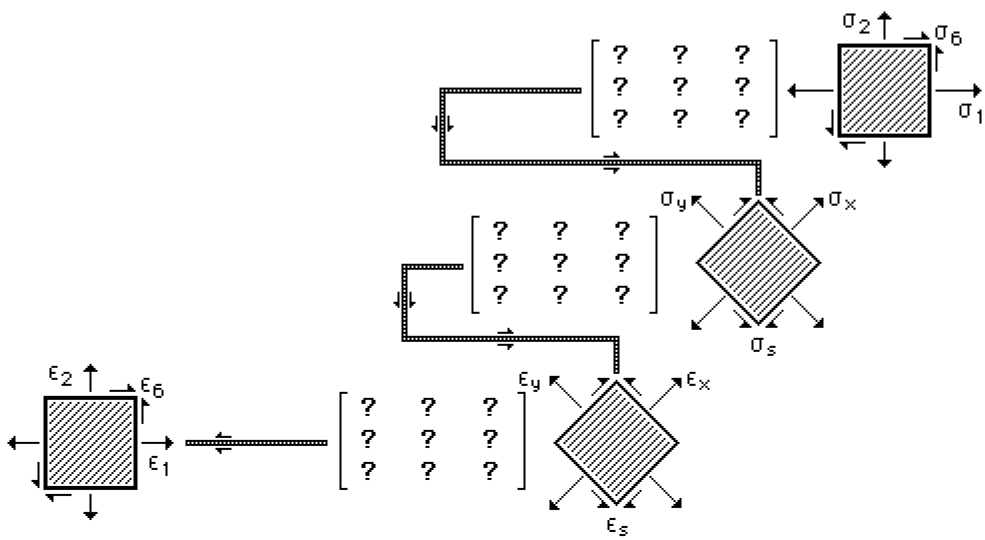

Prob. 3.3 Express on-axis stress in terms of off-axis strain.

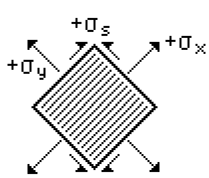

$$\begin{Bmatrix} \sigma_x \\ \sigma_y \\ \sigma_s \end{Bmatrix} = \begin{bmatrix} ? & ? & ? \\ ? & ? & ? \\ ? & ? & ? \end{bmatrix} \begin{Bmatrix} \epsilon_1 \\ \epsilon_2 \\ \epsilon_6 \end{Bmatrix}$$

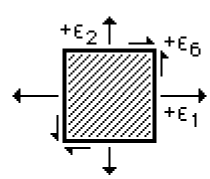

Prob. 3.4 Express on-axis strain in terms of off-axis stress.

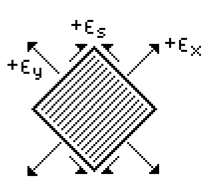

$$\begin{Bmatrix} \epsilon_x \\ \epsilon_y \\ \epsilon_s \end{Bmatrix} = \begin{bmatrix} ? & ? & ? \\ ? & ? & ? \\ ? & ? & ? \end{bmatrix} \begin{Bmatrix} \sigma_1 \\ \sigma_2 \\ \sigma_6 \end{Bmatrix}$$

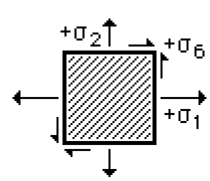

Prob. 3.5 Determine the absolute value and the ply orientation when shear coupling is maximum:

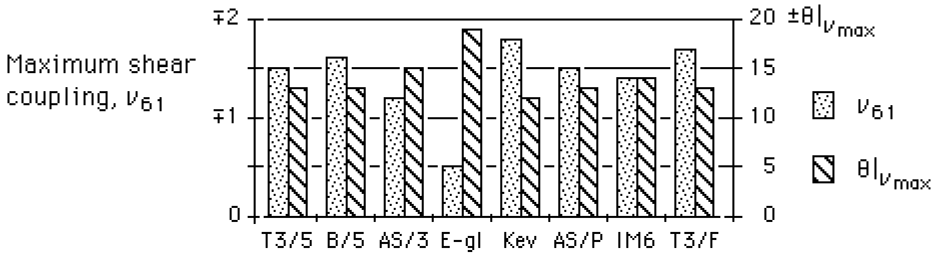

Prob. 3.6 How does a [45] deform under uniaxial tensile stress: A, B or C?

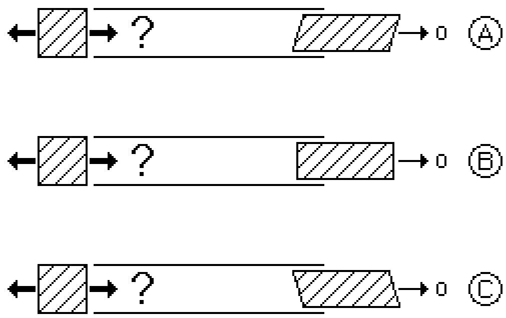

Prob. 3.7 If a positive torque is applied to a [45] tube, what will be the resulting length: A, B or C?

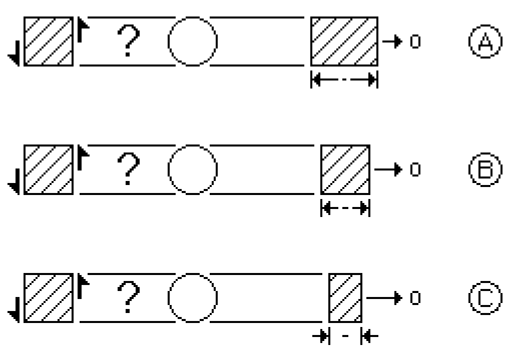

Prob. 3.8 Under a torque loading of [-45] and [+45] tubes connected by a butt join, what is the final shape: A, B or C?

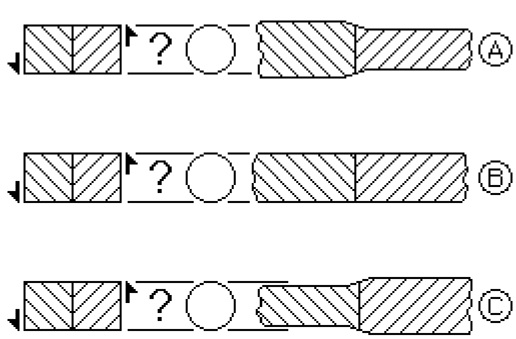

Prob. 3.9 **Under a tensile loading of [0] and [90] plate connected by a butt joint, what is the final shape: A, B or C?**

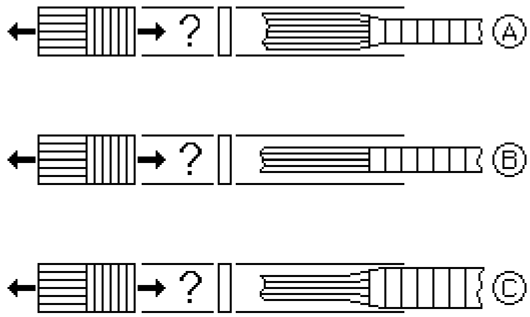

Prob. 3.10 **Identify the components of the stiffness matrix, and their relations for each of the polar plots of the stiffness below:**

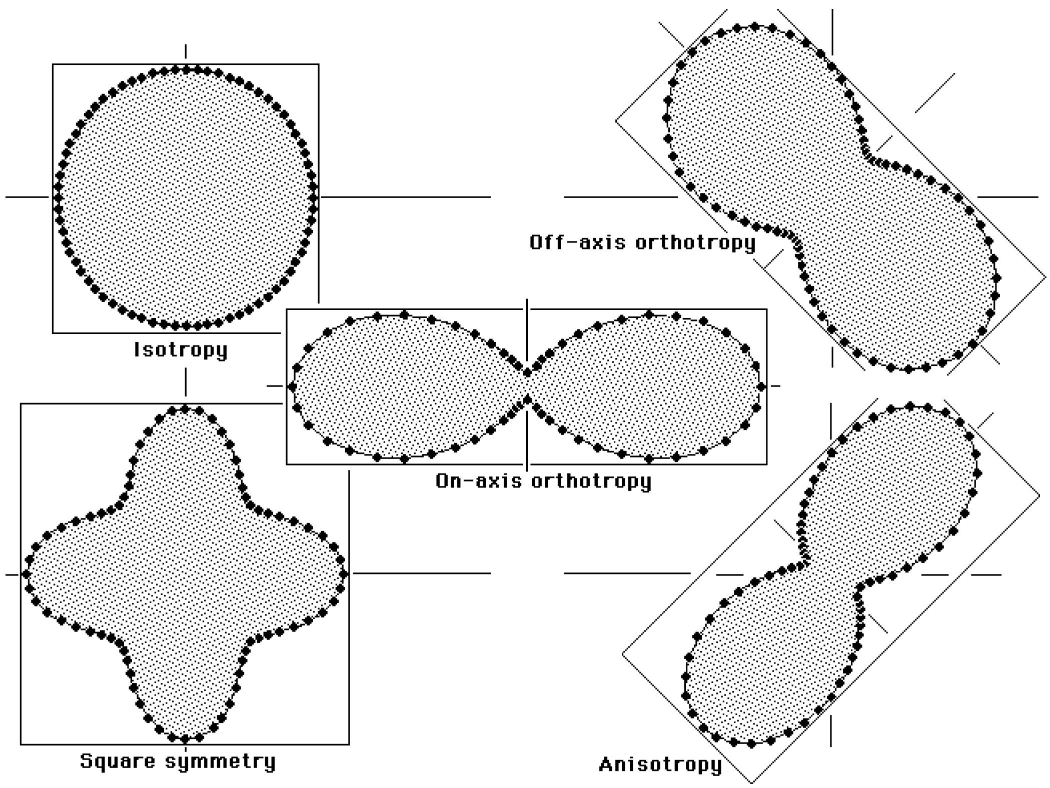

Prob. 3.11 **Identify the compliance components if the axis of transformation is about the 1-axis. These components are analogous to those in Figure 3.10, except the angle of rotation has changed from the 3- to 1-axis.**

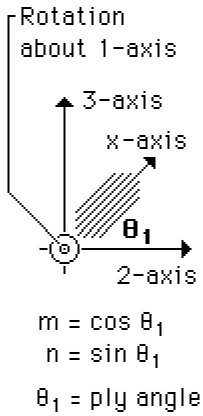

	S??	S??	S??	S??
S??	m^4	n^4	$2m^2n^2$	m^2n^2
S??	n^4	m^4	$2m^2n^2$	m^2n^2
S??	m^2n^2	m^2n^2	m^4+n^4	$-m^2n^2$
S??	$4m^2n^2$	$4m^2n^2$	$-8m^2n^2$	$(m^2-n^2)^2$
S??	$2m^3n$	$-2mn^3$	$2mn^3-2m^3n$	mn^3-m^3n
S??	$2mn^3$	$-2m^3n$	$2m^3n-2mn^3$	m^3n-mn^3

	S??	S??	S??	S??	S??
S??	m^2	n^2	0	0	0
S??	n^2	m^2	0	0	0
S??	mn	-mn	0	0	0
S??	0	0	m^2	n^2	0
S??	0	0	n^2	m^2	0
S??	0	0	-mn	mn	0
S??	0	0	0	0	1

Prob. 3.12 **Identify the power of transformation relations for a rotation about the 2-axis. The powers are analogous to those identified in Figure 3.11 except the rotation is about the 3-axis.**

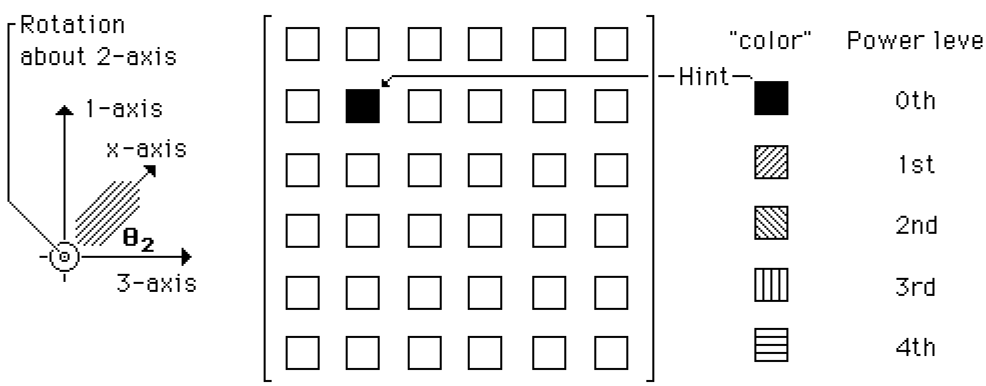

Prob. 3.13 **Find the angle or point of inflection in the transformed stiffness matrix in Figure 3.23 for all the composite materials listed in Table 3.4. Are the angles precisely or approximately invariant? As longitudinal stiffness goes to inifinity, show that this angle becomes 30 degree.**

Section 4

IN-PLANE STIFFNESS

A symmetric laminate subjected to in-plane loads is one of the simplest examples of a composite structure. The effective stiffnesses of the laminate are derived from the average plane-stress stiffness of unidirectional plies having multiple ply angles. The compliance matrix is the inverse of the stiffness matrix. Stresses and strains in each ply can be calculated from these effective constants and the applied laminate stresses or strains. Laminate stiffness in extension and shear have infinite combinations, which provide design options are not possible with isotropic materials. Hygrothermal expansion strains and resulting residual stresses are simple extensions of the in-plane effective stiffnesses.

4.1 LAMINATE CODE

Laminate code is needed for design and manufacturing, and it reflects the layup process. There is no standardized code that is universally accepted. The code may be based on one of the following considerations:

- For an unsymmetric construction, the limits of integration go from the bottom of the laminate to the top.
- For a symmetric construction, the limits of integration go from the mid-plane to the top surface. The laminate stiffness value is then doubled.
- The ply laying process in manufacturing moves away from the surface of the tool. The exact direction depends on the male or female tool.
- Repeating sub-laminates where lamination begins from the outer surface and goes toward the mid-plane may be used.

For symmetric laminates subjected to in-plane loads only, the stacking sequence of plies is not important. Therefore, we can use any convention for the laminate code. When we are building symmetric laminates for flexure, or unsymmetric laminates for any load, explicit rules that govern the code are essential. We prefer a laminate code that goes from the top surface to the bottom surface.

Three alternative laminate codes representing the same laminate are shown in the following; viz., total laminate, symmetric laminate, and percentage of ply angles. Subscript T stands for total, and S or s, symmetric:

Total laminate	Symmetric laminate	Percent 0, ±45, 90
$[0/90_2/45/-45_2/45/90_2/0]_T$	$[0/90_2/45/-45]_S$	[20/40/40]
$[0/90_2/0/90_4/0/90_2/0]_T$	$[0/90_2]_{2S}$	[33/0/67]

(4.1)

If a laminate consists of repeating sub-laminates, a number representing the multiple units may be placed before the letter T or S. In the second row in the above we can represent a laminate consisting of 2 such sub-laminates with a repeating index 2 before subscript S.

A third laminate code is shown in the last column. It shows the percentage of ply angles in a [/4] family of laminates. There is a variation of this code; i.e., the sequence of ply angles is [0], [90], and [±45].

4.2 LAMINATED PLATE THEORY

The notations for laminates are direct extensions of those for unidirectional plies. Transformation relations are intended to connect between the new and old coordinate systems. In composite materials, it is convenient to assign the on- versus off-axis, as well as the laminate versus the ply axes. In the figure below, we show both the 1- 2 and 1'-2' axes as the old and new, respectively. Then we show the 1-2 as the laminate axes, and x-y as the ply axes with a positive ply orientation.
In addition to the usual assumptions for a linearly elastic material and linear strain-displacement relations, three principal geometric assumptions are:

- the laminate is symmetric;
- the laminate is thin: **h** << **a**, **b**, where **h** = thickness, **a** = length, and **b** = width;
- ply strain is constant across the laminate thickness, and is equal to the laminate strain.

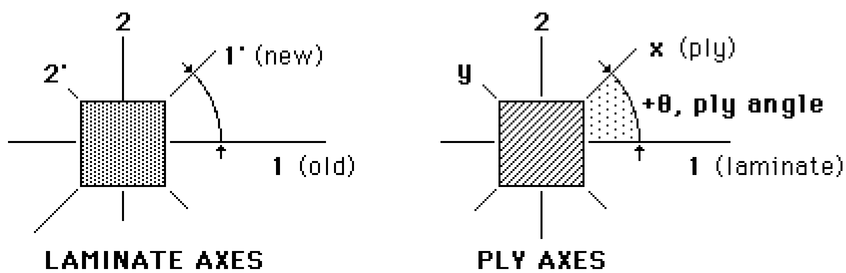

FIGURE 4.1 REFERENCE COORDINATE SYSTEMS FOR LAMINATE AND PLY AXES

For a symmetric laminate under in-plane stress or deformation, ply strain and laminate strain are assumed to be equal. Ply stress varies from ply angle to ply angle.

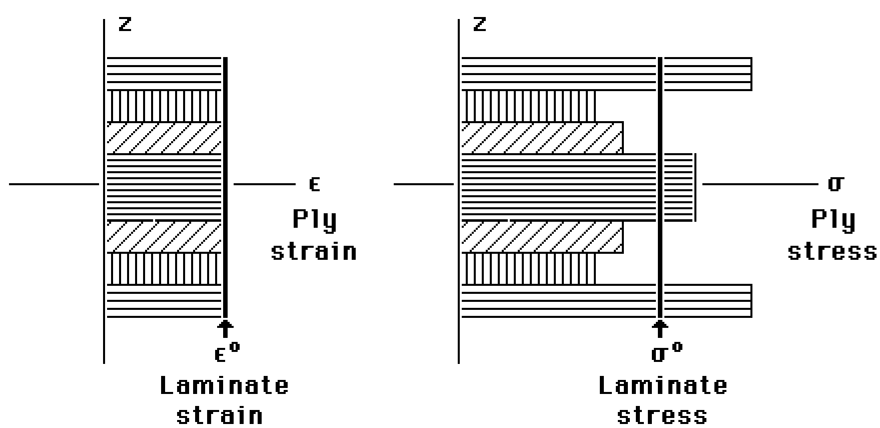

FIGURE 4.2 STRESS AND STRAIN DISTRIBUTIONS IN A SYMMETRIC LAMINATE

With the assumptions in the last figure where ply and laminate strains are equal, we can derive the effective in-plane stiffness of a laminate [A] in the following equations:

$$\{\varepsilon\} = \{\varepsilon^o\},\ \varepsilon_i = \varepsilon_i^o,\ i = 1,2,6$$

$$\{N\} = \int_{-h/2}^{h/2}\{\sigma\}dz = \int_{-h/2}^{h/2}[Q]\{\varepsilon\}dz = \left[\int_{-h/2}^{h/2}[Q]dz\right]\{\varepsilon^o\} = [A]\{\varepsilon^o\},\ \text{in N/m} \tag{4.2}$$

The stiffness of the laminate can be normalized. These normalized material properties are useful for direct comparison with other materials because the properties are intensive, independent of the thickness of the laminate.

$$[A] = \int_{-h/2}^{h/2}[Q]dz,\ [A^*] = \frac{1}{h}[A],\ \text{in Pa};\ [a] = [A]^{-1},\ [a^*] = h[a],\ \text{in Pa}^{-1}$$

$$\{\sigma^o\} = \frac{1}{h}\{N\} = [A]\{\varepsilon^o\};\ \{\varepsilon^o\} = [a]\{N\} = [a^*]\{\sigma^o\} \tag{4.3}$$

These relations are identical to those for an off-axis unidirectional ply. The in-plane behavior is anisotropic in general. The shear coupling coefficients are present. When they vanish the laminate becomes orthotropic. A laminate can also be square symmetric (as is the case of a balanced fabric), or quasi-isotropic (as in the case of a [π/3] or [π/4] laminate.)

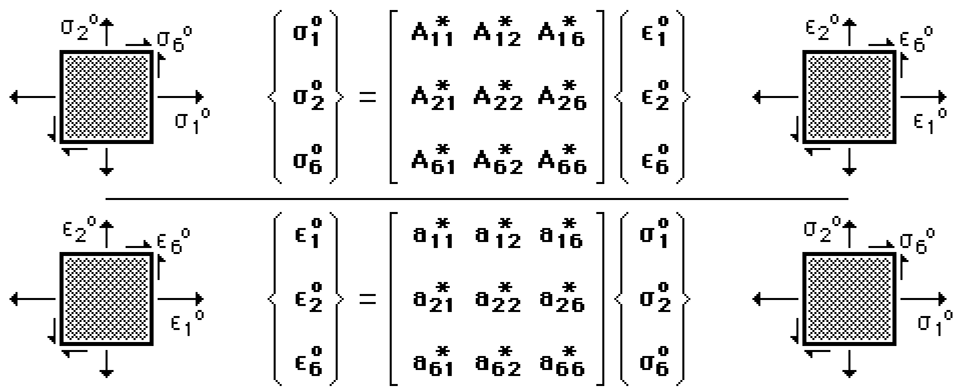

FIGURE 4.3 STRESS AND STRAIN RELATIONS OF A SYMMETRIC LAMINATE

MATRIX INVERSION

The inversion of the stiffness matrix is the compliance matrix. The inversion process is the same as that for the ply stiffness. It is also the same whether the in-plane stiffness is normalized or not; i.e., [A*] or [A].

$$[a] = [A]^{-1},\ |A| = (A_{11}A_{22}-A_{12}^2)A_{66}+2A_{12}A_{26}A_{16}-A_{11}A_{26}^2-A_{22}A_{16}^2$$

$$a_{11} = (A_{22}A_{66}-A_{26}^2)/|A|,\ a_{22} = (A_{11}A_{66}-A_{16}^2)/|A|,\ a_{12} = (A_{16}A_{26}-A_{12}A_{66})/|A|$$

$$a_{66} = (A_{11}A_{22}-A_{12}^2)/|A|,\ a_{16} = (A_{12}A_{26}-A_{22}A_{16})/|A|,\ a_{26} = (A_{12}A_{16}-A_{11}A_{26})/|A| \tag{4.4}$$

IN-PLANE ENGINEERING CONSTANTS

Engineering constants are defined from the components of a normalized compliance patterned after similar relations for an off-axis ply:

$$E_1^o = 1/a_{11}^*,\quad E_2^o = 1/a_{22}^*,\quad E_6^o = 1/a_{66}^*$$

$$\nu_{21}^o = -a_{21}/a_{11},\quad \nu_{61}^o = a_{61}/a_{11},\quad \nu_{62}^o = a_{62}/a_{11}$$

$$\nu_{12}^o = -a_{12}/a_{22},\quad \nu_{16}^o = a_{16}/a_{66},\quad \nu_{26}^o = a_{26}/a_{66} \tag{4.5}$$

Again, the normalization by columns as described in Table 2.11 on page 2-10 is used for the definition of the coupling constants above.

4.3 STIFFNESS MATRIX EVALUATION BY THE MULTIPLE ANGLE METHOD

The integration of Equation 4.3 can be performed using many different methods. Four methods will be shown and their features described. A ply group is defined as plies with the same angle grouped or banded together. Within each of the **m** ply groups, in which the ply stiffness matrix remains constant, the integration can be replaced by a summation:

$$[\mathbf{A}] = \int_{-h/2}^{h/2} [\mathbf{Q}]dz = \sum_{i=1}^{m} [\mathbf{Q'}]^{(i)} \left[z^{(i)} - z^{(i-1)} \right], \quad [\mathbf{A}^*] = \frac{1}{h}[\mathbf{A}]$$

$[Q']^{(i)}$ = off-axis stiffness of the i-th ply group with angle $\theta^{(i)}$ (4.6)

This is a direct summation replacing the integration. From this summation we can develop three other methods of evaluation: the multiple angle method, the cash register method, and the rule-of-mixtures method.

The multiple angle method is an extension of the multiple angle transformation in Figure 3.12 on page 3-8. Instead of integrating the stiffness across the thickness, we integrate the trigonometric functions, shown as follows:

$$A_{11} = \int_{-h/2}^{h/2} Q_{11}dz = \int_{-h/2}^{h/2} [U_1 + U_2\cos 2\theta + U_3 \cos 4\theta]dz = U_1 h + U_2 V_1 + U_3 V_2$$

$$A_{16} = \int_{-h/2}^{h/2} Q_{16}dz = \int_{-h/2}^{h/2} \left[\frac{U_2}{2}\sin 2\theta - U_3 \sin 4\theta \right]dz = \frac{U_2}{2} V_3 - U_3 V_4 \qquad (4.7)$$

We can define the integrated trigonometric functions of multiple angles and the corresponding normalized integrals:

$$V_1 = \int_{-h/2}^{h/2} \cos 2\theta dz, \; V_2 = \int_{-h/2}^{h/2} \cos 4\theta dz, \; V_3 = \int_{-h/2}^{h/2} \sin 2\theta dz, \; V_4 = \int_{-h/2}^{h/2} \sin 4\theta dz$$

$$V_i^* = \frac{1}{h} V_i = V^*_{[1,2,3,4]} = \frac{1}{h} \int_{-h/2}^{h/2} [\cos 2\theta, \cos 4\theta, \sin 2\theta, \sin 4\theta]dz \qquad (4.8)$$

Note the similarity between the in-plane stiffness and the ply stiffness in Figure 3.12 on page 3-8 where material and geometry are separated. For a given material, Us stay constant. For a given laminate, the V*s remain constant.

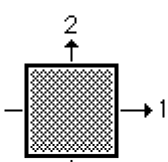

$$\begin{Bmatrix} A^*_{11} \\ A^*_{22} \\ A^*_{12} \\ A^*_{66} \\ A^*_{16} \\ A^*_{26} \end{Bmatrix} = \begin{bmatrix} U_1 & U_2 & U_3 & 0 & 0 \\ U_1 & -U_2 & U_3 & 0 & 0 \\ U_4 & 0 & -U_3 & 0 & 0 \\ U_5 & 0 & -U_3 & 0 & 0 \\ 0 & 0 & 0 & \frac{U_2}{2} & U_3 \\ 0 & 0 & 0 & \frac{U_2}{2} & -U_3 \end{bmatrix} \begin{Bmatrix} 1 \\ V_1^* \\ V_2^* \\ V_3^* \\ V_4^* \end{Bmatrix}$$

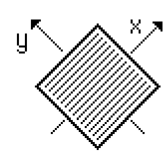

FIGURE 4.4 MULTIPLE-ANGLE FORMATIONS OF NORMALIZED IN-PLANE STIFFNESSES

We show in the following equation an example of the normalized in-plane stiffness [A*] using the multiple angle method for a $[0_3/90]$ cross-ply laminate:

$$\left.\begin{aligned}
&V_1^* = 0.5,\ V_2^* = 1,\ V_3^* = V_4^* = 0,\ A_{16} = A_{26} = 0\\
&A_{11}^* = U_1+0.5U_2+U_3 = 76.37+0.5\text{x}85.73+19.71 = 138.95 \text{ GPa}\\
&A_{22}^* = U_1-0.5U_2+U_3 = 76.37-0.5\text{x}85.73+19.71 = 53.22 \text{ GPa}\\
&A_{12}^* = U_4-U_3 = 22.61-19.71 = 2.9 \text{ GPa},\ A_{66}^* = U_5-U_3 = 26.88-19.71 = 7.17 \text{ GPa}
\end{aligned}\right] \tag{4.9}$$

The in-plane stiffness of a laminate is the matrix products of two parts. One part is the linear combinations of the stiffness matrix of the unidirectional ply. The other part is the average trigonometric functions which reflect the ply orientations of the laminates. When the ply material is changed, only the first part is changed. When the ply orientation is changed, the second part is changed. Thus, materials and geometric characteristics of a laminate stiffness can be separated.

4.4 EXAMPLE OF THE CASH REGISTER METHOD

This is a method of determining the in-plane stiffness [A] by counting plies in each ply orientation.

$$\left.\begin{aligned}
&\mathbf{[A]} = \int_{-h/2}^{h/2}[Q]dz = \sum_{i=1}^{m}[Q']^{(i)}h^{(i)} = \sum_{i=1}^{m}[Q']^{(i)}h_o n^{(i)} = \sum_{i=1}^{m}\mathbf{[A^o]^{(i)}n^{(i)}},\ [A^*] = \frac{1}{h}[A]\\
&\text{where } h^{(i)} = \text{thickness of i-th ply group; } h_o = \text{unit ply thickness;}\\
&\qquad n^{(i)} = \text{plies in i-th ply group; } [A^o] = [Q']^{(i)}h_o = \text{unit ply stiffness}
\end{aligned}\right| \tag{4.10}$$

This is easier to use than direct summation. Plies can be added and subtracted, and hybrids (laminates with two or more materials) can be evaluated. The unit of the stiffness is N/m. The data needed for this method are listed in Table 4.1.

TABLE 4.1 PLY STIFFNESS TO BE USED FOR THE CASH REGISTER METHOD IN SI

Fiber	T300	B(4)	AS	E-glass	Kev 49	AS 4	IM6	T300	T300	T300
Matrix	N5208	N5505	H3501	epoxy	epoxy	PEEK	epoxy	Fbrt934	Fbrt934	Fbrt934
h_o, mm	0.125	0.125	0.125	0.125	0.125	0.125	0.125	0.100	0.325	0.175
[A°]/0 (unit ply stiffness), MN/m								tape	cloth	cloth
11	22.73	25.62	17.35	4.90	9.58	16.84	25.52	14.89	24.11	11.57
22	1.29	2.32	1.13	1.05	0.69	1.12	1.41	0.97	24.11	11.57
21=12	0.36	0.53	0.34	0.27	0.24	0.31	0.45	0.29	1.21	0.51
66	0.90	0.70	0.89	0.52	0.29	0.64	1.05	0.46	1.48	0.72
16=26	0.00	0.00	0.00	0.00	0.00	0.00	0.00	0.00	0.00	0.00
[A°]/90, MN/m										
11	1.29	2.32	1.13	1.05	0.69	1.12	1.41	0.97	24.11	11.57
22	22.73	25.62	17.35	4.90	9.58	16.84	25.52	14.89	24.11	11.57
21=12	0.36	0.53	0.34	0.27	0.24	0.31	0.45	0.29	1.21	0.51
66	0.90	0.70	0.89	0.52	0.29	0.64	1.05	0.46	1.48	0.72
16=26	0.00	0.00	0.00	0.00	0.00	0.00	0.00	0.00	0.00	0.00
[A°]/±45, MN/m										
11=22	7.08	7.95	5.68	2.14	2.97	5.28	8.01	4.57	14.14	6.76
21=12	5.29	6.56	3.90	1.11	2.40	4.01	5.91	3.66	11.18	5.32
66	5.82	6.72	4.45	1.35	2.45	4.33	6.51	3.82	11.45	5.53
16, 26	±5.36	±5.82	±4.06	±0.96	±2.22	±3.93	±6.03	±3.48	±0.00	±0.00

We show in the following equation an example of the in-plane stiffness [A], in N/m, using the cash register method for a $[0/90/45_2]$ laminate, using the data in the table above.

$$
\left.\begin{aligned}
&h = 8h_o = 0.001\ \mathrm{m},\ [A^*] = [A]/h = 1000[A],\ \ A_{ij} = 2\left[A_{ij}{}^{o(0)} + A_{ij}{}^{o(90)} + 2A_{ij}{}^{o(45)}\right] \\
&A_{11} = 2\mathrm{x}(22.73+1.29+2\mathrm{x}7.08) = 76.36\ \mathrm{MN/m},\ \text{or } A_{11}{}^* = 76.36\ \mathrm{GPa} \\
&A_{22} = 2\mathrm{x}(1.29+22.73+2\mathrm{x}7.08) = 76.36\ \mathrm{MN/m},\ \text{or } A_{22}{}^* = 76.36\ \mathrm{GPa} \\
&A_{12} = 2\mathrm{x}(0.36+0.36+2\mathrm{x}5.29) = 22.6\ \mathrm{MN/m},\ \text{or } A_{12}{}^* = 22.6\ \mathrm{GPa} \\
&A_{66} = 2\mathrm{x}(0.9+0.9+2\mathrm{x}5.82) = 26.88\ \mathrm{MN/m},\ A_{16} = A_{26} = 2\mathrm{x}2\mathrm{x}(5.36) = 21.44\ \mathrm{MN/m}
\end{aligned}\right] \tag{4.11}
$$

Note that the factor of 2 is needed for symmetric laminates. Although the laminate is not balanced, the two shear coupling components are always equal for pi/4 laminates.

We show in the equation below a stiffness component calculation of a hybrid, with a T300/5208 cross-ply sub-laminate and 2 plies of boron/5505 unidirectional at 45 degrees. The unit ply data can be found in the Table 4.1 above.

$$
\left[[0/90]^{cfrp}/45_2{}^{bfrp}\right]_S \qquad A_{11} = 2\mathrm{x}(22.73+1.29+2\mathrm{x}7.95) = 79.84\ \mathrm{MN/m} \tag{4.12}
$$

4.5 EXAMPLES OF RULE-OF-MIXTURES METHOD

The last method of summation, the rule-of-mixtures method, is derived as follows:

$$
\begin{aligned}
&\mathbf{[A^*]} = \frac{1}{h}[A] = \frac{1}{h}\sum_{i=1}^{m}[Q']^{(i)}h^{(i)} = \sum_{i=1}^{m}[Q']^{(i)}\frac{h^{(i)}}{h} = \sum_{i=1}^{m}\mathbf{[Q']^{(i)}v^{(i)}} \\
&\text{where } v^{(i)} = \text{fraction of the i-th ply group}
\end{aligned} \tag{4.13}
$$

Unlike the absolute matrix in Equation 4.11, the resulting normalized matrix need not be doubled for symmetric laminates.

The rule-of-mixtures method is based on the product of the ply stiffness and the ply fraction. The data needed for this method are listed in Table 4.2 below.

TABLE 4.2 [A*] TO BE USED IN THE RULE OF MIXTURES METHOD IN SI

Fiber	T300	B(4)	AS	E-glass	Kev 49	AS 4	IM6	T300	T300	T300
Matrix	N5208	N5505	H3501	epoxy	epoxy	PEEK	epoxy	Fbrt934	Fbrt934	Fbrt934
						APC2		4-mil	13-mil	7-mil
[Q]^0, GPa								tape	cloth	cloth
Qxx	181.81	204.98	138.81	39.17	76.64	134.70	204.15	148.87	74.19	66.13
Qyy	10.35	18.59	9.01	8.39	5.55	8.95	11.26	9.71	74.19	66.13
Qxy	2.90	4.28	2.70	2.18	1.89	2.51	3.60	2.91	3.71	2.91
Qss	7.17	5.59	7.10	4.14	2.30	5.10	8.40	4.55	4.55	4.10
[Q]^90, GPa										
11	10.35	18.59	9.01	8.39	5.55	8.95	11.26	9.71	74.19	66.13
22	181.81	204.98	138.81	39.17	76.64	134.70	204.15	148.87	74.19	66.13
12	2.90	4.28	2.70	2.18	1.89	2.51	3.60	2.91	3.71	2.91
66	7.17	5.59	7.10	4.14	2.30	5.10	8.40	4.55	4.55	4.10
16=26	0.00	0.00	0.00	0.00	0.00	0.00	0.00	0.00	0.00	0.00
[Q']^±45, GPa										
11=22	56.66	63.62	45.41	17.12	23.79	42.26	64.06	45.65	43.50	38.62
12	42.32	52.44	31.21	8.84	19.19	32.06	47.26	36.55	34.40	30.42
66	46.59	53.76	35.60	10.80	19.60	34.66	52.05	38.19	35.24	31.61
16, 26	±42.87	±46.60	±32.45	±7.69	±17.77	±31.44	±48.22	±34.79	±0.00	±0.00

We show in the following equation an example of the normalized in-plane stiffness [A*] using the rule of mixtures method for a $[0_3/90]$ cross-ply laminate:

$$\left.\begin{array}{l} v^{(0)} = 0.75,\ v^{(90)} = 0.25;\ A_{11}^* = 0.75\times181.81+0.25\times10.35 = 138.95\text{ GPa} \\ A_{22}^* = 0.75\times10.35+0.25\times181.81 = 53.22\text{ GPa},\ A_{16} = A_{26} = 0 \\ A_{12}^* = 0.75\times2.9+0.25\times2.9 = 2.9\text{ GPa},\ A_{66}^* = 0.75\times7.17+0.25\times7.17 = 7.17\text{ GPa} \end{array}\right] \tag{4.14}$$

Note that the results are the same as those in Equation 4.9. If the laminate is a hybrid, this method is equally applicable provided that the correct ply material data and ply fractions are used. Care must be exercised if the unit ply thicknesses are different. This occurs when unidirectional and fabric composites are combined.

4.6 SAMPLE CALCULATIONS OF IN-PLANE STIFFNESS

Sample 1: Find engineering constants of $[0_3/90]$ for T300/5208.

From Equations 4.14, 4.4, and 4.5, we can calculate [A*], [a*], and engineering constants, respectively:

$$\left.\begin{array}{l} [A^*] = \begin{bmatrix} 138.95 & 2.90 & 0 \\ & 53.22 & 0 \\ \text{symm} & & 7.17 \end{bmatrix}\text{GPa},\ [a^*] = \begin{bmatrix} 7.20 & -0.39 & 0 \\ & 18.81 & 0 \\ \text{symm} & & 139.5 \end{bmatrix}\text{TPa}^{-1} \\ E_1^o = 1/7.20 = 138.88\text{ GPa},\ E_2^o = 1/18.81 = 53.15\text{ GPa},\ \nu_{21}^o = 0.39/7.20 = 0.054 \end{array}\right] \tag{4.15}$$

The laminate Poisson's ratio is nearly zero. This is a consequence of the 90-degree ply that limits the Poisson's contraction. Because of the low Poisson's ratio of this orthotropic laminate,

$$A_{11}^*/E_1^o = 138.95/138.88 = 1.001 \tag{4.16}$$

We can go directly from the engineering constants of plies to those of a laminate with less that 0.1 percent error. By applying the rule-of-mixtures equation to obtain the longitudinal engineering constant:

$$E_1^o = 0.75\times181+0.25\times10.3 = 138.33\text{ GPa} \tag{4.17}$$

The same accuracy of the rule-of-mixtures relation holds for a variety of composite materials, as shown in the figure below, where the two columns for each material are the comparison between the prediction by laminated plate theory and that by the rule of mixtures. There is no discernible difference between the two.

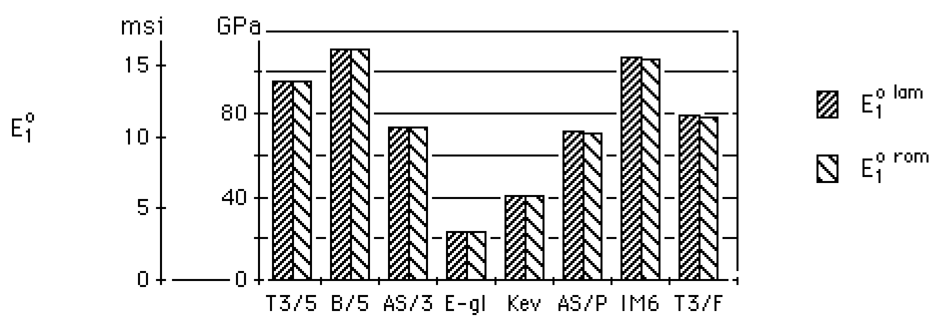

FIGURE 4.5 EXACT AND APPROXIMATE PREDICTIONS OF LONGITUDINAL STIFFNESSES

In the polar diagram below, the in-plane normal and shear moduli of a cross-ply laminate are compared. At [0] and [90] orientations, the in-plane stiffness is essentially identical with the longitudinal Young's modulus. At [45] orientation, the difference is the greatest,. The precise quantity will be covered in the next sub-section.

Under pure shear stress, the shear component of the stiffness matrix and the shear moduli are identical when the ply orientation starts with [0] and increases with 45-degree intervals. In between these angles, the two moduli are different.

This laminate is square symmetric; i.e., the two principal directions at [0] and [90], or at [45] and [-45], have identical properties. This symmetry also exists in a balanced fabric. The number of independent elastic constants are 3, consisting of one each of Young's modulus, Poisson's ratio, and shear modulus. For isotropic material, there is a relation among the 3 moduli. There are only 2 independent elastic moduli.

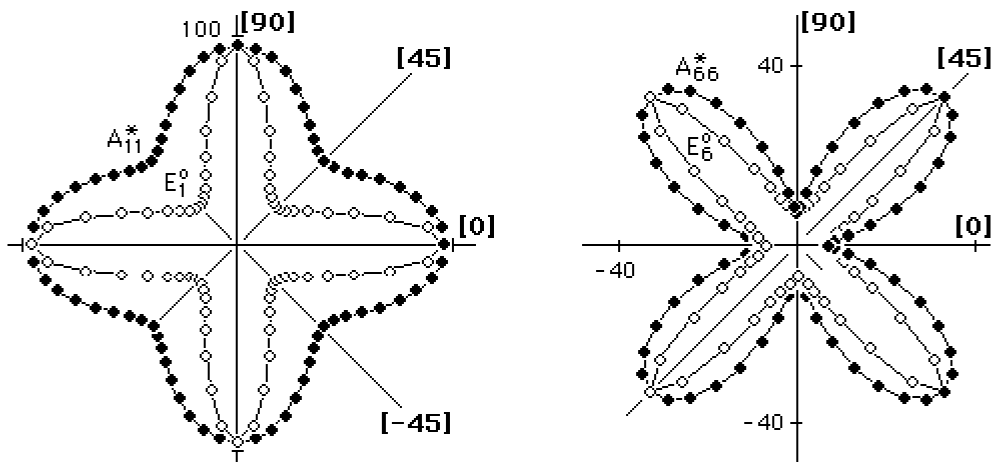

FIGURE 4.6 POLAR DIAGRAMS OF THE MODULI OF A [0/90] CROSS LAMINATE

Sample 2: Find engineering constants of [±45] for T300/5208.
From Equations 4.14, 4.4, and 4.5, we can calculate [A*], [a*], and engineering constants, respectively:

$$[A^*] = \begin{bmatrix} 56.66 & 42.32 & 0 \\ & 56.66 & 0 \\ \text{symm} & & 46.59 \end{bmatrix} \text{GPa},\ [a^*] = \begin{bmatrix} 39.93 & -29.82 & 0 \\ & 39.92 & 0 \\ \text{symm} & & 21.46 \end{bmatrix} \text{TPa}^{-1}$$

$$E_1^o = 1/39.9 = 25.05 \text{ GPa},\ E_2^o = 1/21.46 = 46.59 \text{ GPa},\ \nu_{21}^o = 29.82/39.9 = 0.75 \quad (4.18)$$

From the off-axis stiffness of [45] in the Table 3.4 on page 3-15,

$$E_1 = 16.74 \text{ GPa},\quad E_2 = 9.46 \text{ GPa},\quad nu_{21} = 0.17 \quad (4.19)$$

Comparing Equations 4.18 and 4.19, we can certainly see the difference between [45] and [±45]. The parallel springs model or the simple rule-of-mixtures equation is certainly not applicable. For representative composite materials, the comparison of the effective engineering constants are shown:

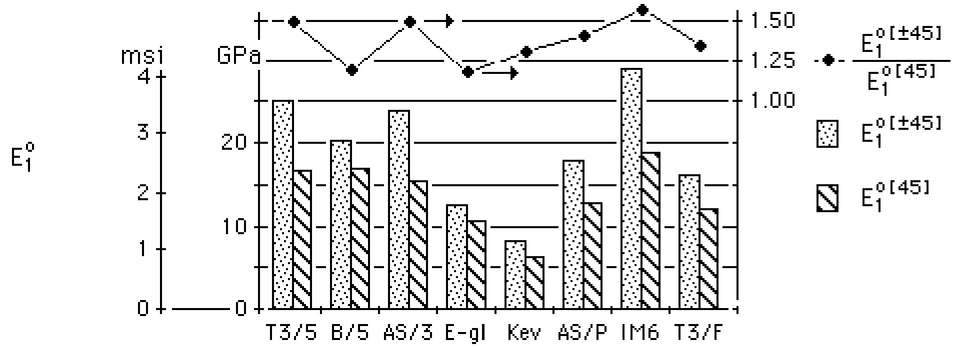

FIGURE 4.7 COMPARISON BETWEEN ANGLE-PLY LAMINATE AND OFF-AXIS PLY

If the lamination angle changes from 45 degrees to an angle between 45 and 0 degree, the same stiffness components of the in-plane stiffness will differ from the corresponding Young's modulus and shear modulus. These differences are shown in the figure below. The material is T300/5208.

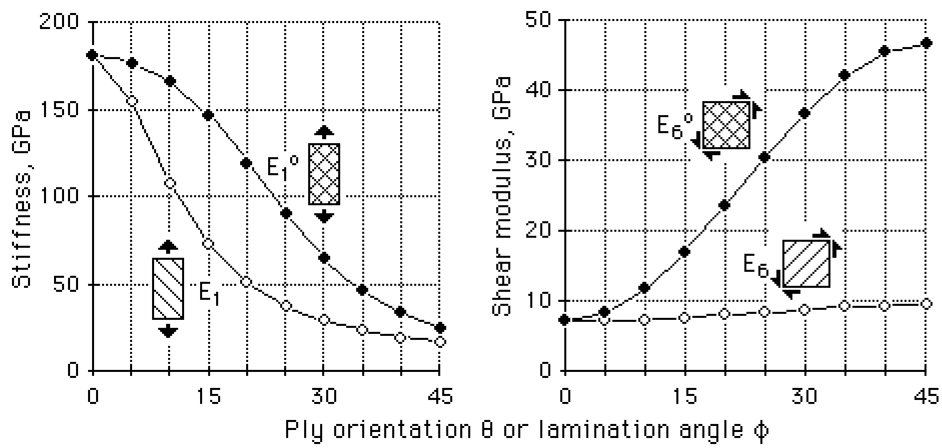

FIGURE 4.8 COMPARISON BETWEEN YOUNG'S AND SHEAR MODULI

Sample 3: Find engineering constants of $[0_2/\pm 45]$ for T300/5208.
For this laminate we can find the constants as in the two previous samples, we have:

$$E_1^o = 103.98 \text{ GPa}, \quad E_2^o = 29.22 \text{ GPa}, \quad E_6^o = 26.88 \text{ GPa} \tag{4.20}$$

If we apply the rule-of-mixtures equation to a $[0_2]$ and [±45] we will have:

$$\begin{aligned} E_1^o &= [181+25.05]/2 = 103 \text{ GPa} \ \ \text{(1 percent error)} \\ E_2^o &= [10.3+25.05]/2 = 17.68 \text{ GPa} \ \ \text{(60 percent error)} \end{aligned} \tag{4.21}$$

The values for the normal stiffness components in Equation 4.20 are exact while those in Equation 4.21 are not reliable, as shown by the relative errors indicated in the parenthesis. However, the shear modulus using the rule-of-mixtures is exact; e.g.,

$$E_6^o = [7.17+46.59]/2 = 26.88 \text{ GPa} \ \ \text{(no error)} \tag{4.22}$$

This simple relation provides the correct answer because the sub-laminates of [0] and [±45] are orthotropic. This is shown in the figure below where a linear relation exists between [0/90] and [±45]. A quasi-isotropic cut-off is shown to remind the designer not to penalize composite materials by selecting a laminate below its quasi-isotropic capability.

The most common quasi-isotropic laminates have equal percentage of plies in [π/3] or [π/4] ply orientations. Problem 4.2 calls for the proof of isotropic laminates.

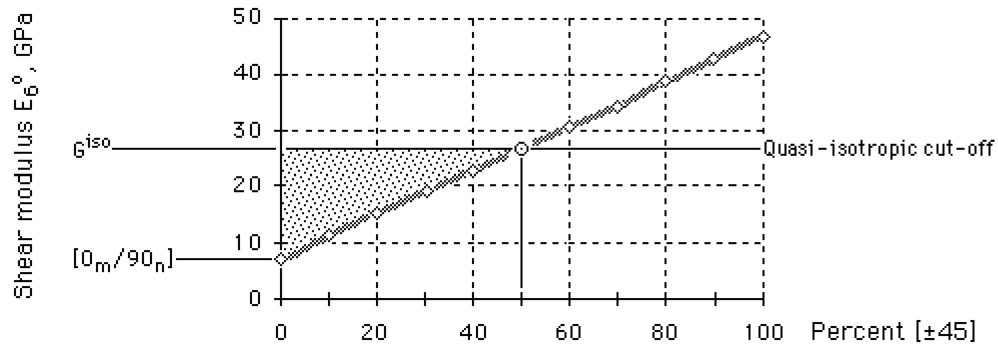

FIGURE 4.9 A LINEAR PLOT FOR THE SHEAR MODULUS OF A [π/4] FAMILY

In the next figure, a carpet plot is shown to cover the range of the longitudinal Young's modulus from a family of [π/4] laminates. The larger Young's modulus of the 2 principal stiffnesses should at least be that of the quasi-isotropic layup. It is assumed in the carpet plot below that all laminates are balanced; i.e., the [45] and [-45] plies are equal in number.

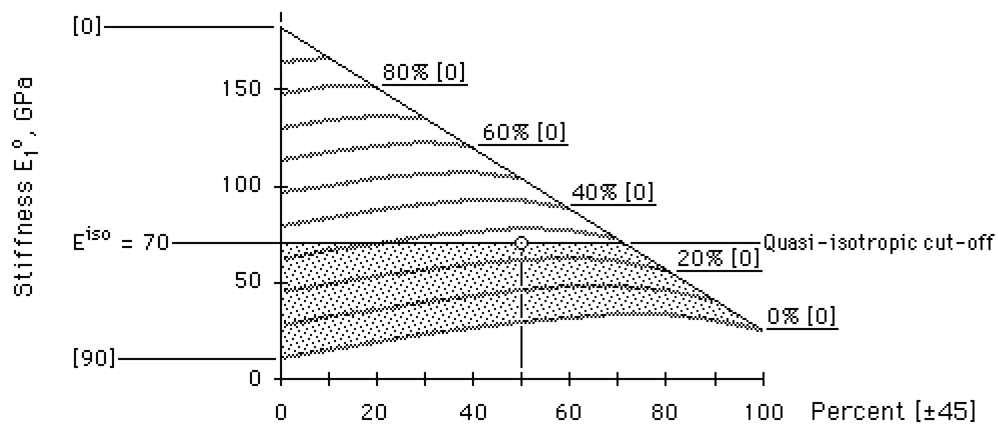

FIGURE 4.10 A CARPET PLOT FOR THE LONGITUDINAL YOUNG'S MODULUS OF [/4] FAMILY

We can generate analogous carpet plots for tri-directional laminates. This is shown in the figure below with the longitudinal Young's modulus of a family of [0] plies and angle-ply sub-laminates. The quasi-isotropic cut-off is based on the [π/3] quasi-isotropic laminate.

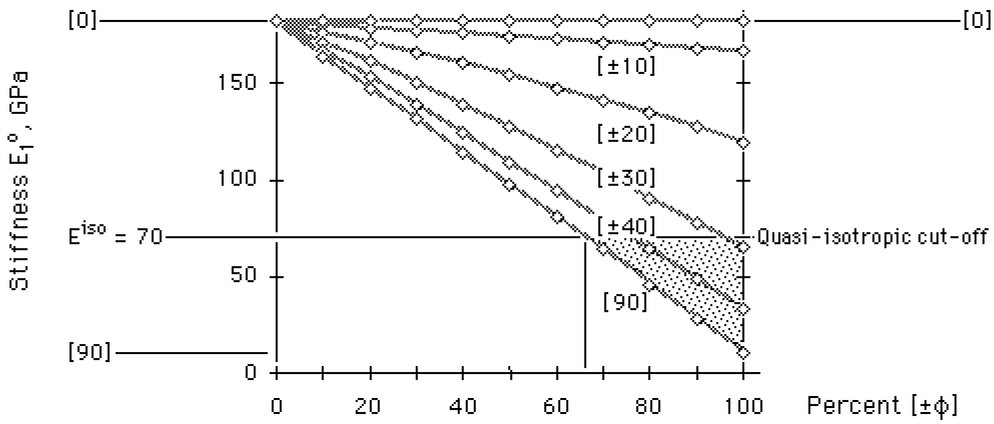

FIGURE 4.11 A CARPET PLOT OF MODULUS OF TRI-DIRECTIONAL LAMINATES

In Figure 4.12 below, we show the laminate shear modulus of [0] and angle-ply sub-laminates. The quasi-isotropic cut-off is based on the [π/3] quasi-isotropic laminate.

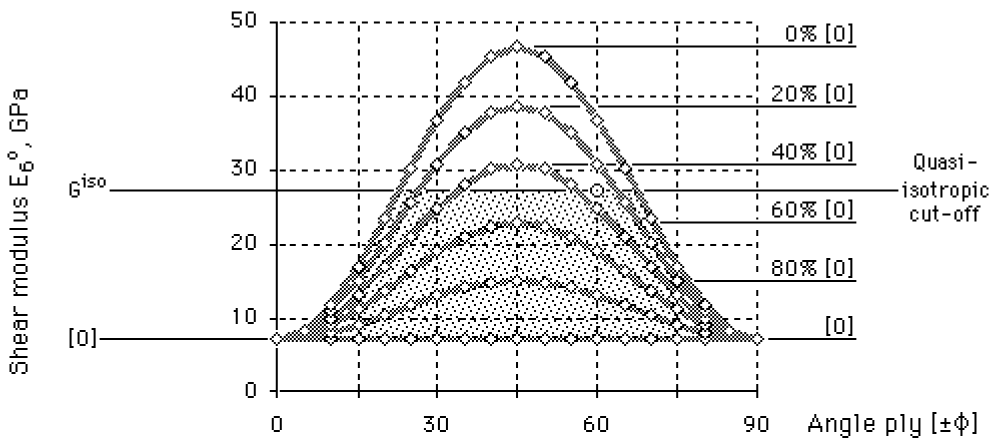

FIGURE 4.12 A CARPET PLOT OF THE SHEAR OF TRI-DIRECTIONAL LAMINATES

Sample 4: Find engineering constants of [0/90/45$_2$], T300/5208.

From Equations 4.14, 4.4, and 4.5, we can calculate [A*], [a*], and engineering constants, respectively:

$$[A^*] = \begin{bmatrix} 76.36 & 22.60 & 21.44 \\ & 76.36 & 21.44 \\ \text{symm} & & 26.88 \end{bmatrix} \text{GPa}, \quad [a^*] = \begin{bmatrix} 17.02 & -1.58 & -12.31 \\ & 17.02 & -12.31 \\ \text{symm} & & 56.83 \end{bmatrix}$$

$$E_1° = 1/17.02 = 58.76 \text{ GPa} = E_2°,\ E_6° = 1/56.83 = 17.60 \text{ GPa}$$

$$\nu_{21}° = 1.58/17.02 = 0.093,\ \nu_{61}° = -12.31/17.02 = -0.723 \qquad (4.23)$$

Although the laminate Poisson's ratio is still small, the A_{11}* is no longer close to $E_1°$ because this laminate is anisotropic. In the figure below, we show the polar plots of the normal and shear moduli as functions of the reference coordinates. For the normal moduli, the unbalanced laminate of [0/90/45$_2$] is the same as the balanced one of [45/-45/0$_2$] rotated 45 degrees clockwise.

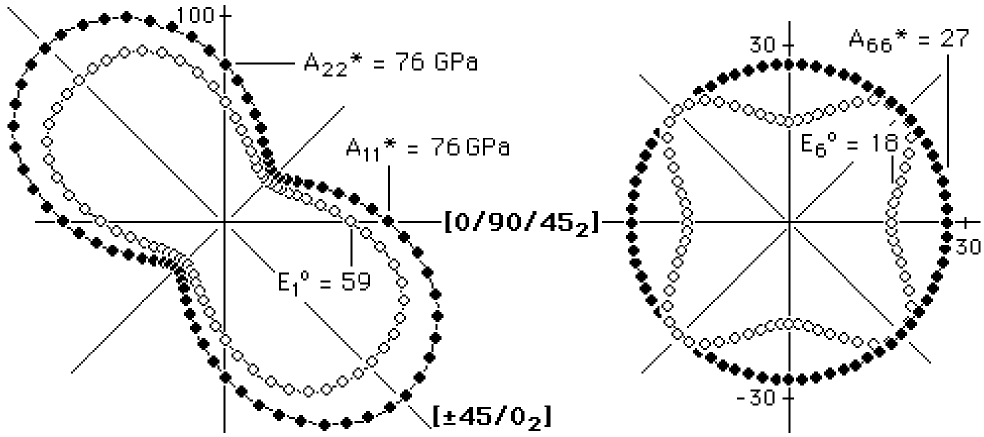

FIGURE 4.13 POLAR PLOTS OF MODULI OF TRI-DIRECTIONAL LAMINATES

Sample 5: Can laminates have unusual Poisson's ratios?

Poisson's ratios for anisotropic materials are not limited to the range between 0 and 1/2 imposed on isotropic materials. Poisson's ratio is not a regular component of the stiffness or compliance matrices. It is a deceptive material property because it is the ratio of two components. It is difficult to rationalize the physical phenomenon of Poisson contraction. In the figure below, we show that the laminate Poisson's ratios are nonlinear functions of the percentage of the off-axis plies. The quasi-isotropic laminate is based on the [π/3] laminate.

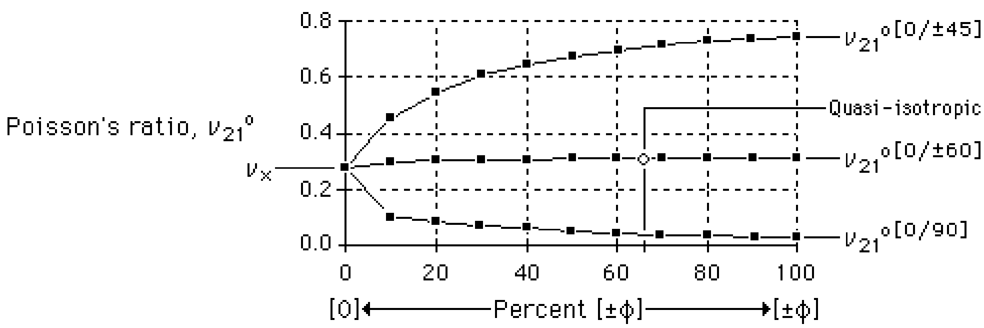

FIGURE 4.14 POISSON'S RATIOS OF TRI-DIRECTIONAL AND CROSS-PLY LAMINATES

We have seen that a [±45] has a Poisson's ratio of 0.747 for T300/5208. We may be tempted to relate this large Poisson's ratio to the scissoring effect of the off-axis plies. This explanation, however, is not valid because laminated plate theory does not permit scissoring, a relative displacement between two off-axis plies. Through micromechanics, we can show that the Poisson's ratio of [±30] can approach 3.0 if the matrix stiffness of the normal epoxy resin is reduced to zero.

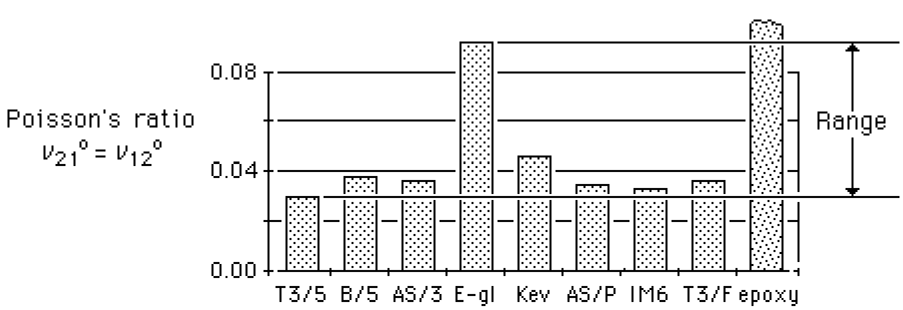

FIGURE 4.15 POISSON'S RATIOS OF [0/90] LAMINATES

Cross-ply laminates have low Poisson's ratio for all representative composite materials. This is shown in Figure 4.15 where the range of variation is between 0.03 and 0.07.

The range of Poisson's ratio for [±45] is between 0.5 and 0.8 for most representative composite materials.

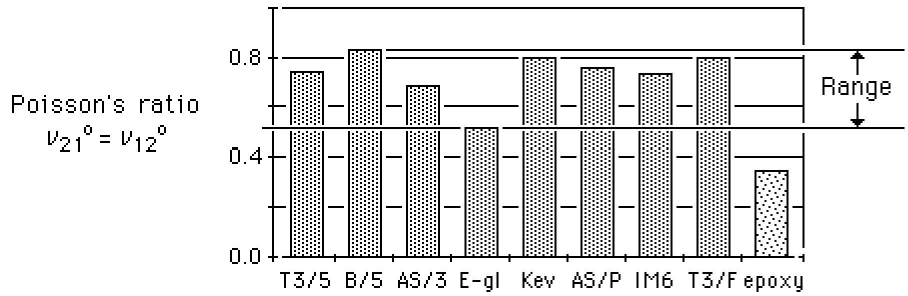

FIGURE 4.16 POISSON'S RATIOS OF [±45] LAMINATES

We can show, for example, that Poisson's ratio can be negative. We are not aware of a simple explanation of this negative Poisson's ratio. Again, the interaction between plies of a laminate is complex and nearly impossible to visualize. A laminate of $[15_2/60]$ gives negative Poisson's ratio in the following figure. The only exception is the E-glass/epoxy composite.

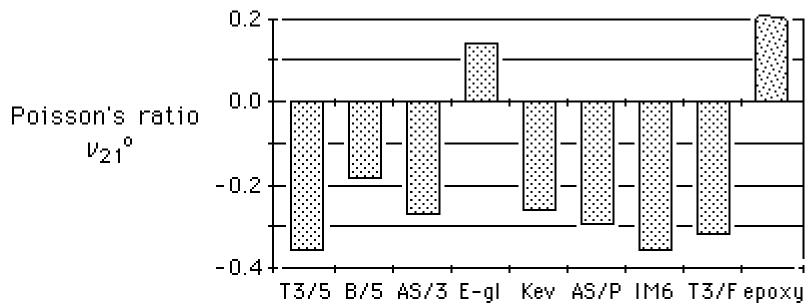

FIGURE 4.17 POISSON'S RATIOS OF $[15_2/60]_S$ LAMINATES

Sample 6: Can we determine shear modulus from uniaxial tests of [45] and [±45]?

Yes, we need to know the transformation relation of compliance at 45 degrees as follows:

$$\text{From } \frac{1}{E^{(45)}} = \frac{1}{4}[S_{xx}+S_{yy}+2S_{xy}+S_{ss}], \text{ then } S_{ss} = \frac{4}{E^{(45)}} - [S_{xx}+S_{yy}+2S_{xy}] \tag{4.24}$$

We can establish the following relations for T300/5208 and E-glass/epoxy composites. The [±45] laminates are calculated for each value of the shear modulus for the same materials. There is no closed form relation for laminates.

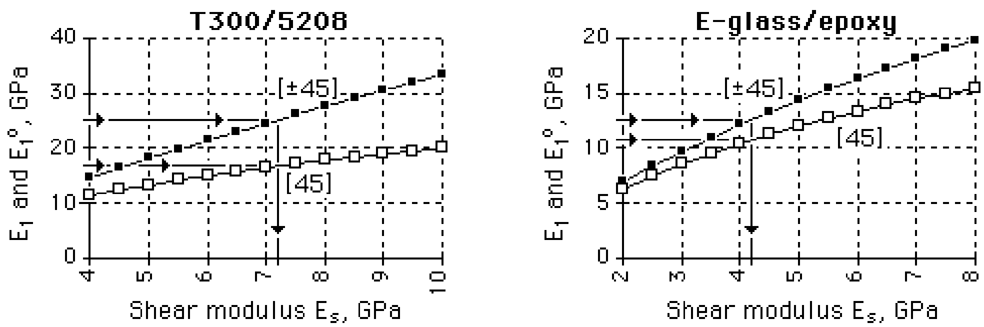

FIGURE 4.18 FIGURES TO BACK-CALCULATE SHEAR MODULUS FOR T300/5208 AND E-GLASS/EPOXY COMPOSITES FROM [45] AND [±45] TEST SPECIMENS

From measured Young's modulus of [45] and [±45], we can use the figures above to find the implied shear modulus. The solid lines with arrows in each figure represent the "perfect" measurements that would recover the original shear modulus of the ply material.

4.7 TRANSFORMATION AND INVARIANTS OF IN-PLANE MODULI

The transformation relations for the in-plane stiffness and compliance matrices follow precisely those for the ply stiffness and compliance, respectively; see Section 3, Ply Stiffness. The invariants associated with the transformation should be maintained as we go from plies to laminates. This is shown in the figures below for the stiffness and compliance.

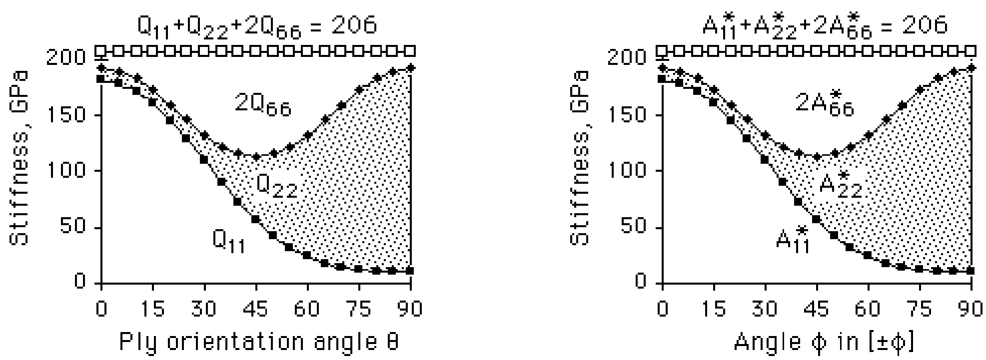

FIGURE 4.19 INVARIANCE OF UNIDIRECTIONAL AND ANGLE-PLY LAMINATES

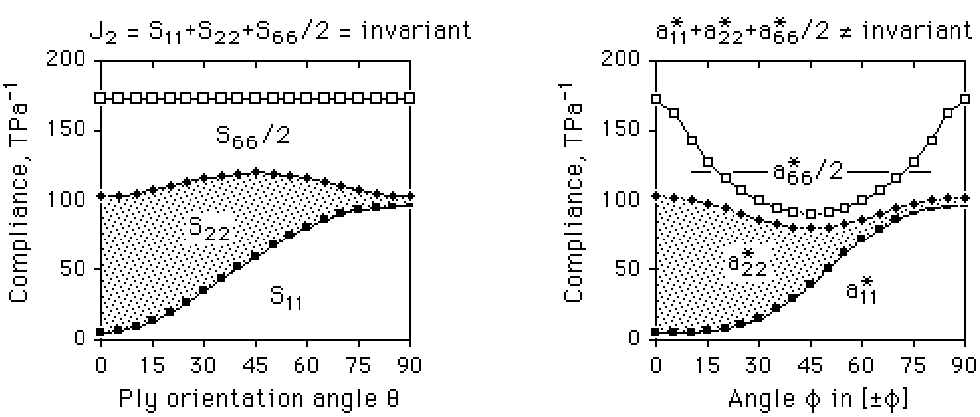

FIGURE 4.20 COMPLIANCE INVARIANCE OF UNIDIRECTIONAL AND ANGLE-PLY LAMINATES

The trace of the compliance does not go from the unidirectional ply to that of a laminate because, in laminated plate theory, strain, not stress, is assumed to be constant.

4.8 PLY STRESS AND PLY STRAIN

It is useful to examine the ply stress and ply strain defined earlier in this section. Figures 3.2 and 3.3 on page 3-3 for the ply stiffness transformation are modified here to suit the ply-by-ply stress analysis of a symmetric laminate under in-plane loading.

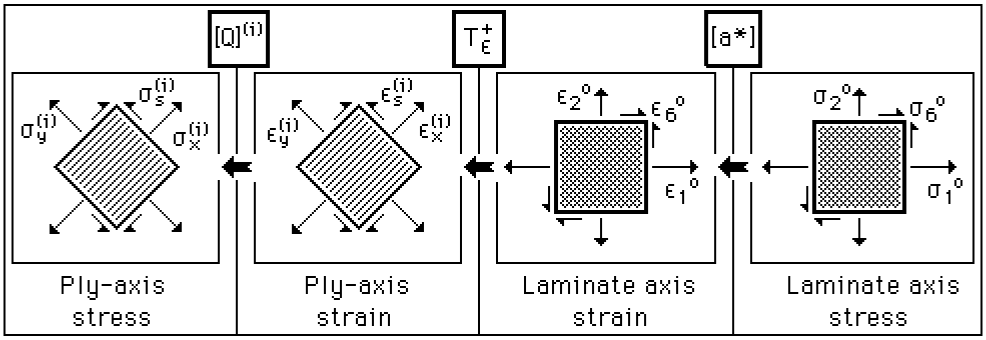

FIGURE 4.21 DETERMINATION OF PLY STRESS AND STRAIN FROM LAMINATE STRESS

The actual formulas for transformation and stress-strain relation are shown in Figure 4.22 below:

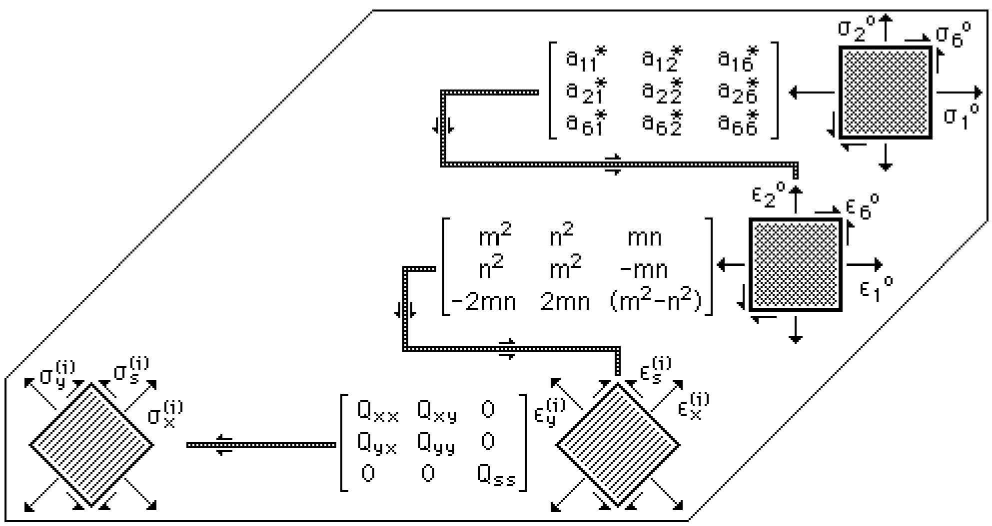

FIGURE 4.22 DETERMINATION OF PLY STRESS AND STRAIN FROM LAMINATE STRESS

Equilibrium check is one way of verifying the ply-by-ply stress analysis. The following relations should be used:

$$\{\sigma^o\} = \frac{\{N\}}{h} = \frac{1}{h}\int_{-h/2}^{h/2}\{\sigma\}dz \neq 0, \quad \{\sigma^f\} = \frac{6\{M\}}{h^2} = \frac{6}{h^2}\int_{-h/2}^{h/2}\{\sigma\}zdz = 0 \qquad (4.25)$$

This is demonstrated by an example given below where a [/4] quasi-isotropic laminate is subjected to a combined in-plane stress of {20,0,40}. The ply strains and ply stress in the laminate axis are shown in the table below. Note that ply strains are equal to laminate strains, as required by laminated plate theory. Ply stresses are different from laminate stress, as expected. The average of the ply stress must be equal to the laminate stress, as required by equilibrium stated in the first part of Equation 4.25.

One important point should be made about the motivation for the ply-by-ply stress analysis of a laminate. Being tensors, both stress and strain components are dependent on the reference coordinates. The components vary. It is difficult to say if the stress or strain is high or low, or safe or unsafe. For scalars, this is easy to do. If the temperature is 100°C, water boils. The most effective way of assessing the magnitudes of stress and strain is by their invariants, which, by definition, are scalars. When we discuss failure criteria, we will make a strong bid for using the quadratic failure criterion, which is a scalar criterion. The maximum stress and maximum strain criteria are not scalar criteria. Because of this and other basic flaws, they are not recommended.

TABLE 4.3 PLY-BY-PLY STRAIN AND STRESS VARIATIONS IN A LAMINATE

θ, degree	ϵ_1	ϵ_2	ϵ_6		σ_1	σ_2	σ_6
-45	0.29	-0.08	1.49		-51	-56	61
45	0.29	-0.08	1.49		76	71	78
90	0.29	-0.08	1.49		3	-15	11
0	0.29	-0.08	1.49		52	0	11
$\{\epsilon^o\}$	0.29	-0.08	1.49	$\{\sigma^o\}$	20	0	40

This numerical values are plotted in the following figures, where the ply layup, ply strains, and ply stresses are shown, respectively. The laminate stresses are also shown as a heavy vertical lines

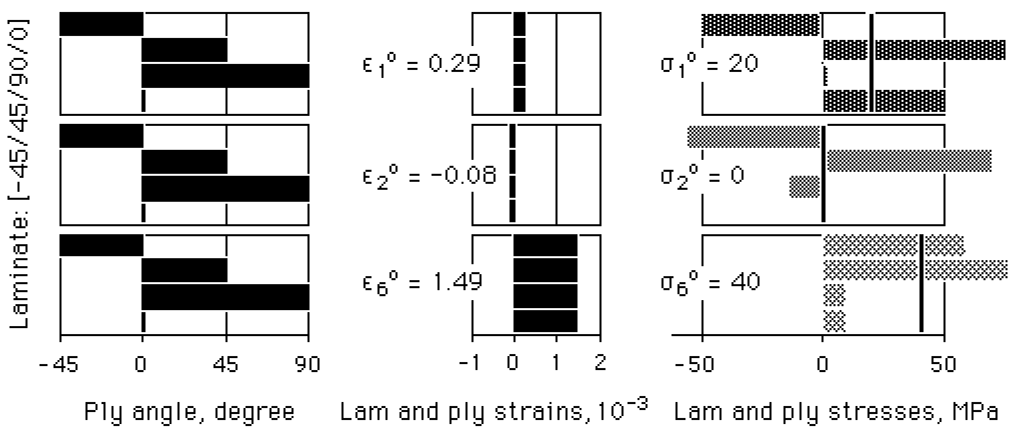

FIGURE 4.23 PLY-BY-PLY STRAIN AND STRESS DISTRIBUTIONS OF A LAMINATE

4.9 RESIDUAL STRESSES

Organic and inorganic matrix composites will have very complicated residual stresses after processing or curing. On the micromechanical level, processing or curing stresses are caused by the volumetric contraction of the matrix, the differential thermal contraction between the matrix and the fiber after cooldown, and non-uniform consolidation or solidification. For organic matrix composites, moisture is absorbed which introduces additional residual stresses. The effects of these stresses are difficult to assess and cannot be measured directly. The empirically measured ply strengths are very much affected by the residual stresses. The effects are, in fact, reflected in the measured strengths. Until reliable predictions of strength based on micromechanics become available, we will back-calculate residual stresses from the temperature-dependent strength data.

Another set of residual stresses originates from the macromechanical or laminate level. Because composite plies are anisotropic, the thermal expansion or contraction in the longitudinal direction is much less than that in the transverse direction. This differential contraction after cooldown, and expansion after moisture absorption will give rise to macromechanical residual stresses among plies in a multidirectional laminate. Using laminated plate theory, these stresses are relatively easy to calculate.

We are only concerned with the macromechanical residual stresses in this section. We assume that temperatures before and after curing and moisture absorbed after curing remain uniform across the laminate thickness. We can extend the theory to deal with a linearly varying temperature across a symmetric plate as a special case.

The stress-free expansion of a unidirectional ply is shown in the figure below. The free on-axis expansions of a ply are:

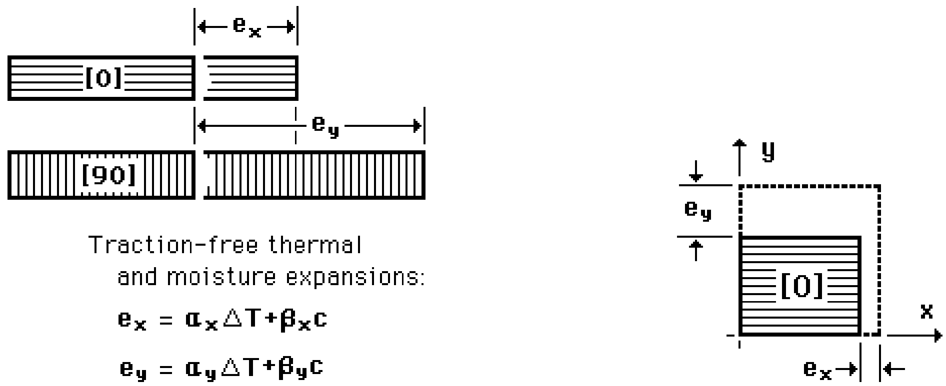

FIGURE 4.24 STRESS-FREE EXPANSIONS OF A UNIDIRECTIONAL PLY. THE REFERENCE STATE IS UNCURED PLIES AT CURE TEMPERATURE; THE EXPANDED STATE IS BASED ON DIFFERENCES IN TEMPERATURE AND MOISTURE CONTENT AFTER CURING

Strengths of unidirectional composites are commonly measured after cooldown and an anticipated exposure to moisture over a long period of time. While temperature is usually uniform within the composite, the moisture is almost always non-uniform. The slow diffusion of moisture is responsible for this non-uniformity. The measured strength or the corresponding ultimate strain is depicted in the figure below. The strain from the original stress-free state at the cure temperature must be the sum of the free expansion and the measured mechanically applied strain at room temperature.

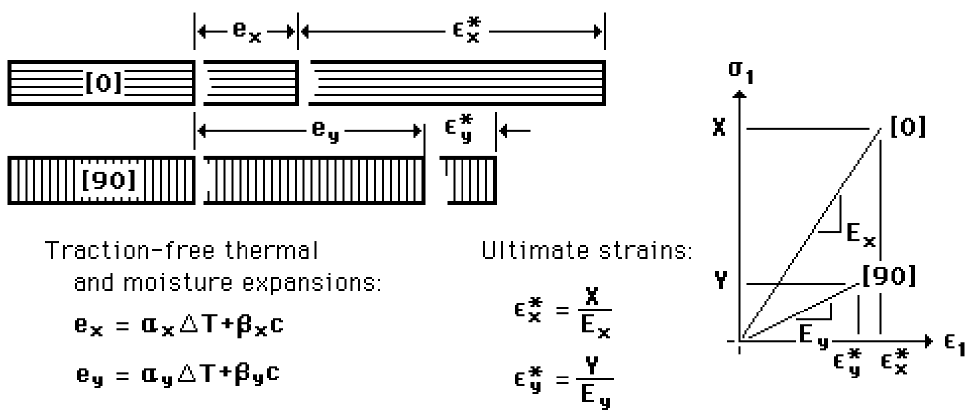

FIGURE 4.25 MEASURED ULTIMATE STRAINS AFTER FREE HYGROTHERMAL EXPANSION OR CONTRACTION

4.10 RESIDUAL STRAINS AFTER CURING

The curing of a multidirectional laminate induces macromechanical curing stresses. This is shown in the figure below. Although the laminate in this figure is a simple cross-ply, the principle is applicable to all laminates. The mathematical formulation in this section is approximate because the process of curing an organic matrix is in general time-dependent and nonlinear. We use only time-independent, linear theory. One simple way to compensate for this deficiency is to use the stress-free temperature in place of the actual cure temperature. We have found that the stress-free temperature can be as much as 50 degrees C below the cure temperature. The simplest method of determining the stress-free temperature is to observe the elevated temperature at which a warped unsymmetric laminate becomes flat.

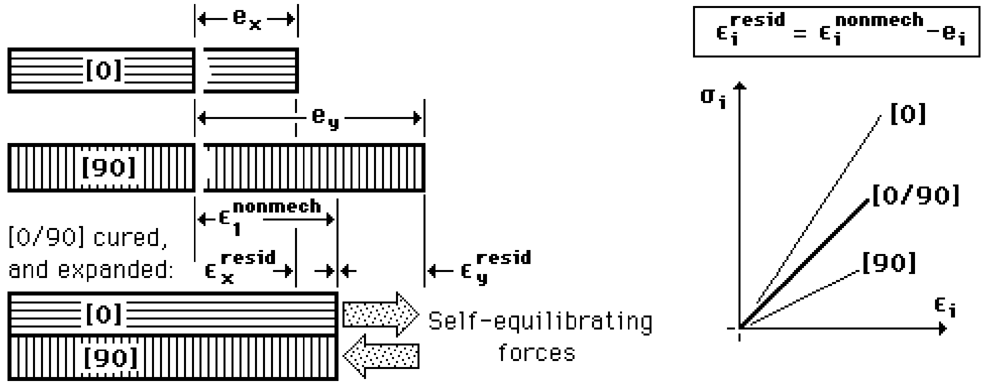

FIGURE 4.26 RELATION BETWEEN NONMECHANICAL, RESIDUAL, AND FREE EXPANSION STRAINS AS DEFINED BY THE EQUATION IN THE FIGURE. ALL STRAINS ARE IN-PLANE AND RELATIVE TO THE MATERIAL AXES. THE LAMINATE IS SYMMETRIC.

In order for the strain components to be additive in the figures above, they all must be in the on- or off-symmetry axes of the plies. The nonmechanical strain is the laminate strain measured from the stress-free state. The residual strain is simply the difference between the nonmechanical strain and the free expansion strain. We will now derive these strains from laminated plate theory.

The nonmechanical stresses are derived from the traction-free nonmechanical strains given in Figure 4.24 above:

$$\sigma_i^n = Q_{ij}e_j, \text{ when } i,j = x,y \text{ on the ply axes: } \sigma_x^n = Q_{xx}e_x+Q_{xy}e_y$$
$$\sigma_y^n = Q_{yx}e_x+Q_{yy}e_y \qquad (4.26)$$

For a on-axis orthotropic material, there is no nonmechanical shear stress.

The transformed nonmechanical stress from the ply- to the laminate-axis:

$$\sigma_1^n = p^n+q^n\cos 2\theta,\ \sigma_2^n = p^n-q^n\cos 2\theta,\ \sigma_6^n = q^n\sin 2\theta$$
$$\text{where } p^n, q^n = \frac{\sigma_x^n \pm \sigma_y^n}{2} = \frac{(Q_{xx}\pm Q_{xy})e_x+(Q_{xy}\pm Q_{yy})e_y}{2} \qquad (4.27)$$

We can now derive the nonmechanical stress components:

$$\sigma_{[1,2,6]}^{(o)n} = \frac{1}{h}\int_{-h/2}^{h/2}\sigma_{[1,2,6]}^{n}dz = \left[p^n+q^nV_1^*,\ p^n-q^nV_1^*,\ q^nV_3^*\right]$$
$$\text{where } V_1^* = \frac{1}{h}\int\cos 2\theta dz, \quad V_3^* = \frac{1}{h}\int\sin 2\theta dz \qquad (4.28)$$

If we limit this calculation to symmetric laminates, the nonmechanical in-plane strains shown in Figure 4.26 above are:

$$\epsilon_i^{(o)r} = \epsilon_i^{(o)n}-e_i,\ i = x,y,s \quad \text{where } \epsilon_i^{(o)n} = a_{ij}^*\sigma_j^{(o)n}$$
$$\epsilon_x^{(o)r} = \epsilon_x^{(o)n}-e_x,\ \epsilon_y^{(o)r} = \epsilon_y^{(o)n}-e_y,\ \epsilon_s^{(o)r} = \epsilon_s^{(o)n} \qquad (4.29)$$

The strains here are in the on- or material symmetry-axis, not in the laminate-axis.

For cross-ply laminates, we have the following unique relations, where nonmechanical stresses are hydrostatic in the plane of the laminate:

$$\text{For [0/90]}, V_1 = V_3 = 0,\ \sigma_1^{(o)n} = \sigma_2^{(o)n} = p^n,\ \sigma_6^{(o)n} = 0$$
$$\text{For [±45]}, V_1 = V_3 = 0,\ \sigma_1^{(o)n} = \sigma_2^{(o)n} = p^n,\ \sigma_6^{(o)n} = 0 \qquad (4.30)$$

To find the resulting strains, we need the compliances of both laminates. We take T300/5208 material, and assume that we have a -100°K temperature difference. Since the compliances for the laminates are equal, the resulting thermal strains are also hydrostatic, as shown in the equation below. The laminates are thermally isotropic.

$$\sigma_1^{(o)n} = p^n = -15.1 \text{ MPa} = \sigma_2^{(o)n},\ \ \sigma_6^{(o)n} = 0:\ \{\epsilon^o\}^n = [a^*]\{\sigma^o\}^n$$
$$\text{For [0/90]}, [a_{11}^* + a_{12}^*] = 10.41 - .31 = 10.10$$
$$\text{For [±45]}, [a_{11}^* + a_{12}^*] = 39.91 - 29.81 = 10.10$$
$$\text{For both [0/90] and [±45]}:\ \epsilon_1^o = [a_{11}^* + a_{12}^*]\sigma_1^o = -0.152 \times 10^{-3} = \epsilon_2^o \qquad (4.31)$$

The quasi-isotropy for hygrothermal properties is simpler to attain than the elastic moduli. The reason is that the hygrothermal are second rank tensors, and the latter, fourth rank tensors. Thus [0/90] are isotropic for hygrothermal properties, while equal ply orientation of [π/3], [π/4], and higher-order laminates are required to attain elastic isotropy. A cross-ply laminate of [0/90] is not isotropic elastically.

The residual strain is a function of temperature difference (usually negative) and moisture concentration. If both are zero, the residual strain is of course zero. If we have a unidirectional composite (without lamination), the residual strain is also zero.

If the operating temperature is equal to the cure temperature, there will be no residual strain due to curing. In this case, the residual strain due to moisture will be a linear function of the moisture concentration. If moisture concentration is zero, the residual strain will be a linear function of temperature difference. If both temperature and moisture are not zero, the residual strain will be nonlinear. This nonlinearity is important if we wish to calculate the "self-destruct" temperature or moisture level.

4.11 EXPANSION COEFFICIENTS

The effective in-plane expansion coefficients are formulated by setting either temperature or moisture at zero; i.e., the free expansion is computed by assuming that it is either due to temperature or moisture, but not both. Having the hygrothermal expansion coefficients, we can calculate the expansion strains as follows:

$$\epsilon_i^{(o)n} = \alpha_i^o \Delta T + \beta_i^o c, \ \text{where}\ \ \alpha_i^o = a_{ij}\int Q_{jk}\alpha_k dz,\ \beta_i^o = a_{ij}\int Q_{jk}\beta_k dz \qquad (4.32)$$

The thermal expansion coefficients can be obtained by integrating the nonmechanical stress using the method of the last sub-section. Free thermal expansions per degrees are by definition thermal expansion coefficients:

$$\alpha_i^o = \frac{1}{\Delta T}\epsilon_i^{(o)n} = \frac{1}{\Delta T} a_{ij}^* \sigma_j^{(o)n} = a_{ij}^*\left[p^n + q^n V_1^*,\ p^n - q^n V_1^*,\ q^n V_3^*\right]$$
$$\text{where}\ \ p^n, q^n = \frac{\sigma_x{}^n \pm \sigma_y{}^n}{2} = \frac{(Q_{xx} \pm Q_{xy})\alpha_x + (Q_{xy} \pm Q_{yy})\alpha_y}{2} \qquad (4.33)$$

The moisture expansion coefficients can be similarly integrated using the same method of the last sub-section where free moisture expansions are replaced by moisture expansion coefficients:

$$\beta_i^o = \frac{1}{c}\epsilon_i^{(o)n} = \frac{1}{c} a_{ij}^* \sigma_j^{(o)n} = a_{ij}^*\left[p^n + q^n V_1^*,\ p^n - q^n V_1^*,\ q^n V_3^*\right]$$
$$\text{where}\ \ p^n, q^n = \frac{\sigma_x{}^n \pm \sigma_y{}^n}{2} = \frac{(Q_{xx} \pm Q_{xy})\beta_x + (Q_{xy} \pm Q_{yy})\beta_y}{2} \qquad (4.34)$$

These laminate expansions can be positive, zero, or negative, and can induce shear by having a nonzero "6" component. By properly designing the laminate layup, unique expansion behavior is possible.

Hygrothermal expansion coefficients for typical composite materials are listed in the table below:

TABLE 4.4 TYPICAL HYGROTHERMAL EXPANSION COEFFICIENTS

Ply Material	T300/ 5208	B/ 5505	AS/ 3501	E-glass/ epoxy	Kevlar/ epoxy
α_x, μ/K	0.02	6.1	-0.3	8.6	-4.0
α_y, μ/K	22.5	30.3	28.1	22.1	79.0
β_x	0.0	0.0	0.0	0.0	0.0
β_y	0.6	0.6	0.44	0.6	0.6

4.12 SAMPLE CALCULATIONS IN EXPANSIONS

Sample 1: Find the free hygrothermal expansions of CFRP T300/5208 at room temperature (22°C), a moisture content of 0.005 or 0.5 percent, and a cure temperature of 122°C.

From Table 4.4 for T300/5208, the expansion coefficients are:

$$\left.\begin{array}{l} e_x = \alpha_x\Delta T+\beta_x c = 0.02\times10^{-6}\times(-100) = -2\times10^{-6} \\ e_y = \alpha_y\Delta T+\beta_y c = 22.5\times10^{-6}\times(-100)+0.6\times0.005 = 0.75\times10^{-3} \end{array}\right] \qquad (4.35)$$

Note that transverse expansion strain can be canceled when the following temperature/moisture combinations exist:

$$\left.\begin{array}{l} \text{At } c = 0.005,\ \Delta T = 0.6\times0.005/22.5\times10^{-6} = 133°K \\ \text{At } \Delta T = -100°K,\ c = 22.5\times10^{-6}\times100/0.6 = 0.00375 \end{array}\right] \qquad (4.36)$$

Sample 2: Find the nonmechanical stress and strain, and residual strain based on the inputs above for [0/90/45$_2$] (curing temperature difference only).

The stiffness and compliance of this laminate can be found in Sub-Section 4.6, Sample 4 on page 4-11, and will not be repeated here. From Equations 4.28,

$$\left.\begin{array}{l} V_1^* = (1/h)\int\cos2\theta dz = [\cos0+\cos180+2\cos90]/4 = 0 \\ V_3^* = (1/h)\int\sin2\theta dz = [\sin0+\sin180+2\sin90]/4 = 0.5 \end{array}\right] \qquad (4.37)$$

Substituting the free expansion strains in Equations 4.35 into 4.28:

$$\left.\begin{array}{l} \sigma_1^{(o)n} = p^n+q^nV_1^* = -15.1 \text{ MPa} \\ \sigma_2^{(o)n} = p^n-q^nV_1^* = -15.1 \text{ MPa} \\ \sigma_6^{(o)n} = q^nV_3^* = 4.1 \text{ MPa} \end{array}\right] \qquad (4.38)$$

The nonmechanical strain can be found using Equations 4.29:

$$\{\varepsilon^o\}^n = [a^*]\{\sigma^o\}^n = \{-0.283,\ -0.283,\ 0.604\}\times 10^{-3} \tag{4.39}$$

The residual strain is found using the same equations, or for the on-axis 0-degree ply, subtracting Equation 4.35 from the last equation:

$$\{\varepsilon\}^{(0)r} = \{\varepsilon^{(0)n} - e\} = \{-0.281,\ 1.97,\ 0.604\}\times 10^{-3} \tag{4.40}$$

For the on-axis 90-degree ply we must first transform Equation 4.39 before we subtract the free expansions:

$$\begin{aligned} &\{\varepsilon\}^{(90)n} = \{-0.283,\ -0.283,\ -0.604\}\times 10^{-3} \\ &\{\varepsilon\}^{(90)r} = \{\varepsilon^{(90)n} - e\} = \{-0.281,\ 1.97,\ -0.604\}\times 10^{-3} \end{aligned} \tag{4.41}$$

For the on-axis 45-degree ply we must transform the nonmechanical strain, then subtract the expansion strain:

$$\{\varepsilon\}^{(45)r} = \{\varepsilon^{(45)n} - e\} = \{0.0209,\ 1.66,\ 0\}\times 10^{-3} \tag{4.42}$$

Sample 3: Find the effective thermal expansion coefficients of $[0/90/45_2]$.

The thermal expansion coefficients can be obtained by using Equation 4.32, or by finding the nonmechanical strain due to one degree temperature change. We will show the latter method. For one degree change in temperature:

$$\begin{aligned} &e_x = \alpha_x \times 1 = 0.02\times 10^{-6}, \quad e_y = \alpha_y \times 1 = 22.5\times 10^{-6} \\ &p^n = [(Q_{xx}+Q_{xy})\alpha_x + (Q_{xy}+Q_{yy})\alpha_y]/2 = 0.151\ \text{MPa} \\ &q^n = [(Q_{xx}-Q_{xy})\alpha_x + (Q_{xy}-Q_{yy})\alpha_y]/2 = -0.082\ \text{MPa} \end{aligned} \tag{4.43}$$

From Equation 4.28 and the V's in Equation 4.37:

$$\{\sigma^o\}^n = \{0.151,\ 0.151,\ -0.041\}\ \text{MPa} \tag{4.44}$$

The nonmechanical strain per one degree is the thermal expansion coefficient. Thus from Equation 4.29:

$$\{\alpha^o\} = \{\varepsilon^o\}^n = [a^*]\{\sigma^o\}^n = \{2.83,\ 2.83,\ -6.04\}\times 10^{-6} \tag{4.45}$$

Sample 4: Find the effective moisture expansion coefficients of $[0/90/45_2]$.

Moisture expansion coefficients can be obtained by finding the nonmechanical strain due to a unit change. For a 100 percent change moisture:

$$\begin{aligned} &e_x = \beta_x \times 1 = 0, \quad e_y = \beta_y \times 1 = 0.6 \\ &p^n = [(Q_{xx}+Q_{xy})\beta_x + (Q_{xy}+Q_{yy})\beta_y]/2 = 3970\ \text{MPa} \\ &q^n = [(Q_{xx}-Q_{xy})\beta_x + (Q_{xy}-Q_{yy})\beta_y]/2 = -2230\ \text{MPa} \end{aligned} \tag{4.46}$$

From Equation 4.28, the V's in Equation 4.37, and Equation 4.31:

$$\begin{aligned} &\{\sigma^o\}^n = \{3970,\ 3970,\ -1120\}\ \text{MPa} \\ &\{\beta^o\} = \{\varepsilon^o\}^n = [a^*]\{\sigma^o\}^n = \{7.51,\ 7.51,\ -1.61\}\times 10^{-2} \end{aligned} \tag{4.47}$$

The nonmechanical strain per 100 percent moisture absorption is by definition the moisture expansion coefficient.

Comparing the moisture expansion coefficients with the thermal coefficients in Equation 4.45, the former is four orders of magnitude higher than the latter. This is expected because moisture absorption is about 1 percent, and the temperature difference between room and cure is about -100. There is a factor of 10,000. Thus moisture expansion of the laminate is about the same magnitude as that of temperature and opposite in sign. One offsets the other under room temperature and a long period time (so moisture can be absorbed).

4.13 SELECTION OF LAMINATE STIFFNESS BY LAMRANK

In Sub-Section 4.6 we showed the variation of laminate stiffness as a function of ply orientations. This is one feature of composite materials that allows us to match precisely the desired laminate stiffness. One fast way of selecting the best laminates for a set of conditions is by the laminate ranking method, or LamRank for short. With personal computers, sorting is a built-in feature, and is easy to use. We will show some results of LamRank in this section.

For the present purpose, we use only symmetric laminates. The maximum number of each laminate family in terms of ply number and ply angles are listed in the table below:

TABLE 4.5 NUMBER OF SUBLAMINATES IN A FAMILY FOR GIVEN NUMBER OF PLIES AND PLY ORIENTATIONS; A GRAND TOTAL OF 12339 MEMBERS OF ALL FAMILIES BELOW

Plies in Sub-laminates	Family using 2 ply angles	Family using 3 ply angles	Family using 4 ply angles	Family using 5 angles	Family of 6 angles
2	3	6	10	15	21
3	4	10	20	35	56
4	5	15	35	70	126
5	6	21	56	126	252
6	7	28	84	210	462
7	8	36	120	330	792
8	9	45	**165**	495	1287
9	10	55	220	715	2002
10	11	66	286	1001	3003
Total	63	282	996	2997	8001
Cumul total	63	345	1341	4338	12339

We recommend that a family of laminates be defined in terms of the number of plies, and the number of ply angles. We further recommend that we limit our laminates to a maximum of ten plies. The basic ply group is called a sub-laminate. For a total laminate, we recommend the use of repeated sublaminates to reach the desired thickness. The are many advantages to using sub-laminates to build a thick total laminate.

- The total laminate is finely dispersed, or spliced. Such a laminate is resistant to delamination.
- It is simpler to design because the combinations of plies having discrete angle is limited, i.e., less than 10. Optimization becomes much simpler to achieve.
- When there are a large number of repeated sublaminates, the total laminate is homogenized. The optimized laminate for in-plane loading is the same for flexural loading.

TABLE 4.6 SUMMARY OF 165 SUBLAMINATES WITH 8 PLIES AND 4 ANGLES

No.	Code	QUADRI-	No.	Code	QUADRI-	No.	Code	QUADRI-	No.	Code	QUADRI-
1	0008	1 Ortho	43	0701	2 Aniso	85	2033	3 Ortho	127	3320	3 Aniso
2	0017	2 Aniso	44	0710	2 Aniso	86	2042	3 Aniso	128	3401	3 Aniso
3	0026	2 Aniso	45	0800	1 Ortho	87	2051	3 Aniso	129	3410	3 Aniso
4	0035	2 Aniso	46	1007	2 Aniso	88	2060	2 Aniso	130	3500	2 Ortho
5	0044	2 Ortho	47	1016	3 Aniso	89	2105	3 Aniso	131	4004	2 Aniso
6	0053	2 Aniso	48	1025	3 Aniso	90	2114	4 Aniso	132	4013	3 Aniso
7	0062	2 Aniso	49	1034	3 Aniso	91	2123	4 Aniso	133	4022	2 Ortho
8	0071	2 Aniso	50	1043	3 Aniso	92	2132	4 Aniso	134	4031	3 Aniso
9	0080	1 Ortho	51	1052	3 Aniso	93	2141	4 Aniso	135	4040	2 Aniso
10	0107	2 Aniso	52	1061	3 Aniso	94	2150	3 Aniso	136	4103	3 Aniso
11	0116	3 Aniso	53	1070	2 Aniso	95	2204	3 Aniso	137	4112	4 Aniso
12	0125	3 Aniso	54	1106	3 Aniso	96	2213	4 Aniso	138	4121	4 Aniso
13	0134	3 Aniso	55	1115	4 Aniso	97	2222	**4 Q-iso**	139	4130	3 Aniso
14	0143	3 Aniso	56	1124	4 Aniso	98	2231	4 Aniso	140	4202	3 Aniso
15	0152	3 Aniso	57	1133	4 Ortho	99	2240	3 Aniso	141	4211	4 Aniso
16	0161	3 Aniso	58	1142	4 Aniso	100	2303	3 Aniso	142	4220	3 Aniso
17	0170	3 Aniso	59	1151	4 Aniso	101	2312	4 Aniso	143	4301	3 Aniso
18	0206	3 Aniso	60	1160	3 Aniso	102	2321	4 Aniso	144	4310	4 Aniso
19	0215	3 Aniso	61	1205	3 Aniso	103	2330	3 Aniso	145	4400	2 Ortho
20	0224	3 Aniso	62	1214	4 Aniso	104	2402	3 Aniso	146	5003	2 Aniso
21	0233	3 Ortho	63	1223	4 Aniso	105	2411	4 Ortho	147	5012	3 Aniso
22	0242	3 Aniso	64	1232	4 Aniso	106	2420	3 Aniso	148	5021	3 Aniso
23	0251	3 Aniso	65	1241	4 Aniso	107	2501	3 Aniso	149	5030	2 Aniso
24	0260	2 Aniso	66	1250	3 Aniso	108	2510	3 Aniso	150	5102	3 Aniso
25	0305	2 Aniso	67	1304	3 Aniso	109	2600	2 Ortso	151	5111	4 Aniso
26	0314	3 Aniso	68	1313	4 Aniso	110	3005	2 Aniso	152	5120	3 Aniso
27	0323	3 Aniso	69	1322	4 Ortho	111	3014	3 Aniho	153	5201	3 Aniso
28	0332	3 Aniso	70	1331	4 Aniso	112	3023	3 Aniso	154	5210	3 Aniso
29	0341	3 Aniso	71	1340	3 Aniso	113	3032	3 Aniso	155	5300	2 Ortho
30	0350	2 Aniso	72	1403	4 Aniso	114	3041	3 Aniso	156	6002	2 Aniso
31	0404	2 Aniso	73	1412	4 Aniso	115	3050	2 Aniso	157	6011	3 Aniso
32	0413	3 Aniso	74	1421	4 Aniso	116	3104	4 Aniso	158	6020	2 Aniso
33	0422	3 Aniso	75	1430	3 Aniso	117	3113	4 Aniso	159	6101	3 Aniso
34	0431	3 Aniso	76	1502	4 Aniso	118	3122	4 Ortso	160	6110	3 Aniso
35	0440	2 Aniso	77	1511	4 Ortho	119	3131	4 Aniho	161	6200	2 Ortho
36	0503	3 Aniso	78	1520	3 Aniso	120	3140	3 Aniso	162	7001	2 Aniso
37	0512	3 Aniso	79	1601	3 Aniso	121	3203	3 Aniso	163	7010	2 Aniso
38	0521	3 Aniso	80	1610	3 Aniso	122	3212	4 Aniso	164	7100	2 Ortho
39	0530	2 Aniso	81	1700	2 Ortho	123	3221	4 Aniho	165	8000	1 Ortho
40	0602	3 Aniso	82	2006	2 Aniso	124	3230	3 Aniso			
41	0611	3 Ortho	83	2015	3 Aniso	125	3302	3 Aniso			
42	0620	2 Aniso	84	2024	3 Aniso	126	3311	3 Aniso			

It is useful to examine the range of variability of the laminate stiffnesses by LamRank. We use a simple laminate code for this purpose. If we limit ourselves to 4-angle families and keep the number of sublaminates below 10, we can have a 4-digit laminate code as follows:

[5111] designates 5 plies of the first angle, 1 each of the next three angles.

If we defined our angles are those of a [π/4] family, we would assign [0] for the first angle, [90], [45] and [-45] for the next three angles. The 4-digit code is easy to remember. The sum of the four digits would be the number of plies of the sub-laminate. In the example here, we have an 8-ply, [π/4] family. There are a total of 165 laminates in this family, and it high-lighted in Table 4.5 above. Each individual member of this family of laminates are listed in Table 4.6. The number of angles and the type of symmetry for each laminate are also identified in the table. For example, [5111] is listed as number 151, has four angles, and is anisotropic. As the size of the family increases, more variation in laminate properties is possible. We have found that the family of 4 angle and 8-ply sub-laminates.

It is very easy to rank the Young's modulus of this family of laminates. Typical results in a decreasing order of stiffness for T300/5208 are shown below. The range is anchored by the longitudinal stiffness of a unidirectional ply and its quasi-isotropic laminate, which is the lower bound stiffness recommended for design.

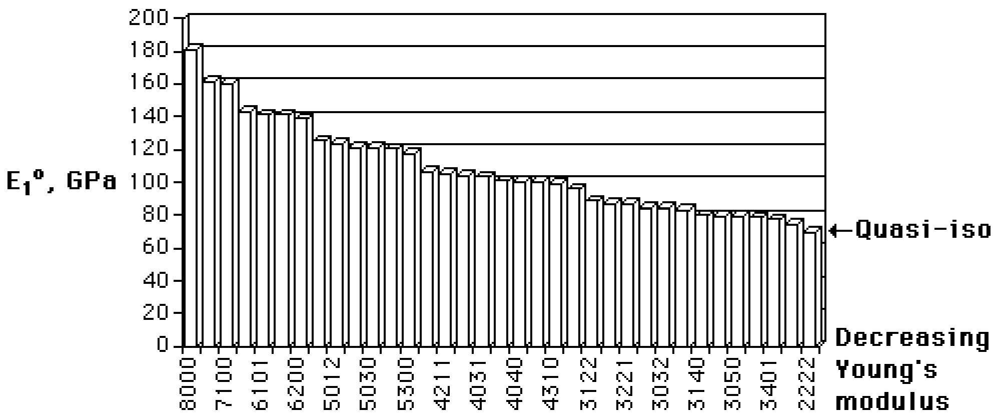

FIGURE 4.27 DECREASING YOUNG'S MODULUS OF [π/4] LAMINATES OF T300/5208

Similarly, we rank the laminates for decreasing shear modulus between the [±45] and the quasi-isotropic laminate.

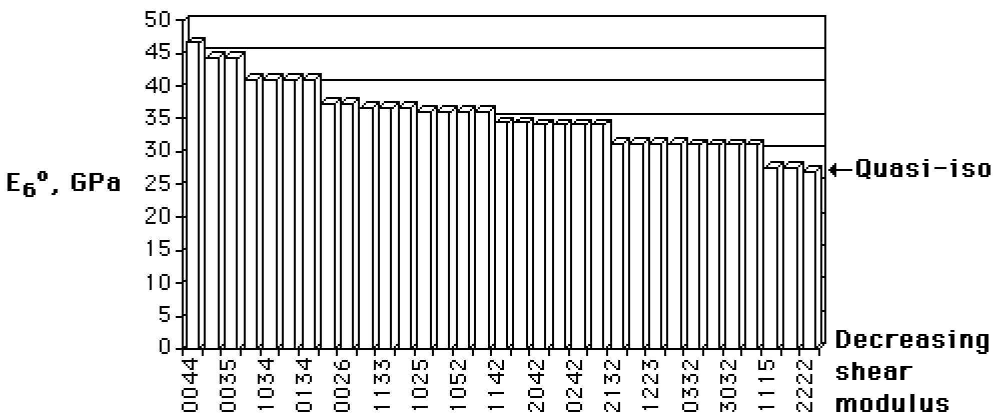

FIGURE 4.28 DECREASING SHEAR MODULUS OF [π/4] LAMINATES OF T300/5208

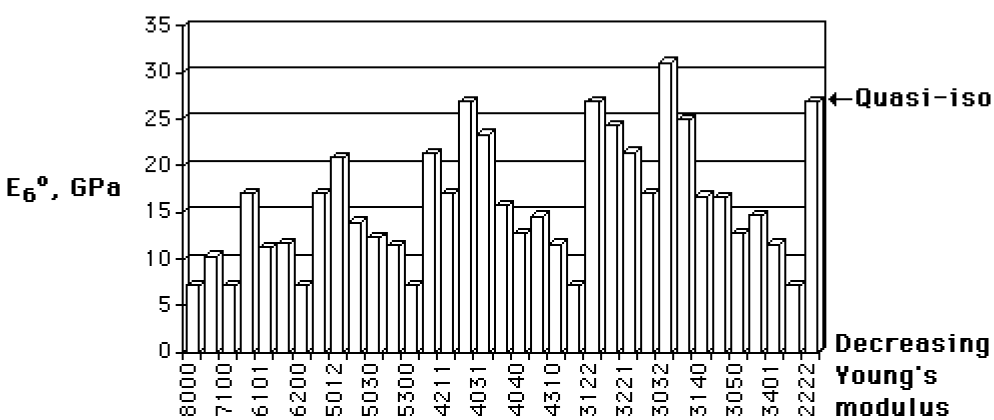

FIGURE 4.29 SHEAR MODULUS VARIATION VERSUS DECREASING YOUNG'S MODULUS

In Figure 4.29, we combine the previous two figures, Figures 4.27 and 4.28, to show how the shear modulus varies as the Young's modulus is ranked in decreasing order. Although a general trend does not exist, it is a simple task to rank laminates by whatever criterion we wish to make. We can as easily rank ratios of the Young's and shear moduli if we desire.

Ranking of laminates by thermal expansion coefficients may also be useful. In the figure below we show the expansion from the lowest value of laminate [6011] to the quasi-isotropic laminate. We rank only one expansion component at a time. As with stress, there are two other components: the 2- or transverse; and the 6- or shear components. The same invariants exist as for stress. Thus, the sum of the two normal components form the first invariant. For T300/5208, this invariant has a value of 22.52. When the figure below shows an increasing order of the first normal component, the second normal component will be in a decreasing order. Each component will have the value of the difference between the first invariant and the first component.

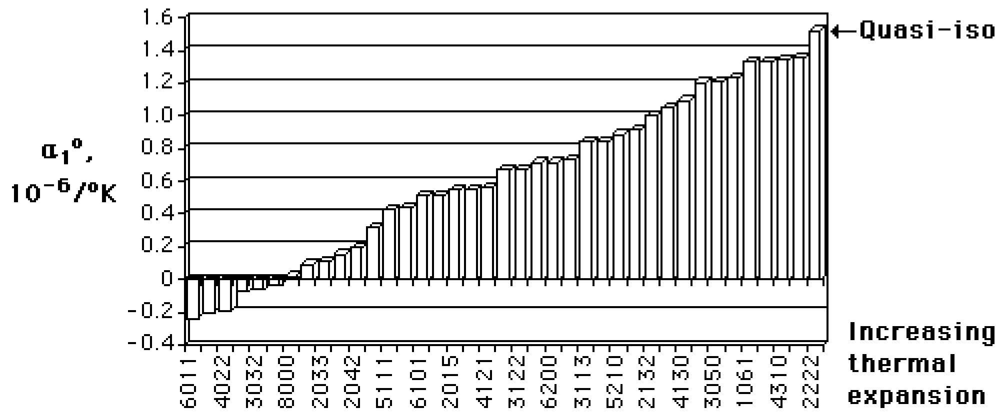

FIGURE 4.30 INCREASING THERMAL EXPANSION UP TO THE QUASI-ISOTROPIC OF [π /4] LAMINATES OF T300/5208

In the figure below, we show an increasing order of the thermal expansion from the quasi-isotropic laminate up to the unidirectional ply. This figure is a continuation of the previous figure. We also show along the vertical axis on the right-hand-side the expansion coefficients of three common metals. To minimize differential thermal stresses in a bonded joint, we can match the thermal expansion along the 1-axis between this composite material, and steel or titanium. This matching is not possible with aluminum. It should be cautioned that matching one component leaves the other components unmatched. For nonorthotropic laminates, the shear components are not zero. This can be very detrimental for bonded joints.

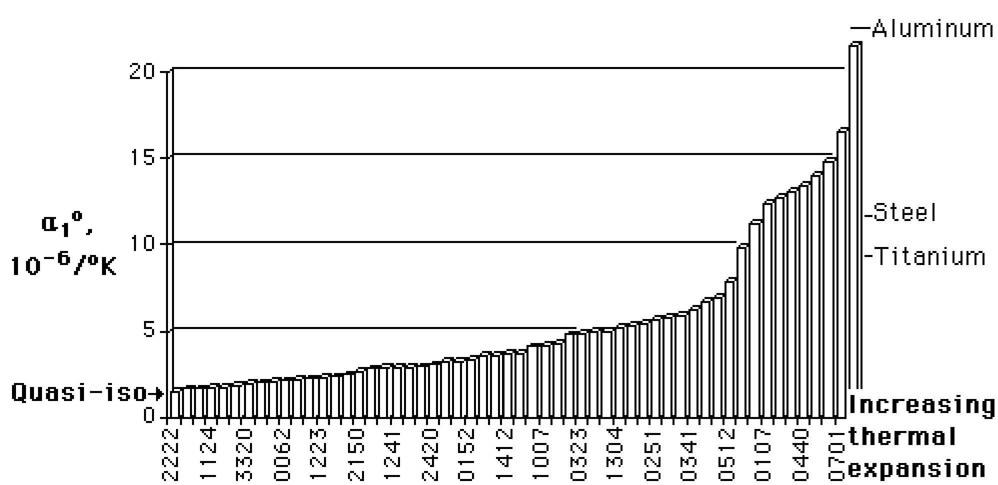

FIGURE 4.31 INCREASING THERMAL EXPANSION FROM THE QUASI-ISOTROPIC OF [π/4] LAMINATES OF T300/5208

Ranking is a powerful approach not only for the laminate stiffness but also laminate strength. In case of multiple loading conditions, laminate ranking provides a fast method of selecting the top laminates. The resulting laminates so selected and ranked are not always intuitively obvious. Thus, we recommend the ranking approach for designing laminates for stiffness, expansion, strength, energy absorption, and other combinations of conditions.

4.14 CONCLUSIONS

It is useful to emphasize that the most effective analysis and design of composite laminates is based on laminated plate theory. The simplest version of this theory is the in-plane behavior, outlined in this section. This represents the minimum level of skill that is required to fully appreciate not only the superior structural performance but also the unique features of composite materials.

The effective stiffness of a laminate is the average plane stress stiffness **[Q]** of the plies. The laminate compliance is the inverse of the stiffness. Effective engineering constants are then determined from the components of the compliance. This pattern is the same for the ply properties. As we will see later, the same pattern holds for the flexural behavior. Because of the matrix inversion, it is not possible to guess the effective engineering constants of a laminate by simply observing the ply composition.

Ply-by-ply stress and strain analysis is the first step toward the investigation of the failure mechanisms and strength of a laminate. It is difficult to assess the value of stress and strain because each has 3 components, and they change with the reference coordinate system. As we will see later, finding the invariants is a more basic step for making a value judgment as to whether or not a ply has failed.

The hygrothermal expansion coefficients are important to determine the residual stresses in a laminate resulting from curing, and absorption of moisture. The residual stress calculation is a simple extension of laminated plate theory. We recommend that these residual stresses be included in the analysis and design of composite structures.

For designing laminates with certain stiffness capability, the are constrained by the invariants of the ply material. The number of ply angles are design options. We prefer laminates with as few angles as possible. Such laminates are easier to select, lower in fabrication cost, stronger because there are fewer plies to fail, and less prone to delamination because the laminates are more homogenized. These guidelines are counter to some accepted practice of the use of balanced laminates only, the preference of tri- or quadri-directional laminates, and the 10-percent rule (which requires a minimum of 10 percent of the total plies to have each ply orientation.)

4.15 PROBLEMS

Prob. 4.1 Compute the ply stress components of the following laminate of T300/5208, subjected to an in-plane stress of {20,0,40} MPa.

Laminate: $[-45/45/0_2]$ σ_i^o = **{20,0,40}** MPa Material: T300/5208

θ, degree	ε_1	ε_2	ε_6		σ_1	σ_2	σ_6
-45	0.19	-0.13	1.49		**?**	**?**	**?**
45	0.19	-0.13	1.49		**?**	**?**	**?**
0_2	0.19	-0.13	1.49		**?**	**?**	**?**
$\{\varepsilon^o\}$	0.19	-0.13	1.49	$\{\sigma^o\}$	**?**	**?**	**?**

FIGURE 4.32 LAMINATE STRAINS AND PLY STRESS CALCULATIONS

Prob. 4.2 Show that [π/3], [π/4], . . . are isotropic in laminate stiffness but not [π/2]. Show that [π/2] is isotropic in expansional coefficients.

Prob. 4.3 Which is a better representation: a 2-d plot of carpet plot in Figure 4.10 or the following 3d plot?

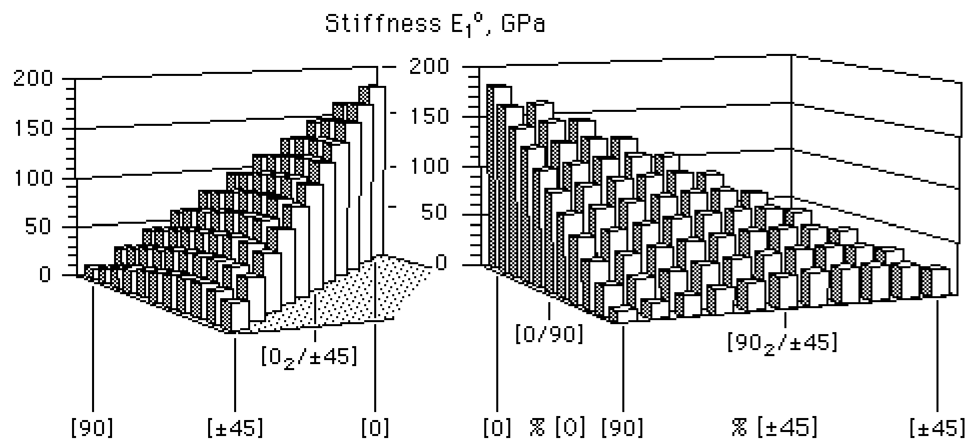

FIGURE 4.33 TWO VIEWS OF 3-D CARPET PLOT FOR T300/5208 LAMINATES

Prob. 4.4 Given the following Poisson's ratios of various T300/5208 laminates, can the large range of these values be rationalized?

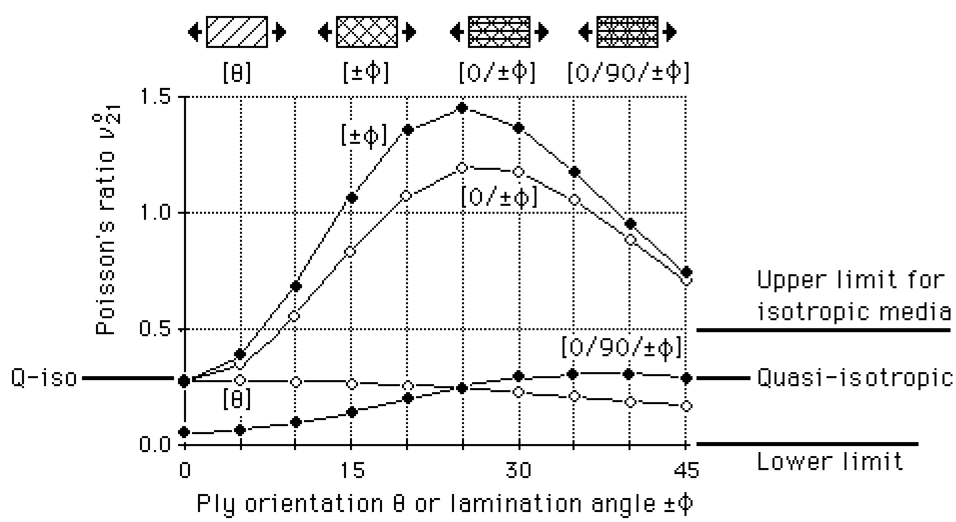

FIGURE 4.34 EFFECTIVE POISSON'S RATIOS OF VARIOUS T300/5208 LAMINATES

Prob. 4.5 Shear modulus of a unidirectional ply is often calculated from test data of a [±45] laminate. What measurements are needed during the test? How can shear modulus be calculated? Under what conditions does uniaxial tensile and compressive tests yield the same shear modulus?

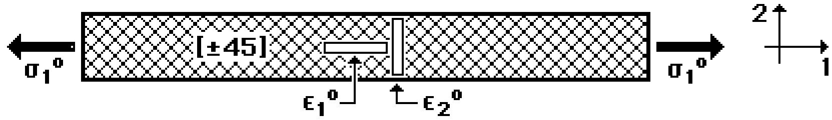

$$\sigma_s = \frac{\sigma_1{}^o}{2},\ \epsilon_s = \epsilon_1{}^o - \epsilon_2{}^o,\ E_s = \frac{\sigma_s}{\epsilon_s} = \frac{\sigma_1{}^o}{2(\epsilon_1{}^o - \epsilon_2{}^o)}$$

FIGURE 4.35 [±45] LAMINATED COUPON FOR SHEAR MODULUS DETERMINATION

Prob. 4.6 **Given the thermal expansion data shown in the figure below, can you show graphically:**

1) What is the expansion coefficient in the 2-direction?

2) What is the expansion coefficients of [0/90]?

3) Are expansion invariants similar to those of strain or stress; see Equation 2.36 on page 2-20?

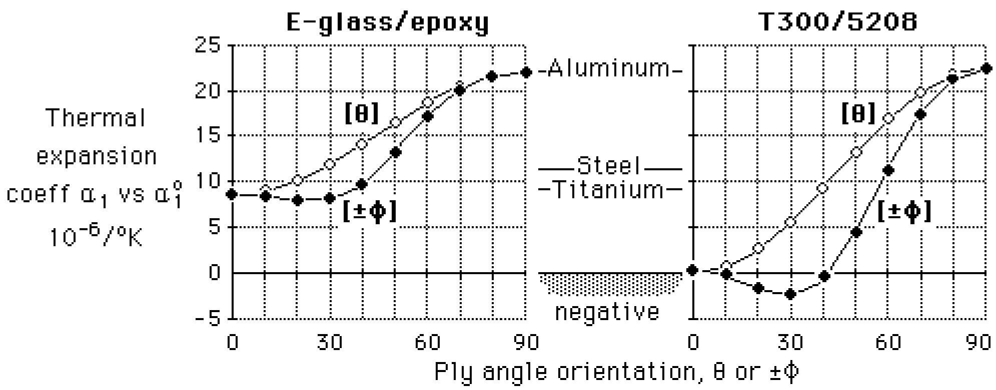

FIGURE 4.36 THERMAL EXPANSION ALONG THE 1-AXIS OF E-GLASS/EPOXY AND T300/5208

Prob. 4.7 **Matching thermal expansions of composite materials with metals in one direction is easy, for example, see Figure 4.34. If steel and titanium are bonded to the composites the other two expansion coefficients will not match those of the metals. Residual stresses can be significant. What would be the best solution to eliminate these stresses?**

Prob. 4.8 **Based on the hygrothermal data listed in Table 4.4 on page 4-19, is it possible to offset curing stresses by moisture absorption? Assuming a curing temperature is 100 degree C above room temperature,**

1) What would be the optimum moisture content for various composite materials, listed in Table 4.4, to have minimum curing stresses?

2) What would be the conditions if these stresses are to be eliminated completely?

3) What happens to curing stresses if composite materials are used in space?

4) What happens if they are used in cryogenic temperatures?

Prob. 4.9 **If a laminate designed to have a zero thermal expansion, does it automatically have a zero moisture expansion?**

Section 5

FLEXURAL STIFFNESS OF SYMMETRIC LAMINATES

Flexural stiffness of laminates depends on the stacking sequence of plies. As before, the normalization of the flexural stress-strain relations is a simple method of describing the behavior of the laminate. Homogenization of laminates will not only increase the strength and toughness, but will also simplify the design.

5.1 LAMINATED PLATE THEORY

Classical assumptions analogous to those used in the in-plane behavior of a laminate are:

- The laminate is symmetric.
- The laminate is thin: **h** << **a**, **b**, where **h** = thickness, **a** = length, and **b** = width.
- Ply and laminate strains are linear functions of the thickness coordinate **z**.
- The normal to the mid-plane of the laminate remains normal, without deformation by bending and stretching. It can only rotate like a rigid body.

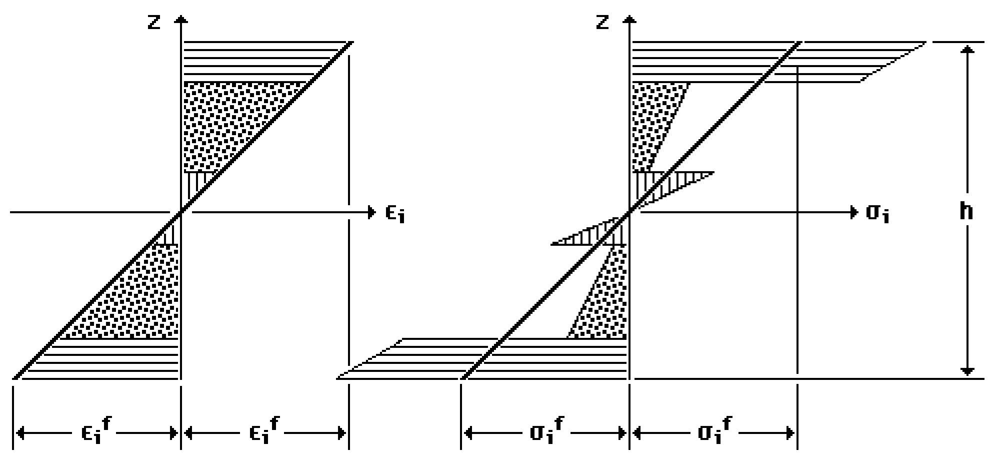

FIGURE 5.1 ASSUMED LINEAR FLEXURAL STRAIN AND STRESS DISTRIBUTIONS

With the assumption of laminated plate theory we can define the following displacements, strains, curvatures, and flexural strains, respectively:

$$
\begin{aligned}
&\text{Displacements: } \mathbf{u} = -z\frac{\partial w}{\partial x},\ \mathbf{v} = -z\frac{\partial w}{\partial y},\ \mathbf{w} = \mathbf{w}(x,y)\\
&\text{Strains:}\\
&\quad \epsilon_1 = \frac{\partial u}{\partial x} = -z\frac{\partial^2 w}{\partial x^2},\ \epsilon_2 = \frac{\partial v}{\partial y} = -z\frac{\partial^2 w}{\partial y^2},\ \epsilon_6 = \frac{\partial u}{\partial y} + \frac{\partial v}{\partial x} = -2z\frac{\partial^2 w}{\partial x \partial y}\\
&\text{Curvatures: } k_1 = -\frac{\partial^2 w}{\partial x^2},\ k_2 = -\frac{\partial^2 w}{\partial y^2},\ k_6 = -2\frac{\partial^2 w}{\partial x \partial y}\\
&\text{Flexural strains: } \epsilon_1{}^f = \frac{h}{2}k_1,\ \epsilon_2{}^f = \frac{h}{2}k_2,\ \epsilon_6{}^f = \frac{h}{2}k_6
\end{aligned}
\tag{5.1}
$$

Displacements **u** and **v** at the mid-plane are zero. The flexural strains are normalized curvatures, and they are defined by the strains at the top and bottom surfaces of the laminate. For symmetric laminates under bending, the surface strains are equal in value and opposite in sign.

As we have pointed out in earlier sections, the sign conventions are more important in understanding composite materials than in the conventional materials which are usually isotropic. When there is no directionally dependent behavior, the signs of stress and strains are immaterial. For composite materials, an incorrect guess of the sign can lead to unconservative designs. The most difficult signs are those related to shear stress and shear strain for the in-plane behavior. For bending, the twisting moment and twisting curvature are also sources of confusion. In defining moment, flexural stress, laminate flexural stiffness, and effective engineering constants, a consistent sign convention must be followed. We prefer to use the convention illustrated in the figure below:

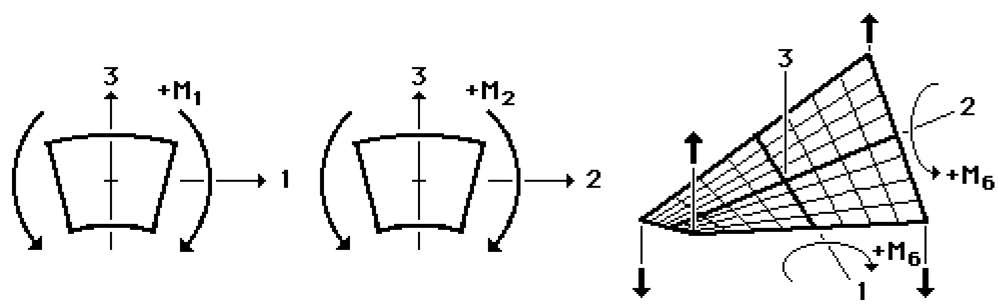

FIGURE 5.2 SIGN CONVENTION FOR MOMENTS (ALL COMPONENTS SHOWN ARE POSITIVE)

In this sign convention, the shear stress in the positive face of the first quadrant is positive. The corner in that quadrant as well as the third quadrant would move in the negative direction along the 3-axis. With the assumptions of laminated plate theory stated earlier, we can define the following integrated variables:

$$
\begin{aligned}
&\{\epsilon\} = z\{k\},\ \epsilon_i = zk_i,\ i, j = 1,2,6\\
&\{M\} = \int_{-h/2}^{h/2}\{\sigma\}z\,dz = \int_{-h/2}^{h/2}[Q]\{\epsilon\}z\,dz = \left[\int_{-h/2}^{h/2}[Q]z^2dz\right]\{k\} = [D]\{k\},\ \text{in N}\\
&[D] = \int_{-h/2}^{h/2}[Q]z^2dz,\ [D^*] = \frac{12}{h^3}[D],\ \text{in Pa; } [d] = [D]^{-1},\ [d^*] = \frac{h^3}{12}[d],\ \text{in Pa}^{-1}\\
&\{\sigma^f\} = \frac{6}{h^2}\{M\} = [D^*]\{\epsilon^f\};\quad \{\epsilon^f\} = \frac{h}{2}\{k\} = [d^*]\{\sigma^f\}
\end{aligned}
\tag{5.2}
$$

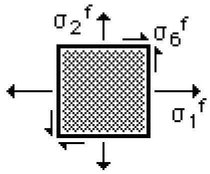

$$\begin{Bmatrix} \sigma_1^f \\ \sigma_2^f \\ \sigma_6^f \end{Bmatrix} = \begin{bmatrix} D_{11}^* & D_{12}^* & D_{16}^* \\ D_{21}^* & D_{22}^* & D_{26}^* \\ D_{61}^* & D_{62}^* & D_{66}^* \end{bmatrix} \begin{Bmatrix} \epsilon_1^f \\ \epsilon_2^f \\ \epsilon_6^f \end{Bmatrix}$$

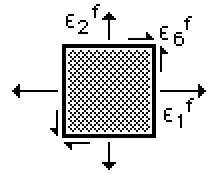

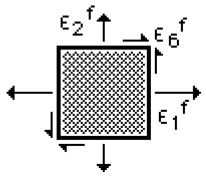

$$\begin{Bmatrix} \epsilon_1^f \\ \epsilon_2^f \\ \epsilon_6^f \end{Bmatrix} = \begin{bmatrix} d_{11}^* & d_{12}^* & d_{16}^* \\ d_{21}^* & d_{22}^* & d_{26}^* \\ d_{61}^* & d_{62}^* & d_{66}^* \end{bmatrix} \begin{Bmatrix} \sigma_1^f \\ \sigma_2^f \\ \sigma_6^f \end{Bmatrix} \quad (5.3)$$

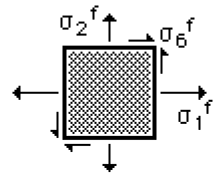

STRESS-STRAIN RELATIONS

Normalization factors analogous to those used in the in-plane behavior of laminates are used to simplify the identity and magnitude of stress, strain, stiffness and compliance matrices of a laminate under bending and twisting. The resulting stress-strain relations are shown in Equation 5.3.

Once the flexural strain (defined as the surface strain) is determined, the interior strain is simply a linear ratio drawn between the outer surfaces and the mid-plane. Ply stresses, on the other hand, are piece-wise linear, shown on the right of Figure 5.1. The stresses are obtained by using the stress-strain relation of each ply with the correct ply angle. In the examples in this book, we prefer to conduct strength analysis using strain as the variable. It is therefore not necessary to know the ply stress. The use of strain eliminates the extra ply-by-ply stress calculation.

In the figure below, a 400-ply thick cross-ply laminate is subjected to both in-plane force of 10 MN/m, and bending of 1 MN. It is difficult to compare the relative magnitudes of the two applied forces which have different units. The easiest way would be to use normalized forces such as the in-plane and flexural stresses, where the ratio is 1:12. We can also compare the in-plane versus flexural strains, where the ratio is 1:9, and the relative Young's and shear moduli.

	θ_1	θ_2		Ply mat	T3/N52[SI]	
[angle, θ_i]	**0.0**	**90.0**	[repeat]	h, #	h, E-3	
[ply#]	**50**	**50**	**2.0**	400	50.00	$[0_{50}/90_{50}]_{2s}$
	{N}MN/m	$\{\sigma^o\}$	$\{\epsilon^o\}$	$\{E^o\}$		$\{\epsilon^o\} = [a^*]\{\sigma^o\}$
1	**10.00**	200.	2.08	91.8		
2	**0.00**	0.	-0.06	91.8		
6	**0.00**	0.	0.00	1.5		
	{M} MN	$\{\sigma^f\}$	$\{\epsilon^f\}$	$\{E^f\}$		$\{\epsilon^f\} = [d^*]\{\sigma^f\}$
1	**1.00**	2400.	18.74	125.2		
2	**0.00**	0.	-0.85	58.3		
6	**0.00**	0.	0.00	1.5		

FIGURE 5.3 EFFECTIVE STRESS, STRAIN AND MODULI OF A CROSS-PLY LAMINATE UNDER COMBINED STRETCHING AND BENDING

In the case of a beam under bending, the usual bending stiffness is derived from the compliance. The section modulus is related to the laminate compliance, the width and thickness of the beam as follows:

$$[D^*] = \frac{12}{h^3}[D] = \frac{1}{I^*}[D],\ [d^*] = \frac{h^3}{12}[d] = I^*[d]$$

$$\text{For a beam: } \mathbf{I^*} = \frac{\mathbf{h^3}}{\mathbf{12}} = \frac{\mathbf{I}}{\mathbf{b}},\ \mathbf{E_1{}^f I} = \frac{\mathbf{b}}{\mathbf{d_{11}}} = \frac{\mathbf{b\,I^*}}{\mathbf{d_{11}^*}} = \frac{\mathbf{I}}{\mathbf{d_{11}^*}} \tag{5.4}$$

MATRIX INVERSION

The inverted stiffness matrix is the compliance matrix. The inversion process is the same as that for the ply and in-plane stiffnesses. It is also the same whether the flexural stiffness is in the absolute or normalized form; i.e., [D] or [D*].

$$[d] = [D]^{-1},\ |D| = (D_{11}D_{22}-D_{12}{}^2)D_{66}+2D_{12}D_{26}D_{16}-D_{11}D_{26}{}^2-D_{22}D_{16}{}^2$$

$$d_{11} = (D_{22}D_{66}-D_{26}{}^2)/|D|,\ d_{22} = (D_{11}D_{66}-D_{16}{}^2)/|D|,\ d_{12} = (D_{16}D_{26}-D_{12}D_{66})/|D|$$

$$d_{66} = (D_{11}D_{22}-D_{12}{}^2)/|D|,\ d_{16} = (D_{12}D_{26}-D_{22}D_{16})/|D|,\ d_{26} = (D_{12}D_{16}-D_{11}D_{26})/|D| \tag{5.5}$$

ENGINEERING CONSTANTS

The engineering constants associated with the flexural moduli are defined by analogous relations such as those for the in-plane case:

$$\mathbf{E_1{}^f = 1/d_{11}^*,\quad \nu_{12}{}^f = -d_{12}/d_{22},\ \nu_{16}{}^f = d_{16}/d_{66}}$$

$$\mathbf{\nu_{21}{}^f = -d_{21}/d_{11},\ E_2{}^f = 1/d_{22}^*,\quad \nu_{26}{}^f = d_{26}/d_{66}}$$

$$\mathbf{\nu_{61}{}^f = d_{61}/d_{11},\ \nu_{62}{}^f = d_{62}/d_{22},\quad E_6{}^f = 1/d_{66}^*} \tag{5.6}$$

5.2 FLEXURAL STIFFNESS EVALUATION

The integration of Equation 5.2 can be replaced by the summation of a laminate with **m** ply groups.

$$[D] = \int_{-h/2}^{h/2}[Q]z^2dz = \frac{1}{3}\sum_{i=1}^{m}[Q']^{(i)}\left[\left[z^{(i)}\right]^3-\left[z^{(i-1)}\right]^3\right],\ \mathbf{[D^*] = \frac{12}{h^3}[D]}$$

$$[Q']^{(i)} = \text{off-axis stiffness of the i-th ply group with angle } \theta^{(i)} \tag{5.7}$$

Index **i**, which designates a ply group, begins from the bottom surface, z = -h/2. For a symmetric laminate the summation may be either from the bottom surface to the mid-plane, or from the mid-plane to the top surface of the laminate. The order of the ply groups is critical for the flexural stiffness. This is fundamentally different from in-plane stiffness, where the location of plies is not important. In-plane stiffness components follow the rule-of-mixtures relations. Thus the analysis and design of laminates for in-plane stiffness are much simpler than those for flexural stiffness. Design for flexural stresses can also be made simple if we use homogenized laminates. The flexural stiffness then approaches that of the in-plane.

We will show how the summation of two typical laminates can be carried out. First, we present the case of a symmetric [0/90] laminate. The plane stress stiffness matrix for the [0] and [90] for T300/5208 are shown in the figure below. The summation is carried out step by step as shown in the figure. Both the absolute and normalized flexural rigidities are shown:

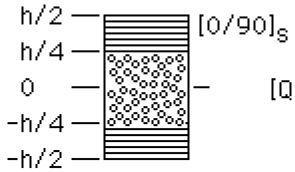

$$[Q]^{(0)} = \begin{bmatrix} 182 & 2.9 & 0.0 \\ 2.9 & 10.3 & 0.0 \\ 0.0 & 0.0 & 7.2 \end{bmatrix}, \quad [Q]^{(90)} = \begin{bmatrix} 10.3 & 2.9 & 0.0 \\ 2.9 & 182 & 0.0 \\ 0.0 & 0.0 & 7.2 \end{bmatrix}$$

$$[D] = \frac{1}{3}\left[[Q]^{(0)}\left[-\frac{h^3}{64}+\frac{h^3}{8}\right]+[Q]^{(90)}\left[\frac{h^3}{64}+\frac{h^3}{64}\right]+[Q]^{(0)}\left[\frac{h^3}{8}-\frac{h^3}{64}\right]\right]$$

$$= \frac{h^3}{12}\left[\frac{7}{8}[Q]^{(0)}+\frac{1}{8}[Q]^{(90)}\right]$$

$$[D^*] = \left[\frac{7}{8}[Q]^{(0)}+\frac{1}{8}[Q]^{(90)}\right] = \begin{bmatrix} 160 & 2.9 & 0.0 \\ 2.9 & 31.8 & 0.0 \\ 0.0 & 0.0 & 7.2 \end{bmatrix}, \text{GPa}$$

FIGURE 5.4 CALCULATION OF THE FLEXURAL STIFFNESS OF A SYMMETRIC [0/90] LAMINATE

We also repeat the summation of the last figure for a symmetric [±45] laminate, where shear coupling components "16" and "26" are similar in value as the normal and Poisson components.

Note that flexural modulus is a weighted average of the ply moduli. This is different from in-plane modulus which is the arithmetic average of the ply moduli. In the case in Figure 5.4, the outer ply contributes to 7/8 of the flexural modulus and the inner one only 1/8.

The same weighted average is true for a different laminate, say, [±45], shown in Figure 5.5.

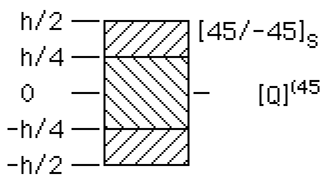

$$[Q]^{(45)} = \begin{bmatrix} 56.6 & 42.3 & 42.9 \\ 42.3 & 56.6 & 42.9 \\ 42.9 & 42.9 & 46.6 \end{bmatrix}, \quad [Q]^{(-45)} = \begin{bmatrix} 56.6 & 42.3 & -42.9 \\ 42.3 & 56.6 & -42.9 \\ -42.9 & -42.9 & 46.6 \end{bmatrix}$$

$$[D] = \frac{1}{3}\left[[Q]^{(45)}\left[-\frac{h^3}{64}+\frac{h^3}{8}\right]+[Q]^{(-45)}\left[\frac{h^3}{64}+\frac{h^3}{64}\right]+[Q]^{(45)}\left[\frac{h^3}{8}-\frac{h^3}{64}\right]\right]$$

$$= \frac{h^3}{12}\left[\frac{7}{8}[Q]^{(45)}+\frac{1}{8}[Q]^{(-45)}\right]$$

$$[D^*] = \left[\frac{7}{8}[Q]^{(45)}+\frac{1}{8}[Q]^{(-45)}\right] = \begin{bmatrix} 56.6 & 42.3 & 32.2 \\ 42.3 & 56.6 & 32.2 \\ 32.2 & 32.2 & 46.6 \end{bmatrix}, \text{GPa}$$

FIGURE 5.5 CALCULATION OF THE FLEXURAL STIFFNESS OF A SYMMETRIC [±45] LAMINATE

Note that the laminate is anisotropic in bending. The shear coupling components change signs as we move from positive to negative ply angles. The shear coupling component of the laminate is 32.3 GPa, or 75 percent of the original shear coupling component of 42.9 GPa.

Similar to the summation of the in-plane stiffness, that of the flexural stiffness can also be formulated using the multiple angle method.

$$
\begin{aligned}
D_{11} &= \int_{-h/2}^{h/2} Q_{11} z^2 dz = \int_{-h/2}^{h/2} [U_1 + U_2 \cos 2\theta + U_3 \cos 4\theta] z^2 dz = U_1 \frac{h^3}{12} + U_2 W_1 + U_3 W_2 \\
D_{16} &= \int_{-h/2}^{h/2} Q_{16} z^2 dz = \int_{-h/2}^{h/2} \left[\frac{U_2}{2} \sin 2\theta - U_3 \sin 4\theta \right] z^2 dz = \frac{U_2}{2} W_3 - U_3 W_4
\end{aligned}
\qquad (5.8)
$$

where the integrated trigonometric functions are expressed in normalized form as follows:

$$
W_i^* = \frac{12}{h^3} W_i = W^*_{[1,2,3,4]} = \frac{12}{h^3} \int_{-h/2}^{h/2} [\cos 2\theta, \cos 4\theta, \sin 2\theta, \sin 4\theta] z^2 dz \qquad (5.9)
$$

The final flexural stiffness components are matrix products of the ply stiffnesses in the Us and the integrated geometric functions in the Ws. The separation of the material and geometric factors takes the same form as those for off-axis ply and in-plane stiffness; i.e., if a ply material is changed, only the Us are changed, and if a lamination is changed, only the Ws are changed. The Ws are weighted averaged of the trignometric functions.

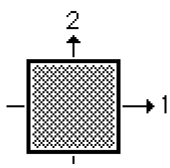

$$
\begin{Bmatrix} D^*_{11} \\ D^*_{22} \\ D^*_{12} \\ D^*_{66} \\ D^*_{16} \\ D^*_{26} \end{Bmatrix} =
\begin{bmatrix}
U_1 & U_2 & U_3 & 0 & 0 \\
U_1 & -U_2 & U_3 & 0 & 0 \\
U_4 & 0 & -U_3 & 0 & 0 \\
U_5 & 0 & -U_3 & 0 & 0 \\
0 & 0 & 0 & \frac{U_2}{2} & U_3 \\
0 & 0 & 0 & \frac{U_2}{2} & -U_3
\end{bmatrix}
\begin{Bmatrix} 1 \\ W^*_1 \\ W^*_2 \\ W^*_3 \\ W^*_4 \end{Bmatrix}
$$

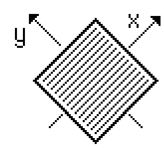

FIGURE 5.6 FLEXURAL STIFFNESS BY THE MULTIPLE ANGLE METHOD

For symmetric laminates, it is convenient to use only one half of the laminate by setting the lower limit of integration to zero, and multiplying the resulting integrals and summations by two:

$$
\begin{aligned}
[D] &= 2\int_0^{h/2} [Q] z^2 dz = \frac{2}{3} \sum_{i=1}^{m/2} [Q']^{(i)} \left[\left[z^{(i)} \right]^3 - \left[z^{(i-1)} \right]^3 \right], \ [D^*] = \frac{12}{h^3} [D] \\
W^*_{[1,2,3,4]} &= \frac{24}{h^3} \int_0^{h/2} [\cos 2\theta, \cos 4\theta, \sin 2\theta, \sin 4\theta] z^2 dz
\end{aligned}
\qquad (5.10)
$$

We have shown the flexural stiffness calculation in two methods: the direct integration or summation in Equation 5.7, and the multiple angle method in Equations 5.8 and 5.9. The latter is useful to show the invariants explicitly.

5.3 SANDWICH PLATES

Sandwich plates are very efficient in flexural stiffness because material is removed near the middle plane of the laminate, which is not highly stressed and contributes a very small amount to the total flexural stiffness. It is assumed that the classical laminated plate theory remains valid; i.e., the normal to the mid-plane does not deform as the plate is being bent and twisted. The stiffness of the core will be zero in in-plane stiffness, and will have infinite transverse shear rigidity.

If we use c* to designate the core fraction, the relative reduction of in-plane and flexure stiffness as functions of the core fraction are expressed.

$$
\begin{aligned}
&A'_{11} = \left[1-c^*\right] = \text{in-plane correction},\ D'_{11} = \left[1-(c^*)^3\right] = \text{flex correction} \\
&\text{specific flexural stiffness} = \frac{1-(c^*)^3}{1-c^*} = \frac{D'_{11}}{A'_{11}},\ \text{where}\ \ c^* = \frac{z_{core}}{h/2} \\
&\text{If } c^* = 0.5,\ A'_{11} = 0.5,\ D'_{11} = 7/8 = 0.875,\ D'_{11}/A'_{11} = 7/4 = 1.75
\end{aligned}
\tag{5.11}
$$

The correction in the in-plane stiffness [A'] is a linear function of the core fraction. The correction in the flexural stiffness [D'] is related to the cube of the core fraction. This is shown in Equation 5.11, where the case for a 50 percent core is also shown as an example.

The same relations are shown graphically in the figure below:

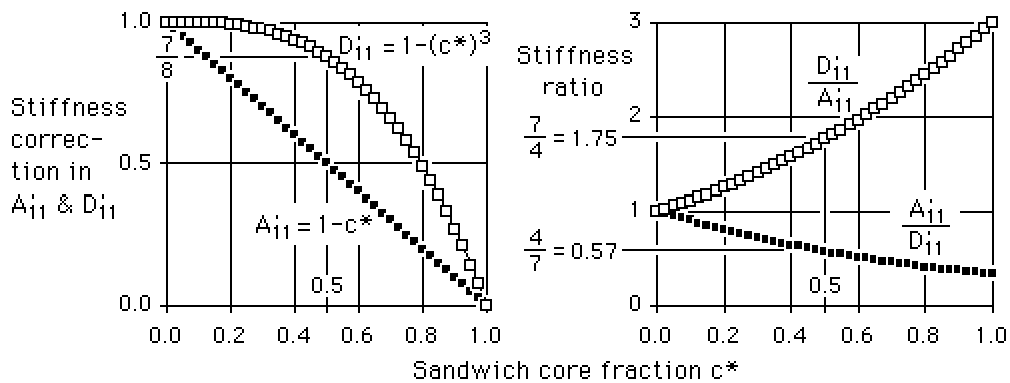

FIGURE 5.7 NORMALIZED REDUCTIONS IN IN-PLANE AND FLEXURAL STIFFNESSES AS FUNCTIONS OF THE CORE FRACTION ARE SHOWN ON THE LEFT AND THEIR RATIOS ON THE RIGHT

For a symmetric laminate with or without a core, the ply stress and laminate stress distributions are piece-wise linear. When there is a core only the facing of the sandwich plate carries stresses. The same assumption of nondeformable normal is applied to the solid laminate on the left in Figure 5.8 below; and the sandwich laminate on the right. An example of the ply stress determination of solid and sandwich plates will be given later in this section.

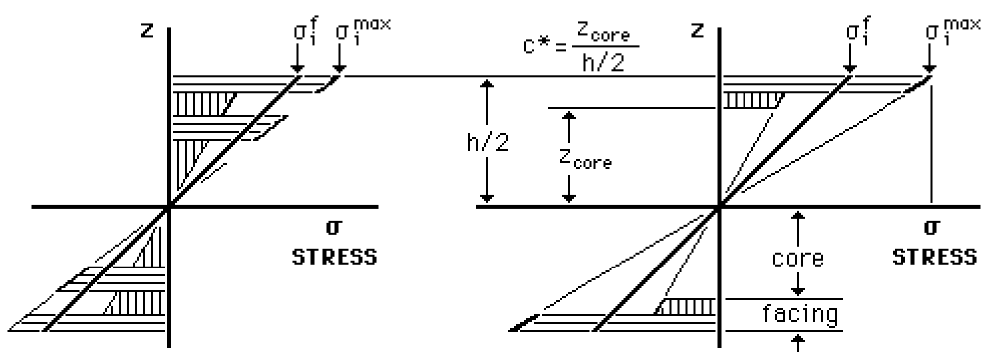

FIGURE 5.8 PLY STRESS AND STRAIN IN A PLATE WITH SANDWICH CORE

The flexural stiffness for a sandwich laminate can be calculated by the same formulas as the solid laminate except the lower limit of integration or summation is that of the top face of the core:

$$[D] = 2\int_{z_c}^{h/2}[Q]z^2dz = \frac{2}{3}\sum_{i=c}^{m/2}[Q']^{(i)}\left[\left[z^{(i)}\right]^3-\left[z^{(i-1)}\right]^3\right],\ [D^*] = \frac{12}{h^3}[D]$$

$$W^*_{[1,2,3,4]c} = \frac{24}{h^3}\int_{z_c}^{h/2}\left[\cos 2\theta, \cos 4\theta, \sin 2\theta, \sin 4\theta\right]z^2dz$$

$$h^* = 2\int_{z_c}^{h/2}z^2dz = \frac{h^3}{12}\left[1-\left[\frac{2z_c}{h}\right]^3\right] = \frac{h^3}{12}\left[1-(c^*)^3\right],\ c^* = \text{core fraction} \qquad (5.12)$$

The normalizing factor for a sandwich plate is the same, as shown in Equation 5.2; i.e., based on the total thickness h. The unity term for the invariants in the multiple angle method shown in Figure 5.6 must be modified to reflect the existence of a symmetric core. The values for the Ws with core will be different from those in Equation 5.10 because of the different limit of integration.

$$\begin{Bmatrix} D^*_{11} \\ D^*_{22} \\ D^*_{12} \\ D^*_{66} \\ D^*_{16} \\ D^*_{26} \end{Bmatrix} = \begin{bmatrix} U_1 & U_2 & U_3 & 0 & 0 \\ U_1 & -U_2 & U_3 & 0 & 0 \\ U_4 & 0 & -U_3 & 0 & 0 \\ U_5 & 0 & -U_3 & 0 & 0 \\ 0 & 0 & 0 & \frac{U_2}{2} & U_3 \\ 0 & 0 & 0 & \frac{U_2}{2} & -U_3 \end{bmatrix} \begin{Bmatrix} 1-(c^*)^3 \\ W^*_{1c} \\ W^*_{2c} \\ W^*_{3c} \\ W^*_{4c} \end{Bmatrix}$$

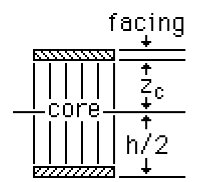

$$c^* = \frac{2z_c}{h}$$
= core fraction

FIGURE 5.9 FLEXURAL STIFFNESS OF A SANDWICH PLATE BY THE MULTIPLE ANGLE METHOD

5.4 TRANSFORMATION OF FLEXURAL MODULI

The transformation of the flexural moduli is the same as that for the anisotropic moduli of a unidirectional ply in Section 3. We can use either the power functions shown in Figure 3.4 on page 3-4 or the multiple angle formulation in Figure 3.12 on page 3-8.

We have seen that invariants in in-plane and ply stiffnesses are defined by coordinate transformations. For a given ply material, the invariants limit the elastic potential independent of the ply orientation. The comparison in the figure below shows the same invariants for off-axis, in-plane, and flexural stiffnesses for T300/5208.

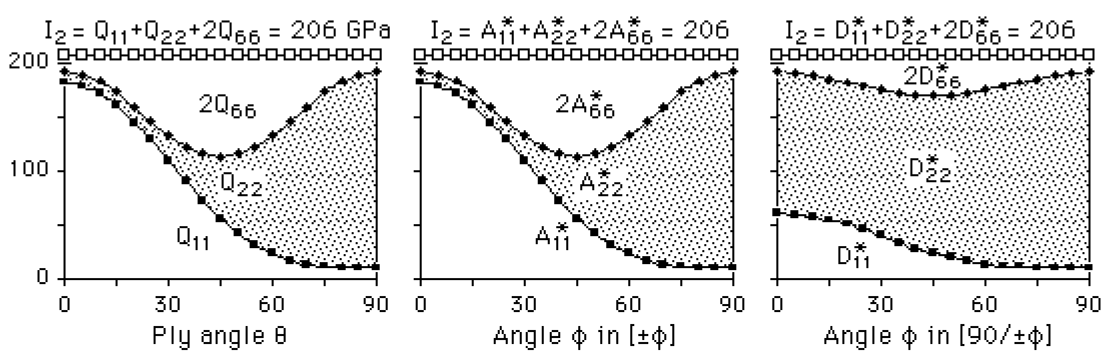

FIGURE 5.10 THE SAME INVARIANTS ARE IMPOSED ON UNIDIRECTIONAL, IN-PLANE AND FLEXURAL STIFFNESS INDEPENDENT OF THE PLY ORIENTATIONS

In designing with composite materials, the invariant values for each ply material must be considered. Directionality of properties by design is unique with composite materials, but the ranges of available properties are dictated by the controlling invariants. With homogenization of laminates, the flexural and in-plane stiffnesses converge. The limits are imposed by the two linear invariants. Designing with composite materials is analogous to using isotropic materials, which also have two independent constants. Thus the most degrees of freedom possible are two for both isotropic and orthotropic materials.

5.5 HOMOGENIZATION OF LAMINATED PLATES

It has been found through experience and demonstrated analytically that ply groups in a laminate should be dispersed or spliced as much as possible to improve laminate strength and toughness. In a finely dispersed laminate, all ply groupings have as few plies as possible. If we have a total of 16 plies each of [0] and [90] degree orientations, the most dispersed symmetric laminate will be [0/90] repeated eight times at the top half of the laminate, and [90/0] eight times at the bottom half, which is shown on the right in the figure below. The least dispersed laminate will be eight [0] and eight [90] at the top, and eight [90] and eight [0] at the bottom. See the "r = 8" and "r = 1" cases in the figure below, the most and the least dispersed or spliced laminates, respectively.

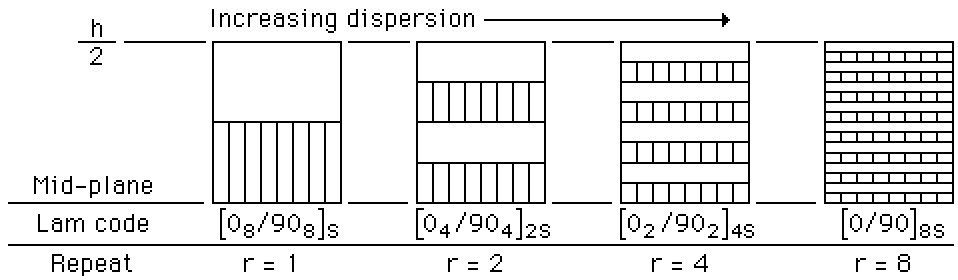

FIGURE 5.11 INCREASING DISPERSION BY INCREASING REPEATING SUB-LAMINATES

The fewer plies in a ply group, the smaller the percentage of this ply group will be in a total laminate. When the ply group fails, the effect is more localized in a dispersed laminate than in a laminate having fewer but thicker ply groups. One way to build up a highly dispersed laminate is to use repeating sub-laminates, which is therefore one of our recommended design practices.

A typical laminate construction is shown in the figure below where the sub-laminates on the left are repeated three times to form the total laminated construction on the right. The core fraction can have any value between 0 and less than unity.

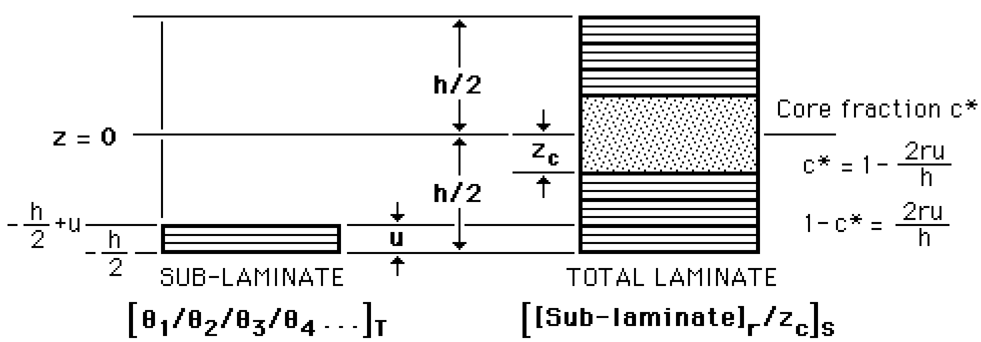

FIGURE 5.12 THE RELATION BETWEEN SUB-LAMINATES AND THE TOTAL SYMMETRIC LAMINATE CONSISTING OF THREE REPEATED SUB-LAMINATES ON EACH SIDE

It is easy to derive the following analytic relations between the stiffness of the sub-laminate and the total symmetric laminated construction. The use of an unsymmetric laminate with the coupling matrix [B] will be covered in the next section. The result shows that it is simple to calculate the stiffness of the total laminate from the stiffness of the sub-laminate and the number of repeats; see Sub-Section 6.2 on page 6-4 for derivation.

$$[A] = 2r[A^o],\ [B] = 0,\ [D] = 2r\left[[D^o]+(r-1)u[B^o]+\frac{(r-1)(2r-1)}{6}u^2[A^o]\right]$$

$$\text{where sub-laminate stiffnesses: } \left[[A^o],[B^o],[D^o]\right] = \int_{-h/2}^{-h/2+u}[Q][1,z,z^2]dz \qquad (5.13)$$

When the dispersion in a laminate is achieved by the use of repeated sub-laminates, we are in effect homogenizing the laminate. This is possible if there are a sufficiently large number of plies available in a laminate. The benefits of homogenization include the following:

- There is increased strength and toughness.
- The flexural stiffness approaches that of the in-plane, and stacking sequence is not important.
- A homogenized laminate with repeated sub-laminates is conceptually simple, and becomes easy to optimize, and can be fabricated using sub-laminates as modules.

A practical problem of homogenization is the number of repeated sub-laminates required to make a laminate homogeneous. A sufficient condition for a solid laminate that is homogenized is when the flexural and in-plane stiffness are equal, as stated in the following equation. This condition is valid for symmetric laminates only. If the laminate has a sandwich core, a correction factor that takes into account the core fraction must also be used as shown. This relation is based on the results in Equation 5.11 on page 5-6.

$$\text{For solid laminates: } \frac{D_{ij}^*}{A_{ij}^*} = 1 \text{ or } D_{ij} = h^2A_{ij}/12$$

$$\text{For sandwich laminates: } \frac{D_{ij}^*}{A_{ij}^*} = \frac{1-(c^*)^3}{1-c^*} \qquad (5.14)$$

In the following figures we show the rate of convergence of the flexural to the in-plane stiffnesses for two cross-ply laminates for both solid and sandwich constructions.

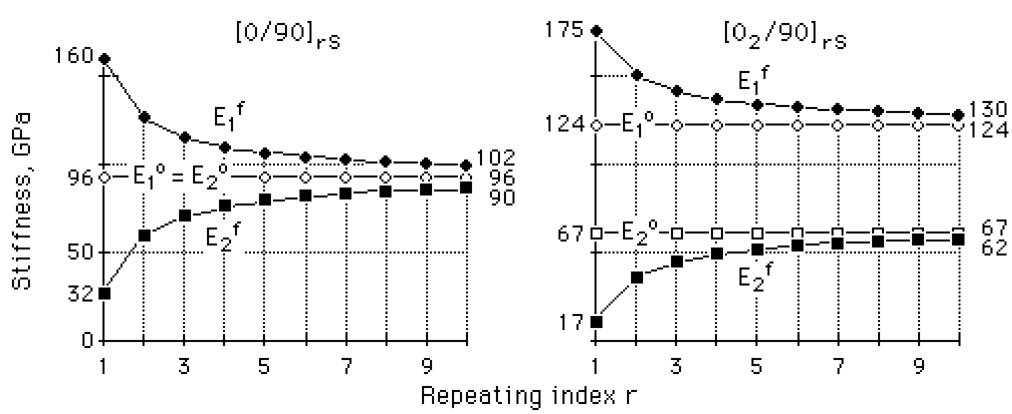

FIGURE 5.13 THE CONVERGENCE OF THE FLEXURAL STIFFNESS TO THE IN-PLANE STIFFNESS AS SUB-LAMINATES INCREASE (PLY IS T300/5208)

In Figure 5.13, the convergence of the flexrural stiffness to the in-plane stiffess comes within 6 GPa when the repeating index is 10. On the left of this figure, we have an equal cross ply laminate when the [0] and [90] plies are equal in number. For both laminates, the convergence toward the respective in-plane stiffnesses is rapid in the initial, low values of the repeating index. The in-plane stiffness values are also indicated in this figure; i.e., for the equal cross-ply laminate the value is 96 GPa, while for the unequal, the values are 124 and 67 GPa, respectively.

When laminates have a symmetric sandwich core, the convergence of the flexural to the in-plane stiffness still holds. As we have indicated in Equation 5.11 and Figure 5.7 on page 5-6, the presence of core reduces the in-plane stiffness linearly, and the flexural stiffness by a cubic relation. In the example in the figure below, we have a core fraction of 0.5 and the ratio between the two reduced stiffnesses would be 7/4 or 1.75, as shown in Figure 5.7 on page 5-7.

The convergence of the flexural stiffness to the corrected in-plane stiffness (by a multiplying ratio of 1.75) is shown for the same two cross-ply laminates used as the facing material in the figure above. When the repeated sub-laminates are 10, the convergence is within 3 GPa or less. This is expected because the face sheets of a sandwich construction approach the in-plane or membrane as the core fraction increases. Therefore the convergence of a sandwich laminate is more rapid than that of a solid laminate.

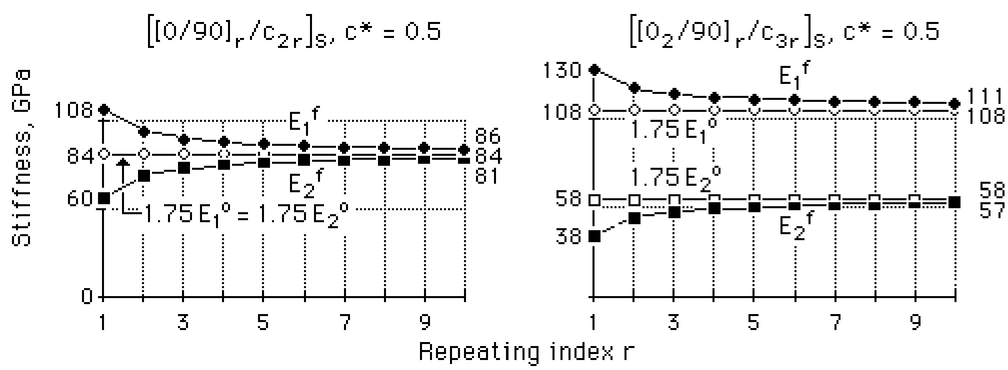

FIGURE 5.14 THE CONVERGENCE OF THE FLEXURAL AND IN-PLANE STIFFNESS AS THE NUMBER OF SUB-LAMINATES INCREASE (PLY MATERIAL IS T300/5208, WITH A CORE FRACTION OF 0.5)

5.6 STACKING SEQUENCE EFFECTS

We have seen that a laminate formed from repeated sub-laminates can approach a homogeneous laminate. Being homogeneous, the laminate has many desirable attributes from the standpoint of strength and ease of design and fabrication.

In Figure 5.15, we show the drastic decrease in the delamination stress as a function of the increasing repeating index, based on a free-edge stress analysis. The increase in strength can also be rationalized by a damage distribution argument; i.e., when the plies in a laminate are dispersed, each ply group represents a smaller percentage of the total laminate.

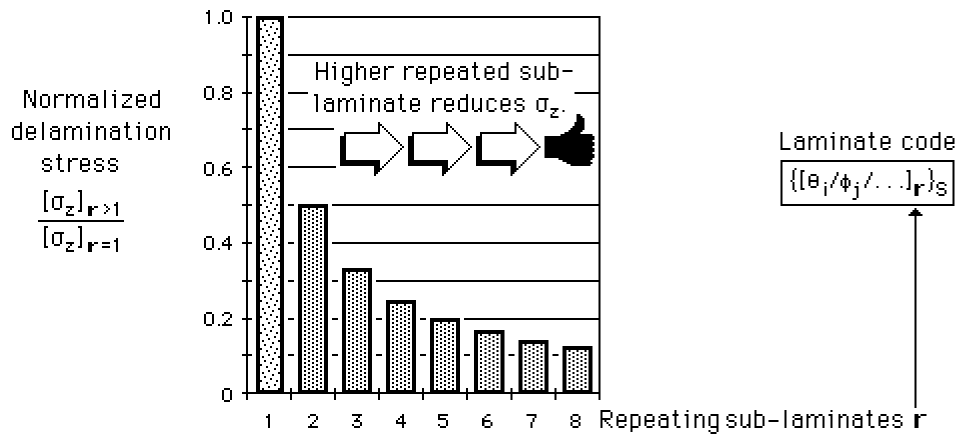

FIGURE 5.15 REDUCTION IN INTERLAMINAR NORMAL STRESS AS THE NUMBER OF REPEATING SUB-LAMINATES INCREASE

Another design consideration is the stacking sequence effects. A family of sub-laminates can be defined by groups of sub-laminates that have the same total number of plies and ply angles. Sub-laminates having no more than 10 plies, and no more than 4 ply angles, will satisfy most practical loading conditions. The selection of the best laminates for given sets of loads is greatly simplified if the selection process is limited to 10 or fewer sub-laminates.

Another stacking sequence effect is the twisting coupling in flexure, analogous to the shear coupling in in-plane. A balanced laminate is defined as one that has an equal number of the plus and minus off-axis plies. The in-plane stiffness is orthotropic; i.e., there is no shear coupling. Balanced laminates are often specified in practical design. The motivation is to limit laminates to an orthotropic symmetry, for which many closed form or simple solutions of stress analysis exist or are readily obtainable. Such a rule, however, penalizes the use of composite laminates. We can show that balanced laminates are in general less efficient than those without this restriction if the combined loading has a shear component.

A balanced laminate is normally restricted to the case of an on-axis orthotropy. If a laminate is orthotropic, it is orthotropic for all coordinate systems, as when a laminate is symmetric it is symmetric in all coordinate systems. With this ground rule, a balanced laminate is not an invariant description because it is dependent on the coordinate axes.

Balanced laminates are intended for in-plane behavior only. In flexural behavior, laminates are not orthotropic in general because the twisting coupling coefficients of off-axis plies do not cancel one another. Each ply occupies a specified position within a laminate, and the shear coupling coefficients do not cancel each other between the plus and minus ply angles

There is a misconception that unbalanced laminates are not recommended because the laminates will warp when temperature and/or moisture content changes. Symmetric laminates, whether balanced or not, will not warp, while unsymmetric laminates will. Material symmetry, such as orthotropy or anisotropy, has no effect on warpage.

In the table below we list three types of laminates, the nonzero components, and the number of independent constants. The flexural compliance or stiffness of a balanced laminate is a truly anisotropic laminate, and will have six independent constants.

TABLE 5.1 THREE COMMON TYPES OF SYMMETRIES OF A COMPOSITE LAMINATE

Material symmetry	Compliance components	Number of independent constants	Conditions when θ = 0 (mat'l symm)
On-axis orthotropic (special ortho)	a_{11} a_{12} 0 a_{21} a_{22} 0 0 0 a_{66}	4	$a_{61} = a_{62} = 0$
Off-axis orthotropic (general ortho)	a_{11} a_{12} a_{16} a_{21} a_{22} a_{26} a_{61} a_{62} a_{66}	4	$a_{61} = a_{62} = 0$
Anisotropic	d_{11} d_{12} d_{16} d_{21} d_{22} d_{26} d_{61} d_{62} d_{66}	6	$d_{61} \neq d_{62} \neq 0$ (no symmetry)

$$d'_{61} = 2m^3nd_{11}-2mn^3d_{22}+2(mn^3-m^3n)(d_{12}-d_{66}/2)+(m^4-3m^2n^2)d_{16}+ \ldots$$

In the figure below, we show three tri-directional laminates where the twisting coupling coefficients are reduced by the position of the off-axis plies, and the degree of homogenization by the number of repeated sub-laminates.

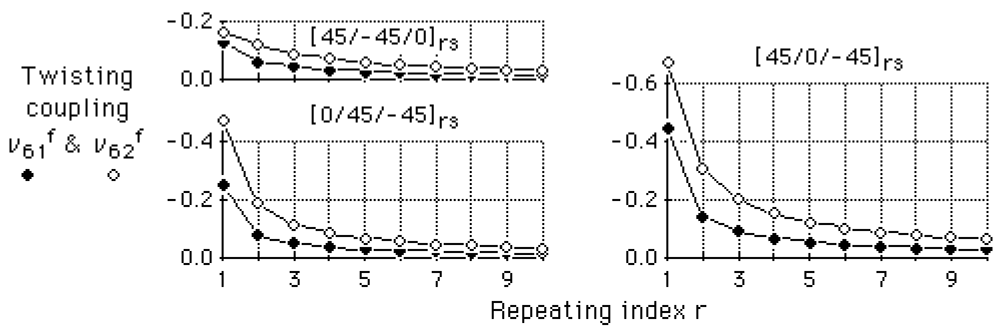

FIGURE 5.16 STACKING SEQUENCE AND REPEATING SUB-LAMINATES ON TWISTING COUPLING OF [0/45/-45] FAMILY

We can also show three quadri-directional laminates where the twisting coupling coefficients are reduced by the position of the off-axis plies, and the degree of homogenization by the number of repeated sub-laminates. The results are very similar to those of the previous figure.

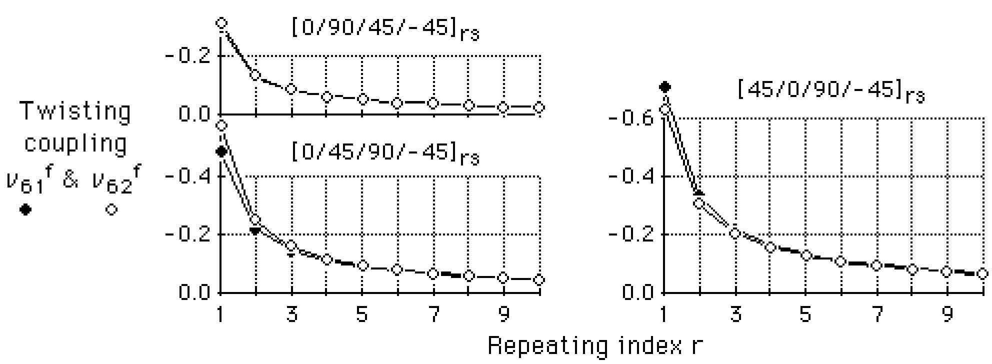

FIGURE 5.17 STACKING SEQUENCE AND REPEATING SUB-LAMINATES ON TWISTING COUPLING OF [0/90/45/-45] FAMILY

The guidelines concerning the positions of the off-axis plies on the twisting couplings are:

- Greater when the plies are far apart as in [45/0/-45] and [45/0/90/-45].

- Smaller when the plies are adjacent to each other as in [0/45/-45], [45/-45/0], and [0/90/45/-45].
- Smaller when the plies are placed furthermost from the mid-plane of the laminate; [45/-45/0] has a lower shear coupling than [0/45/-45].
- Smaller when repeat index increases, as homogenization of the laminate increases.

The stacking sequence effect can also be illustrated by polar plots as in Figure 5.18. The laminate is [45/0/-45] of T300/5208. On the left is the in-plane stiffness and the effective Young's modulus along the 1-axis. The laminate is balanced and orthotropic. The two planes of symmetry are self-evident. If this polar plot is rotated, the planes of symmetry rotate with it. The symmetry is not disturbed. It is orthotropic for all coordinate transformations. Only in its material symmetry axes is the laminate called on-axis, as opposed to an off-axis orientation. The number of independent constants remain at four, as described in Table 5.1 on the last page.

The flexural stiffness and flexural Young's modulus along the 1-axis for the same laminate are shown on the right. This material under flexure is not orthotropic. There is no plane of symmetry, and it is therefore truly anisotropic. If a new laminate consisting of this as a sub-laminate is created, the homogenization process will begin. The anisotropic figure on the right will eventually change to the laminate on the left, then fexural and in-plane moduli are equal.

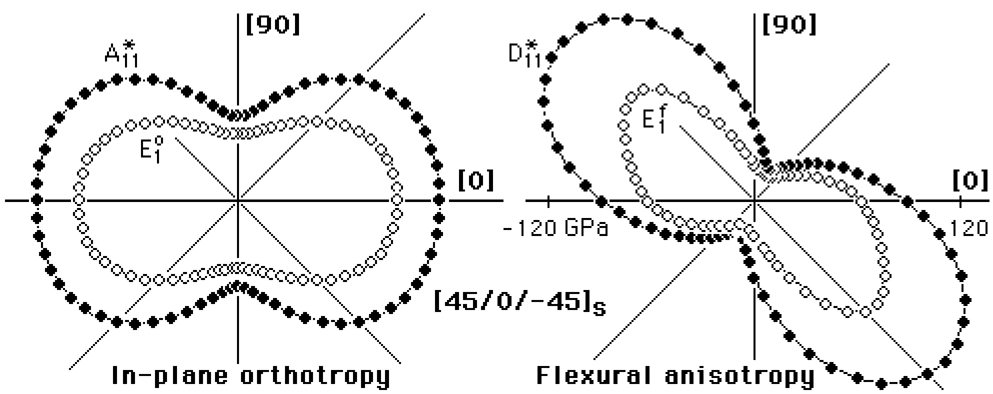

FIGURE 5.18 POLAR PLOTS OF IN-PLANE AND FLEXURAL STIFFNESSES. NOTE THE DIFFERENCE BETWEEN ORTHOTROPIC AND ANISOTROPIC FIGURES.

5.7 PLY STRESS AND PLY STRAIN

Analogous to the ply-by-ply analysis of stress and strain for in-plane loading, the ply strain for the flexural loading is diagrammed in the figure below for a given value of **z**. The corresponding ply stress is simply the ply strain multiplied by the on-axis ply stiffness **[Q]**.

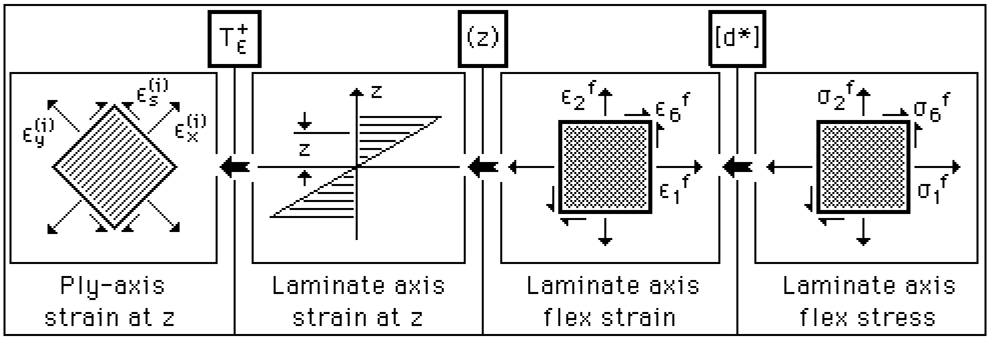

FIGURE 5.19 A PROGRESSION OF PLY STRAIN ANALYSIS STEPS FROM RIGHT TO LEFT

There is no conceptual difference between the flexural and the in-plane stress analysis. The position of each ply must be identified to reflect the linearly decreasing laminate strain from the top or bottom surface to the mid-plane of the laminate. The other differences between a solid and a sandwich plate must be included in the evaluation of the flexural stiffness, as described earlier in this section in Equation 5.11 on page 5-6.

The ply stress analysis is straightforward. The laminate flexural stiffness and compliance must first be calculated for both the solid and sandwich plates. From imposed moment or flexural stress, the flexural strain can be computed. The maximum ply strain for each ply angle is based on the maximum distance from the mid-plane. The ply stress is approximately the ply strain multiplied by the ply stiffness. This is acceptable when the Poisson's ratio of the laminate is small. All these operations are by matrix algebra. The maximum ply stresses are shown in Figure 5.19.

$[0/90]_{2s}$	$[0/90/c_2]_s$
$[D^*] = \begin{bmatrix} 128 & 2.9 & 0 \\ & 63.9 & 0 \\ & & 7.17 \end{bmatrix}$ GPa	$[D^*] = \begin{bmatrix} 108 & 2.5 & 0 \\ & 60.0 & 0 \\ & & 6.27 \end{bmatrix}$ GPa
$[d^*] = \begin{bmatrix} 7.8 & -0.35 & 0 \\ & 15.7 & 0 \\ & & 139 \end{bmatrix}$ TPa^{-1}	$[d^*] = \begin{bmatrix} 9.25 & -0.4 & 0 \\ & 16.7 & 0 \\ & & 159 \end{bmatrix}$ TPa^{-1}
$\sigma_1^f = \frac{6M_1}{h^2} = 500$ MPa	$\sigma_1^f = \frac{6M_1}{h^2} = 500$ MPa
$\{\epsilon^f\} = [d^*]\{\sigma^f\} = \{3.90, -0.18, 0\}\ 10^{-3}$	$\{\epsilon^f\} = [d^*]\{\sigma^f\} = \{4.62, -0.02, 0\}\ 10^{-3}$
$\sigma_i^{max} = Q_{ij}^{(i)}\epsilon_j^f = Q_{ij}^{(i)} d_{jk}^* \sigma_k^f$	$\sigma_i^{max} = Q_{ij}^{(i)}\epsilon_j^f = Q_{ij}^{(i)} d_{jk(core)}^* \sigma_k^f$
$\sigma_1^{max(0)} = 181 \times 3.90 = 709$ MPa	$\sigma_1^{max(0)} = 181 \times 4.62 = 840$ MPa
$\sigma_1^{max(90)} = 10.3 \times 3.9 \times 0.75 = 30$ MPa	$\sigma_1^{max(90)} = 10.3 \times 4.62 \times 0.75 = 36$ MPa

FIGURE 5.20 PLY STRESS ANALYSIS OF SOLID AND SANDWICH PLATES UNDER BENDING

We wish to reiterate that strength analysis can be based on ply strains as easily as ply stresses. We recommend the use of ply strains, which are simpler to determine from the flexural strain. Only a simple ratio that identifies the position of the ply will suffice. Ply stresses need an extra matrix multiplication, and are not really necessary for strength analysis. This issue will be discussed again when we present failure criteria. We will now plot the flexural and ply stresses in the solid and sandwich laminates given in Figure 5.20.

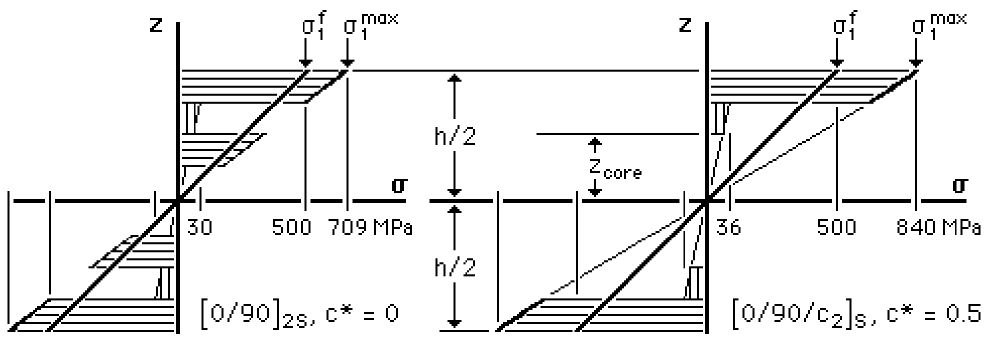

FIGURE 5.21 FLEXURAL STRESS AND PLY STRESS IN SOLID AND SANDWICH PLATES

It is a recommended practice to verify equilibrium of the in-plane and flexural stresses; the integrated stresses must satisfy the applied loads. For the plates described above, the in-plane load is zero, and the flexural stress must be balanced by the applied moment. The following relations for static equilibrium must be satisfied:

$$\{\sigma^o\} = \frac{\{N\}}{h} = \frac{1}{h}\int_{-h/2}^{h/2}\{\sigma\}dz = 0, \quad \{\sigma^f\} = \frac{6\{M\}}{h^2} = \frac{6}{h^2}\int_{-h/2}^{h/2}\{\sigma\}zdz \neq 0 \tag{5.15}$$

5.8 BEAMS

The determination of the deflection and strength of statically determinate beams made of composite laminates is a special case of laminated plate theory. The only difference from the homogeneous beam is in the material properties.

For statically determinate beams, we know the bending moment **M** at each point along the beam. We can calculate the stress in the beam from

$$M_1 = \frac{M}{b}, \sigma_1{}^f = \frac{6M_1}{h^2} = \frac{Mc}{I}, M_2 = M_6 = \sigma_2{}^f = \sigma_6{}^f = 0 \tag{5.16}$$

From any strength of materials book we can find the maximum moment and maximum deflection for beams with simple loads and simple end conditions. We will show the formulas for three beams for concentrated and uniformly distributed loads in Table 5.2. The maximum moment and deflection are normalized with respect to a cantilever beam with concentrated and distributed loads, respectively.

TABLE 5.2 MAXIMUM MOMENTS AND DEFLECTIONS OF SIX SIMPLE BEAMS

LOADED BEAMS	M_{max}	M*	δ_{max}	δ*
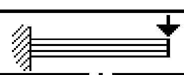 P	PL	1	$PL^3/3E^fI$	1
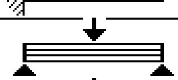	PL/4	1/4	$PL^3/48E^fI$	1/16
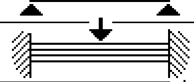	PL/8	1/8	$PL^3/192E^fI$	1/64
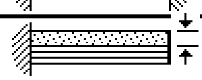 q	$qL^2/2$	1	$qL^4/8E^fI$	1
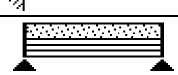	$qL^2/8$	1/4	$5qL^4/384E^fI$	5/48
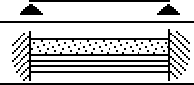	$qL^2/12$	1/6	$qL^4/384E^fI$	1/48

Formulas for the moments and deflections are simple, and are the same for homogeneous as well as laminated composite materials. The Young's modulus along the beam axis is the only constant that distinguishes one material from another. For the composite beam, the Young's modulus is defined in Equation 5.6; i.e.,

$$E = E_1^f = \frac{1}{d_{11}^*}, \ \epsilon_1^f = \frac{h}{2} k_1 = \frac{h d_{11} M_1}{2} = \frac{h d_{11}^* M}{2bI} = \frac{hM}{2E_1^f I} \qquad (5.17)$$

The stress distribution across the beam is, however, significantly different between a homogeneous and a laminated composite material, as shown in Figure 5.8. Having plies with different elastic constants, the stress in each ply is piece-wise linear, and varies from ply to ply. The ply stress and ply strain determination in a laminated composite material is calculated following the laminated plate theory, as stated in Equation 5.2 and shown in a flow diagram in Figure 5.19 on page 5-13.

From the calculated strain we can determine the strength/stress ratio or the factor of safety, including the effect of residual stress due to curing and moisture absorption. The strength analysis will be described in Sections 8 and 9.

5.9 TUBING

There are many useful applications of composite laminates formed in thin wall tubing of symmetric cross sections. The analysis of the bending of tubing is very similar to the analysis of beams in the previous subsection. The Young's modulus of the laminate along the tubing will be that of the in-plane stiffness. We only need to define the section modulus of various cross sections. A few simple cross sections are defined in the figure below. The wall thickness must be symmetric and thin for this one-dimensional solution.

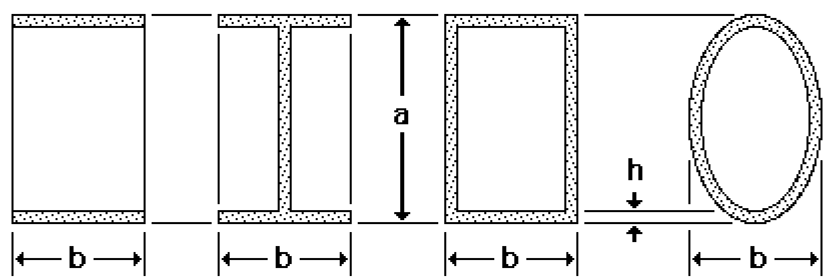

Moment of inertia	$a^2bh/2$	$(6a^2b+a^3)h/12$	$(3a^2b+a^3)h/6$	$(3a^2b+a^3)\pi h/32$
Eq. width	$b_{eq} = b$	$b_{eq} = b+a/6$	$b_{eq} = b+a/3$	$b_{eq} = \pi(3b+a)/16$

FIGURE 5.22 AREA MOMENT OF INERTIA AND EQUIVALENT WIDTH OF VARIOUS THIN WALL TUBING

Using the moment of inertia in the figure above in conjunction with Table 5.2 on the previous page, the maximum moment and deflection of the six beams can be readily computed. The Young's modulus of the thin wall along the tube axis is determined by the in-plane stiffness derived from laminated plate theory.

We also show, in the figure above, the equivalent width or width correction for each of the three cross sections on the right. The baseline width is the open sandwich construction on the extreme left of this figure. The added material in the remaining three sections can be represented by an increase in the width. The wall thickness **h** remains the same for all sections.

By modifying Equation 5.17, we can determine the curvature using the correct Young's modulus and the moment of inertia for various sections in Figure 5.22:

$$E = E_1^o = \frac{1}{a_{11}^*}, \ \epsilon_1^f = \frac{a}{2} k_1 = \frac{a d_{11} M_1}{2} = \frac{a d_{11}^* M}{2bI} = \frac{aM}{2E_1^o I}, M_{eq} = b_{eq} M_1 \qquad (5.18)$$

Since different sections will each have a different area moment of inertia, we can also claim the increase in the sectional stiffness by using a higher equivalent width, or a lower equivalent moment in Equation 5.18. Regardless of which method we use for determining the curvature, we can calculate the maximum ply strain in the tubing from the flexural strain-curvature relations in Equation 5.1.

This strain at the outer fiber of the tubing will be used for the calculation of the strength ratio to be described in Section 9 on laminate strength. The quadratic failure criterion is preferable because the two conjugate roots correspond to the strength ratios at the top and bottom faces, where $z = -a/2$. The roots are obtained from the same calculation. We only have to apply the criterion once and obtain both roots, $\mathbf{R}^{+}$ and $\mathbf{R}^{-}$, immediately. If we use the maximum stress or maximum strain criterion, we must apply the criterion twice, one for each of the top and bottom faces.

Thin wall tubing is susceptible to buckling. The Euler-type column buckling is easy to determine by using the same sectional stiffness in Equation 5.18. For a column with fixed/free ends:

$$\text{Fixed/free: } P_{critical} = \frac{\pi^2 E_1^o I}{4L^2}, \text{ Hinged/hinged: } P_{critical} = \frac{\pi^2 E_1^o I}{L^2}, \quad \text{where } L = \text{length} \tag{5.19}$$

Solutions for cases with more complicated end conditions can be found in strength of materials books, for example, in R. J. Roark, *Formulas for Stress and Strain*, McGraw-Hill.

5.10 CONCLUSIONS

There are no shortcuts in the evaluation of the flexural stiffness of symmetric laminates. The position of each ply must be evaluated. Flexural stiffness cannot be orthotropic if off-axis plies, balanced or not, exist. Homogenization by having many repeated sub-laminates simplifies the design of laminates. Twisting coupling resulting from off-axis plies will reduce as shown in Figure 5.16. Ultimately, the in-plane and flexural moduli are equal. There is no longer a stacking sequence dependency. Then sizing the best laminate for resisting flexural loads is the same as sizing for in-plane loads. For a symmetric sandwich constructions with thin face sheets, the face sheets are subjected principally to in-plane loads, and can then be designed the same as the in-plane case. When a laminate has many repeated sub-laminates, it is also resistant to delamination.

The analysis and design of beams are simple and direct when the structure is statically determinate. Only the effective flexural Young's modulus along the axis of the beam is required for all beam formulas. This Young's modulus is calculated from the reciprocal of one of the diagonal terms in the compliance matrix.

5.11 PROBLEMS

Prob. 5.1 Determine the flexural stiffness of [0/90] and [±45] laminates resulting from a process of homogenization by a factor of 2 and infinite repeats.

Laminate	[D*], GPa	Laminate	[D*], GPa
$[0/90]_s$	$\begin{bmatrix} 160 & 2.9 & 0.0 \\ 2.9 & 31.8 & 0.0 \\ 0.0 & 0.0 & 7.2 \end{bmatrix}$	$[45/-45]_s$	$\begin{bmatrix} 56.6 & 42.3 & 32.2 \\ 42.3 & 56.6 & 32.2 \\ 32.2 & 32.2 & 46.6 \end{bmatrix}$
$[0/90]_{2s}$	$\begin{bmatrix} ? & ? & ? \\ ? & ? & ? \\ ? & ? & ? \end{bmatrix}$	$[45/-45]_{2s}$	$\begin{bmatrix} ? & ? & ? \\ ? & ? & ? \\ ? & ? & ? \end{bmatrix}$
$[0/90]_{\infty}$	$\begin{bmatrix} ? & ? & ? \\ ? & ? & ? \\ ? & ? & ? \end{bmatrix}$	$[45/-45]_{\infty}$	$\begin{bmatrix} ? & ? & ? \\ ? & ? & ? \\ ? & ? & ? \end{bmatrix}$

FIGURE 5.23 FLEXURAL STIFFNESS OF [0/90] AND [±45] RESULTING FROM HOMOGENIZATION

Prob. 5.2 **Show that for a symmetric sandwich plate having homogenized anisotropic face sheet, the following stiffness components are valid, where c* is the core fraction, and [B] the in-plane-flexure coupling (see Equation 6.4).**

$$\left[\begin{array}{c|c} A_{ij}^* & B_{ij}^* \\ \hline 3B_{ij}^* & D_{ij}^* \end{array}\right]_c = [1-c^*]\left[\begin{array}{c|c} \begin{bmatrix} A_{11}^* & A_{12}^* & A_{16}^* \\ A_{21}^* & A_{22}^* & A_{26}^* \\ A_{61}^* & A_{62}^* & A_{66}^* \end{bmatrix} & \begin{bmatrix} 0 & 0 & 0 \\ 0 & 0 & 0 \\ 0 & 0 & 0 \end{bmatrix} \\ \hline \begin{bmatrix} 0 & 0 & 0 \\ 0 & 0 & 0 \\ 0 & 0 & 0 \end{bmatrix} & \dfrac{[1-(c^*)^3]}{[1-c^*]}\begin{bmatrix} A_{11}^* & A_{12}^* & A_{16}^* \\ A_{21}^* & A_{22}^* & A_{26}^* \\ A_{61}^* & A_{62}^* & A_{66}^* \end{bmatrix} \end{array}\right]$$

FIGURE 5.24 STIFFNESS MATRIX OF A HOMOGENIZED ANISOTROPIC SANDWICH PLATE

Prob. 5.3 **It can be shown that the interlaminar normal stresses along a free edge can be reduced if a fanned or spirally stacked composite laminate is used. This is achieved by separating the [45] from [-45] plies in a [/4] family of laminates, shown in the figure below:**

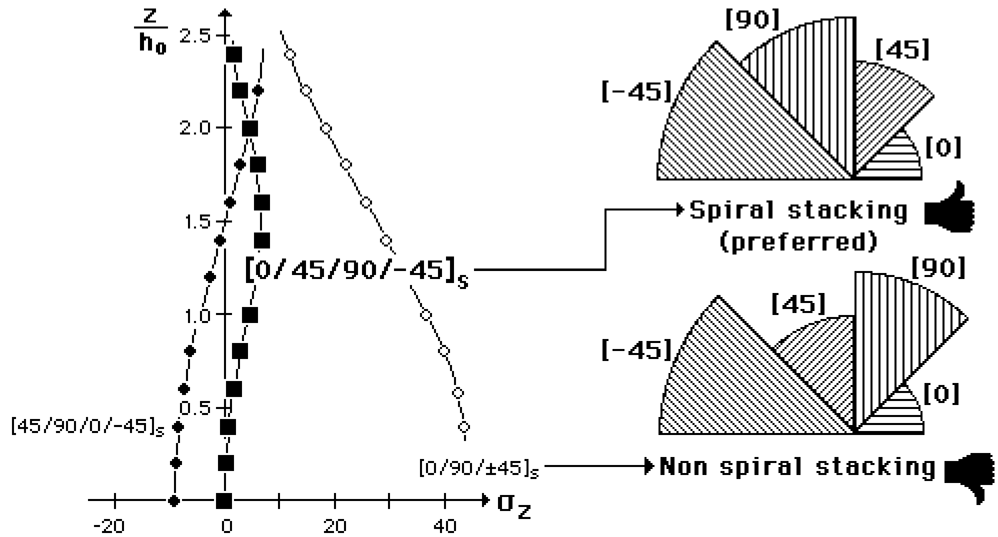

FIGURE 5.24 DELAMINATION RESISTANCE OF FANNED OR SPIRALLY STACKED LAMINATES

Is homogenization of spirally stacked laminates more difficult to achieve than non-spirally stacked? What is unique about [/3] family of laminates as far as spiral stacking is concerned?

Prob. 5.4 Plot polar plot of flexural stiffness that bridges between the two envelopes in Figure 5.18. The envelopes in this figure is no repeated sub-laminate, or repeat index is equal to unity. Try repeat indices of 2 and 3 that would illustrate the trend for larger repeats.

Section 6

STIFFNESS OF GENERAL LAMINATES

The most general laminate is one that does not have a mid-plane symmetry. The coupling between in-plane and flexure can be maximized or minimized by varying the number of repeated sub-laminates. An unsymmetric structure can also be simplified by using a thin wall, or stiffened construction. An unsymmetric laminate will twist under hygrothermal loading. Its shape is therefore not stable. This laminate warps, not the unbalanced laminate. Although most composites now in use are symmetrically laminated, there are opportunities to utilize unsymmetric laminates to produce an anticlastic surface from a flat tool, and a flat structure with unique pre-stress.

6.1 LAMINATED PLATE THEORY

The same assumptions found in the last sections are used for a general, unsymmetric laminate. The plate is thin, the strain is linear, and under stress the normal to the mid-plane of the laminate does not deform:

$$\text{Linear strain} = \{\boldsymbol{\epsilon}\} = \{\boldsymbol{\epsilon}^{\mathbf{o}}\} + z\{\mathbf{k}\} = \{\boldsymbol{\epsilon}^{\mathbf{o}}\} + z^*\{\mathbf{k}\}$$
$$\text{where } z^* = \frac{2z}{h},\ -1 \le z^* \le 1 \qquad (6.1)$$

Using the same normalized stresses and strains as before, there is no difference between the laminate and ply strains, but the laminate and ply stresses are statically equivalent. Ply stresses are piece-wise linear. The stresses and strains are shown in the figure below:

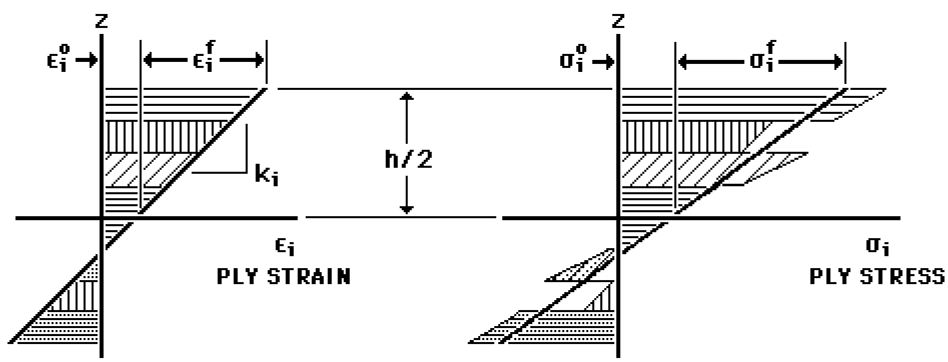

FIGURE 6.1 PLY STRESS AND STRAIN AND LAMINATE STRESS AND STRAIN

In the equation below, we use the linear relation in Equation 6.1 to express the in-plane loads in terms of the in-plane and coupling matrices of an unsymmetric laminate.

$$\{\mathbf{N}\} = \int_{-h/2}^{h/2}\{\boldsymbol{\sigma}\}\mathbf{d}z = \int_{-h/2}^{h/2}[\mathbf{Q}]\{\boldsymbol{\epsilon}\}\mathbf{d}z = \int_{-h/2}^{h/2}[Q]\left[\{\epsilon^o\}+z\{k\}\right]dz$$
$$= \left[\int_{-h/2}^{h/2}[Q]dz\right]\{\epsilon^o\} + \left[\int_{-h/2}^{h/2}[Q]z\,dz\right]\{k\} = [\mathbf{A}]\{\boldsymbol{\epsilon}^{\mathbf{o}}\}+[\mathbf{B}]\{\mathbf{k}\} \qquad (6.2)$$

Similarly, flexural loads can be related to the coupling and flexural matrices of the same laminate.

$$\begin{aligned}\{\mathbf{M}\} &= \int_{-h/2}^{h/2}\{\boldsymbol{\sigma}\}\mathbf{z}\,\mathbf{dz} = \int_{-h/2}^{h/2}[\mathbf{Q}]\{\boldsymbol{\epsilon}\}\mathbf{z}\,\mathbf{dz} = \int_{-h/2}^{h/2}[Q]\left[\{\epsilon^o\}+z\{k\}\right]zdz \\ &= \left[\int_{-h/2}^{h/2}[Q]zdz\right]\{\epsilon^o\}+\left[\int_{-h/2}^{h/2}[Q]z^2dz\right]\{k\} = \mathbf{[B]\{\epsilon^o\}+[D]\{k\}}\end{aligned} \qquad (6.3)$$

Like the case for the stiffness of symmetric laminates, the integrations above can be replaced by summation when all plies and ply groups are discrete and homogeneous:

$$\begin{aligned}\mathbf{[A]} &= \int_{-h/2}^{h/2}[Q]dz = \sum_{i=1}^{m}[Q']^{(i)}\left[z^{(i)}-z^{(i-1)}\right] = \text{in-plane matrix} \\ \mathbf{[B]} &= \int_{-h/2}^{h/2}[Q]zdz = \frac{1}{2}\sum_{i=1}^{m}[Q']^{(i)}\left[\left[z^{(i)}\right]^2-\left[z^{(i-1)}\right]^2\right] = \text{coupling matrix} \\ \mathbf{[D]} &= \int_{-h/2}^{h/2}[Q]z^2dz = \frac{1}{3}\sum_{i=1}^{m}[Q']^{(i)}\left[\left[z^{(i)}\right]^3-\left[z^{(i-1)}\right]^3\right] = \text{flexural matrix} \\ &\text{where } [Q']^{(i)} = \text{off-axis stiffness of the i-th ply group with angle } \theta^{(i)}\end{aligned} \qquad (6.4)$$

As in previous sections, we prefer to use normalized over absolute variables. The advantages of normalized variables include consistent units for stresses, strains, and laminate effective moduli. Direct comparison of the relative magnitudes of variables can be readily made. To this end, the in-plane stress, flexural stress, and flexural strain are defined as follows:

$$\{\boldsymbol{\sigma}^o\} = \frac{\mathbf{1}}{\mathbf{h}}\{\mathbf{N}\},\ \{\boldsymbol{\sigma}^f\} = \frac{\mathbf{6}}{\mathbf{h}^2}\{\mathbf{M}\},\ \{\boldsymbol{\epsilon}^f\} = \frac{\mathbf{h}}{\mathbf{2}}\{\mathbf{k}\} \qquad (6.5)$$

The advantage of normalized stresses and strains can be seen in the examples given in the table below. This comparison is similar to Figure 5.3 on page 5-3 covering a cross-ply laminate. We compare two quasi-isotropic laminates: one is solid, and the other has a sandwich core of 100 equivalent ply thickness. The resulting total number of plies are 80 and 280, respectively; the total thicknesses are 10 and 35 mm, respectively. The applied loads along the 1-direction for both laminates are the same; viz., a uniaxial load of 10 MN/m, and a bending moment of 0.1 MN. Even for symmetric laminates it is difficult to see the relative magnitudes of the applied loads because their units are different: MN/m versus MN.

		$[0/90/45/-45]_{10S}$			$[(0/90/45/-45)_{10}/c_{100}]_S$		
	[repeat]	[z/core]	h, #	h, E-3	[z/core]	h, #	h, E-3
	10.0	**0.0**	80	10.00	**100.0**	280	35.00
{N}MN/m		$\{\sigma^o\}$	$\{\epsilon^o\}$	$\{E^o\}$	$\{\sigma^o\}$	$\{\epsilon^o\}$	$\{E^o\}$
1	**10.00**	1000.	14.35	62.4	286.	14.35	17.8
2	**0.00**	0.	-4.25	62.4	0.	-4.25	17.8
6	**0.00**	0.	0.00	23.7	0.	0.00	6.8
{M} MN		$\{\sigma^f\}$	$\{\epsilon^f\}$	$\{E^f\}$	$\{\sigma^f\}$	$\{\epsilon^f\}$	$\{E^f\}$
1	**0.10**	6000.	81.45	66.9	490.	10.92	40.3
2	**0.00**	0.	-22.58	63.7	0.	-3.19	39.9
6	**0.00**	0.	-1.77	22.0	0.	-0.05	14.8

FIGURE 6.2 NORMALIZED IN-PLANE AND FLEXURAL STRESSES, STRAINS, AND MODULI

Using normalized stresses and strains listed in the table above, as defined in Equation 6.5, we can see the relative importance of the applied in-plane load to two different laminates. We compare 1000 and 286 MPa in-plane stresses in two laminates. We can also compare the relative importance of the in-plane versus flexural stresses for the same laminate. We compare 1000 versus 6000 MPa for the first laminate. The same comparisons of the resulting in-plane and flexural strains can be made. The key is that with normalization, all applied loads are in Pa; strains are dimensionless. Direct comparison between in-plane strain and curvature, for example, cannot be made. They must be normalized by using the last relation in Equation 6.5.

For the same reason that we normalized loads and deformation, all stiffness components should also be normalized so as to have the same unit in Pa. This is done in the following relations.

$$[A^*] = \frac{1}{h}[A],\ [B^*] = \frac{2}{h^2}[B],\ [D^*] = \frac{12}{h^3}[D],\ \text{in GPa} \qquad (6.6)$$

The normalization of the in-plane and flexural stiffnesses follows the conventional practice. The in-plane stiffness is corrected by the laminate thickness. That is the same factor used between stress resultant and the average laminate stress. The factor used for the flexural stiffness is a normalized moment of inertia of a rectangular section. The factor for the coupling component is more arbitrary. We believe that the factor of 2 is the best choice, as we will see in the resulting Equation 6.8 below.

PARTIAL INVERSION

With in-plane and flexure coupling, the stiffness matrix is now 6x6. A partial matrix inversion brings a useful result:

$$\{\epsilon^o\} = [a]\{N\} - [a][B]\{k\};\ \text{when } \{k\} = 0,\ \boldsymbol{\{\epsilon^o\} = [a]\{N\} = [a^*]\{\sigma^o\}}$$

$$\{M\} = [B][a]\{N\} + \big[[D] - [B][a][B]\big]\{k\},\ \text{in N} \qquad (6.7)$$

The relations are for all laminates, symmetric or not. The underlined relation is applicable to a situation where there is no change in curvature; i.e., {k} = 0. This simple relation is satisfied when a cylindrical shell is subjected to loading such as internal or external pressure, axial tension or compression, and torque. There is no need to have a symmetric wall if the load is axisymmetric. An unsymmetric layup is acceptable for this application.

LAMINATE STIFFNESS AND COMPLIANCE

The fully inverted stiffness matrix in both absolute and normalized terms is shown below:

	ABSOLUTE	NORMALIZED
STIFFNESS	$\begin{Bmatrix} N_i \\ \hline M_i \end{Bmatrix} = \left[\begin{array}{c\|c} A_{ij} & B_{ij} \\ \hline B_{ij} & D_{ij} \end{array}\right] \begin{Bmatrix} \epsilon_j^o \\ \hline k_j \end{Bmatrix}$	$\begin{Bmatrix} \sigma_i^o \\ \hline \sigma_i^f \end{Bmatrix} = \left[\begin{array}{c\|c} A_{ij}^* & B_{ij}^* \\ \hline 3B_{ij}^* & D_{ij}^* \end{array}\right] \begin{Bmatrix} \epsilon_j^o \\ \hline \epsilon_j^f \end{Bmatrix}$
COMPLIANCE	$\begin{Bmatrix} \epsilon_i^o \\ \hline k_i \end{Bmatrix} = \left[\begin{array}{c\|c} \alpha_{ij} & \beta_{ij} \\ \hline \tilde{\beta}_{ij} & \delta_{ij} \end{array}\right] \begin{Bmatrix} N_j \\ \hline M_j \end{Bmatrix}$	$\begin{Bmatrix} \epsilon_i^o \\ \hline \epsilon_i^f \end{Bmatrix} = \left[\begin{array}{c\|c} \alpha_{ij}^* & \frac{1}{3}\beta_{ij}^* \\ \hline \tilde{\beta}_{ij}^* & \delta_{ij}^* \end{array}\right] \begin{Bmatrix} \sigma_j^o \\ \hline \sigma_j^f \end{Bmatrix}$

(6.8)

Factors of 3 and 1/3 in the coupling matrices are the results of the particular normalization recommended in Equation 6.6 above. The total matrices are not symmetric, but we have uniform units. All normalized stress and stiffness have the same units in Pa. Strains are dimensionless. Compliance is 1/Pa. Thus all sub-matrices can be compared. A summary of the normalization is shown below for both the stiffness and compliance matrices:

$$A^*_{ij}, B^*_{ij}, D^*_{ij} = \left[\frac{1}{h}A_{ij}, \frac{2}{h^2}B_{ij}, \frac{12}{h^3}D_{ij}\right] \quad \alpha^*_{ij}, \beta^*_{ij}, \delta^*_{ij} = \left[h\alpha_{ij}, \frac{h^2}{2}\beta_{ij}, \frac{h^3}{12}\delta_{ij}\right] \tag{6.9}$$

In the absolute representation of the stress-strain relations, all sub-matrices have different units; e.g., [A] in N/m, [B] in N, and [D] Nm. As we have just discussed, direct comparison of stiffness components cannot be made unless their units are properly normalized.

6.2 REPEATED SUB-LAMINATES

We wish to find the applied stress resultants, applied moments, and the stiffness matrix of a laminate with respect to a plane other than the mid-plane. In the figure below, primed matrices are calculated using the new reference plane, **d** is the distance between the new and old reference planes.

d = **z - z'** = transfer distance (6.10)

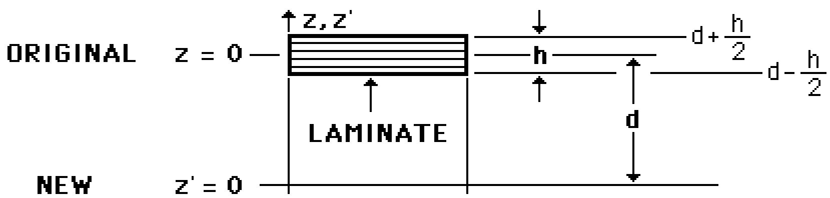

FIGURE 6.3 ORIGINAL AND NEW MID-PLANES FOR THE PARALLEL AXIS THEOREM

In the following equations, we show how the stress resultant and moment are transferred to the new axis:

$$\begin{aligned} & z = z'-d,\ dz = dz';\ -\frac{h}{2} \le z \le \frac{h}{2},\ d-\frac{h}{2} \le z' \le d+\frac{h}{2} \\ & \mathbf{\{N'\}} = \int_{d-h/2}^{d+h/2}\{\sigma\}dz' = \int_{-h/2}^{h/2}\{\sigma\}dz = \mathbf{\{N\}} \\ & \mathbf{\{M'\}} = \int_{d-h/2}^{d+h/2}\{\sigma\}z'dz' = \int_{-h/2}^{h/2}\{\sigma\}(z+d)dz = \mathbf{\{M\}+d\{N\}} \end{aligned} \tag{6.11}$$

We can derive the transferred stress-strain relations. First we express the stress resultant in terms of in-plane strain and curvature:

$$\begin{aligned} \{N'\} &= \int_{d-h/2}^{d+h/2}\{\sigma\}dz' = \int_{d-h/2}^{d+h/2}[Q]\left[\{\epsilon^{o'}\}+z'\{k'\}\right]dz' = \int_{-h/2}^{h/2}[Q]\left[\{\epsilon^{o'}\}+(z+d)\{k'\}\right]dz \\ &= [A]\{\epsilon^{o'}\}+\left[[B]+d[A]\right]\{k'\} = [A']\{\epsilon^{o'}\}+[B']\{k'\} \end{aligned} \tag{6.12}$$

Now, the moment is expressed in terms of the same in-plane strain and curvature:

$$\begin{aligned} \{M'\} &= \int_{d-h/2}^{d+h/2}\{\sigma\}z'dz' = \int[Q]\left[\{\epsilon^{o'}\}+z\{k'\}\right]z'dz' = \int_{-h/2}^{h/2}[Q]\left[\{\epsilon^{o'}\}+(z+d)\{k'\}\right](z+d)dz \\ &= \left[[B]+d[A]\right]\{\epsilon^{o'}\}+\left[[D]+2d[B]+d^2[A]\right]\{k'\} = [B']\{\epsilon^{o'}\}+[D']\{k'\} \end{aligned} \tag{6.13}$$

This parallel axis theorem can be expressed in terms of absolute and normalized variables:

d* = **d / h** = normalized transfer distance, **h** = thickness (6.14)

$$[A'] = [A],\ [B'] = [B]+d[A],\ [D'] = [D]+2d[B]+d^2[A]$$

$$[A'^*] = [A^*],\ [B'^*] = [B^*]+2d^*[A],$$

$$[D'^*] = [D^*]+12d^*[B^*]+12d^{*2}[A^*] \qquad (6.15)$$

Sub-laminates consist of a small assemblage of plies that can be repeated to form a thick laminate. Typical sub-laminates may have up to 10 plies and 4 ply angles, and they provide sufficient range of laminate properties in most practical applications. The advantages of sub-laminates are:

- An easy selection of optimum ply angles if the limits of 10-ply and 4-angle are imposed.
- A damage tolerant laminate resulting from maximum splicing or dispersion of plies.
- A simple, repeatable layup module resulting in lower cost and fewer errors in production.

The design process consists of two steps: determining first the optimum ply angles, and then the required number of repeating sub-laminates. The laminate code with sub-laminate in brackets, index r for repeat, and z_c for half-depth of sandwich core is:

$$\left[[\text{sub-lam}]_r/z_c\right]_S,\ \left[[\text{sub-lam}^+]_{r+}/c/[\text{sub-lam}^-]_{r-}\right]_T \qquad (6.16)$$

For unsymmetric constructions, different sub-laminates and different repeat indices can be used for the top and bottom faces, where c is the core.

In the case of a symmetric laminate, we can use the parallel axis theorem to derive the laminate stiffness matrix in terms of the sub-laminate and the repeating index. The definition of terms is shown in the figure below. The stiffness matrices for the sub-laminate, its location and thickness u are also shown.

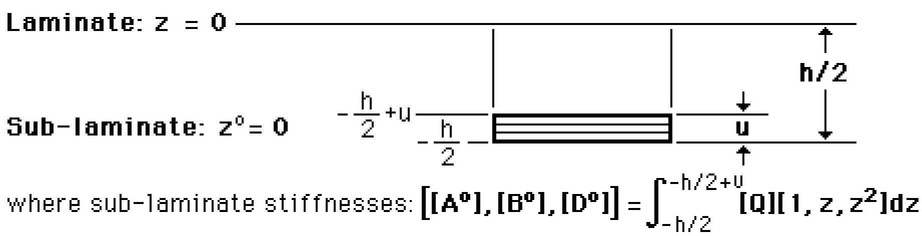

FIGURE 6.4 POSITION AND THICKNESS OF THE STIFFNESSES OF A SUB-LAMINATE

The relation between the sub-laminate and the total laminate is shown below:

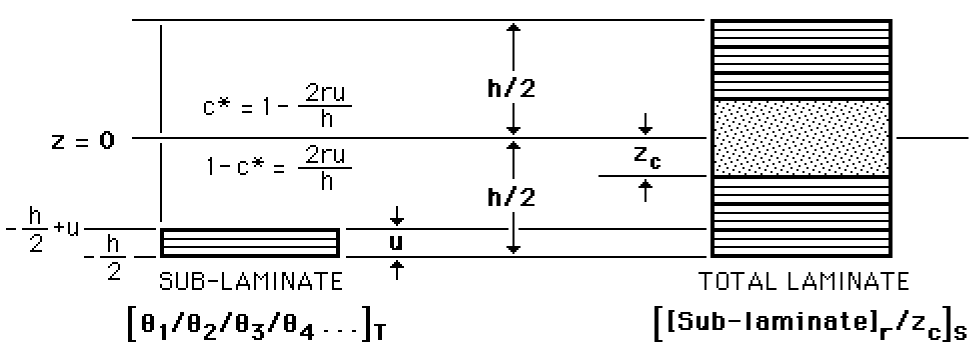

FIGURE 6.5 RELATION BETWEEN SUBLAMINATES AND TOTAL LAMINATE

In the derivation of the stiffnesses, the following series for the repeating index r were used:

$$\sum_{i=1}^{r} i = \frac{r(r+1)}{2}, \ \sum_{i=1}^{r} i^2 = \frac{r(r+1)(2r+1)}{6} \tag{6.17}$$

The stiffness matrices of the total laminate are, based on Equation 5.13 on page 5-9:

$$[A] = 2r[A^o],\ [B] = 0,\ [D] = 2r\left[[D^o]+(r-1)u[B^o]+\frac{(r-1)(2r-1)}{6}u^2[A^o]\right]$$
$$\text{where sub-laminate stiffnesses: } \left[[A^o],[B^o],[D^o]\right] = \int_{-h/2}^{-h/2+u}[Q][1, z, z^2]dz \tag{6.18}$$

If the total construction is unsymmetric but is built with the same sub-laminate, the equation above can be modified to include the repeating indices designating the top and bottom sections of the construction:

$$[A] = (r^+ + r^-)[A^o],\ [B] = (r^+ - r^-)[-[B^o]-(r^+ + r^- - 1)u[A^o]/2]$$
$$[D] = (r^+ + r^-)[D^o]+[r^+(r^+ - 1)+r^-(r^- - 1)]u[B^o]+[r^+(r^+ - 1)(2r^+ - 1)+r^-(r^- - 1)(2r^- - 1)]u^2[A^o]/6 \tag{6.19}$$

It is recommended to build a thick laminate from repeated sub-laminates. This is a good practice for in-plane loading. For bending and twisting, the use of sub-laminate will also lead to a stronger laminate, from being highly dispersed. Having fewer plies in a sub-laminate makes optimization of ply angles considerably simpler. In most practical cases, the sub-laminate does not need to have more than 10 plies. The effect of the stacking sequence of a thick laminate is important only when sub-laminates are not used. If many sub-laminates are used, the stacking sequence effect becomes negligible. This has been discussed in the previous section on homogenization. Thus, the use of sub-laminates is a very powerful option in the design of composite laminates for both in-plane and flexural loadings. The closed form relations above make the use of sub-laminates easy and simple.

6.3 UNSYMMETRIC CROSS-PLY LAMINATES

The integration or summation of the stiffness components cannot be further simplified for general, unsymmetric laminates, and must consider the entire laminate on a ply-by-ply basis. The location of a sandwich core is in general unsymmetric with respect to the mid-plane. The highly coupled in-plane and flexural behavior is also conceptually different from that of a symmetric laminate, and can be viewed as an opportunity to provide unique structural performances not possible with conventional constructions.

One of the simplest unsymmetric laminates is the cross-ply laminate of [0/90] shown in the figure below. The ply material is T300/5208, and the unit for the stiffness matrix is GPa. The in-plane and flexural stiffness matrices are identical. In fact, they are numerically equal to the homogeneous [0/90] cross-ply laminate shown in the last section.

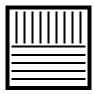

$[0/90]_{rT}$

$$\left[\begin{array}{c|c} A^*_{ij} & B^*_{ij} \\ \hline 3B^*_{ij} & D^*_{ij} \end{array}\right] = \left[\begin{array}{ccc|ccc} 96.0 & 2.9 & 0 & -\frac{42.8}{\mathbf{r}} & 0 & 0 \\ 2.9 & 96.0 & 0 & 0 & \frac{42.8}{\mathbf{r}} & 0 \\ 0 & 0 & 7.2 & 0 & 0 & 0 \\ \hline -\frac{128.6}{\mathbf{r}} & 0 & 0 & 96.0 & 2.9 & 0 \\ 0 & \frac{128.6}{\mathbf{r}} & 0 & 2.9 & 96.0 & 0 \\ 0 & 0 & 0 & 0 & 0 & 7.2 \end{array}\right]$$

FIGURE 6.6 NORMALIZED STIFFNESS MATRIX OF A CROSS-PLY LAMINATE, HAVING COUPLING COMPONENTS WHICH DECAY WITH REPEATING INDEX

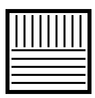

$[0/90]_{T}$

$$\left[\begin{array}{c|c} \alpha^*_{ij} & \frac{1}{3}\beta^*_{ij} \\ \hline \tilde{\beta}^*_{ij} & \delta^*_{ij} \end{array}\right] = \left[\begin{array}{ccc|ccc} 25.9 & -0.8 & 0 & 11.6 & 0 & 0 \\ -0.8 & 25.9 & 0 & 0 & -11.6 & 0 \\ 0 & 0 & 139 & 0 & 0 & 0 \\ \hline 34.7 & 0 & 0 & 25.9 & -0.8 & 0 \\ 0 & -34.7 & 0 & -0.8 & 25.9 & 0 \\ 0 & 0 & 0 & 0 & 0 & 139 \end{array}\right]$$

FIGURE 6.7 NORMALIZED COMPLIANCE MATRIX OF A CROSS-PLY LAMINATE WITH NO REPEAT

The equality between [A*] and [D*] is a necessary condition for homogeneity for symmetric laminates as described in the last section. The unsymmetric laminate above is obviously not homogeneous. Thus mid-plane symmetry is a required additional condition for homogeneity. The repeating index is responsible for the decay of the coupling terms. As the number of repeats increases the unsymmetric laminate becomes a homogeneous laminate.

The normalized compliance matrix is shown in Figure 6.7 above; the unit is 1/TPa. The compliance matrix below, however, is for only one repeat. The effect of repeated sub-laminates is not explicit.

The in-plane and flexural compliance matrices above remain the same, but they are no longer equal to those of a homogeneous cross-ply laminate; e.g., the "11" component here is 25.9 as compared with 10.4 for a homogeneous cross-ply laminate. The ply material is T300/5208.

Since a matrix inversion is required to obtain the compliance matrix, we cannot transfer the simple 1/r decay of the coupling component from the stiffness matrix to that of the compliance matrix. In the figure below, we show that the "11" component of the coupling matrices decreases in value with the number of repeats. Note that stiffness decays as 1/r, and the compliance decays faster than 1/r.

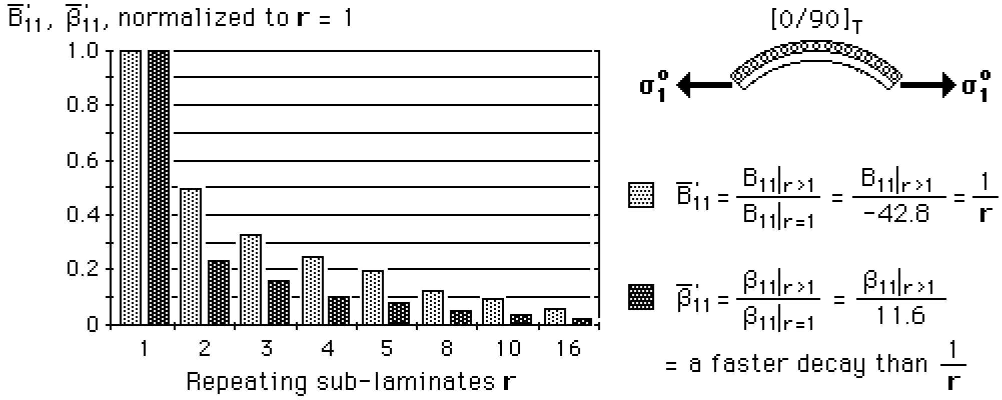

FIGURE 6.8 NORMALIZED DECAY OF THE COUPLING STIFFNESS AND COMPLIANCE COMPONENTS

The coupling components here are responsible for the bending curvature when a laminate is stretched. As the repeating index increases, this coupling effect decays. The coupling effect is shown in the figure above where the neutral axis, defined by zero strain, is shifted from the mid-plane.

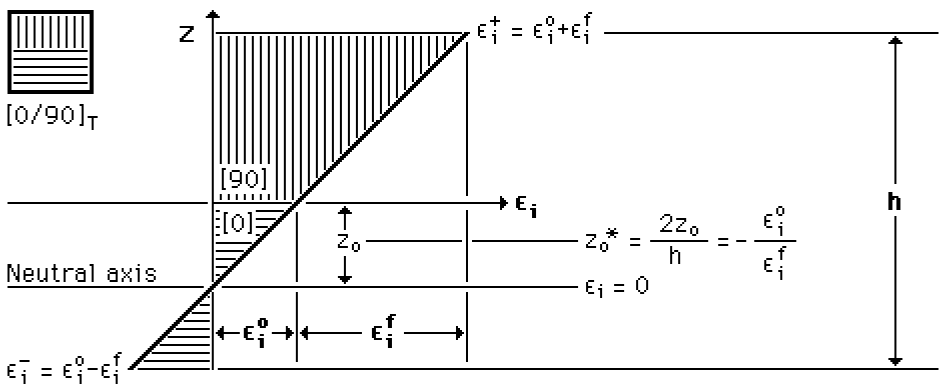

FIGURE 6.9 SHIFTING OF THE NEUTRAL AXIS OF AN UNSYMMETRIC LAMINATE

The coupling effect can be illustrated by simple loading cases such as uniaxial tensile and simple bending. The resulting strains and the shifts in the neutral axis are shown in Equation 6.20, and plotted in Figure 6.10 below:

$$\left.\begin{array}{l}
\text{Uniaxial tensile } \sigma_1^o\text{:}\quad \epsilon_1^o = \alpha^*_{11}\sigma_1^o,\ \ \epsilon_2^o = \alpha^*_{21}\sigma_1^o,\ \ \epsilon_1^f = \tilde{\beta}^*_{11}\sigma_1^o;\ \ z_o^* = -\dfrac{\alpha^*_{11}}{\beta^*_{11}} \\
\text{Bending moment } \sigma_1^f\text{:}\quad \epsilon_1^f = \delta^*_{11}\sigma_1^f,\ \ \epsilon_2^f = \delta^*_{21}\sigma_1^f,\ \ \epsilon_1^o = \dfrac{1}{3}\beta^*_{11}\sigma_1^f;\ \ z_o^* = -\dfrac{\beta^*_{11}}{3\delta^*_{11}}
\end{array}\right] \qquad (6.20)$$

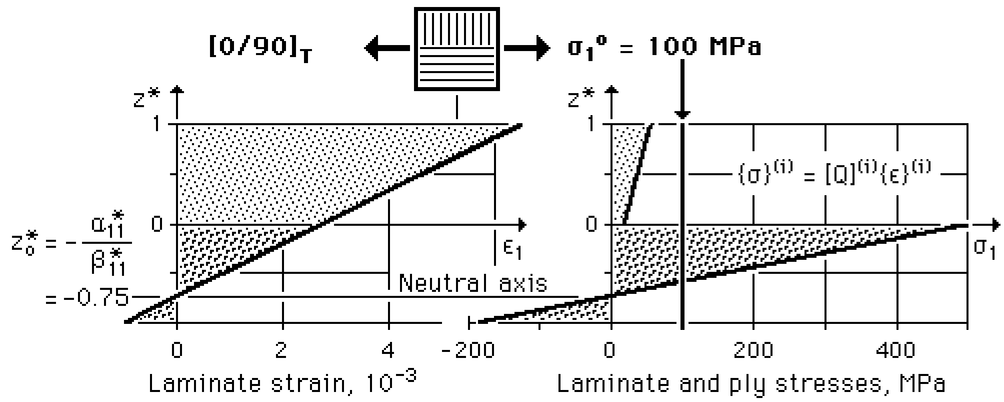

FIGURE 6.10 STRAIN AND STRESS VARIATIONS ACROSS THE THICKNESS OF AN UNSYMMETRIC CROSS-PLY LAMINATE SUBJECTED TO A UNIAXIAL TENSILE STRESS

As the repeating index increases, the distance to the neutral axis for the uniaxial tensile case goes to infinity. The strain becomes in-plane as the flexural strain goes to zero. For the bending case, the neutral axis approaches that of the mid-plane. The in-plane strain goes to zero. If the direction of the uniaxial stress changes from that along the 1-axis to the 2-axis, the sign of the coupling components changes. The shift of the neutral axis is in the opposite direction; i.e., +0.75. Neutral axis is meaningful only for beams. There is no equivalent neutral plane for anisotropic laminates. Matrices [A], [B], [D] completely define the elastic behavior of a laminate, as shown in Equation 6.4.

The ply stress at the neutral axis in Figure 6.10 is also zero. However, the stress is not always zero when the strain is zero. In fact, ply stress may be zero at more than one location. Strain, on the other hand, is linear and can only be zero in at most one location. There cannot be an inflection in the strain. This nondeformable normal to the mid-plane is one of the basic assumptions of the classical theory.

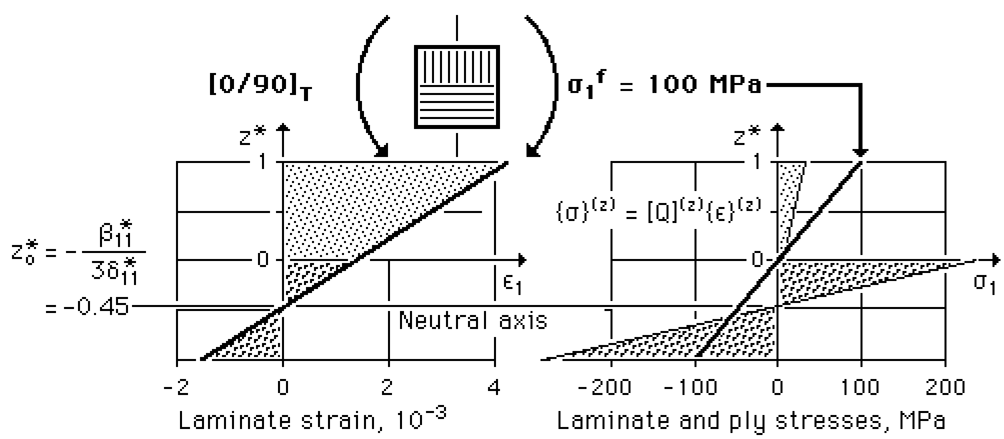

FIGURE 6.11 STRAIN AND STRESS VARIATIONS ACROSS THE THICKNESS OF AN UNSYMMETRIC CROSS-PLY LAMINATE SUBJECTED TO BENDING

In Figure 6.11 we show the stress and strain distributions of the same unsymmetric laminate subjected to a bending moment. A shift in the neutral axis is shown. Ply stress also vanishes at this neutral axis. If the same bending moment is applied along a constant value on the 2-axis, the shift of the axis will be in the positive direction; i.e., +0.45. The location of the neutral axis will vary with the reference coordinate axis. Neutral axis only applies to one bending. Thus, its concept is more useful for beams than for plates.

Homogenization by increasing the repeating index can be seen by the increase in the reciprocal of a typical compliance component, plotted in the figure below. As the repeats increase to infinity, we recover the Young's modulus of a homogeneous [0/90] laminate, which is 96 GPa. Thus we cannot define engineering constants for unsymmetric laminates. When a laminate is not repeated, the apparent Young's modulus is less than 40 percent of the modulus of a homogeneous laminate.

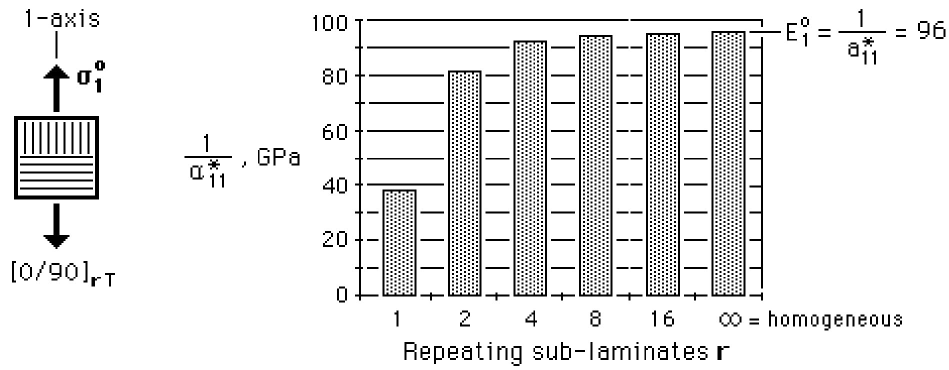

FIGURE 6.12 CONVERGENCE OF THE EFFECTIVE YOUNG'S MODULUS AS THE NUMBER OF REPEATS INCREASE

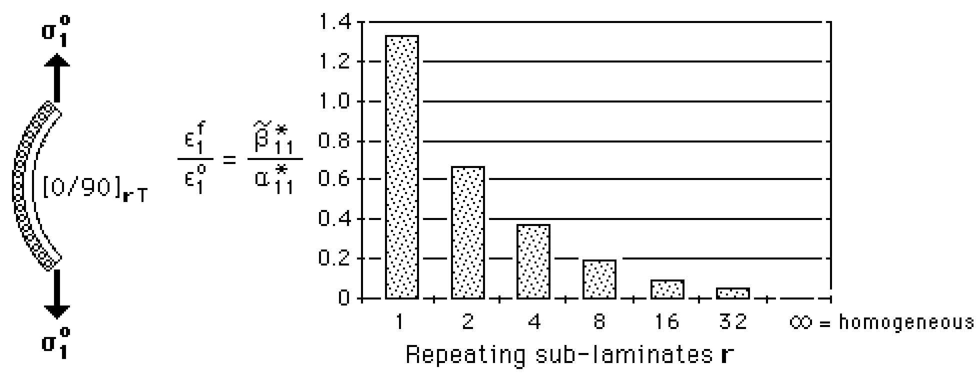

FIGURE 6.13 WARPAGE OF AN UNSYMMETRIC LAMINATE VS REPEAT INDEX

An unsymmetric laminate with a nonzero "11" coupling component, like that shown in Figure 6.6 on page 6-6, will warp under uniaxial tensile stress. The ratio between the flexural strain over the in-plane strain is a measure of the warpage. In the figure above, this ratio decreases as the repeating index increases. With many repeats, we recover the homogeneous laminate where warping vanishes.

6.4 OTHER UNSYMMETRIC LAMINATES

Another simple unsymmetric laminate, an angle-ply laminate, is shown in Figure 6.14. The in-plane and flexural stiffness of this unsymmetric laminate are equal to the corresponding stiffness matrix of a homogeneous [±45] laminate. The presence of nonzero coupling matrix differentiates between the two laminates if the repeating index is low in number. As the index becomes large, the laminate becomes homogenized.

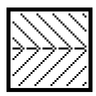

$[45/-45]_{rT}$

$$\left[\begin{array}{c|c} A_{ij}^* & B_{ij}^* \\ \hline 3B_{ij}^* & D_{ij}^* \end{array}\right] = \left[\begin{array}{ccc|ccc} 56.6 & 42.3 & 0 & 0 & 0 & -\frac{21.4}{\mathbf{r}} \\ 42.3 & 56.6 & 0 & 0 & 0 & -\frac{21.4}{\mathbf{r}} \\ 0 & 0 & 46.6 & -\frac{21.4}{\mathbf{r}} & -\frac{21.4}{\mathbf{r}} & 0 \\ \hline 0 & 0 & -\frac{64.3}{\mathbf{r}} & 56.6 & 42.3 & 0 \\ 0 & 0 & -\frac{64.3}{\mathbf{r}} & 42.3 & 56.6 & 0 \\ -\frac{64.3}{\mathbf{r}} & -\frac{64.3}{\mathbf{r}} & 0 & 0 & 0 & 46.6 \end{array}\right]$$

FIGURE 6.14 STIFFNESS MATRIX OF AN UNSYMMETRIC ANGLE-PLY LAMINATE

In the figure below, we show the compliance matrix of the most unsymmetric angle-ply [±45] laminate; i.e., the repeat index is unity. As was the case of the unsymmetric [0/90] laminate, the in-plane and flexural compliance matrices below are significantly higher than the corresponding matrices of a homogeneous [±45] laminate; e.g., the "66" component is 53.4 for the unsymmetric laminate as compared with 21.46 for the homogeneous laminate shown in Equation 4.18.

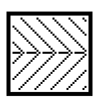

$[45/-45]_{T}$

$$\left[\begin{array}{c|c} \alpha_{ij}^* & \frac{1}{3}\beta_{ij}^* \\ \hline \tilde{\beta}_{ij}^* & \delta_{ij}^* \end{array}\right] = \left[\begin{array}{ccc|ccc} 47.7 & -22.3 & 0 & 0 & 0 & 11.6 \\ -22.3 & 47.7 & 0 & 0 & 0 & 11.6 \\ 0 & 0 & 53.4 & 11.6 & 11.6 & 0 \\ \hline 0 & 0 & 34.7 & 47.7 & -22.3 & 0 \\ 0 & 0 & 34.7 & -22.3 & 47.7 & 0 \\ 34.7 & 34.7 & 0 & 0 & 0 & 53.4 \end{array}\right]$$

FIGURE 6.15 THE MOST UNSYMMETRIC ANGLE-PLY [±45] LAMINATE COMPLIANCE

The difference between the unsymmetric and homogeneous laminates is illustrated by the apparent shear modulus as a function of the repeating index in the figure below. The difference in the value of the "66" component, cited above, is reflected in the apparent shear modulus, as measured by the reciprocal of the "66" component of the in-plane compliance. When the repeating index is four, the apparent shear modulus reaches within 3 GPa of the fully homogenized laminate of 46.6 GPa. The convergence is rapid.

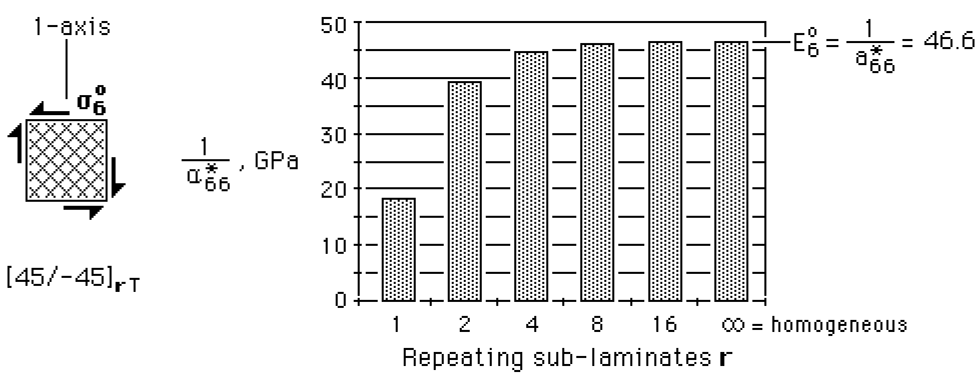

FIGURE 6.16 CONVERGENCE OF SHEAR MODULUS OF AN UNSYMMETRIC LAMINATE TO THAT OF A FULLY HOMOGENIZED [±45] LAMINATE

The next common laminate would be the generalized [π/4] laminate. The coupling matrix is fully populated, and every component is dependent on **1**/**r**. The in-plane stiffness is the same as in the homogeneous [π/4] laminate which happens to be quasi-isotropic.

The flexural stiffness has different dependency on the repeating index. The twisting coupling components are proportional to the reciprocal of the square of the repeat, and they decay with **1**/**r**. Flexural stiffness would become orthotropic and homogeneous more rapidly as the repeating index increases. The rate of decay is $\mathbf{1/r^2}$. This is shown in Figure 6.17. The Poisson and shear components, the "12" and "66" components, are the same in the in-plane and flexural matrices.

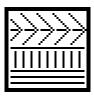

$[0/90/45/-45]_{rT}$

$$\left[\begin{array}{c|c} A^*_{ij} & B^*_{ij} \\ \hline 3B^*_{ij} & D^*_{ij} \end{array}\right] = \left[\begin{array}{ccc|ccc} 76.4 & 22.6 & 0 & -\frac{20.6}{r} & \frac{9.8}{r} & -\frac{5.4}{r} \\ 22.6 & 76.4 & 0 & \frac{9.8}{r} & \frac{0.9}{r} & -\frac{5.4}{r} \\ 0 & 0 & 26.9 & -\frac{5.4}{r} & -\frac{5.4}{r} & \frac{9.8}{r} \\ \hline -\frac{61.7}{r} & \frac{29.6}{r} & -\frac{16.1}{r} & 109.(r) & 22.6 & -\frac{16.1}{r^2} \\ \frac{29.6}{r} & \frac{2.6}{r} & -\frac{16.1}{r} & 22.6 & 44.(r) & -\frac{16.1}{r^2} \\ -\frac{16.1}{r} & -\frac{16.1}{r} & \frac{29.6}{r} & -\frac{16.1}{r^2} & -\frac{16.1}{r^2} & 26.9 \end{array}\right]$$

.

FIGURE 6.17 STIFFNESS MATRIX OF UNSYMMETRIC [/4] LAMINATES WITH VARYING DEPENDENCE ON THE REPEATING INDEX

The normal flexural components "11" and "22" are dependent on the repeating index, and are also bound by the same first linear invariant of symmetric laminates:

$$\text{Linear invariants: } I_1 = A^*_{11}+A^*_{22}+2A^*_{12} = D^*_{11}+D^*_{22}+2D^*_{12} = 198 \text{ GPa}$$

$$\text{When } A^*_{12} = D^*_{12},\ A^*_{11}+A^*_{22} = D^*_{11}+D^*_{22} = 153 \text{ GPa}$$

$$\text{Other invariants: } I_2 = A^*_{11}+A^*_{22}+2A^*_{66} = D^*_{11}+D^*_{22}+2D^*_{66} = 206 \text{ GPa}$$

$$I_1 = B^*_{11}+B^*_{22}+2B^*_{12} = 0,\ I_2 = B^*_{11}+B^*_{22}+2B^*_{66} = 0, \text{ or } B^*_{12} = B^*_{66} \qquad (6.21)$$

The compliance matrix is shown in the figure below for the case of the repeat index of unity; i.e., the most unsymmetric [π/4] laminate. The matrix is fully populated.

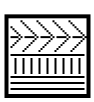

$[0/90/45/-45]_T$

$$\left[\begin{array}{c|c} \alpha^*_{ij} & \frac{1}{3}\beta^*_{ij} \\ \hline \tilde{\beta}^*_{ij} & \delta^*_{ij} \end{array}\right] = \left[\begin{array}{ccc|ccc} 27.7 & -10.0 & -6.4 & 8.6 & -9.1 & 5.5 \\ -10.0 & 18.2 & -3.0 & -4.2 & 4.8 & 3.1 \\ -6.4 & -3.0 & 65.9 & -1.8 & 0.7 & -26.7 \\ \hline 25.7 & -12.7 & -5.4 & 18.9 & -12.8 & 8.2 \\ -27.3 & 14.4 & 2.0 & -12.8 & 39.9 & 12.9 \\ 16.6 & 9.2 & -80.2 & 8.2 & 12.9 & 84.3 \end{array}\right]$$

FIGURE 6.18 COMPLIANCE MATRIX FOR THE MOST UNSYMMETRIC [Pi/4] LAMINATE, WITH A UNITY REPEATING INDEX. THE PLY MATERIAL IS T300/5208

Engineering constants are those derived from simple tests such as uniaxial loading, pure shear loading, simple bending or pure twisting. For combined stresses, the engineering constants are no more useful than the components of the compliance matrix above.

Engineering constants for unsymmetric laminates are uncommon and difficult to measure directly because in-plane and flexural deformations are coupled. The constants can also be improperly used. For example, a direct comparison between equivalent constants of unsymmetric laminates should not be made. As we have illustrated earlier in this section, effective engineering constants are meaningful only for laminates with many repeated sub-laminates; i.e., the asymmetry is small. In the equation below we emphasize the difference between engineering constants and the compliance components for symmetric and unsymmetric laminates, in Latin and Greek letters respectively:

ENGINEERING CONSTANTS NOT DEFINED

$$\begin{array}{ll} E_1^o = \dfrac{1}{a_{11}^*} \neq \dfrac{1}{\alpha_{11}^*} & E_1^f = \dfrac{1}{d_{11}^*} \neq \dfrac{1}{\delta_{11}^*} \\ E_2^o = \dfrac{1}{a_{22}^*} \neq \dfrac{1}{\alpha_{22}^*} & E_2^f = \dfrac{1}{d_{22}^*} \neq \dfrac{1}{\delta_{22}^*} \\ E_6^o = \dfrac{1}{a_{66}^*} \neq \dfrac{1}{\alpha_{66}^*} & E_6^f = \dfrac{1}{d_{66}^*} \neq \dfrac{1}{\delta_{66}^*} \end{array} \tag{6.22}$$

If we use repeated [π/4] sub-laminates, the convergence to the engineering constants of a homogenized [π/4] can occur as shown in the figure below. Using T300/5208 as the ply material, the convergence to the homogeneous constants approximates within 5 percent when the repeating index is as low as 4. From the standpoint of practicality, unsymmetric and symmetric [π/4] laminates are hardly distinguishable within 5 percent error. This may make fabrication easier and less costly because less control is needed in the stacking.

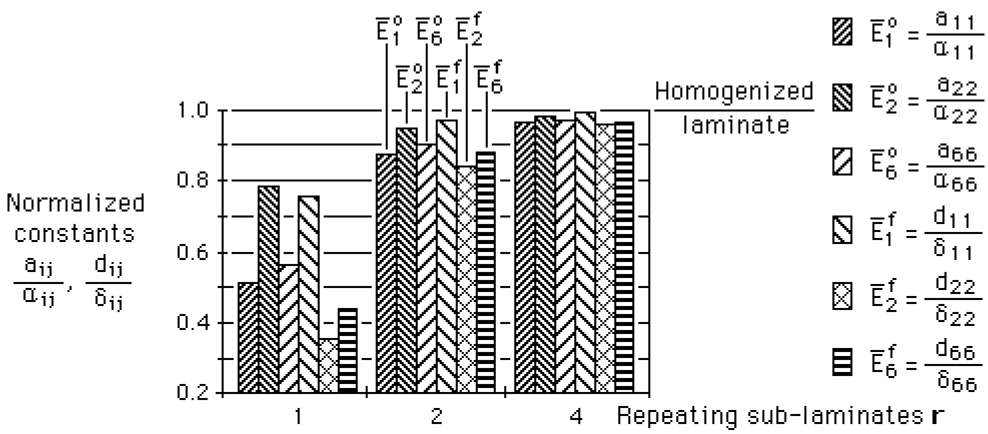

FIGURE 6.19 CONVERGENCE OF THE UNSYMMETRIC LAMINATES VS REPEATS

6.5 HYGROTHERMAL WARPAGE

Hygrothermal expansion or contraction of an unsymmetric laminate, even with uniformly distributed temperature and moisture, will cause warping. The shape and degree of warpage will depend on the coupling coefficients in the equation below, and the nonmechanical stresses:

$$\begin{Bmatrix} \epsilon_i^{(o)n} \\ \epsilon_i^{(f)n} \end{Bmatrix} = \begin{bmatrix} \alpha_{ij}^* & \frac{1}{3}\beta_{ij}^* \\ \tilde{\beta}_{ij}^* & \delta_{ij}^* \end{bmatrix} \begin{Bmatrix} \sigma_j^{(o)n} \\ \sigma_j^{(f)n} \end{Bmatrix} \tag{6.23}$$

From Equation 4.27 on page 4-17, we know how to determine the nonmechanical in-plane stresses. The flexural stresses can be similarly determined, as shown in the equation below:

$$\sigma_{[1,2,6]}^{(f)n} = \frac{6M^n}{h^2} = \frac{6}{h^2}\int_{-h/2}^{h/2}\sigma_{[1,2,6]}^{n}\,z\,dz$$

where $\sigma_1^n = p^n+q^n\cos2\theta,\ \sigma_2^n = p^n-q^n\cos2\theta,\ \sigma_6^n = q^n\sin2\theta$

$$p^n, q^n = \frac{\sigma_x^n \pm \sigma_y^n}{2} = \frac{(Q_{xx}\pm Q_{xy})e_x+(Q_{xy}\pm Q_{yy})e_y}{2} \qquad (6.24)$$

The integration in the equation above is shown below. The hygrothermal flexural stresses are unique in that the two normal components remain equal in value, and opposite in sign. They always appear together. It is not possible to have one without the other.

$$\sigma_{[1,2,6]}^{(f)n} = \left[\,q^nV_{1B}^*,\ -q^nV_{1B}^*,\ q^nV_{3B}^*\,\right]$$

where $\displaystyle\int_{-h/2}^{h/2} p^n z\,dz = p^n\int_{-h/2}^{h/2} z\,dz = 0$, then $\sigma_1^n = -\sigma_2^n = qV_{1B}^*$ (6.25)

The normalized combinations of the cosine and sine functions are shown below:

$$V_{1B}^* = \frac{6}{h^2}\int \cos2\theta\, z\,dz = \frac{3}{h^2}\sum_{i=1}^{m}\left[\cos2\theta\right]^{(i)}\left[\left[z^{(i)}\right]^2-\left[z^{(i-1)}\right]^2\right]$$

$$V_{3B}^* = \frac{6}{h^2}\int \sin2\theta\, z\,dz = \frac{3}{h^2}\sum_{i=1}^{m}\left[\sin2\theta\right]^{(i)}\left[\left[z^{(i)}\right]^2-\left[z^{(i-1)}\right]^2\right] \qquad (6.26)$$

For a [0/90] cross-ply laminate of T300/5208 composite having a temperature difference of -100°K, we know from Figure 6.6 on page 6-6 that the two coupling compliances are equal but opposite in sign, having a value of 34.7.

Non zero $\{\sigma\}^n$: $\sigma_1^{(o)n} = \sigma_2^{(o)n} = -15.1$ MPa; $\sigma_1^{(f)n} = -\sigma_2^{(f)n} = -12.3$ MPa

then, non zero $\{\varepsilon\}^n$: $\varepsilon_1^{(o)n} = (\alpha_{11}^*+\alpha_{12}^*)\sigma_1^{(o)n} + \dfrac{\beta_{11}^*}{3}\sigma_1^{(f)n} = \varepsilon_2^{(o)n} = -0.52\times10^{-3}$

$\varepsilon_1^{(f)n} = \tilde{\beta}_{11}^*\sigma_1^{(o)n} + (\delta_{11}^*-\delta_{12}^*)\sigma_1^{(f)n} = -\varepsilon_2^{(f)n} = -0.85\times10^{-3}$ (6.27)

The two normal flexural strains are equal for a [0/90] laminate, and the deformed "saddle" shape is shown in the figure below. We can repeat the calculation above from other ply ratios of cross-ply laminates. Although the bending moments due to a temperature difference of 100°K remain equal in value and opposite in sign, the resulting flexural strains are not equal, and change with the ply ratios.

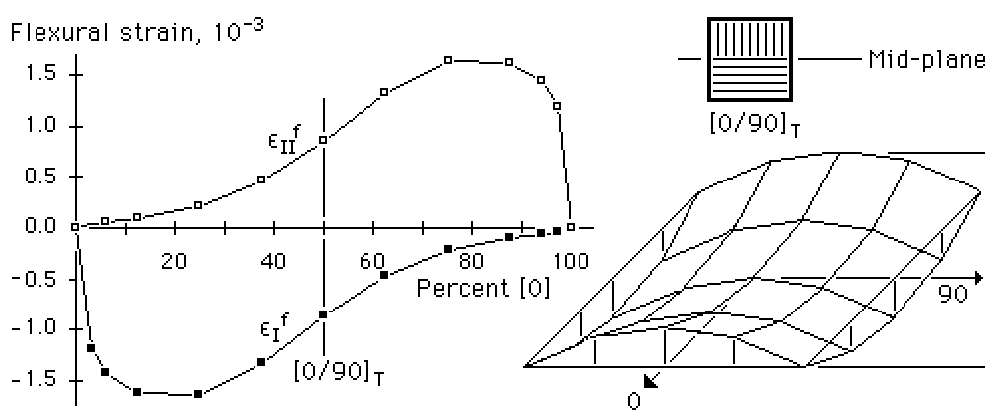

FIGURE 6.20 THERMAL FLEXURAL STRAINS OF A CROSS-PLY LAMINATE OF T300/5208

Similarly we can determine the nonmechanical strains of a [±45] of T300/5208 composite, having a temperature difference of -100°K. The calculation is shown in the following. The compliance used for this laminate can be found in Figure 6.14 on page 6-10.

$$\text{Non zero } \{\sigma\}^n:\ \sigma_1^{(o)n} = \sigma_2^{(o)n} = -15.1 \text{ MPa};\ \sigma_6^{(f)n} = -24.6 \text{ MPa}$$

$$\text{then, non zero } \{\epsilon\}^n:\ \epsilon_1^{(o)n} = (\alpha^*_{11}+\alpha^*_{12})\sigma_1^{(o)n} + \frac{\beta^*_{16}}{3}\sigma_6^{(f)n} = \epsilon_2^{(o)n} = -0.52\times10^{-3}$$

$$\epsilon_6^{(f)n} = 2\tilde{\beta}^*_{61}\sigma_1^{(o)n} + \delta^*_{66}\sigma_6^{(f)n} = -\epsilon_2^{(f)n} = -1.70\times10^{-3} \qquad (6.28)$$

The deformed shape of a [0/90] is shown below. The "saddle" shape is the same as the one above except the axes are rotated 45 degrees. As the ply ratio changes, the resulting flexural strains also change.

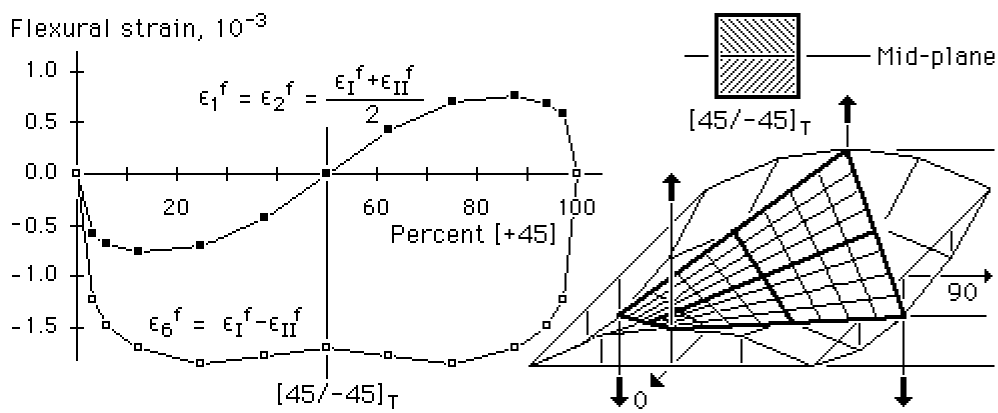

FIGURE 6.21 THERMAL FLEXURAL STRAINS OF A ANGLE-PLY LAMINATE OF T300/5208

We have illustrated the warpage of unsymmetric laminates due to changes in temperature and/or moisture content. The theory is straightforward. Since hygrothermal stresses are predictable, they should be included in design.

6.6 THIN WALL CONSTRUCTION

A thin wall construction has thin face sheets relative to the total thickness of a sandwich or stiffened construction. The face sheets can use different materials and thicknesses. The face sheets should be symmetric to avoid stretching/flexure coupling. With these limitations, laminated plate theory for an unsymmetric construction can be greatly simplified. A typical construction is shown in the figure below:

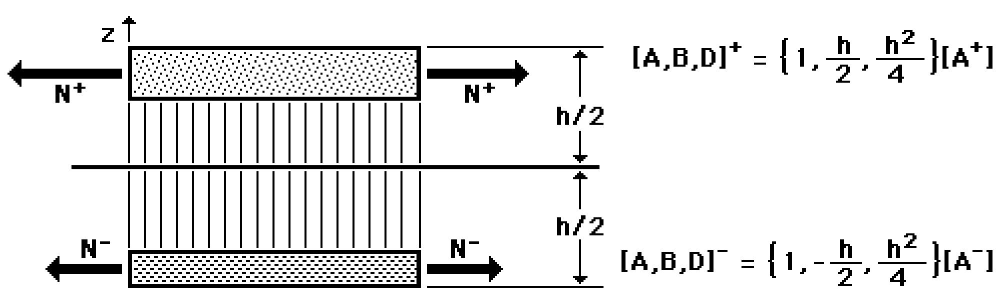

FIGURE 6.22 A THIN WALL, UNSYMMETRIC CONSTRUCTION

The in-plane stiffness matrices of the face sheets will control the stiffness of the entire construction. The total stiffness of this construction is simply the sum of the top and bottom faces. The forces acting on the entire thin wall construction are controlled by the in-plane stress resultants acting on the top and bottom face sheets. From these resultants, the total in-plane and flexural loads are defined.

Total stiffnesses:

$$[A] = [A^+ + A^-],\ [B] = \frac{h}{2}[A^+ - A^-],\ [D] = \frac{h^2}{4}[A^+ + A^-]$$

Total forces:

$$\{N\} = \{N^+ + N^-\},\ \{M\} = \frac{h}{2}\{N^+ - N^-\}$$

Face sheet forces:

$$\{N^+\} = \left\{\frac{N}{2} + \frac{M}{h}\right\},\ \{N^-\} = \left\{\frac{N}{2} - \frac{M}{h}\right\} \qquad (6.29)$$

When the in-plane stiffnesses of the face sheets are equal, we have a symmetric construction, for which [B] vanishes.

The resulting stresses and strains at the top and bottom face sheets, and the in-plane and curvature of the construction are:

$$\{N^+\} = [A^+]\{\epsilon^+\},\ \{N^-\} = [A^-]\{\epsilon^-\};\ \ \{\epsilon^+\} = [a^+]\{N^+\},\ \{\epsilon^-\} = [a^-]\{N^-\}$$

$$\{\epsilon^o\} = \frac{\{\epsilon^+ + \epsilon^-\}}{2},\ \{k\} = \frac{\{\epsilon^+ - \epsilon^-\}}{h};\ \ \{\epsilon^+\} = \{\epsilon^o\} + \frac{h\{k\}}{2},\ \{\epsilon^-\} = \{\epsilon^o\} - \frac{h\{k\}}{2} \qquad (6.30)$$

We can show the following stiffness and compliance matrices by matrix inversion of the stiffness components in Equation 6.29 or normalization by Equation 6.9:

$$[\alpha] = \frac{[a^+ + a^-]}{4},\ [\beta] = \frac{[a^+ - a^-]}{2h},\ [\delta] = \frac{[a^+ + a^-]}{h^2}$$

$$[A^*] = \frac{[A^+ + A^-]}{h},\ [B^*] = \frac{[A^+ - A^-]}{h},\ [D^*] = \frac{3[A^+ + A^-]}{h}$$

$$[\alpha^*] = \frac{h[a^+ + a^-]}{4},\ [\beta^*] = \frac{h[a^+ - a^-]}{4},\ [\delta^*] = \frac{h[a^+ + a^-]}{12} \qquad (6.31)$$

These relations for unsymmetric construction are more easily obtained than the complete laminated plate theory, which requires a 6x6 matrix and its inversion.

The simplified theory of thin wall construction is useful for design, although the intrinsic errors introduced by this approach must be explained. We will make a comparison between the unabridged and simplified theories to illustrate the errors.

The simplest comparison is the strain variation across a thin face sheet shown in the figure below. Let us assume that the top face sheet shown is 10 percent of the half-thickness h/2 of the total construction. Since linear strain across the entire construction is assumed, it varies from 0.9 to unity. The average strain would be 0.95 of the top face sheet, with 5 percent error. The error introduced by the approximation of the strain in a thin wall construction is the same as the ratio of the face sheets to the total thicknesses.

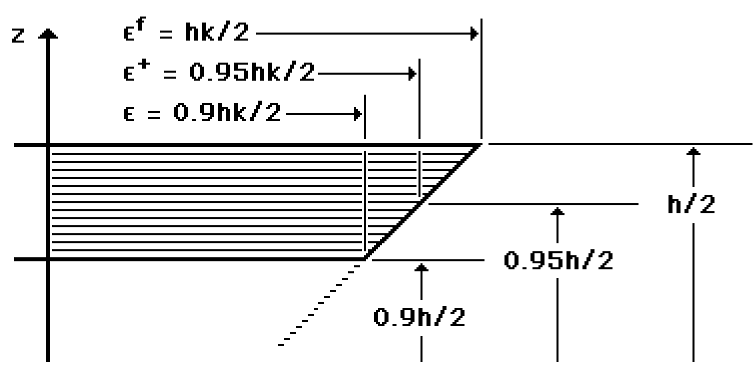

FIGURE 6.23 STRAIN ACROSS THE TOP FACE OF A THIN WALL CONSTRUCTION

A comparison of the elastic constants of the construction can be made. The laminates have 80 and 98 percent core, respectively. The results using the unabridged, exact theory, and those obtained with thin wall theory are listed in the table here. We can say that a thin wall construction with 98 percent core will have, in the worst case, a 2 percent error. This happens in the flexural stiffness. For "thick wall" construction of, for example, 80 percent core, the worst-case error of simplified theory is 20 percent.

TABLE 6.1 COMPARISON OF ELASTIC MODULI BETWEEN EXACT AND THIN WALL THEORIES

Laminate	$[90/c_8/0]$, $c^* = 0.80$			$[90/c_{98}/0]$, $c^* = 0.98$		
	EXACT THEORY	THIN WALL	PERCENT ERROR	EXACT THEORY	THIN WALL	PERCENT ERROR
A_{11}^*	19.1	19.1	0.0	1.91	1.91	0.0
B_{11}^*	15.4	17.1	11.0	1.70	1.71	0.6
D_{11}^*	47.7	57.3	20.0	5.65	5.73	1.4
α_{11}^*	252	256	0.2	2564	2565	0.1
β_{11}^*	249	229	8.7	2200	2290	0.4
δ_{11}^*	103	86	21.0	872	855	2.0

Thus, a simplified theory of unsymmetric constructions is useful if it can capture the salient features of composite materials without the burden of a complete laminated plate theory. In fact, unsymmetric designs are used in practice for structural and non-structural reasons. The thin wall theory gives excellent results provided the wall is thin: the wall thicknesses are less than 10 percent of the total thickness, and the loading is primarily in-plane.

6.7 STIFFENED PANELS

The repeating section of a panel stiffened with one rib along the 1-axis is shown in the figure below. The stiffness of this panel can be obtained by applying the parallel axis theorem to the plate and the rib.

The stiffnesses of the face plate and the rib are:

$$[A,B,D]^p = \int_{-h'/2}^{h'/2} [Q]^p [1,z,z^2]dz,\ [A_{11},B_{11},D_{11}]^r = \frac{a}{b}\int_{-h''/2}^{h''/2}[Q_{11}]^r[1,z,z^2]dz$$

$$\text{If rib along the z-axis: } A_{11}{}^r = \frac{h''}{h}\int_{-a/2}^{a/2} Q_{11}{}^r dy,\ B_{11}{}^r = 0,\ D_{11}{}^r = \frac{h''^2}{12}A_{11}{}^r \qquad (6.32)$$

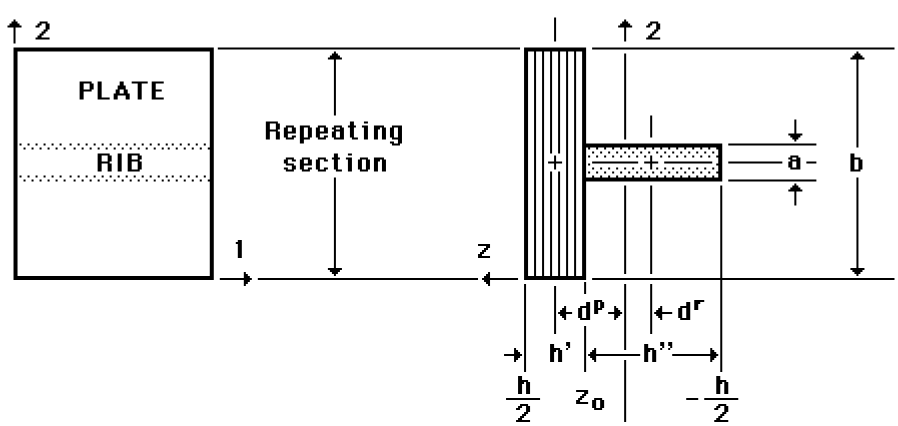

FIGURE 6.24 A REPEATING SECTION OF STIFFENED PANEL BY A RIB IN THE 1-AXIS

Using the parallel axis theorem, we can combine the stiffness of the plate and the rib:

$$A_{11} = A_{11}{}^{p}+A_{11}{}^{r},\ B_{11} = B_{11}{}^{p}+d^{p}A_{11}{}^{p}+B_{11}{}^{r}+d^{r}A_{11}{}^{r}$$
$$D_{11} = D_{11}{}^{p}+2d^{p}B_{11}{}^{p}+(d^{p})^{2}A_{11}{}^{p}+D_{11}{}^{r}+2d^{r}B_{11}{}^{r}+(d^{r})^{2}A_{11}{}^{r} \qquad (6.33)$$

If the plate and the rib are symmetrical with respect to their own mid-plane, the coupling matrix [B] will be identically zero, and the last equations become:

$$A_{11} = A_{11}{}^{p}+A_{11}{}^{r},\ B_{11} = d^{p}A_{11}{}^{p}+d^{r}A_{11}{}^{r},$$
$$D_{11} = D_{11}{}^{p}+(d^{p})^{2}A_{11}{}^{p}+D_{11}{}^{r}+(d^{r})^{2}A_{11}{}^{r} \qquad (6.34)$$

The other components of the stiffness of the stiffened panel are assumed to be unaffected by the rib; i.e., components other than the "11" are:

$$A_{ij} = A_{ij}{}^{p},\ B_{ij} = B_{ij}{}^{p}+d^{p}A_{ij}{}^{p},$$
$$D_{ij} = D_{ij}{}^{p}+2d^{p}B_{ij}{}^{p}+(d^{p})^{2}A_{ij}{}^{p} \qquad (6.35)$$

This assumption is valid when the rib is small relative to the plate; i.e., a/b is small.

If the plate is symmetric about its mid-plane, the last equation can be further simplified. If the rib runs in the 2-direction, the subscript 2 will simply replace subscript 1. All the "11" components will be changed to the "22" components. If there are ribs in both directions, both "11" and "22" components will appear. If the stiffened panel is used as the top cover of the thin wall construction described earlier, the in-plane stiffnesses of the plate and the rib will be those of the face sheet:

$$A_{11} = A_{11}{}^{p}+A_{11}{}^{r} = A_{11}{}^{+},$$
$$\text{all other components: } A_{ij}{}^{p} = A_{ij}{}^{+},\ 0 < A_{12}{}^{+} < A_{21}{}^{+} \qquad (6.36)$$

Similar expressions can be obtained for the bottom face.

The method for the stiffened panel shown above can be applied to a more complicated geometry than the plate and the rib. For example, pultruded sections of complex geometry can be similarly analyzed. The width of the repeating section b has not entered the calculation. Only the ratio a/b has been used. The calculation is intended to apply to unit width.

If the actual width is needed, all components of the stiffness matrix [A] must be multiplied by the actual width; e.g., if the width is less than 1 meter, the panel stiffness will be reduced proportionally.

As a sample problem, find the "11" component in the stiffness matrix of a stiffened panel consisting of T300/5208, 160 plies of [±45] as the plate, and 40 plies of [0] as the rib. The dimensions are shown in the figure below. The total thickness of the panel is h = 0.04 m; the width of the rib a = 0.005 m; and the width of the repeating section b = 0.05 m.

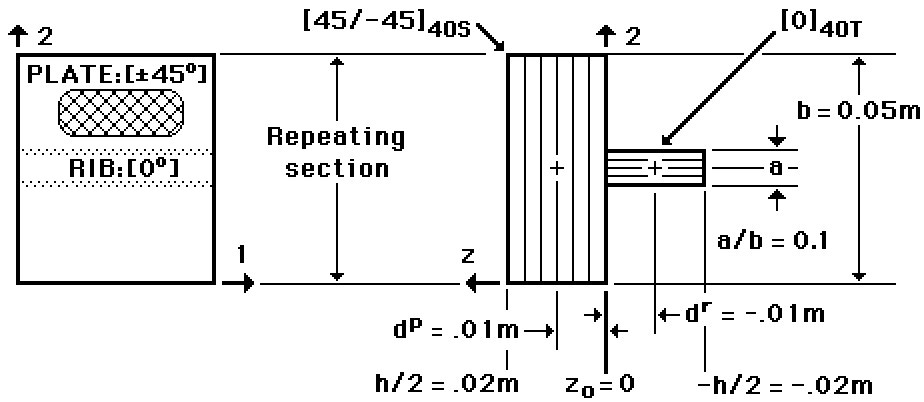

FIGURE 6.25 A SAMPLE STIFFENED PANEL.

For the face plate, the components of the stiffness matrix are designated with a superscript p:

$$\begin{aligned}
&\text{For the 160-ply [45/-45] plate, } h' = 160h_o = 0.02\,\text{m} \\
&A_{11}^* = 56.66\text{ GPa},\ A_{11}^p = A_{11}^*h' = 56.66\text{x}0.02 = 1133\text{ MN/m},\ B_{11}^p = 0 \\
&D_{11}^p = A_{11}^*(h')^3/12 = 37.77\text{ kNm}
\end{aligned} \tag{6.37}$$

For the rib, the components of the stiffness matrix are designated with a superscript **r**:

$$\begin{aligned}
&\text{For the 40-ply [0] rib, } h'' = 0.02\,\text{m},\ (h'')^3/12 = 0.666\text{x}10^{-6}\,\text{m}^3,\ a/b = 0.1 \\
&Q_{xx} = 181.81\text{ GPa},\ A_{11}^r = (a/b)Q_{xx}h'' = 0.1\text{x}181.81\text{x}.02 = 363.6\text{ MN/m} \\
&B_{11}^r = 0,\ D_{11}^r = (a/b)Q_{xx}(h'')^3/12 = 12.11\text{ kNm}
\end{aligned} \tag{6.38}$$

We can find the "11" components of the stiffness matrix by substituting the values above into Equation 6.28:

$$\begin{aligned}
&d^p = -d^r = 0.01\text{ m},\ h = h'+h'' = 0.04\text{ m},\ h^3/12 = 5.33\text{x}10^{-6}\text{ m}^3 \\
&A_{11} = A_{11}^p + A_{11}^r = 1133+364 = 1497\text{ MN/m, B} \\
&B_{11} = d^pA_{11}^p + d^rA_{11}^r = 0.01(1133-364) = 7.69\text{ MN} \\
&D_{11} = D_{11}^p + (d^p)^2A_{11}^p + D_{11}^r + (d^r)^2A_{11}^r = 37.77\text{x}10^3 + 0.0001\text{x}1133\text{x}10^6 \\
&\qquad + 12.11\text{x}10^3 + 0.0001\text{x}364\text{x}10^6 = 199.5\text{ kNm}
\end{aligned} \tag{6.39}$$

It is more meaningful to convert the absolute stiffness components to normalized ones. Since all normalized stiffness components have the same unit, direct comparison of their influence can be assessed.

$$\begin{aligned}
&A_{11}^* = A_{11}/h = 1497/0.04 = 37.4\text{ GPa},\ B_{11}^* = 2B_{11}/h^2 = 9.6\text{ GPa} \\
&D_{11}^* = 12D_{11}/h^3 = 199.5/5.33\text{x}10^{-6} = 37.4\text{ GPa}
\end{aligned} \tag{6.40}$$

Note that the coupling component is small relative to the in-plane and flexural stiffness. The other components of the stiffness matrix are the same as the comparable components for the plate only, which will not be illustrated here.

6.8 CONCLUSIONS

Unsymmetric laminates represent the ultimate challenge in the design of composite materials. Such laminates provide a unique structural behavior which does not exist in conventional materials. Designers often avoid them because their highly coupled deformation is difficult to analyze. Unsymmetric laminates should not be confused with unbalanced laminates, although these are often avoided for the same reason.

Our recommendation is that the most efficient laminate construction should be selected, and unsymmetric or unbalanced laminates should not be arbitrarily excluded. Individuals involved with design should at least be aware of the negative aspects of avoiding all unsymmetric and/or unbalanced laminates.

When the anticipated temperature and moisture content are constant during the life of a structure, unsymmetric laminates will not warp after the initial curing and moisture saturation. Shape stability will not be an issue. When there is a situation of minimum thickness, an unsymmetric laminate is only one half as thick as a symmetric laminate. For a cylindrical shell with axisymmetric loading, there is no reason for using symmetric construction; an unsymmetric construction will be satisfactory. Other opportunities for unsymmetric construction may come from the desired residual stresses, or the twisting of a composite mold for the easy removal of a cured part. Then is it possible to have a special unsymmetric laminate that does not warp? We will pose this question in one of our problems in the next sub-section.

6.9 PROBLEMS

Prob. 6.1 What consequence will the normalization factor of the coupling sub-matrix [B] in Equation 6.6 has on the final constitutive relation in Equation 6.8?

Prob. 6.2 What consequence will the use of tensorial strain and curvature, as defined in Equation 2.1 have on the constitutive relation in Equation 6.8? The use of additional factors are analogous to those shown in Equation 3.8 for plane stress.

Prob. 6.3 How can you derive the formula for the measurement of warpage in an unsymmetric laminate, assuming that the warped surface, shown below, is quadratic resulting from homogeneous non-mechanical flexural stresses?

$$w = ax^2+bxy+cy^2+dx+ey+f \tag{6.41}$$

where w = out-of-plane displacement

Prob. 6.4 Can unsymmetric laminates be shape stable? (Hint: one yes answer was found by Steven J. Winkler and Stephen C. Hill, " Minimizing Hygrothermal Effects on the Dimensional Stability and Mechanical Properties of Composite Plates and Tubes," Paper Number 2-I, Proceedings International Conference on Composite Materials (ICCM/8), Honolulu, July 1991.

Section 7

MICROMECHANICS

One outstanding feature of the use of composite materials is the opportunity to build material and structure simultaneously. The design options provided by composite materials are based not only on laminated plate theory but also micromechanics that relate the fiber and matrix contributions to the properties of complete structures. In this section, we will introduce simple micromechanics models from which the stiffness of plies, intact as well as degraded, can be described. Micromechanics of strengths and their dependence on temperature and moisture effects are empirically based. They are useful in optimizing composite structures for stiffness and strength.

7.1 BACKGROUND

Micromechanics establishes the relation between the properties of the constituents and those of the unit composite ply. Extensive literature is available in this area. The rule of mixtures is the simplest relation. It states that the composite property is the sum of the corresponding property of each constituent multiplied by its volume fraction. This rule is surprisingly accurate for many micromechanics formulas.

Micromechanics can be used effectively to guide property improvement by engineers. Most current designers of laminates and composite structures use only macromechanics, which is limited to the use of measured ply data to select the optimum laminates for a structure. We believe that designers can benefit by extending their scope to include micromechanics as a practical design tool. We propose the use of an integrated micro- and macromechanics which can include the following features:

- The predictions of stiffness constants, expansion coefficients, fabrics, and random composites can be based on micromechanics models. Designers may use them to control deformations from mechanical and thermal loads.

- The prediction of the successive ply failures after the first ply failure can be achieved by replacing cracked plies with a lower effective matrix modulus.

- The empirical data fit of hygrothermal properties of composite materials can be achieved by using exponents applied to micromechanical variables.

Almost all available micromechanics models are approximate. The two most common models of micromechanics are shown below. They parallel and series models are known to yield the upper and lower bounds of the properties.

- The parallel model is based on a uniform strain and gives the upper-bound

- The series model is based on a constant stress and gives the lower-bound

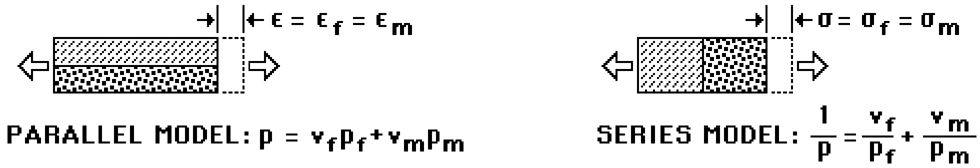

FIGURE 7.1 MICROMECHANICS OF PARALLEL- AND SERIES-CONNECTED MODELS

These elementary models have limited utility because the resulting predictions are often far apart. An example can be seen in the figure below where the property ratio between the constituents is ten. For most practical composite materials, the property ratios are higher than ten. The elementary models, therefore, must be improved to be useful.

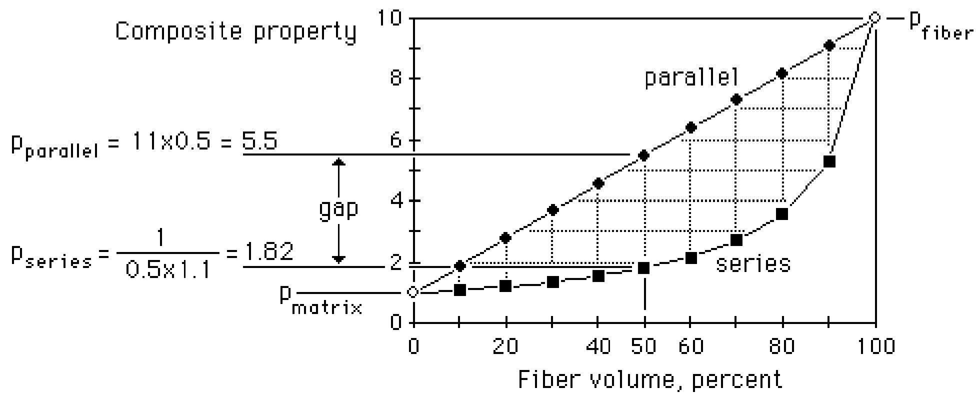

FIGURE 7.2 NUMERICAL PREDICTIONS OF PARALLEL AND SERIES MODELS FOR A 10:1 FIBER/ MATRIX RATIO

Models beyond the strength-of-materials models above are numerous. Three models based on idealized geometry are shown in the figure below.

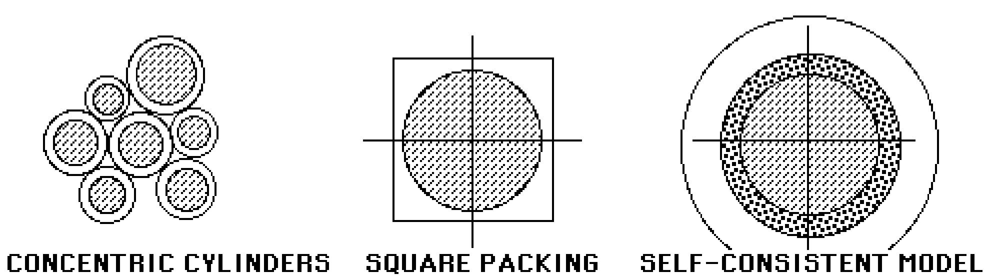

FIGURE 7.3 IDEALIZED MICROMECHANICS MODELS

Nearly every model proposed makes some idealizations of the shape, symmetry, and boundary conditions at infinity and at the interface. Specifically the models above are idealized as follows:

1) A concentric cylinder model yields closed-form results for composite bulk modulus and approximate results for composite shear modulus. This model requires concentric composite assemblages with either constant or decreasing diameters. Real composite materials are not aggregates of composite assemblages with a constant fiber volume.

2) The square-packing model is a popular model for easy computation, and it provides not only the effective composite modulus, but also the stress distribution. This model is realistic for boron fibrous composites, but not for composites with small diameter fibers such as glass and graphite.

3) The self-consistent model can provide simple solutions. The theory, however, is limited by the approximation that each fiber is uniformly encased of a matrix material.

Micromechanics models are often limited by the idealized fiber cross-section and fiber packing symmetry, as well as the assumed continuity at the interface. The models are further limited by a lack of the properties of anisotropic fibers, as well as shrinkage stresses which are often ignored. We believe that the realistic use of micromechanics formulas is for sensitivity studies; i.e., the change of known properties due to some micromechanical change. The relative rather than the absolute change is often adequate for the purpose of design. We will rely on various forms of the rule-of-mixtures relations to forward-calculate the ply properties from the constituent properties. But for other properties such as the transverse and shear moduli of a unidirectional ply, we will back-calculate the constituent properties from baseline ply data.

7.2 SPECIFIC GRAVITY, VOLUME AND MASS FRACTIONS, AND VOID

The composite specific gravity, and the volume and mass fractions of the constituents are related by the rule of mixtures relations. This approach is reasonable for scalar quantities as specific gravity.

Rule of mixtures, specific gravity: $\gamma = v_f \gamma_f + v_m \gamma_m$

Fiber mass fraction: $m_f = \dfrac{v_f \gamma_f}{\gamma}$, matrix mass fraction: $m_m = \dfrac{v_m \gamma_m}{\gamma}$

Void volume fraction: $v_v = 1 - \gamma \left[\dfrac{m^f}{\gamma^f} + \dfrac{m^m}{\gamma^m} \right]$ (7.1)

For mechanics analysis, volume fractions of the constituents are commonly used. For materials characterization, mass fractions are often reported. Conversion between the volume and mass fractions is simple. For typical composite materials, these properties are listed in the table below:

TABLE 7.1 VOLUME AND MASS FRACTIONS OF TYPICAL COMPOSITE MATERIALS

Fiber Matrix	T300 N5208	B(4) 5505	AS 3501	E-glass epoxy	Kev 49 epoxy	Boron Al
Fiber sp gr, γ_f	1.75	2.60	1.75	2.60	1.44	2.60
Matrix sp gr, γ_m	1.20	1.20	1.20	1.20	1.20	3.50
γ_f / γ_m	1.46	2.16	1.46	2.16	1.20	0.74
Comp sp gr, γ	1.58	1.89	1.56	1.82	1.36	3.09
Fiber volume	0.70	0.50	0.66	0.45	0.70	0.45
Fiber mass	0.78	0.69	0.75	0.64	0.74	0.38
Matrix volume	0.30	0.50	0.33	0.54	0.29	0.55
Matrix mass	0.22	0.31	0.25	0.36	0.26	0.62

Void content is determined by comparing the measured composite specific gravity with theoretical one, which is computed using the measured fiber content and the specific gravity of the constituents. It is however difficult to extract the void content from the specific gravity of the composite when the void content is less than 2 percent.

7.3 LONGITUDINAL YOUNG'S MODULUS AND POISSON'S RATIO

The micromechanics formula for the stiffness of a unidirectional composite follows the rule-of-mixtures relation, where the longitudinal fiber and matrix strains are assumed to be the equal. This is the parallel model in Figure 7.1.

Rule of mixtures: $E_x = v_f E_{fx} + (1 - v_f) E_m \hat{=} v_f E_{fx}$, $\quad \nu_x = v_f \nu_f + v_m \nu_m$

Back-calculation: $E_{fx} = \dfrac{E_x}{v_f}$, $\quad \nu_f = \dfrac{\nu_x - v_m \nu_m}{v_f}$ (7.2)

We can also back-calculate the fiber longitudinal stiffness and Poisson's ratio. If a value of 0.35 is used as the matrix Poisson's ratio for typical organic matrix, the back-calculated fiber Poisson's ratios are shown, including the average which coincides with the commonly accepted value of 0.2

TABLE 7.2 BACK CALCULATED FIBER POISSON'S RATIOS OF VARIOUS COMPOSITES

Fiber Matrix	T300 N5208	B(4) 5505	AS 3501	E-glass epoxy	Kev 49 epoxy	
Ply Poisson, ν_x	0.28	0.23	0.30	0.26	0.34	
Fiber volume	0.70	0.50	0.66	0.45	0.70	
Back-calc ν_f	0.25	0.11	0.27	0.15	0.33	Ave: 0.2

7.4 TRANSVERSE MODULUS

For the transverse modulus, we recommend a modified rule-of-mixtures relation using the stress partitioning parameter, as outlined in Section 9 of *Introduction to Composite Materials* by Tsai and Hahn. This relation is based on series-connected constituents in a composite ply, but modified by a stress partitioning parameter, the ratio of the average matrix to average fiber stresses.

The unique feature of this relation, shown in the equation below, lies in two additional variables: the transverse stiffness of the fiber, and the stress partitioning parameter. We treat this stress partitioning parameter as an empirical constant. We back-calculate this parameter from the data of a glass/epoxy composite assuming glass fiber is isotropic.

$$\text{Modified RoM equation: } \frac{(1+v_y^*)}{E_y} = \frac{1}{\underbrace{E_{fy}}_{\text{Transverse stiffness of fiber}}} + \frac{v_y^*}{E_m}, \quad v_y^* = \underbrace{\eta_y}_{\text{Stress partitioning parameter}} \frac{v_m}{v_f}$$

$$\text{For an isotropic fiber, } E_{fy} = E_{fx} = E_f^{iso}, \quad \eta_y = \frac{\dfrac{1}{E_y} - \dfrac{1}{E_f}}{\dfrac{1}{E_m} - \dfrac{1}{E_y}} \frac{v_f}{v_m} = \frac{\bar{\sigma}_m}{\bar{\sigma}_f} \tag{7.3}$$

The key assumption is that glass fiber is isotropic. The Young's and shear moduli of the fiber are:

$$E_f^{iso} = E_{fx} = \frac{E_x}{v_f} = 85.3 \text{ GPa}, \; G_f^{iso} = \frac{E_f^{iso}}{2(1+\nu_f)} = 35.5 \text{ GPa, assuming } \nu_f = 0.2 \tag{7.4}$$

By substituting the values of glass/epoxy composite materials the stress partitioning parameter is:

$$\begin{gathered} E_{fx} = E_{fy} = 85.3 \text{ GPa}, E_y = 8.27 \text{ GPa}, E_m = 3.4 \text{ GPa}; \\ v_y^* = \frac{\dfrac{1}{8.27} - \dfrac{1}{85.3}}{\dfrac{1}{3.4} - \dfrac{1}{8.27}} = 0.630; \; \eta_y = v_y^* \frac{v_f}{v_m} = 0.630 \frac{0.45}{0.55} = 0.516 \end{gathered} \tag{7.5}$$

The stress partitioning parameter is intended to cover the highly complex boundary conditions in the plane transverse to the fiber axis in a unidirectional ply. Instead of idealizing a repeated fiber packing arrangement in a matrix, as shown in Figure 7.3 on page 7-3, we intend to characterize the random dispersion of the fiber by this partitioning parameter. We assume that if the randomness of the fiber packing is similar between different composite materials, the parameter will be the same. The similarity between the glass/epoxy and graphite/epoxy composites in the figure below justifies the use of the same partitioning parameter:

If the graphite fiber in T300/5208 is isotropic, we can back-calculate the fiber stiffness from the measured longitudinal stiffness of the ply, and the shear modulus in the equation below.

$$E_f^{iso} = E_{fx} = \frac{E_x}{v_f} = 258 \text{ GPa}, \quad G_f^{iso} = \frac{E_f^{iso}}{2(1+\nu_f)} = 108 \text{ GPa, assuming } \nu_f = 0.2 \tag{7.6}$$

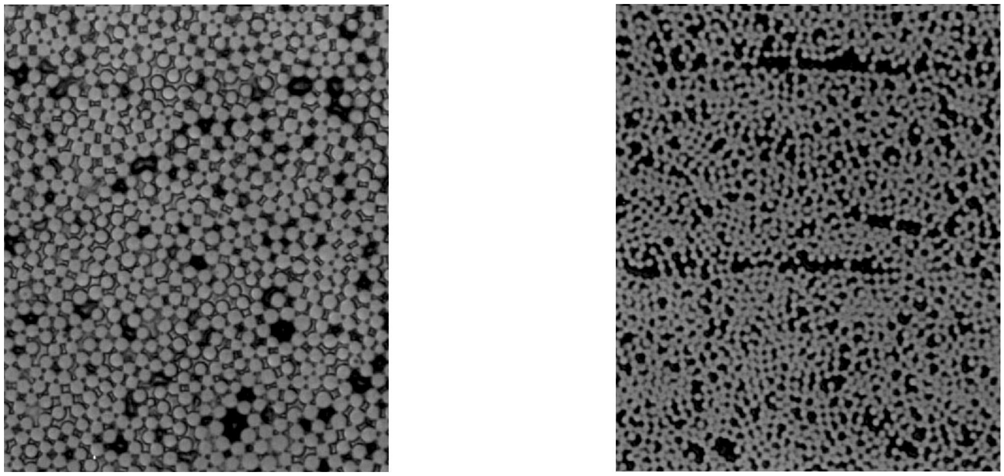

GLASS/EPOXY 220X GRAPHITE/EPOXY 220X

FIGURE 7.4 COMPARISON OF THE TRANSVERSE PLANES OF GLASS/EPOXY AND GRAPHITE/EPOXY UNIDIRECTIONAL PLIES

Since we have assumed that the stress partitioning parameter for T300/5208 is the same for glass/epoxy, we can back-calculate the implied transverse fiber stiffness of T300 fiber:

$$\frac{1}{E_{fy}} = \frac{(1+v_y^*)}{E_y} - \frac{v_y^*}{E_m}, \quad v_y^* = 0.516\frac{0.30}{0.70} = 0.22, \; E_{fy} = 18.7 \text{ GPa} \tag{7.7}$$

Thus, T300 graphite fiber is highly orthotropic. The transverse to longitudinal modulus ratio is 18.7/258, or 7 percent. In the figure below, we plot the absolute and normalized transverse fiber stiffness as functions of the stress partitioning parameter. The transverse ply stiffness is not sensitive to the stress partitioning parameter.

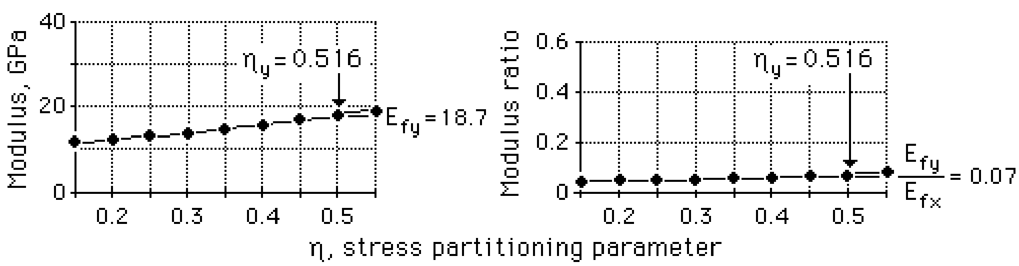

FIGURE 7.5 THE ABSOLUTE AND NORMALIZED TRANSVERSE STIFFNESS OF THE GRAPHITE FIBER IN A T-300/5208 PLY MATERIAL DERIVED FROM THE PARTITIONING PARAMETER

With the transverse fiber stiffness, we can now calculate the transverse stiffness of T300/5208 for different fiber volume fractions using the equation below. In this equation, the stress partitioning parameter, and the transverse stiffness of the fiber are fixed. The independent variable is the fiber volume.

$$\frac{1}{E_y} = \frac{1}{(1+v_y^*)}\left[\frac{1}{E_{fy}} + \frac{v_y^*}{E_m}\right] = \frac{1}{1+0.516\,\frac{v_m}{v_f}}\left[\frac{1}{18.7} + \frac{0.516}{3.4}\,\frac{v_m}{v_f}\right] \qquad (7.8)$$

The position occupied by T300/5208, designated as "T" in the figure below, is defined by the transverse fiber stiffness of the fiber at 18.7 GPa, and the transverse stiffness of the ply at 10.3 GPa. We can generate similar positions for other typical composite materials.

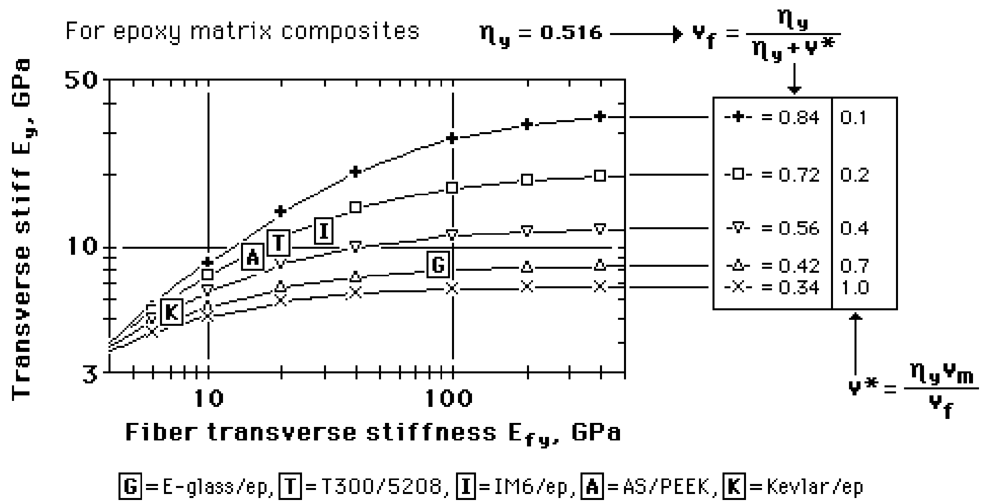

FIGURE 7.6 TRANSVERSE YOUNG'S MODULUS OF EPOXY MATRIX UNIDIRECTIONAL COMPOSITES AS FUNCTIONS OF FIBER YOUNG'S MODULI, AND FIBER VOLUME FRACTIONS.

If the fiber volume fraction is increased, the material point will move directly up, while maintaining the same transverse fiber stiffness. If the fiber stiffness is increased while the fiber volume remains constant, the material point moves to the right along a constant fiber fraction line. The curves are useful for discovering the sensitivities of some of the micromechanical variables. Note that graphite fibers of T300, IM6, and AS are grouped in one band, while glass and Kevlar are located separately.

To summarize the steps of the modified rule-of-mixtures equation for the prediction of the transverse stiffness of a unidirectional T300/5208 ply, we have the following:

1) From an isotropic fibrous composite such as glass/epoxy, we back-calculate the stress partitioning parameter, and obtained 0.516 as the value for the transverse Young's modulus using Equation 7.5 on page 7-4.

2) From the measured transverse ply stiffness of T300/5208 (10.3 GPa) and the partitioning parameter above, we can forward-calculate the transverse stiffness of the T300 fiber; the value is 18.7 GPa from Equation 7.7 on page 7-5.

3) From the fiber transverse stiffness and the partitioning parameter, we can now forward calculate the transverse ply stiffness as a function of fiber and matrix volume fractions for T300/5208 (use Equation 7.8 on page 7-5).

7.5 LONGITUDINAL SHEAR MODULUS

A nearly identical process can be used for the prediction of the longitudinal shear modulus of a unidirectional ply, and it is summarized in the figures below. The calculation is based on knowing the longitudinal shear modulus of the E-glass/epoxy composite, the fiber shear modulus computed from the isotropic relation in Equation 7.4 on page 7-4 using a fiber Poisson's ratio of 0.2. The shear modulus of the epoxy matrix is also computed from the same isotropic relation.

Modified RoM equation: $\frac{(1+v_s^*)}{E_s} = \frac{1}{G_{fx}} + \frac{v_s^*}{E_m}, \quad v_s^* = \eta_s \frac{v_m}{v_f}$

Longitudinal shear modulus of fiber (G_{fx}); Stress partitioning parameter (η_s)

For E-glass fiber, $G_{fx} = G_f^{iso}, \quad \eta_s = \frac{\frac{1}{E_s} - \frac{1}{G_f}}{\frac{1}{G_m} - \frac{1}{E_s}} \frac{v_f}{v_m} = \frac{\bar{\sigma}_m}{\bar{\sigma}_f} = 0.316$ (7.9)

Once we back-calculate the stress partitioning parameter, with a value of 0.316, we can forward-calculate the longitudinal shear modulus of the fiber for T300/5208, where the longitudinal shear of the ply is 7.17 GPa. This is shown in the equation below.

$$\frac{1}{G_{fx}} = \frac{(1+v_s^*)}{E_s} - \frac{v_s^*}{G_m}, \quad v_s^* = \eta_s \frac{v_m}{v_f} = 0.136, G_{fx} = 19.6 \text{ GPa} \tag{7.10}$$

The resulting fiber shear modulus is 19.6 GPa, which is small compared with 108 GPa for the assumed isotropic fiber calculation in Equation 7.6. The modulus ratio is 19.6/108, or 18 percent. Curves similar to those in Figure 7.5 are shown for the shear modulus of the T300 fiber:

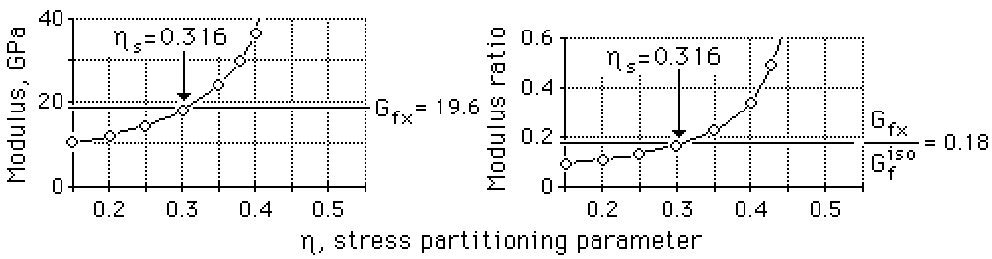

FIGURE 7.7 THE ABSOLUTE AND NORMALIZED SHEAR MODULI OF THE GRAPHITE FIBER DERIVED FROM THE STRESS PARTITIONING PARAMETER

The slopes of the curves above are much steeper than comparable curves for the transverse stiffnesses shown in Figure 7.6. The value of the stress partitioning parameter, therefore, has a more profound influence on the fiber shear modulus than on the fiber transverse stiffness.

Once we know the fiber shear modulus and the stress partitioning parameter we can calculate the shear modulus of the unidirectional T300/5208 as a function of the fiber and matrix volume fractions. The relation is shown in the equation below:

$$\frac{1}{E_s} = \frac{1}{(1+v_s^*)}\left[\frac{1}{G_{fx}} + \frac{v_s^*}{G_m}\right] = \frac{1}{1+0.316\frac{v_m}{v_f}}\left[\frac{1}{19.6} + \frac{0.316}{1.26}\frac{v_m}{v_f}\right] \tag{7.11}$$

As was the case of the transverse stiffness for typical composite materials in Figure 7.6 on page 7-5, we show below the longitudinal ply shear modulus as a function of fiber volume fraction and shear modulus. Typical composite materials are shown as blocks below:

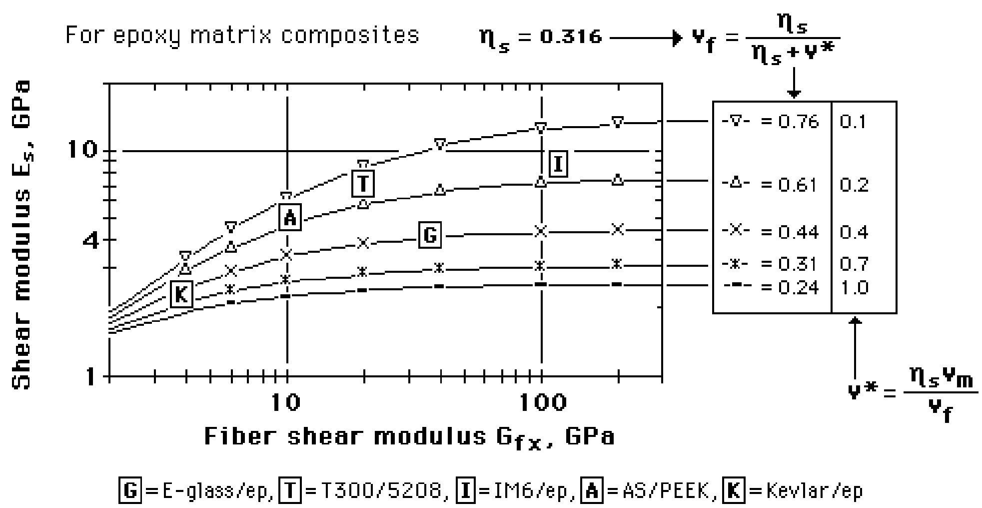

FIGURE 7.8 SHEAR MODULI AS FUNCTIONS OF FIBER SHEAR MODULI AND VOLUME

The same comments on the sensitivities of the stress partitioning parameter in Figure 7.6 apply here for the shear modulus of the unidirectional plies. Fiber volume and fiber shear modulus have nonlinear effects on the ply shear modulus. These curves can serve a useful purpose in defining the probable range of shear modulus of a new material where stiffness data is incomplete.

TABLE 7.3 STRESS PARTITIONING PARAMETERS FOR TRANSVERSE AND SHEAR MODULI

Stiff	E-glass/ep	T300/52	Kevlar/ep	AS4/PEEK	IM6/epoxy
E_x	38.60	181.00	76.00	134.00	203.00
E_y	8.27	10.30	5.50	8.90	11.20
E_s	4.14	7.17	2.30	5.10	8.40
v_f	0.45	0.70	0.60	0.66	0.66
η_y	0.5161	→ 0.5161	→ 0.5161	→ 0.5161	→ 0.5161
η_s	0.3162	→ 0.3162	→ 0.3162	→ 0.3162	→ 0.3162

The most important assumption of the modified rule-of-mixtures relations that we have proposed is the equal stress partitioning parameters. As long as the shape and dispersion of the unidirectional fibers between the two composite materials retain the similarity shown in Figure 7.4 on page 7-4, we believe that the partitioning parameter will be reasonably accurate.

With the exception of the glass fiber, all graphite and Kevlar fibers show a high degree of orthotropy. This is shown in the table below. The ratios of the transverse to the longitudinal stiffnesses are surprisingly close; i.e., with an average of 0.072. Thus fiber orthotropy is a significant effect, and must be included in any micromechanics prediction of stiffness and strength of composite materials. The last row of this table shows the ratio of the transverse stiffness and the longitudinal shear modulus of anisotropic fibers. For isotropic fibers, this ratio is 2.4 for a Poisson's ratio of 0.3. For anisotropic fibers, this ratio will be different from 2.4. The values of the last row vary from 0.26 to 2.51. A similar range of variations was found for unidirectional plies of various composite materials, and it is shown in Figure 3.20.

TABLE 7.4 BACK-CALCULATED TRANSVERSE STIFFNESS AND LONGITUDINAL SHEAR MODULI OF FIBERS IN TYPICAL UNIDIRECTIONAL EPOXY-MATRIX COMPOSITE MATERIALS

Stiff	E-glass/ep	T300/52	Kevlar/ep	AS4/PEEK	IM6/epoxy	
E_x	38.60	181.00	76.00	134.00	203.00	
v_f	0.45	0.70	0.60	0.66	0.66	
E_{fx}	85.78	258.57	126.67	203.03	307.58	
E_m	3.40	3.40	3.40	3.40	3.40	
η_y	0.5161	→ 0.5161	→ 0.5161	→ 0.5161	→ 0.5161	
E_{fy}	85.78	18.69	6.98	15.61	28.70	
E_{fy}/E_{fx}	1.000	0.072	0.055	0.077	0.093	← Ave: 0.072 (orthotropic fibers)
η_s	0.3162	→ 0.3162	→ 0.3162	→ 0.3162	→ 0.3162	
G_{fx}	35.74	19.68	2.78	10.13	109.24	
E_{fy}/G_{fx}	2.40	0.95	2.51	1.54	0.26	

7.6 EXPANSION COEFFICIENTS

The thermal and moisture expansion coefficients of unidirectional epoxy matrix composites can be expressed in the following simplified micromechanics formulas:

$$\alpha_x = \beta_x = 0;\ \alpha_y = v_m(1+\nu_m)\alpha_m,\ \beta_y = v_m(1+\nu_m)\beta_m \tag{7.12}$$

The relations are a simplified version of a more complete theory developed by R. A. Schapery, "Thermal Expansion Coefficients of Composite Materials Based on Energy Principles," *Journal of Composite Materials*, Vol. 2 (1968), p. 380.

7.7 EFFECTIVE STIFFNESS OF DEGRADED PLIES

Pressure vessels made by filament winding can resist internal pressure if an impervious liner is installed. Without this liner, the vessel would "weep" or leak fluid at a very low pressure. The leakage is associated with micro cracks in the composite shell of the vessel. In order to fully utilize the strength potential of composite laminates, it is useful to develop a micromechanics model that can describe plies in a laminate having micro cracks. A finite element shear lag analysis of a [0/90] laminate, shown below, is used to predict the loss of laminate stiffness as the number of micro cracks increases with increasing uniaxial stress. A saturation level is reached when the spacing between cracks reaches an aspect ratio of unity, which remain essentially the same for all organic-matrix composites. This model, developed by Jose Luis Perez Aparicio in his PhD thesis in the Mechanical Engineering Department, Stanford University in 1992, is different from discounting the [90] ply from the laminate when micro cracks are formed. We recommend the model below based on the ply stiffness reduction proportional to the number of micro cracks at a saturation level.

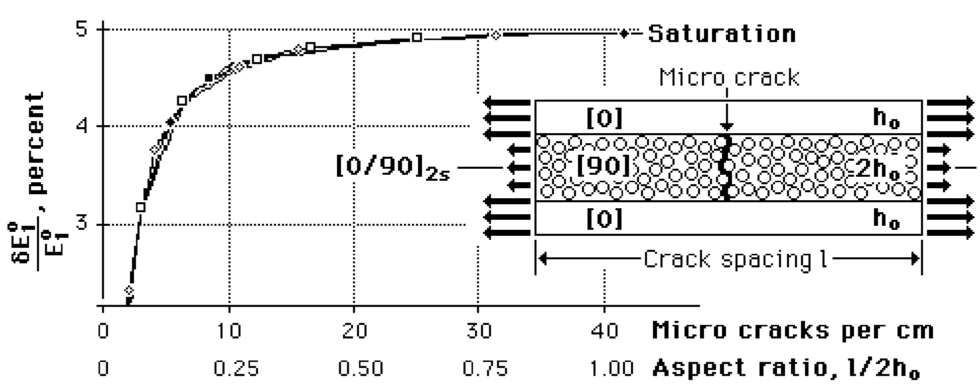

FIGURE 7.9 A SHEAR LAG ANALYSIS OF A [0/90] YIELDS THE LOSS LAMINATE STIFFNESS AS MICRO CRACKS MULTIPLY AND REACH A SATURATION LEVEL (SEE PHOTOMICROGRAPH FIGURE 9.14 ON PAGE 9-9)

We will now attempt to model a degraded ply as a homogeneous material, and continue to apply laminate plate theory. A ply with uniformly spaced micro cracks is replaced by a homogeneous ply with the same fibers but a matrix of lower effective stiffness.

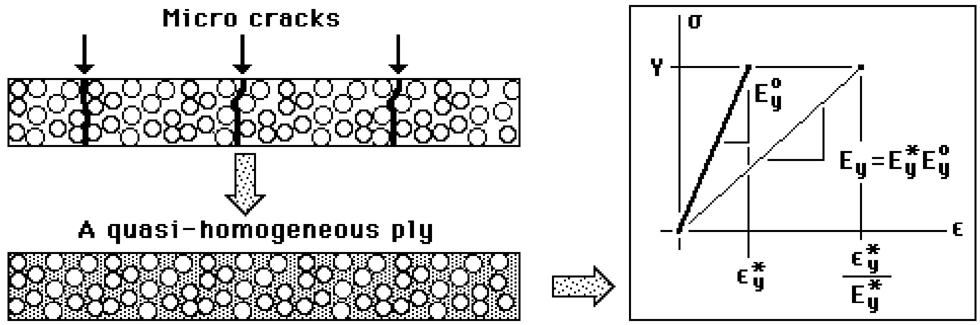

FIGURE 7.10 REPLACING A PLY WITH MICRO CRACKS BY ONE WITH LOWER MATRIX STIFFNESS. THE DEGRADATION FACTOR IS USED TO ACCOUNT FOR THE DECREASED LAMINATE STIFFNESS AND INCREASED FAILURE STRAIN

Taking advantage of the micromechanics relations for the transverse and shear moduli of a unidirectional ply, which we have just presented, it is easier to use the reduced or degraded matrix modulus than the decreased ply stiffness. Only one matrix degradation factor is needed for the former, as compared with two factors for the decreased ply stiffness; i.e., one each for the transverse and shear moduli. The matrix modulus degradation can be back-calculated from the loss of laminate stiffness due to the presence of micro cracks. In the figure above, we show that the loss of transverse stiffness of a unidirectional ply shifts the stress-strain curve from the intact ply to a degraded ply that is less stiff. The failure strain of the degraded ply is increased proportionally.

It is simple to use the modified rule-of-mixtures relation of micromechanics to establish the loss of ply stiffness from the matrix modulus degradation. The relations for the four basic ply stiffnesses are shown below:

$$E_x^{degraded} = E_x^{intact}, \quad \nu_x^{degraded} = E_m^* \nu_x^{intact}$$

$$\frac{1}{E_y^{degraded}} = \frac{1}{(1+\nu_y^*)}\left[\frac{1}{E_{fy}} + \frac{1}{E_m^*}\frac{\nu_y^*}{E_m}\right], \quad \frac{1}{E_s^{degraded}} = \frac{1}{(1+\nu_s^*)}\left[\frac{1}{G_{fx}} + \frac{1}{E_m^*}\frac{\nu_s^*}{G_m}\right] \tag{7.13}$$

matrix degradation factor

It is assumed that matrix degradation does not affect the longitudinal stiffness of the unidirectional ply. Loss of stiffness along the fiber direction will be covered later by a fiber degradation factor. The transverse and shear moduli of a degraded ply are lowered by the reduced matrix modulus shown in the equation above. We reduce the Poisson's ratio by the same degradation factor. The rationale is that as micro cracks multiply, plies in a laminate become uncoupled; i.e., they operate almost independently. Plies are detached from one another and the laminate Poisson's coupling is expected to vanish as well. The same rationale can be applied to other interactions among plies. One such example is when the interaction in the quadratic failure criterion is reduced as cracks increase in a laminate stressed beyond the first ply failure.

We now show the micromechanics modeling of a degraded T300/5208 ply in the figure below. The matrix degradation factor has a range from unity, when the ply is intact, toward zero. The implied losses in the transverse and shear moduli are calculated using the relations shown in Equation 7.13. The numerical results shown below are for a matrix degradation factor of 0.2 which leads to the loss of the moduli 0.31 and 0.24, respectively.

Thus we need only one matrix degradation factor to deduce the degraded transverse and shear moduli of a ply with micro cracks.

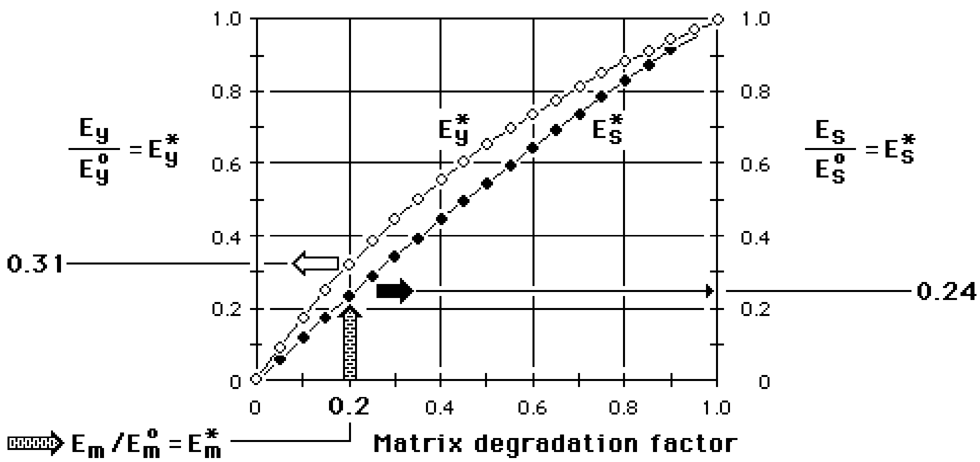

FIGURE 7.11 NORMALIZED REDUCTION OF THE TRANSVERSE AND SHEAR MODULI OF T300/5208 FROM THE REDUCTION OF THE MATRIX MODULUS DEGRADATION FACTOR. THE NUMERICAL RESULTS OF A FACTOR OF 0.2 ARE SHOWN.

From the micromechanics formulas, we can predict the loss of laminate stiffness for two composite materials, with two cross-ply laminates each, as shown in the figure below. The predicted loss in laminate stiffness are relatively flat, meaning that the stiffness loss is not sensitive to the matrix degradation factor.

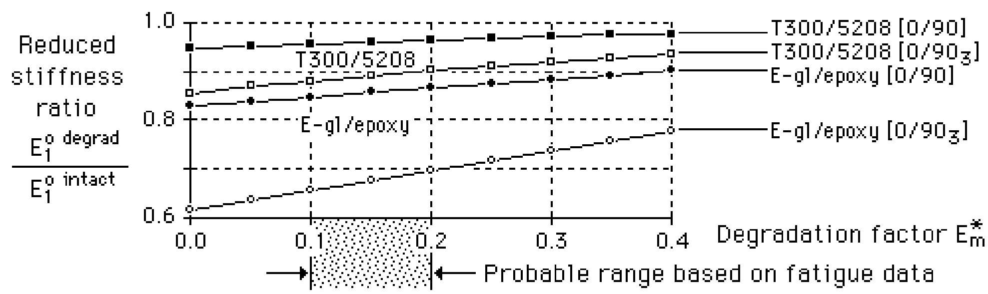

FIGURE 7.12 MICROMECHANICS PREDICTION OF THE LAMINATE STIFFNESS REDUCTION AS A FUNCTION OF MATRIX DEGRADATION FACTOR

From the loss of laminate stiffness due to tension-tension fatigue tests reported in "Stiffness-Reduction Mechanisms in Composite Laminates," *ASTM STP 775* (1982), p.103, by A. L, Highsmith and K. L. Reifsnider, we can back-calculate the matrix degradation factor that would match the reduction in laminate stiffness from fatigue loading. The best fit matrix degradation factor fell between 0.1 and 0.2 for graphite/epoxy composite material. The ply discount method, which is often assumed, is not correct. The degradation factor based on fatigue data is not zero.

From micromechanics calculation for typical composite materials the normalized reduction in the transverse and shear moduli as functions of a constant matrix degradation factor are listed in the following table.

TABLE 7.5 NORMALIZED REDUCTION OF THE TRANSVERSE AND SHEAR MODULI DUE TO THE MATRIX DEGRADATION FACTOR FOR TYPICAL COMPOSITE MATERIALS

Degrade	T300/52	B/5505	AS4/35	E-gl/ep	Kev/ep	AS4/PK	IM6/ep	T300/F9
E_m	→ 3.40	→ 3.40	→ 3.40	→ 3.40	→ 3.40	→ 3.40	→ 3.40	→ 3.40
E_m^*	→ 0.15	→ 0.15	→ 0.15	→ 0.15	→ 0.15	→ 0.15	→ 0.15	→ 0.15
E_y	10.30	18.50	8.96	8.27	5.50	8.90	11.20	9.65
E_y^*	0.24	0.15	0.24	0.16	0.30	0.24	0.20	0.20
E_s	7.17	5.60	7.10	4.14	2.30	5.10	8.40	4.55
E_s^*	0.21	0.15	0.18	0.16	0.36	0.24	0.16	0.22

Degraded plies can exist only in laminates. Furthermore, the loss in ply stiffness is possible only when plies are subjected to transverse tensile strains. Under transverse compressive strains, the transverse stiffness of the intact as well as degraded plies are essentially the same. Thus, as progressive failures of plies occur in a laminate, degradation described here applies only to plies under transverse tensile strain. We identify the difference between the tensile and compressive degradation as selective or bi-modulus degradation. The latter expression is borrowed from its use to describe moduli of materials which have different tensile and compressive moduli. More detailed failure analysis on a ply-by-ply basis will be given in the section on laminate strength.

7.8 HYGROTHERMAL EFFECTS

Since we are not aware of any general theory that governs the hygrothermal effects we will use a non-dimensional temperature **T*** as a state variable for the temperature and moisture effects:

- Hygrothermal effects follow power law functions of **T***;
- Changes in stiffness and strength of constituents also follow a function of **T***, and are not time dependent;
- Micromechanics formulas remain valid for the range of temperature and moisture changes;
- Laminated plate theory and failure criteria remain valid and only the stiffness and strength properties are changed. Ply degradation due to micro cracking and fiber failure can be modeled the same way with hygrothermally induced property changes only.

We use micromechanics because we can reduce the number of variables. If we ignore micromechanics and assess the hygrothermal effects on the ply or laminate levels, we will have to run many more tests, and will find sensitivity studies of materials design much more difficult.

The non-dimensional temperature is defined in the figure below. This is intended for organic-matrix composite material where the glass transition temperature plays a major role. At the transition temperature, the matrix transitions from a rigid, glassy state to a highly pliable state. Moisture content suppresses the glass transition temperature by a linear coefficient **g**.

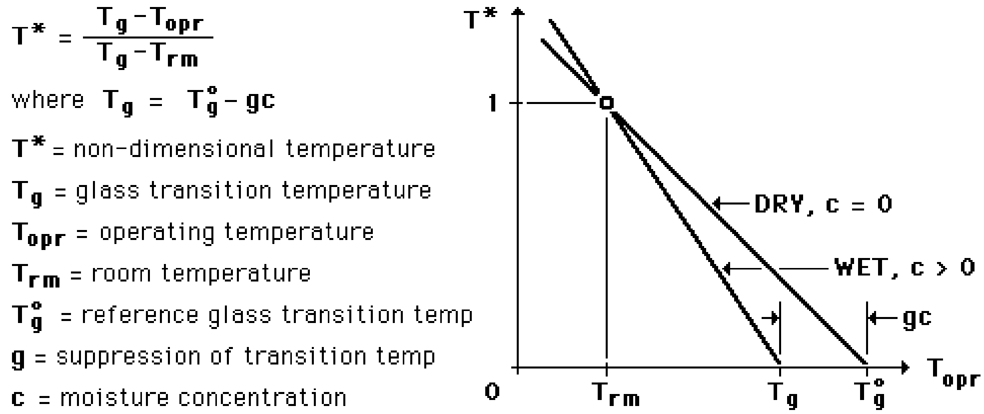

FIGURE 7.13 NON-DIMENSIONAL TEMPERATURE VS OPERATING TEMPERATURE.

In Figure 7.13 above we show a linear relation between the non-dimensional temperature and the operating temperature. If we wish to have nonlinear relations, a power law would be one of the simplest, and takes only one exponent. The sensitivity of this exponent is shown in Figure 7.14.

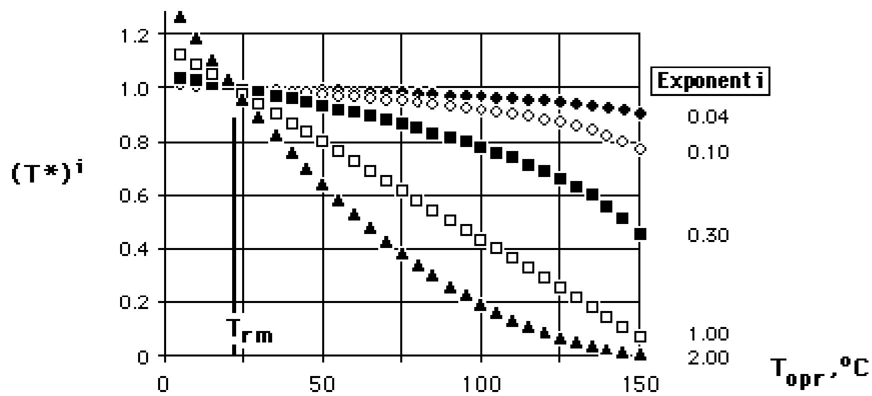

FIGURE 7.14 THE NON-DIMENSIONAL TEMPERATURE WITH VARIOUS POWER VERSUS THE OPERATING TEMPERATURE

The effect of moisture content on the non dimensional temperature **T*** is shown in Figure 7.15.

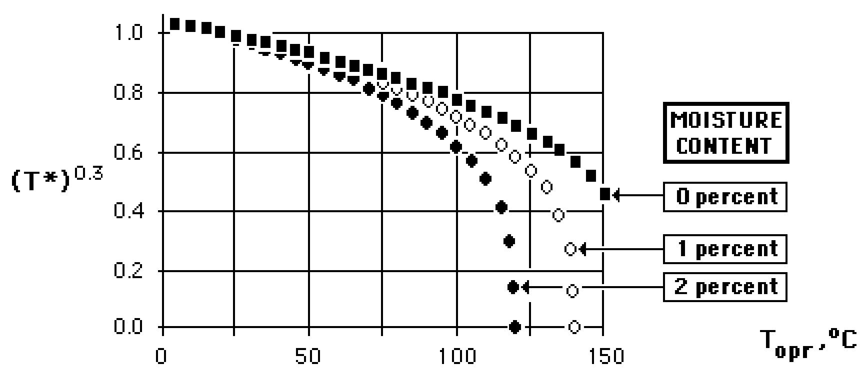

FIGURE 7.15 EFFECTS OF MOISTURE CONTENT ON THE NON-DIMENSIONAL TEMPERATURE TO A CONSTANT EXPONENT OF 0.3

7.9 MICROMECHANICS OF STRENGTHS

The predictions of strengths of an orthotropic ply from the constituents are more complicated than the prediction of elastic constants. We will limit to ratios of strength as functions of strengths of the fiber and matrix, fiber volume fractions, and temperature.

The strengths and ultimate strains of various composite materials are listed in the table below.

TABLE 7.6 STRENGTHS AND ULTIMATE STRAINS OF TYPICAL COMPOSITE MATERIALS.

Ply		T3/52	B4	AS/35	E-gl	Kev	IM6	T3/F
Strengths, MPa								
Longi tens	X^o	1500	1260	1447	1062	1400	3500	1314
Longi compr	X'^o	1500	2500	1447	610	235	1540	1220
Trans tens	Y^o	40	61	51.7	31	12	56	43
Trans compr	Y'^o	246	202	206	118	53	150	168
Longi shear	S^o	68	67	93	72	34	98	48
Ultimate strain, E-03								
Longi tens	x^o	8.29	6.18	10.49	27.51	18.42	17.24	8.88
Longi compr	y^o	3.88	3.30	5.77	3.75	2.18	5.00	4.46
Trans tens	x'^o	8.29	12.25	10.49	15.80	3.09	7.59	8.24
Trans compr	y'^o	23.88	10.92	22.99	14.27	9.64	13.39	17.41
Longi shear	s^o	9.48	11.99	13.10	17.39	14.78	11.67	10.55

Let us assume that we have measured the five strengths of a unidirectional ply at a reference state, for example, room temperature with 0.5 percent moisture (c = 0.005). We will designate this reference state by superscript o. The five strengths and ultimate strain based on uniaxial and shear tests are listed in the table below. Under uniaxial compressive and longitudinal shear stresses, the resulting strains are nonlinear. The ultimate strains below are calculated using the initial or tangent moduli.

It is assumed that stiffness and strength of the constituents and the interface are power functions of the non-dimensional temperature. The respective hygrothermal exponents are listed in the figure below. For example, from left to right in the figure, exponent "c" controls the matrix strength; "a", matrix stiffness; "b", interfacial strength and stress partitioning parameter; "h", fiber strength; and "f", fiber stiffness.

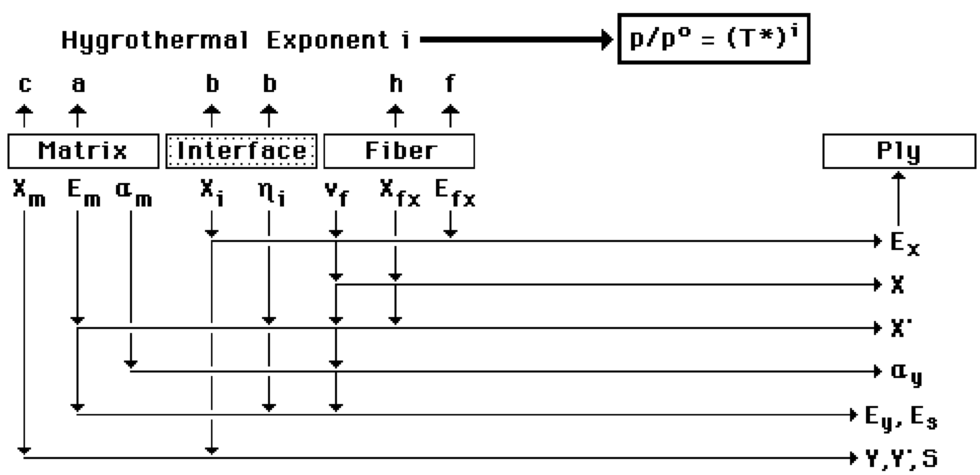

FIGURE 7.16 HYGROTHERMAL EFFECTS ON PROPERTIES ARE EMPIRICALLY FITTED BY VARIOUS EXPONENTS TO THE NON DIMENSIONAL TEMPERATURE

We list the exponents of T* to empirically fit the matrix stiffness and strength data as functions of moisture and temperature. Typical values for organic matrix composites are also listed.

$$\begin{aligned} &\text{Matrix stiffness ratio} = E_m/E_m^o = (T^*)^a && \text{where } a = 0.5 \\ &\text{Stress partitioning ratio} = \eta_y/\eta_y^o = \eta_s/\eta_s^o = (T^*)^b && b = 0.2 \\ &\text{Matrix strength ratio} = X_m/X_m^o = (T^*)^c && c = 0.9 \end{aligned} \qquad (7.14)$$

We list the exponents of T* to empirically fit the fiber stiffness and strength data as functions of moisture and temperature. Typical values for organic matrix composites are listed.

$$\text{Fiber stiffness ratio} = E_{fx}/E^o_{fx} = E_{fy}/E^o_{fy} = E_{fs}/E^o_{fs} = (T^*)^f$$

$$\text{Fiber strength ratio} = X_{fx}/X^o_{fx} = (T^*)^h \qquad \text{where } f = h = 0.004 \tag{7.15}$$

The values for fiber stiffness and strength are nearly zero in terms of the non-dimensional temperature. They are reasonable because the temperature used is primarily intended to describe matrix properties which depend on the glass transition temperature and its shift due to absorbed moisture. A different temperature parameter may be used to describe the hygrothermal effects on fiber. It is deemed unnecessary for the present approach where temperature is relatively low; i.e., less than 300 °C.

With these back-calculated constituent properties as functions of T*, we can derive the ply stiffness and strength in terms of T* and appropriate exponents following earlier postulates in our micromechanics.

$$E_x/E^o_x = (v_f/v^o_f)(T^*)^f;\ \nu_x = \text{constant};$$

$$E_y/E^o_y,\ E_s/E^o_s \text{ are nonlinear functions of } (T^*)^a,\ (T^*)^b, \text{ and } v_f \tag{7.16}$$

For ply strength, the following relations are based on the rule of mixtures for the longitudinal tensile and compressive strengths. For the compressive strength, we also include the loss of the foundation shear modulus that would reduce the buckling strength. The transverse and shear strengths are assumed to be controlled by the matrix strength.

$$X/X^o = (v_f/v^o_f)(T^*)^h;\ X'/X'^o = (v_f/v^o_f)(T^*)^h(E_s/E^o_s)^n, \text{ where } n = 0.1$$

$$Y/Y^o = Y'/Y'^o = S/S^o = (T^*)^c \tag{7.17}$$

We first assume that the rule-of-mixtures equation holds for the longitudinal strength. While this is not a startling postulate, we need to recognize that fiber strength in this equation is difficult to measure because: (1) the fiber diameter is small, (2) fiber strength data has a wide scatter, and (3) fiber strength also decreases with the length of the test specimen. For a given baseline material, we can back-calculate the fiber strength. Thus the variation of the longitudinal tensile and compressive strengths can be described by the following dimensionless ratios:

For longitudinal compressive strength, we expect an additional failure by instability. This mode can be included by adding the change in the ply shear modulus or the foundation modulus. The loss in the longitudinal compressive strength resulting from the reduction in the shear modulus can be most conveniently modeled by a power law relation. This relation is shown in the figure below. Also shown is the case, when a shear modulus reduction of 0.3 and an exponent **n** of 0.2, the loss in compressive strength reduction is to 78 percent. We recommend a value between 0 and 0.2, which means that the relative reduction of the compressive strength is considerably less than that of the shear modulus.

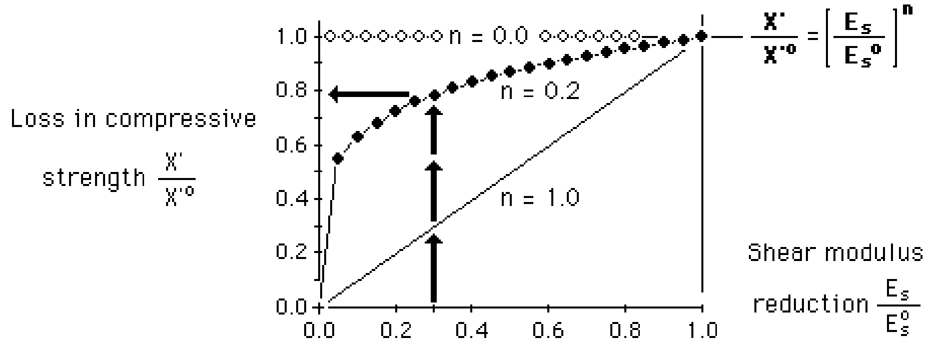

FIGURE 7.17 NORMALIZED LOSS IN THE LONGITUDINAL COMPRESSIVE STRENGTH DUE TO THE REDUCTION IN SHEAR MODULI RESULTING FROM MATRIX CRACKING.

7.10 MICROMECHANICS OF WOVEN COMPOSITES

The predictions of elastic constants of fabrics, filament-wound and braided structures can be made if it is possible to replace the woven composite by a multidirectional laminate consisting of the same fiber angles and ply group ratios. Only then can the micromechanics formulas for stiffness be applied to the plies without modification.

In the table below, we show three ply materials and see how close [0/90] laminates can represent balanced woven fabrics of the same fibers and fiber volume fractions.

Thus, under each of the three ply materials, we list in the first column the engineering constants of the unidirectional ply. In the second column, we list the predicted effective laminate stiffness of a [0/90] cross-ply laminate. A heavy border is drawn around the predicted values. These laminate stiffnesses can be compared with those measured from a balanced woven fabric or cloth, listed in the third column. The same bases of comparison apply to the other two ply materials. For the stiffnesses in the x- and y-directions, the [0/90] laminate is higher than those measured from the fabric. This is not unexpected when the fibers in the fabric are not straight, and is true for graphite and Kevlar/epoxy composites. The laminate stiffness is 19 and 14 percent higher than the fabric stiffness. For the case of glass/epoxy composite, the laminate stiffness is 18 percent less than the fabric stiffness. There was apparently a difference in the fiber volume fractions that may account for the lower laminate stiffness. The Poisson's ratio and shear moduli of the [0/90] laminates are close to those of the fabrics.

TABLE 7.7 COMPARISON OF STIFFNESS AND STRENGTH PREDICTIONS OF [0/90] LAMINATES WITH BALANCED WOVEN FABRICS OR CLOTHS

Type	Graphite/epoxy			E-glass/epoxy			Kevlar/epoxy		
Fiber	T300	T300	T300	E-glass	E-glass	F161	Kev 49	Kev 49	Kev 49
Matrix	F934	F934	F934	epoxy	epoxy	6581	epoxy	epoxy	N5209
	[0]	[0/90]		[0]	[0/90]		[0]	[0/90]	
	tape	laminate	cloth	tape	laminate	cloth	tape	laminate	cloth
Stiffness									
Ex	148.00	79.2	66.00	38.60	23.6	29.6	76.00	41.0	35.8
Ey	9.65	79.2	66.00	8.27	23.6	26.9	5.50	41.0	35.8
nu/x	0.30	0.04	0.04	0.26	0.09	0.12	0.34	0.05	0.09
Es	4.55	4.6	4.10	4.14	4.1	6.24	2.30	2.3	1.79
Strengths									
X	1314	664	375	1062	545	489	1400	704	582
X'	1220	899	279	610	306	390	235	165	189
Y	43	664	368	31	545	444	12	704	582
Y'	168	899	278	118	306	305	53	165	189
S	48	49	46	72	80	133	34	34	84

The predicted strengths of [0/90] are also compared with corresponding strengths measured from fabrics in the table above. With only the exception on one compressive strength of glass-epoxy fabric, cross-ply laminates have higher strengths than the fabrics.

This is not unexpected because the fibers in fabrics are bent. The fibers in contact will cause local stress concentrations that would reduce tensile strengths. Bent fibers would reduce buckling strengths which, in turn, will reduce compressive strengths.

7.11 MICROMECHANICS OF RANDOM COMPOSITES

The simplest method of prediction of the elastic constants of random composites is based on the quasi-isotropic laminated composite materials of [p/3] and [p/4]; see Problem 4.2 on page 4-26. The results for typical composite materials are listed in the table below, which is the same as Table 3.3 on page 3-13.

TABLE 7.8 PREDICTED ISOTROPIC CONSTANTS OF RANDOM COMPOSITE MATERIALS FROM QUASI-ISOTROPIC LAMINATE

Type	CFRP	BFRP	CFRP	GFRP	KFRP	CFRTP	CFRP	CFRP	CCRP	CCRP
Fiber/cloth	T300	B(4)	AS	E-glass	Kev 49	AS 4	IM6	T300	T300	T300
Matrix	N5208	N5505	H3501	epoxy	epoxy	PEEK	epoxy	Fbrt 934	Fbrt 934	Fbrt 934
						APC2		4-mil tp	13-mil c	7-mil c
Linear combinations of [Q], GPa										
U1*	76.37	87.70	59.66	20.45	32.44	57.04	85.88	62.47	58.84	52.37
U4*	22.61	28.36	16.96	5.51	10.54	17.28	25.43	19.73	19.05	16.66
U5*	26.88	29.67	21.35	7.47	10.95	19.88	30.23	21.37	19.89	17.85
* invariant										
Quasi-isotropic constants										
E, GPa	69.68	78.53	54.84	18.96	29.02	51.81	78.35	56.24	52.67	47.0
nu	0.30	0.32	0.28	0.27	0.32	0.30	0.30	0.32	0.32	0.32
G, GPa	26.88	29.67	21.35	7.47	10.95	19.88	30.23	21.37	19.89	17.8
Sp. Gr.	1.60	2.00	1.60	1.80	1.46	1.60	1.60	1.50	1.50	1.50

For two-dimensional random composites the quasi-isotropic constants are related to the invariants in the table above by the equation below:

$$E^{iso} = \left[1-\nu^{iso\,2}\right]U_1, \quad \nu^{iso} = \frac{U_4}{U_1}, \quad G^{iso} = U_5 \qquad (7.18)$$

The effective Young's moduli in absolute and specific terms are shown as columns in the figure below, the same as Figure 3.21 on page 3-14. These values are the lower bound of the composite materials. Note that graphite and boron composites are higher than aluminum and steel in specific stiffness, and also in specific strength as shown in Figure 1.5 on page 1-4.

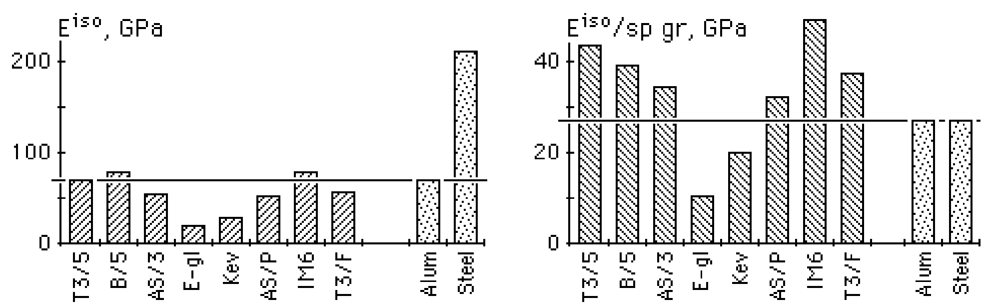

FIGURE 7.18 ABSOLUTE AND SPECIFIC QUASI-ISOTROPIC YOUNG'S MODULI

For three-dimensional random composites, an approach similar to that for two-dimensional composites can be applied. See Problem 7.2 below.

7.12 CONCLUSIONS

The micromechanics formulas in this section are simple to use. They provide sufficient insight for determining the trend in sensitivity studies and for giving direction to materials improvement. Micromechanics will continue to play a critical role in establishing ply with micro cracks, and the hygrothermal dependency of the stiffness and strength of composites. Using a matrix degradation factor, we can extend the traditional failure criteria from the first ply failure to progressive failures on a ply-by-ply basis.

With readily workable micromechanics formulas we can successfully integrate micro- and macro-mechanics to provide a powerful tool for the efficient use of composite materials. Examples of the integrated micro-macro analysis, Mic-Mac for short, is an example of the utility of our simplified micromechanics formulas.

7.13 PROBLEMS

Prob. 7.1 Fill in the missing reduced transverse and shear moduli for typical composite materials:

Degrade	T300/52	B/5505	AS4/35	E-gl/ep	Kev/ep	AS4/PK	IM6/ep	T300/F9
E_m	→ 3.40	→ 3.40	→ 3.40	→ 3.40	→ 3.40	→ 3.40	→ 3.40	→ 3.40
E_m^*	→ 0.20	→ 0.20	→ 0.20	→ 0.20	→ 0.20	→ 0.20	→ 0.20	→ 0.20
E_y	10.30	18.50	8.96	8.27	5.50	8.90	11.20	9.65
E_y^*	0.31	?	?	?	?	?	?	?
E_s	7.17	5.60	7.10	4.14	2.30	5.10	8.40	4.55
E_s^*	0.24	?	?	?	?	?	?	?

FIGURE 7.19 REDUCED TRANSVERSE AND SHEAR MODULI RESULTING FROM A MATRIX DEGRADATION FACTOR OF 0.2

Prob. 7.2 For many 3-dimensionally reinforced composite materials made through stitching, weaving and braiding processes, it is a common practice to report the fiber volume fractions of various configurations. The elastic moduli of a 3-dimensionally random fibrous composite can be found, for example, in R. M. Christensen's *Mechanics of Composite Materials*, John Wiley, 1979. What are the effective elastic moduli as functions of fiber volume fractions? (Hint: use Equations 7.2, 7.8 and 7.11 for the fiber volume dependency of engineering constants.)

Section 8

FAILURE CRITERIA

Failure criteria are needed to extend the uniaxial and pure shear test data of unidirectional composite materials to combined stresses. Quadratic criteria are the most general form in use today. To be analytically sound and consistent, the most versatile criterion must include simple transformation relations and failure mode interactions. Being invariant strain-space envelopes are preferred over stress-space envelopes. Strength ratios are preferred over failure indices because the former can be used as a scaling factor.

8.1 INTRODUCTION

Failure criteria are necessary for design and for guiding materials improvement. The most frequently used criteria are extensions of similar criteria for isotropic materials based on maximum stress, maximum strain, or a stress or strain quadratic invariant. Unlike the analytical formulation of the elastic deformation of previous sections, these criteria are empirical and have no analytical foundation. It is curve fitting. The formulation of the criteria, however, must still be consistent with established principles of mechanics .

One of the most common failure criteria for isotropic materials is the von Mises criterion. The envelope on the plane without shear stress is defined by this criterion shown in the figure below. Also shown in this figure is the Tresca failure criterion where failure is defined by either the maximum normal or the maximum shear stress. Both criteria give nearly the same strength under combined stresses. Also shown is the corresponding shear strengths. This strength is not independent, and can be expressed in terms of the uniaxial strength. Although these criteria are often limited to yielding, we intend to extend them to orthotropic composite materials. Since composite materials are strong, resilient and have no yielding, the criteria are applied to the ultimate.

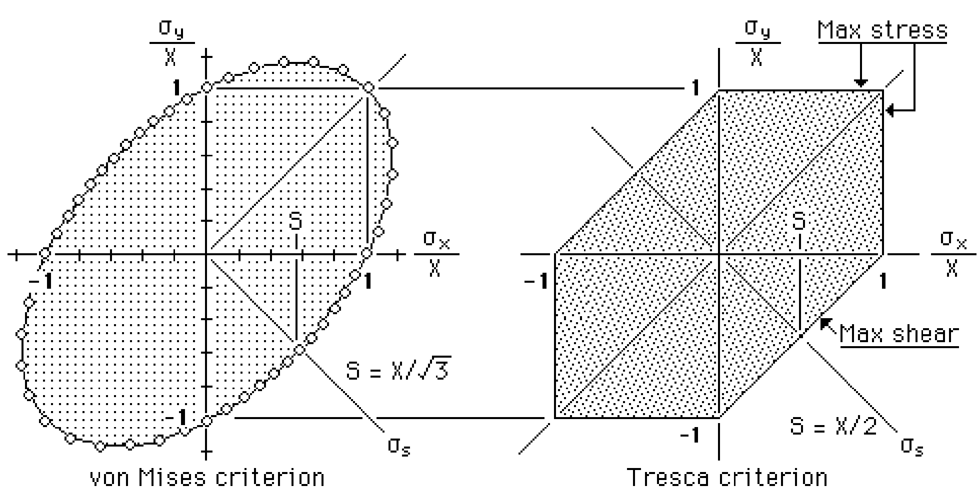

FIGURE 8.1 FAILURE ENVELOPES FOR ISOTROPIC MATERIALS

If tensile and compressive strengths are different, the von Mises failure criterion above can be modified as shown Figure 8.2, where, in this case, the tensile is less than the compressive strength. For isotropic materials, the corresponding shear strength can be expressed in terms of the tensile and compressive strengths.

To recognize different tensile and compressive strengths of composite and other isotropic materials, the Tresca criterion can also be modified as shown in the figure below. The maximum stress criteria in the 1st and 3rd quadrants have different values. The criteria in the 2nd and 4th quadrants are no longer the maximum shear stress. They are simply lines connecting the anchor points of the tensile and compressive strengths: **X** and **X'**.

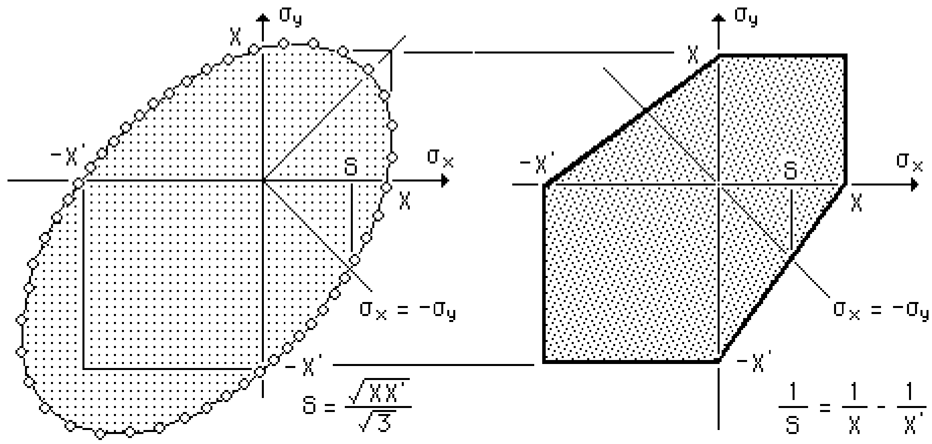

FIGURE 8.2 FAILURE CRITERIA FOR AN ISOTROPIC MATERIAL HAVING DIFFERENT TENSILE AND COMPRESSIVE STRENGTHS

The modes of failure of composite materials are more complicated than those of isotropic materials. In addition to the different tensile and compressive strengths, the strengths along the fibers are different from those transverse to them. Thus there are four uniaxial strengths; i.e., **X**, **X'**, **Y**, and **Y'**. Shear strength is also independent. This makes a total of five strengths. The objective of a failure criterion is to select an envelope that will define the strength of an orthotropic ply under combined stresses. This is important because all plies in a laminate are under combined stresses. There are many failure criteria., and they can be selected by different reasoning processes. Two key issues in comparing the merits of failure criteria are the identification and interaction of the ply failure modes, and the degradation of ply properties as failure progresses toward the ultimate laminate failure.

Having a failure criterion, ply-by-ply strength analysis can be determined, from which the first ply failure, next ply failure, and last ply failure can all be derived. In this section, we will cover various failure criteria of a unidirectional ply. In the next section, failure of a laminate consisting of arbitrarily selected plies will be determined. This is done by letting all plies remain intact until the first ply failure occurs. The FPF envelope is then defined. We will also describe the laminate load carrying capability beyond the FPF.

8.2 BASIC STRENGTH DATA

It is assumed that the strengths of a unidirectional or fabric ply listed in Table 8.1 can be determined from relatively simple tests. Failure criteria are envelopes that define the strength of a unit ply under combined stresses or strains. The envelope must pass through the measured strengths. These strengths are the anchors of failure envelopes. Another necessary condition is that the envelope must be closed. Open envelopes imply infinite strengths under certain combined stresses which is unacceptable.

Each of these basic strength has its unique failure mode. Some pictures of the failures will be shown. Suffice to say, the actual mechanisms of failure are not well understood.

TABLE 8.1 STRENGTH OF VARIOUS COMPOSITE MATERIALS

Test and strength data					T3N	B4	AS	E-gl	Kev	IM6	T3F
Loading	Specimen	Strengths, MPa									
Uniaxial	[0]	Longi tens	X	□	1500	1260	1447	1062	1400	3500	1314
Uniaxial	[0]	Longi compr	X'	⊡	1500	2500	1447	610	235	1540	1220
Uniaxial	[90]	Trans tens	Y	■	40	61	52	31	12	56	43
Uniaxial	[90]	Trans compr	Y'	◘	246	202	206	118	53	150	168
Shear	[0]or[90]	Longi shear	S	◇	68	67	93	72	34	98	48

The five distinctive modes of failure of a unidirectional ply are based on the five strengths listed in the table above. Some general characteristics of failure modes of unidirectional composite materials can be described as follows:

1) Tensile failure of a [0] ply, designated by **X**, is not a cleavage type; there is no necking before failure. It is by a sudden explosion in the case of glass/epoxy composites, where matrix is stripped from the fiber after fiber failure like an explosion. The bushy appearance is shown on the left of the figure below. For graphite/epoxy composites, the failure is often preceded by splitting the ply into parallel strips before the ultimate failure; shown on the right of the figure.

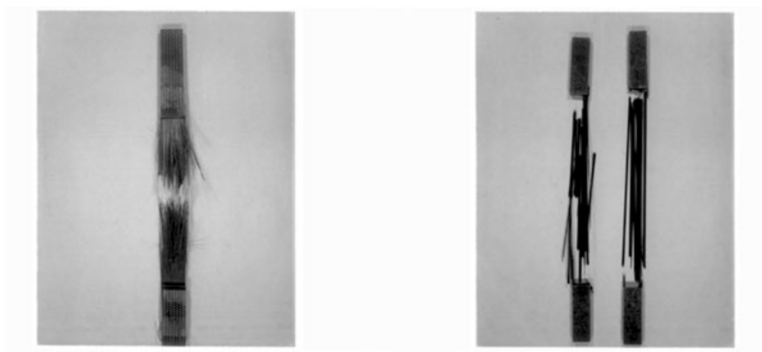

FIGURE 8.3 UNIAXIAL TENSILE FAILURES OF UNIDIRECTIONAL GFRP AND CFRP

2) Compressive failure of a [0] ply, designated by **X'**, is a shear-type failure (along a 45-degree cleavage plane), or a stability failure by a kink band formation. Compressive strength is affected by both the fiber and matrix properties and the interfacial strength. In Figure 8.4, compressive failures of unidirectional CFRP are shown. Both examples are shear-type failures on the macro scale, triggered by failures by micro buckling or kink band formulation.

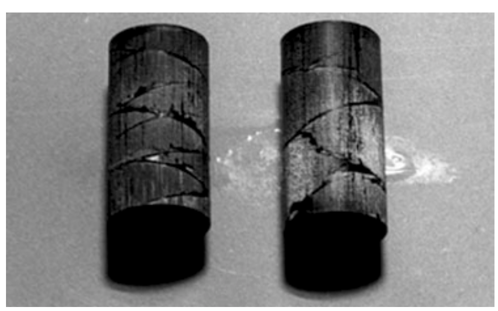

FIGURE 8.4 UNIAXIAL COMPRESSIVE FAILURE OF UNIDIRECTIONAL CFRP

3) Tensile failure of a [90] ply, designated by **Y**, is a cleavage type failure along the fibers, transverse to the applied uniaxial load. In terms of fracture, the failure is caused by a crack opening mode.

4) Compressive failure of a [90] ply, designated by **Y'**, is a shear type failure, along a 45-degree plane to the applied uniaxial load and normal to the parallel fibers.

5) Longitudinal shear failure of [0] or [90], designated by **S**, is precipitated by transverse cracking, similar to the transverse tensile failure. In terms of crack propagation, it is propelled by a shear mode parallel to the axis of the fibers.

Using these data as anchors, we can employ appropriate failure criteria to predict the strength of an orthotropic ply subjected to combined stresses or strains.

8.3 QUADRATIC CRITERION IN STRESS SPACE

One of the simplest failure criteria for anisotropic materials is the extension of the von Mises criterion to a quadratic criterion, which is based on scalar products of stress or strain components. We postulate that the criterion in stress space consists of the sum of a linear and a quadratic invariant as shown in the equations below. For an orthotropic or transversely isotropic ply under plane stress relative to the symmetry axes x-y, the strength parameters **F**s can be defined as the strength parameters in stress space:

$\boxed{F_{ij}\sigma_i\sigma_j + F_i\sigma_i = 1}$, when expanded in the symmetry axes:

$$\boxed{F_{xx}\sigma_x^2 + 2F_{xy}\sigma_x\sigma_y + F_{yy}\sigma_y^2 + F_{ss}\sigma_s^2 + F_x\sigma_x + F_y\sigma_y = 1}$$

where for orthotropy: $F_{xs} = F_{ys} = F_s = 0$; only **six** strength parameters.

$$F_{xy} = \text{interaction term} = F^*_{xy}\sqrt{F_{xx}F_{yy}}\text{; for closed envelopes: } -1 \le F^*_{xy} \le 1 \tag{8.1}$$

The quadratic criterion is the simplest functional relation form by scalar products. We show a more general relation in Figure 8.23. As more general relations are proposed, more material constants will be needed. There is a point of diminishing return. We consider the quadratic relation shown above the best compromise between flexibility and practicality.

$$\text{If } \sigma_x \ne 0,\ \left.\begin{matrix} F_{xx}X^2 + F_xX = 1 \\ F_{xx}X'^2 - F_xX' = 1 \end{matrix}\right\} \text{ roots: } F_{xx} = \frac{1}{XX'},\ F_x = \frac{1}{X} - \frac{1}{X'}$$

$$\text{If } \sigma_y \ne 0,\ \left.\begin{matrix} F_{yy}Y^2 + F_yY = 1 \\ F_{yy}Y'^2 - F_yY' = 1 \end{matrix}\right\} \text{ roots: } F_{yy} = \frac{1}{YY'},\ F_y = \frac{1}{Y} - \frac{1}{Y'}$$

$$\text{If } \sigma_s \ne 0,\ F_{ss} = \frac{1}{S^2}$$

$$\boxed{\frac{\sigma_x^2}{XX'} + \frac{2F^*_{xy}\sigma_x\sigma_y}{\sqrt{XX'YY'}} + \frac{\sigma_y^2}{YY'} + \frac{\sigma_s^2}{S^2} + \left[\frac{1}{X} - \frac{1}{X'}\right]\sigma_x + \left[\frac{1}{Y} - \frac{1}{Y'}\right]\sigma_y = 1} \tag{8.2}$$

The strength parameters can be computed from the five strength data by solving simultaneous equations shown in Equation 8.2. This is done by imposing simple tests like uniaxial tension and compression, and pure shear. By substituting the stresses into the failure criterion, we can solve for **F**s, the strength parameters.

The sixth and missing parameter is the interaction term, which can only be determined from a combined-stress test where both normal stress components are nonzero. Unfortunately, combined-stress tests are difficult to perform. For the time being we can treat the interaction term as an empirical constant. The values for the interaction term, among the most frequently cited failure criteria, are listed below.

TABLE 8.2 INTERACTION TERMS FOR VARIOUS QUADRATIC FAILURE CRITERIA

Criteria	Uniaxial strengths	F_{xy}	F^*_{xy} (T300-5208)
Tsai-Hill	$X = X'$, $Y = Y'$	$-\frac{1}{2X^2}$	$-0.014 \le -\frac{Y}{2X} \le -0.008$
Hoffman	$X \neq X'$, $Y \neq Y'$	$-\frac{1}{2XX'}$	$-0.041 \le -\frac{1}{2}\sqrt{\frac{YY'}{XX'}} \le -0.022$
Tsai-Wu	$X \neq X'$, $Y \neq Y'$	$\frac{F^*_{xy}}{\sqrt{XX'YY'}}$	$-1 \le F^*_{xy} \le 0$ (all materials)

Limits are imposed on the normalized interaction term for having closed envelopes, as stated in Equation 8.1. It will be postulated later in this section (Figure 8.18) that a tighter limits may be imposed from failure mode considerations such that the limits can be between -1 and 0; i.e., no positive value.

Three orthogonal views of various failure envelopes are shown in the figures below. Because of the severe anisotropy, the scale for the stress along the fiber axis is about five times that of the stress in the transverse and shear direction. The first is the Tsai-Hill criteria where the compressive strengths are assumed to be equal to the tensile strengths. The interaction term is practically zero. The symbols for strengths, defined in Table 8.1, are used as anchors in the envelopes.

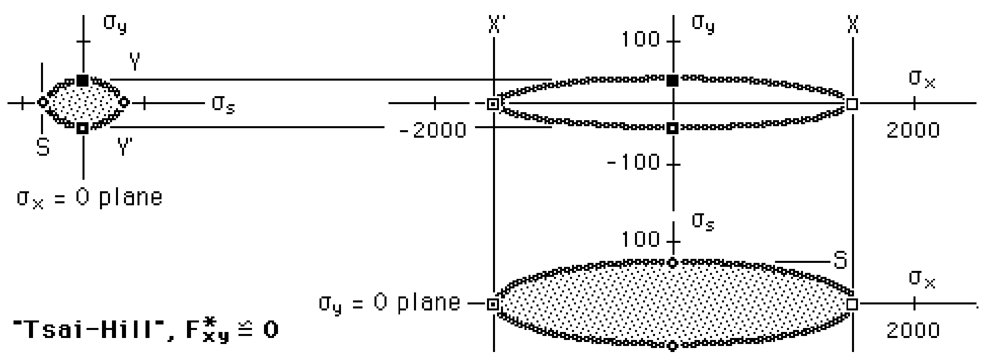

FIGURE 8.5 FAILURE ENVELOPE OF THE TSAI-HILL CRITERION FOR A MODIFIED T300/5208 (USE LOWER TENSILE OR COMPRESSIVE STRENGHT)

The Hoffman criterion takes into account the difference between tensile and compressive strengths, but keeps the interaction term negative but vanishingly small. It is essentially zero. This criterion is a special case of the more general Tsai-Wu quadratic criterion when the interaction term is assumed to be zero. Three views of this criterion are shown (not to scale) in Figure 8.6.

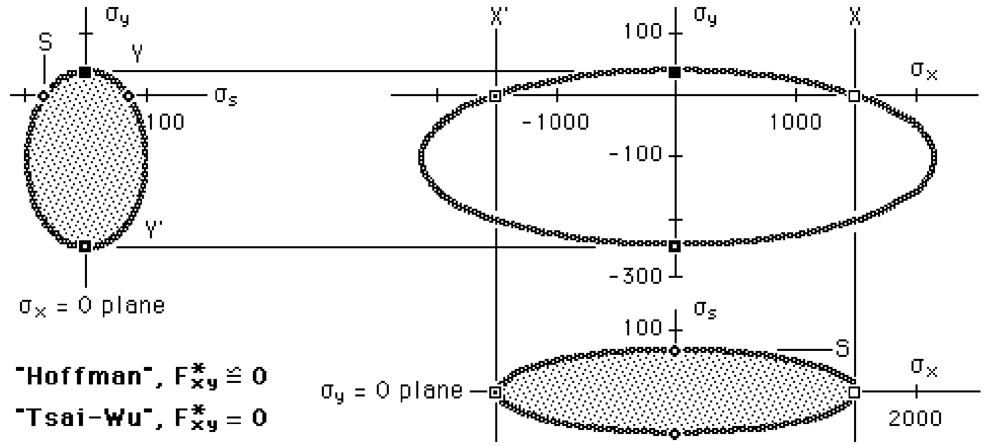

FIGURE 8.6 FAILURE ENVELOPE OF THE HOFFMAN OR TSAI-WU CRITERION FOR ZERO INTERACTION TERM FOR T300/5208

Tsai-Wu criterion can have different values for the interaction term. One example, shown in the figure below, is the case when the normalized interaction term is -1/2. This is a popular criterion because classical von Mises criterion can be recovered when anisotropy is reduced to isotropy and tensile and compressive strengths are equal. Three views of this envelope are shown (not to scale) below. Only the view in the normal stress plane is different as the value of the interaction term changes. This can be seen comparing Figures 8.6 and 8.7.

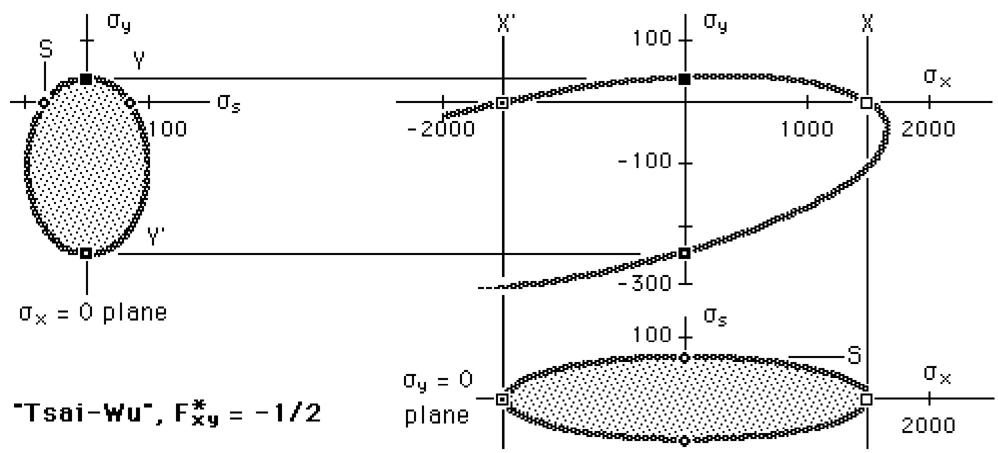

FIGURE 8.7 FAILURE ENVELOPE OF TSAI-WU CRITERION HAVING AN INTERACTION TERM OF -1/2 FOR T300/5208

A variation of the quadratic criterion is seen in the figure below the Hashin criterion where the quadratic relation is limited to the transverse-shear stress plane. The maximum stress criterion is used for the tensile and compressive failures of the fibers. It is assumed that fiber failure can be uncoupled from the matrix failure. In composites, both fiber and matrix contribute the overall stiffness and strength. Dissecting a highly complex failure modes to two parts is not more realistic or rational than the quadratic formation for the entire composite. Mathematically, inequalities are more difficult to manipulate than equalities.

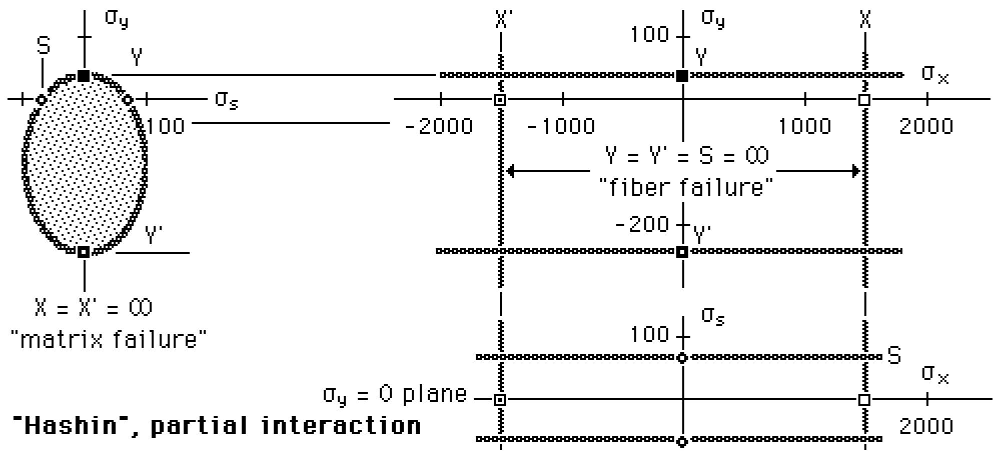

FIGURE 8.8 FAILURE ENVELOPE OF THE HASHIN CRITERION FOR T300/5208

The Dassault Company found that for most of their applications it was only necessary to take into account the interaction between the longitudinal-shear stress plane. Transverse failure is assumed not to be a controlling factor, and is to occur at infinity. The interaction is shown in shaded area in the figure below. Like Hashin's criterion, we can view the Dassault criterion as a hybrid, having partial interaction. Again, there are inequalities in this criterion and for the added operational difficulties, it does not seem to add more insight nor utility to the failure criterion of composites.

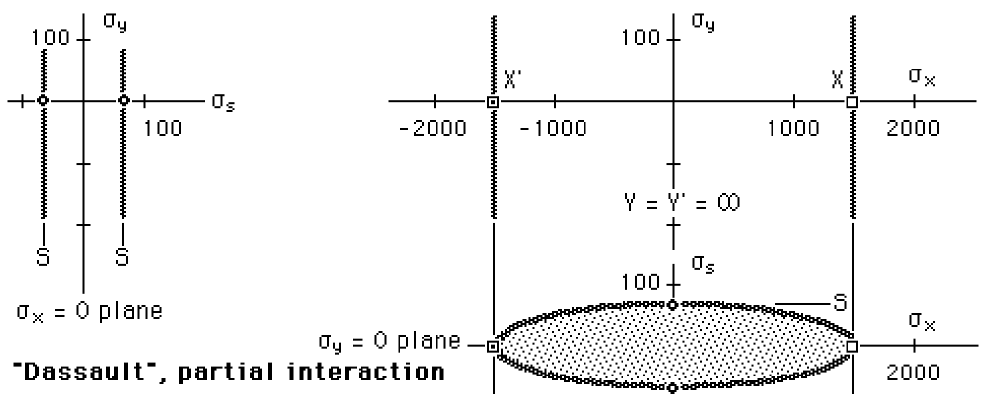

FIGURE 8.9 FAILURE ENVELOPE OF THE DASSAULT CRITERION FOR T300/5208

The quadratic criterion can be taken to limiting cases, such as letting fiber or matrix strength go to infinity; i.e., the fiber or matrix failure mode can be suppressed. In the equations below we show the results of the limiting cases, which result in the maximum stress criterion. In this sense, quadratic criteria are more general than non-interactive and partially interactive criteria.

Let $\sigma_s = 0$ (the principal stress plane)

If $X = X' = \infty$ (infinite fiber strength): $\dfrac{\sigma_y^2}{YY'} + \left[\dfrac{1}{Y} - \dfrac{1}{Y'}\right]\sigma_y = 1,\ \sigma_y = Y, -Y'$

If $Y = Y' = \infty$ (infinite matrix strength): $\dfrac{\sigma_x^2}{XX'} + \left[\dfrac{1}{X} - \dfrac{1}{X'}\right]\sigma_x = 1,\ \sigma_x = X, -X'$ (8.3)

The resulting maximum stress criterion can be viewed in the figure below, where failure mode interactions are assumed to be non-existent. An analogous criterion can be based on strains. The latter will appear like boxes in strain space.

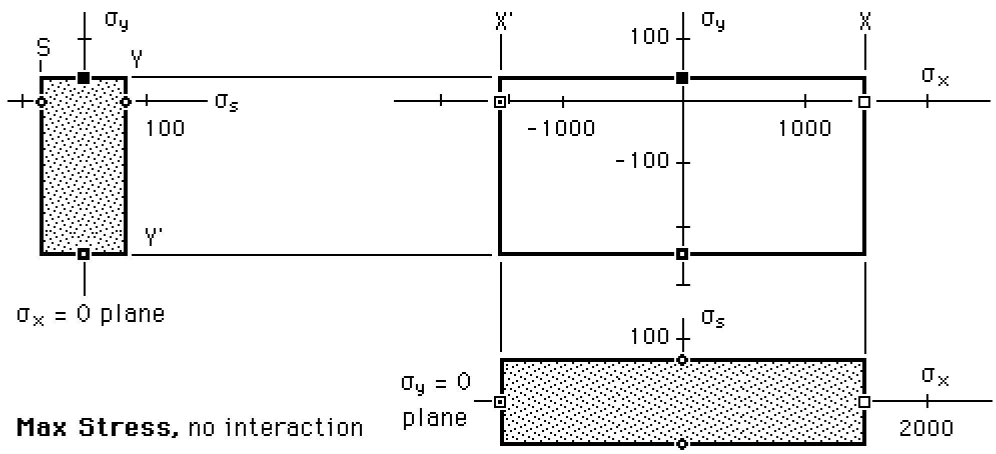

FIGURE 8.10 FAILURE ENVELOPE OF THE MAXIMUM STRESS CRITERION

Aside from the assumed non-interacting failure modes, there is another concern of assigning critical or ultimate values to each component of a tensor like those for stress and strain. In this case failure assessment must be made in the on-axis coordinate system. If critical values are assigned to an invariant or scalar, it is no longer necessary to examine the on-axis system. It would be true for all coordinate systems. Such invariant description is guaranteed in the Tsai-Wu and Tsai-Hill quadratic criteria. They are therefore simple to apply.

We have illustrated some of the most popular failure criteria in use by various companies and commercial finite element analysis programs. We believe that the Tsai-Wu quadratic criterion with full interactive failure modes is likely to provide the most consistent failure prediction. It is often claimed that the two limitations of this criterion are the uncertainty of the interaction term and, secondly, the identification of failure modes. We will show in the next section how a more restrictive interaction term may be estimated. Identification of failure modes remains subjective, and very much in doubt in many failure criteria. Failures under simple stresses are difficult to explain, as seen in Figures 8.3 and 8.4, those under combined stresses are much more contentious.

8.4 FAILURE MODE INTERACTIONS

Using five of the basic strength data, we can only determine five out of six strength parameters needed for an orthotropic material under plane stress. The missing data is the interaction term. If it is assumed that longitudinal failure is preceded by matrix cracking, the dominant crack will run parallel to the unidirectional fibers, as shown in the figure below. A small lateral tension would tend to facilitate the crack extension. Then, strength under tension-tension would be lower than that under pure tension. Conversely, tension-compression would retard the crack propagation. The resulting strength from this combined stress would be greater than the strength of pure tension. The shaded area in the figure below would be the admissible range of the slopes at the anchor point of the longitudinal strength **X**. The slope of the failure envelope through this anchor point would be negative.

If there is no mode interaction, a line through the tensile strength anchor point would be vertical. The slope would be infinity. The minimum slope, on the other hand, would be a straight line connecting **X** and **Y**, the longitudinal and transverse tensile strengths, respectively. The minimum slope would be **-Y/X** = -40/1500 = -0.027, or the admissible inclination of the tangent would be between -1.6 and -90 degrees for T300/5208.

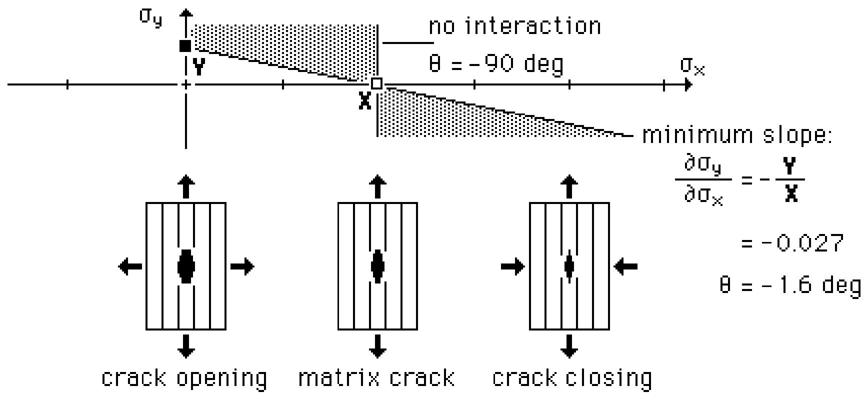

FIGURE 8.11 ADMISSIBLE RANGE OF TANGENT AT THE LONGITUDINAL TENSILE STRENGTH

If the crack is oriented perpendicular to the fiber instead of parallel to the fiber shown in the figure above, the admissible range of the interaction term, or the slope, would be positive. This occurs when the fiber strength is low, which is not the case for most modern composite materials.

We can use the same argument to establish the slope of the failure envelope at the anchor of the longitudinal compressive strength. The range is bounded by a vertical line indicating no interaction, and a straight line connecting **Y** and **X'**. The shaded area in the figure below shows the admissible range of the value of the interaction term.

It is assumed that compressive failure is by shear along a 45-degree plane. A small lateral compression would reduce the maximum shear stress, resulting in higher compressive strength than the uniaxial compression. A small lateral tension would increase the maximum shear stress, resulting in a lower compressive strength. The slope through this anchor point would be positive, having a minimum value of **Y**/**X'** = 40/1500 = 0.027, or the admissible angle will be between 1.6 and 90 degrees for T300/5208 ply material.

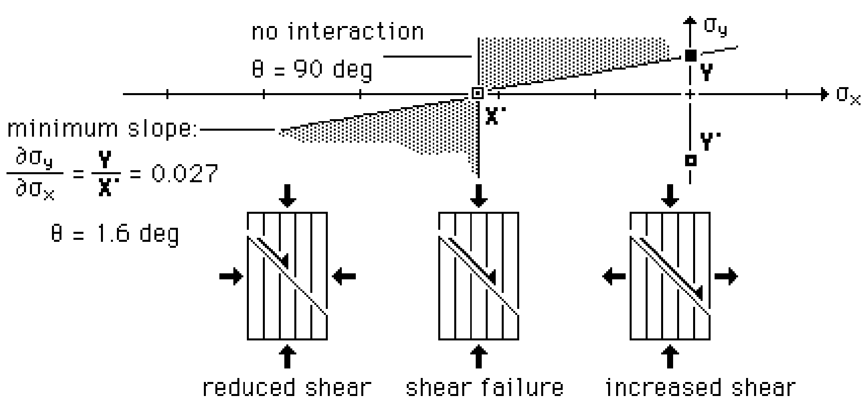

FIGURE 8.12 ADMISSIBLE RANGE OF TANGENT AT THE LONGITUDINAL COMPRESSIVE STRENGTH

If we had assumed that the failure is caused by matrix failure, instead of the shear failure just described, the same range of values for the interaction term would remain; i.e., a lateral compression would increase the strength, and a lateral tension would decrease the strength.

If we had assumed that fiber failure occurs before the composite failure, then the cracks would be normal to the fibers. The resulting interaction would lead to a negative slope.

We can then examine the transverse tensile failure for a unidirectional ply. We assume that a crack that would lead to a transverse failure would run parallel to the transverse fibers, shown in the figure below.

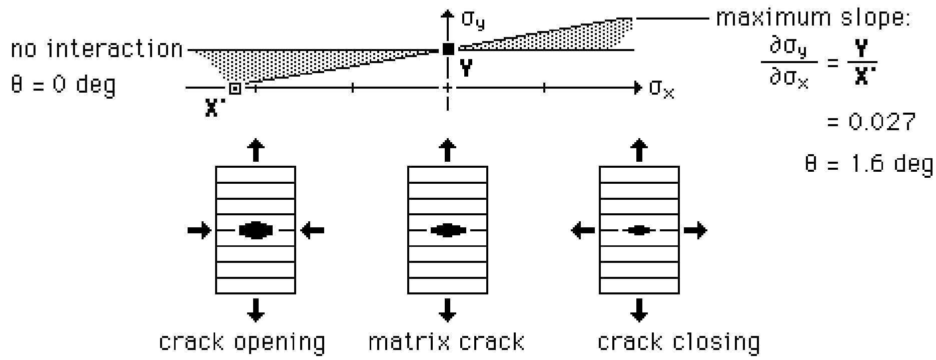

FIGURE 8.13 ADMISSIBLE RANGE OF TANGENT AT THE TRANSVERSE TENSILE STRENGTH

The admissible range of values for the interaction term is shown as the shaded area, where a small lateral compression would cause the crack to open. The strength would be lower than the uniaxial tensile strength. A small lateral tension, on the other hand, would increase the tensile strength. The slope through this anchor point would be positive, with a maximum value of **Y/X'** = 40/1500 = 0.027, or the angle of inclination of the tangent will be between 0 and 1.6 degrees for T300/5208 ply material.

Finally we can rationalize the mode interaction at the transverse compressive strength. If shear failure controls, lateral compression would increase the compressive strength and lateral tension would decrease the strength. The slope through this anchor point would be positive. The maximum value for the slope would be **Y'/X** = 246/1500 = 0.16, or the angle of inclination will be between 0 and 9 degrees for T300/5208 ply material.

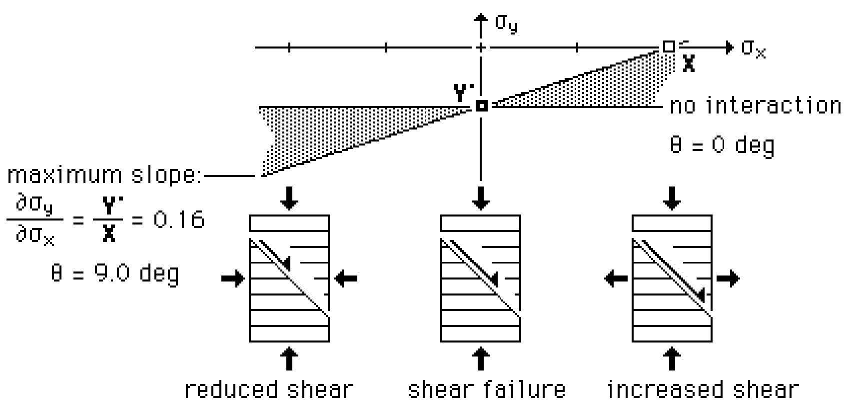

FIGURE 8.14 ADMISSIBLE RANGE OF TANGENT AT THE TRANSVERSE COMPRESSIVE STRENGTH

A summary of the failure mode interactions of a unidirectional composite material around the four uniaxial strengths can be defined by the range of the inclination of the tangents to the quadratic failure envelope. When the tangent is normal to the stress axis in space, no failure mode interaction is assumed. This is the case of the maximum stress criterion.

8.5 ADMISSIBLE VALUES FOR THE INTERACTION TERM

In order to narrow the value for the interaction term of the quadratic failure criterion, we can further impose the following rationalizations:

1) We assume that there is one failure criterion for the entire range of combined stresses or strains. We can have only one value for all the strength parameters,

one of which is the interaction term. We do not wish to have different values for the interaction term in different quadrants or octants in stress or strain space. There would be too many material parameters to determine. We must pay attention to the shape of the failure envelope in all quadrants. A forced fitting of data in one quadrant can lead to an unreasonable shape of the envelope elsewhere.

2) It is assumed that the failure envelope must be closed. The condition for a closed ellipsoid bounds the normalized interaction term between +1, and -1. This requirement ensures that there are no combined stresses or strains that would lead to infinite strength. In Figure 8.15 we show a series of failure envelopes in strain space (to be covered later in the next sub-section) having a varying interaction term between -2 and +2. Note the open surface at each end of the figure. Implicitly assumed is that all envelopes must pass through the initial strengths which act as anchor points.

3) The inclination of tangents to the failure envelopes at the four anchor points must be within the four corresponding admissible ranges cited in Figure 8.15. The slope and the inclination of the tangents are derived in the equations below in the normal stress plane where shear stress vanishes:

$$\frac{\partial}{\partial\sigma_x}\left[F_{ij}\sigma_i\sigma_j+F_i\sigma_i\right] = 2F_{xx}\sigma_x+2F_{xy}\left[\sigma_y+\sigma_x\frac{\partial\sigma_y}{\partial\sigma_x}\right]+2F_{yy}\sigma_y\left[\frac{\partial\sigma_y}{\partial\sigma_x}\right]+F_x+F_y\left[\frac{\partial\sigma_y}{\partial\sigma_x}\right] = 0$$

$$\frac{\partial\sigma_y}{\partial\sigma_x} = -\frac{2F_{xx}\sigma_x+2F_{xy}\sigma_y+F_x}{2F_{xy}\sigma_x+2F_{yy}\sigma_y+F_y};\ \theta = \text{inclination} = \arctan\left[\frac{\partial\sigma_y}{\partial\sigma_x}\right] \qquad (8.4)$$

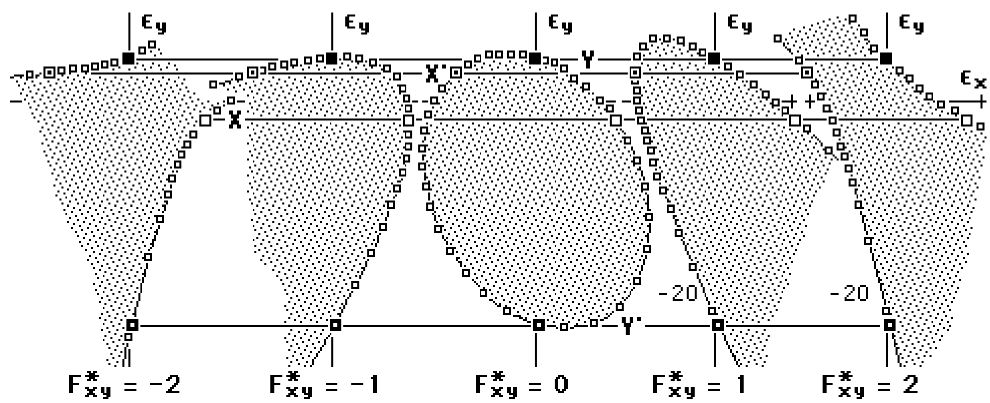

FIGURE 8.15 A RANGE OF VALUES FOR THE INTERACTION TERM OF THE QUADRATIC FAILURE CRITERION SHOWING THE NECESSARY BOUNDS BETWEEN -1 AND +1 IF THE FAILURE ENVELOPES ARE TO BE CLOSED

Our quadratic criterion is analytical: it is a closed-formed, single-valued function. Differentiation is elementary. The inclinations at the four anchor points as functions of the normalized interaction terms are easily found:

$$\text{When } \sigma_x = X,\ \sigma_y = 0,\ \theta]_{\mathbf{X}} = \arctan\left[-\frac{2F_{xx}X+F_x}{2F^*_{xy}\sqrt{F_{xx}F_{yy}}\,X+F_y}\right]$$

$$\text{when } \sigma_x = -X',\ \sigma_y = 0,\ \theta]_{\mathbf{X'}} = \arctan\left[-\frac{-2F_{xx}X'+F_x}{-2F^*_{xy}\sqrt{F_{xx}F_{yy}}\,X'+F_y}\right]$$

$$\text{when } \sigma_y = Y,\ \sigma_x = 0,\ \theta]_{\mathbf{Y}} = \arctan\left[-\frac{2F^*_{xy}\sqrt{F_{xx}F_{yy}}\,Y+F_x}{2F_{yy}Y+F_y}\right]$$

$$\text{when } \sigma_y = -Y',\ \sigma_x = 0,\ \theta]_{\mathbf{Y'}} = \arctan\left[-\frac{-2F^*_{xy}\sqrt{F_{xx}F_{yy}}\,Y'+F_x}{-2F_{yy}Y'+F_y}\right] \qquad (8.5)$$

By knowing the range of the inclination as a result of the failure mode interactions, we can define the range of the interaction term. The results of the first two relations of Equations 8.5 are shown in the next figure. The admissible range of the interaction term is defined by the admissible inclinations at the longitudinal tensile and compressive strengths. At the longitudinal tensile strength point, the inclination goes from -60 to -2 degrees as the interaction term goes from -1 to +1. At the longitudinal compressive strength point, the inclination goes from +2 to +60 degrees as the interaction term goes from -1 to +1. The failure mode interaction does not narrow the range of the interaction term for this ply material at these two anchor points.

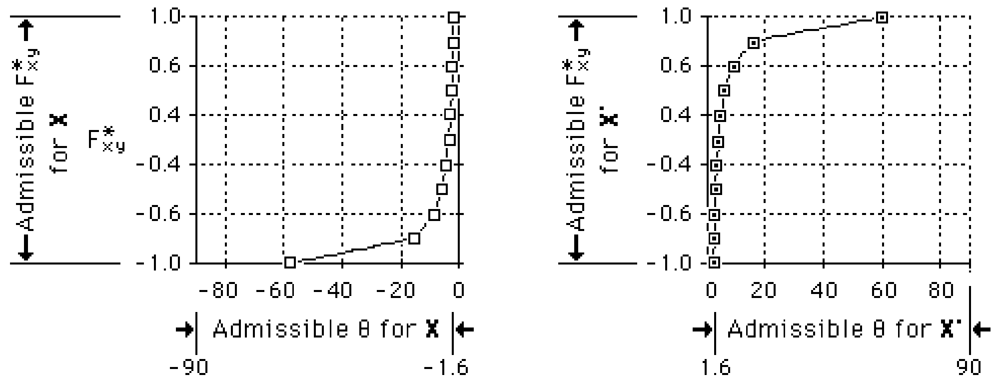

FIGURE 8.16 ADMISSIBLE RANGES OF THE INTERACTION TERM AND THE INCLINATIONS OF THE TANGENTS TO THE FAILURE ENVELOPE

Next we show the range of the interaction term as defined by the transverse tensile and compressive strengths given by the last two relations in Equation 8.5. The range of the inclination goes from 1.1 to 0 degrees as the interaction term goes from -1 to zero at the transverse tensile point; it goes from 6 to 0 degrees as the interaction term goes from -1 to zero.

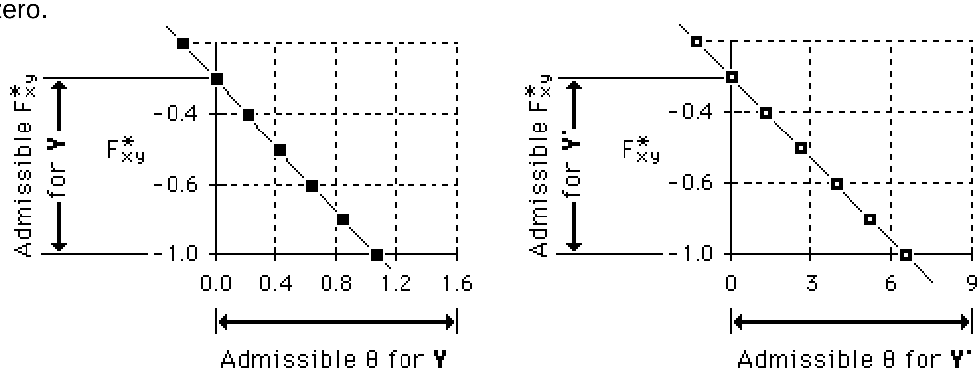

FIGURE 8.17 ADMISSIBLE RANGES OF THE INTERACTION TERM AND THE INCLINATIONS OF THE TANGENTS TO THE FAILURE ENVELOPE

The admissible range of the interaction term is narrowed by the range of admissible inclinations. From this figure, the range for this composite ply of T300/5208 is between 0 and -1. Positive value is not admissible by the inclination at the transverse tensile and compressive strengths, although it is admissible by the inclination at the longitudinal tensile and compressive strengths.

While the admissible range of the value for the interaction term for T300/5208 at the transverse tensile and compressive strength points is cut in half, it still covers a range from 0 to -1. It is nonetheless assuring that one value of the interaction term is adequate to satisfy four independently defined range of admissible inclinations.

Additional rationalization and/or biaxial test data will be required to more narrowly define the value for the interaction term. By repeating the process of determining the range of interaction term of T300/5208 through the admissible range of the inclinations at each of the four anchor points, the ranges for other composite plies are shown in Figure 8.18.

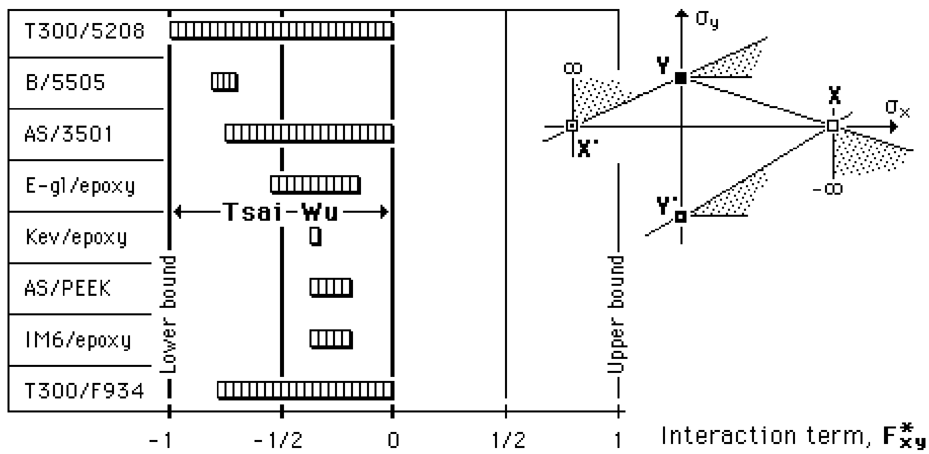

FIGURE 8.18 ADMISSIBLE RANGES OF THE NORMALIZED INTERACTION TERMS

Judging from the ranges of the interaction term for a vairety of materials in the figure above, the upper and lower bounds of the interaction term can be reduced from ±1 to zero and -1, respectively. A new Tsai-Wu range is more restrictive than the geometric range to ensure closed elliptic surface, as indicated in Table 8.2. It is recommended that -1/2 be used as a good approximation for all materials. Unless is otherwise specified, Tsai-Wu criterion implies that this -1/2 is used for the normalized interaction term.

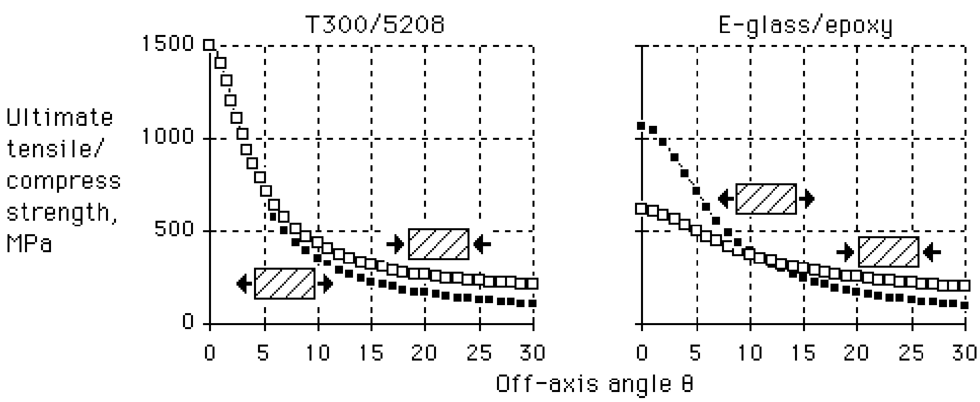

FIGURE 8.19 OFF-AXIS UNIAXIAL TENSILE AND COMPRESSIVE STRENGTHS

A natural question concerns the sensitivity of the value of the interaction term in the strength prediction of composite materials under combined stresses. The off-axis uniaxial tensile and compressive strengths are insensitive to the interaction term. In fact, in the uniaxial strengths shown in Figure 9.19 show no discernible difference between the full range of values for the interaction term from -1 to +1. For a more restrictive range of interaction term between -1/2 and zero, the sensitivity will be even smaller.

The reason for the lack of sensitivity arises from the highly orthotropic strength properties of composite materials. If the failure envelope is drawn with the same scale along the fiber and its transverse, the envelope will be a highly elongated body, like a thin sausage. The interaction term affect the ends of this elongated body more than the middle of the same body. The off-axis uniaxial tensile and compressive tests traverse near the portion of the failure envelope where the shape is not sensitive to the value of the interaction.

In fact, the sensitivity of the interaction term depends on the ply material, and the externally imposed stresses. The insensitivity of the interaction term on the 2-dimensional pressure on a 0-degree specimen, and a uniaxial compression on a 45-degree specimens for two ply materials for the entire range of admissible value for the interaction term is shown in the figure below. Horizontal lines mean complete insensitivity of the interaction term.

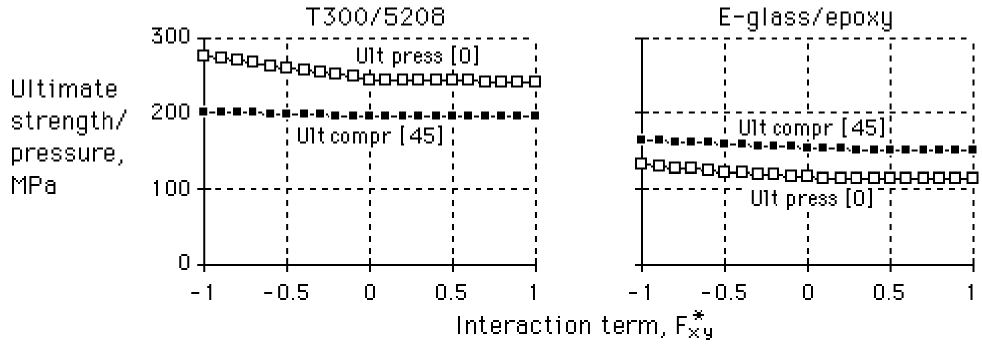

FIGURE 8.20 PLANE (2-D) PRESSURE AND UNIAXIAL COMPRESSIVE STRENGTHS OF T300/5208 AND E-GLASS/EPOXY COMPOSITE MATERIALS FOR A FULL RANGE OF THE INTERACTION TERM

8.6 QUADRATIC CRITERION IN STRAIN SPACE

The plane stress criterion can be represented in strain space by a straightforward substitution of the stress-strain relation. The resulting failure criterion is not based on plane strain because we ignore the nonzero strain along the thickness direction. We are actually representing the plane stress failure criterion in strain space. This is acceptable if we recognize that all failure criteria are purely empirical and are not analytical. They are not derived from fundamental principles.

$$\mathbf{F_{ij}\sigma_i\sigma_j} = F_{ij}[Q_{ik}\epsilon_k][Q_{jl}\epsilon_l] = [F_{ij}Q_{ik}Q_{jl}]\epsilon_k\epsilon_l = \mathbf{G_{kl}\epsilon_k\epsilon_l}, \text{therefore } \boxed{\mathbf{G_{kl} = Q_{ki}Q_{lj}F_{ij}}}$$

$$\mathbf{F_i\sigma_i} = F_i[Q_{ij}\epsilon_j] = [F_iQ_{ij}]\epsilon_j = \mathbf{G_j\epsilon_j}, \text{ therefore } \boxed{\mathbf{G_j = Q_{ji}F_i}} \qquad (8.6)$$

For an orthotropic material, the scalar equation in strains can be expanded as follows:

$$\boxed{\mathbf{G_{ij}\epsilon_i\epsilon_j + G_i\epsilon_i = 1}} \quad \text{when expanded:}$$

$$\boxed{\mathbf{G_{xx}\epsilon_x^2 + 2G_{xy}\epsilon_x\epsilon_y + G_{yy}\epsilon_y^2 + G_{ss}\epsilon_s^2 + G_x\sigma_x + G_y\epsilon_y = 1}}, \text{ where}$$

$$G_{xx} = F_{xx}Q_{xx}^2 + 2F_{xy}Q_{xx}Q_{xy} + F_{yy}Q_{xy}^2, \; G_{yy} = F_{xx}Q_{xy}^2 + 2F_{xy}Q_{xy}Q_{yy} + F_{yy}Q_{yy}^2$$

$$G_{xy} = F_{xx}Q_{xx}Q_{xy} + F_{xy}(Q_{xx}Q_{yy} + Q_{xy}^2) + F_{yy}Q_{xy}Q_{yy},$$

$$G_{ss} = F_{ss}Q_{ss}^2, \; G_x = F_xQ_{xx} + F_yQ_{xy}, \; G_y = F_xQ_{xy} + F_yQ_{yy} \qquad (8.7)$$

If we know the strength parameter **[F]** and **{F}** in stress space and the plane stress stiffness **[Q]**, we can immediately calculated **[G]** and **{G}** using the relations in Equation 8.7.

The representation of failure envelopes in strain space is preferred because strain is usually specified in laminated plate theory; i.e., strain is at most a linear function of the thickness. The failure envelope for a given ply angle is fixed in strain space and is independent of plies having different angles in the same laminate. These envelopes can thus be viewed as material properties. On the other hand, failure envelopes of a multidirectional laminate in stress space are functions for each laminate. This will be illustrated in the next section in Figure 9.4.

In the figure below, we show the failure envelopes of T300/5208 in strain space for three values of the interaction term; i.e., 0 and -1/2. Also shown are the four anchors of the basic uniaxial strengths. Due to Poisson's ratios, the basic uniaxial strengths in strain space are in combined strain space. The longitudinal tensile and compressive strengths are connected by a line having a slope equal to the major Poisson's ratio of the ply material, in a negative value. For this material, the slope is -0.28. The transverse tensile and compressive strengths are almost along the vertical or transverse stress axis, because the minor Poisson's ratio is very small or close to zero.

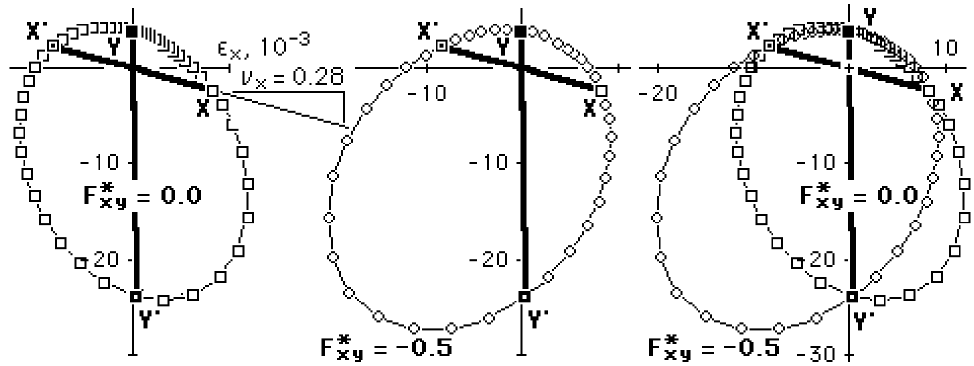

FIGURE 8.21 SINGLE AND SUPERPOSED ENVELOPES IN STRAIN SPACE WITH TWO INTERACTION TERMS

The sensitivity of the interaction term on the failure envelopes can be seen when they are superposed. The most pronounced difference is in thrid quadrant. Compression-compression tests would be effective to measure which interaction term is more reasonable.

Typical strength data for the same composite materials as those in Table 8.1, on page 8-2, are shown in the following table. Engineering constants are also included.

TABLE 8.3 STRENGTH OF VARIOUS COMPOSITE MATERIALS IN SI

Fiber	T300	B(4)	AS	E-glass	Kev 49	AS 4	H-IM6	T300	T300	T300
Matrix	N5208	N5505	3501	epoxy	epoxy	PEEK	epoxy	F934	F934	F934
Engineering constants, GPa or dimensionless								4-mil tp	13-mil c	7-mil c
Ex	181.00	204.00	138.00	38.60	76.00	134.00	203.00	148.00	74.00	66.00
Ey	10.30	18.50	8.96	8.27	5.50	8.90	11.20	9.65	74.00	66.00
nu/x	0.28	0.23	0.30	0.26	0.34	0.28	0.32	0.30	0.05	0.04
Es	7.17	5.59	7.10	4.14	2.30	5.10	8.40	4.55	4.55	4.10
Max stress, MPa										
X	1500	1260	1447	1062	1400	2130	3500	1314	499	375
X'	1500	2500	1447	610	235	1100	1540	1220	352	279
Y	40	61	52	31	12	80	56	43	458	368
Y'	246	202	206	118	53	200	150	168	352	278
S	68	67	93	72	34	160	98	48	46	46
Max strain, eps*, E-03										
x	8.29	6.18	10.49	27.51	18.42	15.90	17.24	8.88	6.74	5.68
x'	8.29	12.25	10.49	15.80	3.09	8.21	7.59	8.24	4.76	4.23
y	3.88	3.30	5.77	3.75	2.18	8.99	5.00	4.46	6.19	5.58
y'	23.88	10.92	22.99	14.27	9.64	22.47	13.39	17.41	4.76	4.21
s	9.48	11.99	13.10	17.39	14.78	31.37	11.67	10.55	10.11	11.22

TABLE 8.4 STRENGTH PARAMETERS IN STRAIN SPACE OF VARIOUS COMPOSITES

Type	CFRP	BFRP	CFRP	GFRP	KFRP	CFRTP	CFRP	CFRP	CCRP	CCRP
Fiber	T300	B(4)	AS	E-glass	Kev 49	AS 4	H-IM6	T300	T300	T300
Matrix	N5208	N5505	3501	epoxy	epoxy	PEEK	epoxy	F934	F934	F934
Strength parameters Fxy* = -0.5								4-mil tp	13-mil c	7-mil c
Gxx	12004	10374	7376	1914	13454	6394	5822	10971	29783	40019
Gyy	10681	27646	7467	18882	47657	4890	14914	12786	32580	40965
Gxy	-3069	-2989	-1746	1712	2069	-1584	-495	-2570	-13120	-17455
Gss	11118	6961	5828	3306	4576	1016	7347	8985	9784	7944
Gx	61	130	39	25	-150	-40	-34	42	-65	-63
Gy	217	214	131	198	351	66	125	168	-52	-61
Strength parameters Fxy* = 0										
Gxx	15544	14823	9889	3669	23445	8136	9259	14999	31418	41879
Gyy	10882	28050	7630	19258	48380	5005	15104	13049	34216	42825
Gxy	3280	6728	2467	5137	16885	1545	4938	4183	3273	3720
Gss	11118	6961	5828	3306	4576	1016	7347	8985	9784	7944
Gx	61	130	39	25	-150	-40	-34	42	-65	-63
Gy	217	214	131	198	351	66	125	168	-52	-61

Since strength parameters in strain space are dimensionless, they are the same for SI and English units. In Figure 8.21 above, we showed the failure envelopes in strain space of T300/5208. In Figure 8.22, we show the failure envelopes of E-glass/epoxy and Kevlar/epoxy composites in strain space. Interaction term of -1/2 and zero are shown.

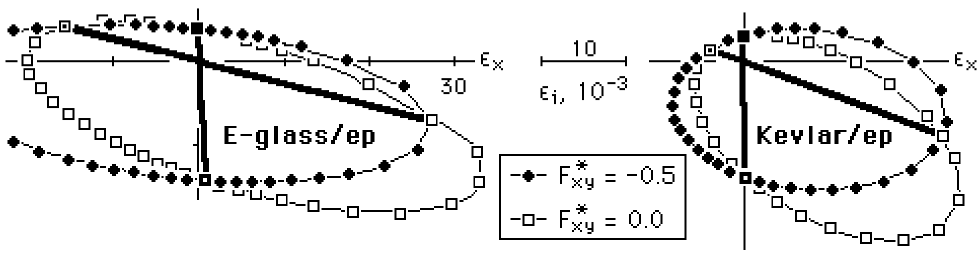

FIGURE 8.22 TSAI-WU ENVELOPES IN STRAIN SPACE FOR GFRP AND KFRP

In the figure below, similar envelopes for AS/PEEK and IM6/epoxy are shown.

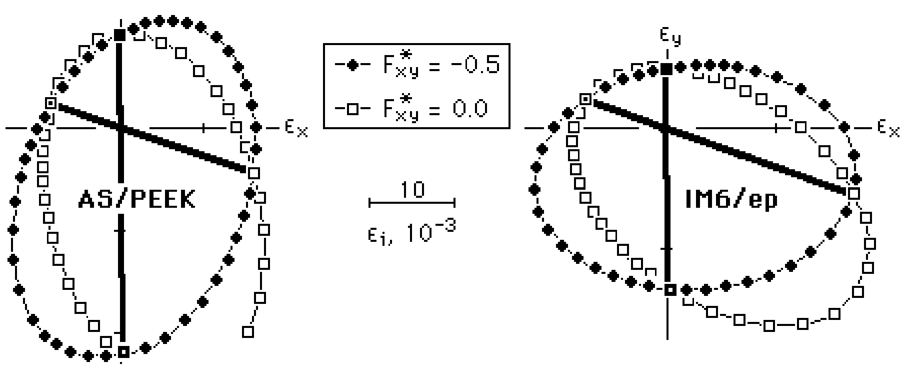

FIGURE 8.23 TSAI-WU ENVELOPES IN STRAIN SPACE FOR AS/PEEK AND IM6/EPOXY COMPOSITES

8.7 TRANSFORMATION OF FAILURE ENVELOPES

We know how to transform an off-axis stress and strain to on-axis orientations. Failure criteria are usually applied in this fashion. We can just as easily transform the failure stress or strain from an on-axis orientation (a point on the failure envelope) to an off-axis orientation equal to the particular ply angle. Failure analysis can be applied in any coordinate axes. This is one of the advantages of the quadratic failure criterion where the transformation relations are well established and need not be reinvented. Such a fully reversible transformation for the maximum stress or maximum strain failure criterion does not exist. For the strength parameters in stress space, the transformation is the same as that of elastic compliance for the fourth rank tensor, and that of strain for the second rank tensor:

$$\begin{Bmatrix} F_{11} \\ F_{22} \\ F_{12} \\ F_{66} \\ F_{16} \\ F_{26} \end{Bmatrix} = \begin{bmatrix} m^4 & n^4 & 2m^2n^2 & m^2n^2 \\ n^4 & m^4 & 2m^2n^2 & m^2n^2 \\ m^2n^2 & m^2n^2 & m^4+n^4 & -m^2n^2 \\ 4m^2n^2 & 4m^2n^2 & -8m^2n^2 & (m^2-n^2)^2 \\ 2m^3n & -2m^3n & 2(mn^3-m^3n) & mn^3-m^3n \\ 2mn^3 & -2mn^3 & 2(m^3n-mn^3) & m^3n-mn^3 \end{bmatrix} \begin{Bmatrix} F_{xx} \\ F_{yy} \\ F_{xy} \\ F_{ss} \end{Bmatrix}$$

$$\begin{Bmatrix} F_1 \\ F_2 \\ F_6 \end{Bmatrix} = \begin{bmatrix} m^2 & n^2 \\ n^2 & m^2 \\ 2mn & -2mn \end{bmatrix} \begin{Bmatrix} F_x \\ F_y \end{Bmatrix} \tag{8.8}$$

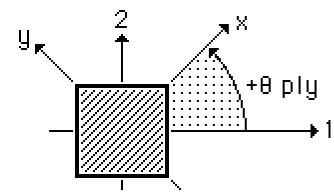

For the strength parameters in strain space, the transformation is the same as that of elastic stiffness for the fourth rank tensor, and that of stress for the second rank tensor. These transformation relations are important and convenient that failure analysis can be done in any coordinate system. In fact, mathematical entities such as stress, strain, failure parameters are defined by their transformation properties. Those entities that cannot be defined by transformation relations are not analytically reliable. Criteria such as Hashin, Dassault, max stress and max strain cannot be transformed. The can only be applied in the on-axis or material coordinate system. This is an intrinsic limitation of non-invariant failure criteria. It is the same dilemma of trying to describe a balanced laminate. A reference coordinate must first be defined before a laminate can be described. Thus being balanced is not as acceptable as being symmetric, anisotropic, thick, heavy or hot.

$$\begin{Bmatrix} G_{11} \\ G_{22} \\ G_{12} \\ G_{66} \\ G_{16} \\ G_{26} \end{Bmatrix} = \begin{bmatrix} m^4 & n^4 & 2m^2n^2 & 4m^2n^2 \\ n^4 & m^4 & 2m^2n^2 & 4m^2n^2 \\ m^2n^2 & m^2n^2 & m^4+n^4 & -4m^2n^2 \\ m^2n^2 & m^2n^2 & -2m^2n^2 & (m^2-n^2)^2 \\ m^3n & -mn^3 & mn^3-m^3n & 2(mn^3-m^3n) \\ mn^3 & -m^3n & m^3n-mn^3 & 2(m^3n-mn^3) \end{bmatrix} \begin{Bmatrix} G_{xx} \\ G_{yy} \\ G_{xy} \\ G_{ss} \end{Bmatrix}$$

$$\begin{Bmatrix} G_1 \\ G_2 \\ G_6 \end{Bmatrix} = \begin{bmatrix} m^2 & n^2 \\ n^2 & m^2 \\ mn & -mn \end{bmatrix} \begin{Bmatrix} G_x \\ G_y \end{Bmatrix} \tag{8.9}$$

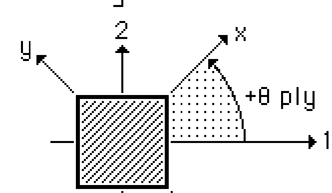

The strain space representation has several advantages over that of stress space:

- It is easier to plot because the envelope is less elongated.
- It is invariant; i.e., the envelope for each ply remains fixed for all laminates.

- It is easy to determine the off-axis ply envelopes.

- It is dimensionless; it is the same in both SI and English units.

As we will discuss in the next section, the advantages of the strain space representation are valid for the first ply failure (FPF) criterion of laminates. Strength capability beyond the FPF becomes nonlinear, and depends on the imposed boundary conditions. Stress and strain boundary conditions will lead to different envelopes beyond the FPF.

The flexibility in the quadratic failure criterion is enhanced by the availability of the interaction term. The experimental determination requires a state of combined stresses. Such tests are not easy to perform. The traditional approach is to use a tubular specimen. Unfortunately, the cost of specimen and that of testing can be prohibitively high and impractical for design data generation.

It should be emphasized that failure criteria are empirical schemes made to fit available experimental data. Since they are not derived from fundamental principles, it is not a question of having a correct or incorrect criterion. The quadratic criterion is better because it is easier to use and more flexible.

The most general failure criterion can be postulated by a function of the power of the cubic, quadratic and linear scalar products. The quadratic criterion that we have been discussing is a special case of this general criterion when the exponents for the cubic term is zero, and the quadratic and linear terms are unity. This is shown in Figure 8.24.

It turns out that these exponents cannot take on arbitrary values if the envelope is totally closed in order to avoid having infinite strength under some combinations of stresses or strains. If we assume that the exponents are equal to 2 for the quadratic and linear terms, the resulting failure envelope is shown in the same figure, together with the conventional quadratic criterion. The envelope having higher exponents is closed, but passes through only two of the four anchor points. The longitudinal tensile and compressive strengths happen to be the same for this material, but the transverse tensile and compressive strengths are different. The solution of the fourth order equation, however, requires that the intercepts of the normal strain axes are symmetrical with respect to the origin. It is therefore incorrect to assign values to the exponents such that the original anchor points are not on the envelope.

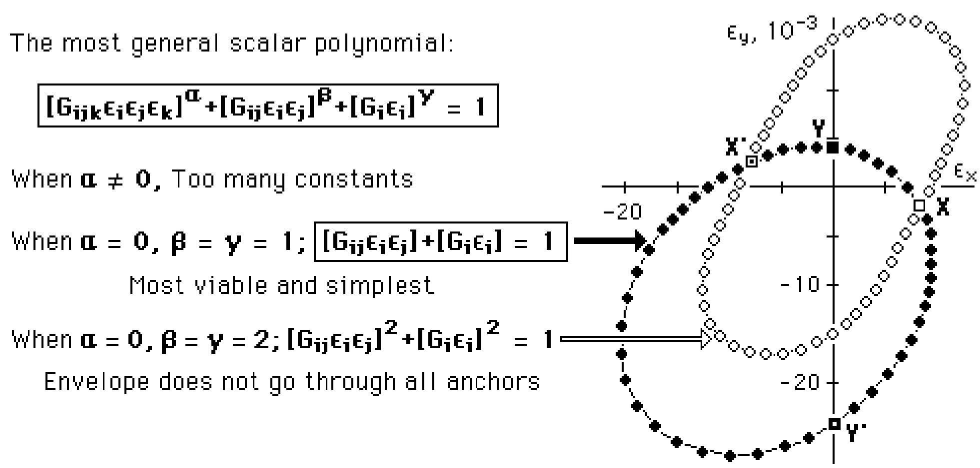

FIGURE 8.24 POSSIBLE EXTENSION OF THE QUADRATIC CRITERION

The present form of the quadratic criterion has the minimum number of strength parameters (five for a 2-dimensional formulation) and one failure mode interaction. Fewer than six parameters would be insufficient. Having more than six parameters would be difficult to apply analytically and experimentally. We believe that the present quadratic criterion has the best combination.

8.8 STRENGTH/STRESS RATIO AND FAILURE INDEX

The strength/stress ratio **R**, or strength ratio for short, is the ratio between the maximum, ultimate or allowable strength, and the applied stresses. We postulate that our material is linearly elastic, and that for each state of combined stresses there is a corresponding state of combined strains. Then the strength ratio remains the same in stress and strain spaces. We also assume proportional loading; i.e., all components of stress and strain increase by the same proportion.

Strength/stress ratio R:

$\sigma_i^{max} = R\sigma_i^{applied}$, or

$\epsilon_i^{max} = R\epsilon_i^{applied}$

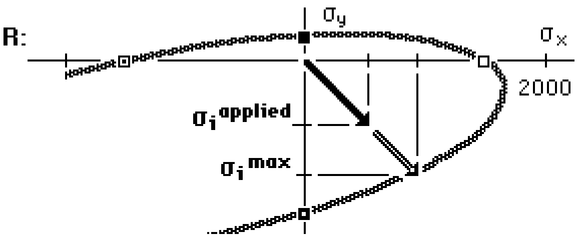

FIGURE 8.25 DEFINITION AND ILLUSTRATION OF STRENGTH RATIO AND PROPORTIONAL LOADING

Numerically **R** can have any positive value but only a value greater than or equal to unity has physical meaning. This ratio is a convenient scaling parameter in design.

- When **R** = 1, failure occurs.
- When **R** > 1, say **R** = 2, the safety factor is two; i.e., the applied stress can increase by a factor of two before failure occurs.
- When **R** < 1, say **R** = 0.5, the applied stress has exceeded the strength by a factor of two. This is not physically possible. The ratio is useful for design; e.g., we can reduce the load by one half, or double the number of plies for a new design.
- Note that when the applied stress or strain component is unity, the resulting strength ratio is the strength. This is an easy method for calculating strength.

Proportional loading means that the loading vectors in stress and strain space are kept in the same direction. Typically such vectors would radiate from the origin of stress or strain space, and extend like rays when the applied stress or strain increases. If initial or residual stresses are present, the applied vectors will radiate from a point different from the origin. In this case, modifications to the strength ratio calculation will have to be made. This subject will be covered in the next section.

The strength ratio can be derived for the quadratic criterion as follows. The value of the stress components in the equation below are that of the applied stress. For a given material, the **F**s are specified. For a given state of applied stresses, we only need to solve the quadratic equation in the strength ratio **R**. The correct answer is the positive square root in the quadratic formula.

Letting σ_i reach maximum values when $F_{ij}\sigma_i|_{max}\sigma_j|_{max} + F_i\sigma_i|_{max} = 1$,

we substitute $R\sigma_i|_{applied}$ for $\sigma_i|_{max}$: $\boxed{[F_{ij}\sigma_i\sigma_j]R^2 + [F_i\sigma_i]R - 1 = 0}$

Solving quadratic equation: $aR^2 + bR - 1 = 0$, $a = F_{ij}\sigma_i\sigma_j$, $b = F_i\sigma_i$

Positive quadratic root = strength ratio $R = -(b/2a) + [(b/2a)^2 + 1/a]^{1/2}$ (8.10)

The absolute value of the conjugate root from negative square root yields the strength ratio when the signs of all the applied stress components are reversed. This is useful for the bending of a symmetric plate because the resulting ply stresses change signs between the positive and negative distance from the mid-plane: designated superscript plus and minus, respectively; i.e.,

$$R^{+} = -(b/2a)+[(b/2a)^2+1/a]^{1/2}, \quad R^{-} = (b/2a)+[(b/2a)^2+1/a]^{1/2} \tag{8.11}$$

Since we assume that the strength ratio based on combined stresses is equal to that based on combined strains, we can determine the strength ratio using the failure criterion in strain space:

$$\boxed{[G_{ij}\epsilon_i\epsilon_j]R^2+[G_i\epsilon_i]R = 1}$$

$$aR^2+bR-1 = 0, \quad \text{where} \quad a = G_{ij}\epsilon_i\epsilon_j = F_{ij}\sigma_i\sigma_j, \quad b = G_i\epsilon_i = F_i\sigma_i$$

$$\text{Strength ratio: } R = -(b/2a)+[(b/2a)^2+1/a]^{1/2} \tag{8.12}$$

Failure index is used for failure analysis in many commercial finite element analysis programs (FEA). In the equation below, we compare the definitions of strength ratio **R**, FEA index **K**, and failure index **k**. While **R** and **k** are reciprocals and are equally valid, **K** is a bad index to use for composite materials.

$$\mathbf{R} = \text{strength ratio:} \quad \boxed{[G_{ij}\epsilon_i\epsilon_j]R^2+[G_i\epsilon_i]R = aR^2+bR = 1}$$

$$\mathbf{K} = \text{FEA index:} \quad G_{ij}\epsilon_i\epsilon_j+G_i\epsilon_i = K^2$$

$$\mathbf{k} = \text{failure index:} \quad \boxed{[G_{ij}\epsilon_i\epsilon_j]\left[\frac{1}{k}\right]^2+[G_i\epsilon_i]\left[\frac{1}{k}\right] = a\left[\frac{1}{k}\right]^2+b\left[\frac{1}{k}\right] = 1} \tag{8.13}$$

Failure occurs when the values of the ratio or indices are unity. All the envelopes are identical. Within the envelope, the material is safe. The value of **R** is higher than unity, and those of **K** and **k** less than unity. When tensile and compressive strengths are equal, all three approaches are equivalent. For composite materials, tensile and compressive strengths are different and the linear term (coefficient b) is not zero. Then the use of **K** is no longer associated with safety factor. In the figures below, we show the difference between the envelopes for **R**, **k** and **K** for values other than zero. Strength ratio and failure index are more useful than FEA index from the standpoint of safety. Having **R** and **1/k** equal to 3/2, we know immediately that the applied load can be raised one and one half times before failure occurs, or the laminate thickness can be reduced to 2/3 before failure occurs.

A FEA index of 2/3, on the other hand, says that the material is safe qualitatively. It is not related to safety in any quantitative way; i.e., we cannot say how much the applied load can be increased or the laminate thickness reduced before failure occurs. A value of **K** less than unity merely shrinks the elliptic envelope proportionally. The origin is not always enclosed in this envelope. In fact, **K** can be imaginary when the origin is outside the envelope.

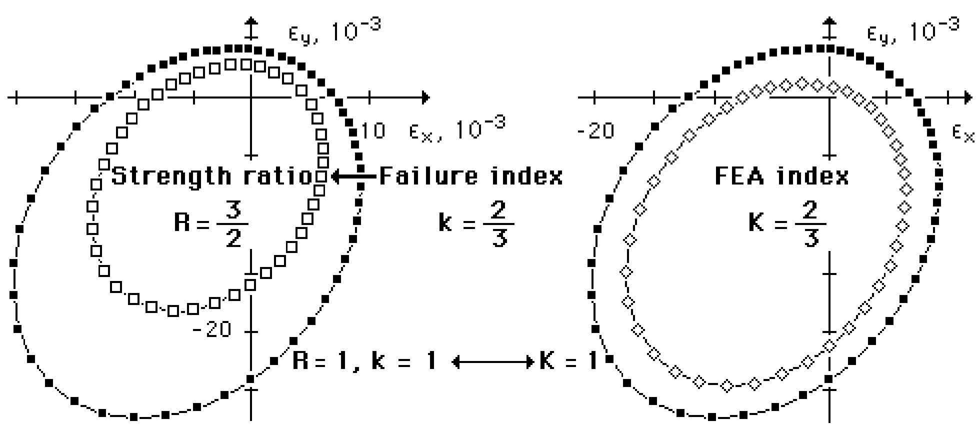

FIGURE 8.26 CONSTANT STRENGTH RATIO R VERSUS FEA INDEX K

Many commercial FEA codes provide options for failure criteria. A common choice is given between Tsai-Hill, Hoffman or Tsai-Wu/0.0, and Tsai-Wu/-0.5. In Tsai-Hill, tensile and compressive strengths are equal. Then **K** and **k** are equal, and **R** is simply the reciprocal. All envelopes are confocal. When linear scalar term exists as a result of different tensile and compressive strengths, Hoffman and Tsai-Wu will be appropriate. Then **K** is no longer is scaling parameter or related to safety. Failure analysis should be based on **k** or **R**, not **K**.

Finally, failure analysis of a symmetric plate under flexure is particularly easy to determine by using the strength ratio.

$$\text{Let } \boxed{\epsilon_i^{f\,max} = z^* k_i^{max} = R z^* k_i^{applied}}\text{, for safety: } R \geq 1$$
$$\boxed{[G_{ij}k_ik_j]\left[Rz^*\right]^2 + [G_ik_i]\left[Rz^*\right] = 1}\text{, or } a\left[Rz^*\right]^2 + b\left[Rz^*\right] - 1 = 0$$
$$R^+z^* = -b/2a + \sqrt{(b/2a)^2 + 1/a}\,; \quad R^-z^* = \left|-b/2a - \sqrt{(b/2a)^2 + 1/a}\right| \tag{8.14}$$

A normalized ply position of z* is defined, where z* = 1, z* = -1 or -1<z*<1. A hyperbolic relation exist between strength ratio and the ply position z*.

The controlling strength ratio is determined by the highest value of z* for each ply angle, which is the furthermost ply from the mid-plane. There are two strength ratios for each ply angle with positive or negative z*. The lower R of the two will be the controlling ratio.

We can similarly derive the safety prediction of a flexural loading situation using failure index, instead of strength ratio. This is done in the following:

$$\text{Let } \boxed{\epsilon_i^{f\,max} = z^* k_i^{max} = \frac{1}{k} z^* k_i^{applied}}\text{, for safety: } k \leq 1, \quad \boxed{k = 1/R}$$
$$\boxed{[G_{ij}k_ik_j]\left[\frac{z^*}{k}\right]^2 + [G_ik_i]\left[\frac{z^*}{k}\right] = 1}\text{, or } a\left[\frac{z^*}{k}\right]^2 + b\left[\frac{z^*}{k}\right] - 1 = 0$$
$$\frac{z^*}{k^+} = -b/2a + \sqrt{(b/2a)^2 + 1/a}\,; \quad \frac{z^*}{k^-} = \left|-b/2a - \sqrt{(b/2a)^2 + 1/a}\right| \tag{8.15}$$

From the following figure, we show the hyperbolic relation between strength ratio and ply position for a homogeneous laminate. The outermost ply from the mid-plane has the lowest and controlling strength ratio. For multidirectional laminates, each ply angle is piecewise hyperbolic. Unlike strain variation across the thickness, strength ratio is not linear. To be safe, the strength analysis of a laminate under flexure should be based on the outer and inner surfaces of a ply or ply group, not the mid point. Some commercial finite element analysis programs, however, use the mid point, which is not as accurate as using the actual outer surfaces.

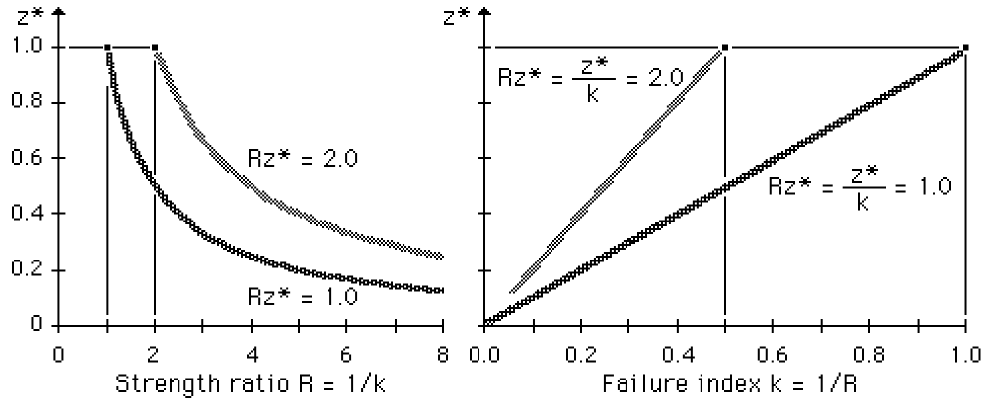

FIGURE 8.27 THE HYPERBOLIC RELATION BETWEEN POSITION IN A LAMINATE FROM THE MID-PLANE AND STRENGTH RATIO, THE PREFERRED LINEAR RELATION BETWEEN THE POSITION AND FAILURE INDEX.

On the right of the same figure we plot the failure index as a function of thickness. This index is linear, which is more convenient to use than the hyperbolic relation of strength ratio. For multidirectional laminates, the failure index will be piece-wise linear. An example of this will be shown in the next section.

8.9 EXPERIMENTAL DATA

Obtaining experimental data to substantiate any failure criterion is a daunting task. First, a multiaxial testing machine is required. Loading frames and independently controlled actuators are difficult to finance, design, and be built and maintained. Only a handful of reliable installations exist in the world. Specimen design and instrumentation are equally challenging.

In a special issue of Fiber Science and Technology, some test data were furnished and compared with various failure criteria. For anisotropic plies, the following data were compared with the Tsai-Wu criterion. This is shown in the figure below.

FIGURE 8.28 TEST DATA OF UNIPLY IN COMBINED STRESS PLANE

If the data are to be believed, quadratic relations in the transverse stress-shear stress plane are more accurate than maximum stress, maximum strain, and Dassault criteria. Data in other combined stresses states are not available for this particular study. Data on laminates from the same source will be cited in the next section.

8.10 CONCLUSIONS

We would like to emphasize again the utility and limitations of failure criteria. We need the criteria to guide design and materials improvement. We can calculate the safety factor and determine the weakness in our strength characteristics so that direction of improvement in materials can be made.

Failure criteria are empirical and phenomenological. Failure modes of composites are more complicated than can be described by simple criteria. We must also recognize the interaction of these modes. The quadratic criterion is more powerful than the non-interactive criteria for its ease of application, mathematical simplicity, invariance, and internal consistency. We therefore recommend the quadratic criterion as the most versatile and easiest to use.

8.11 PROBLEMS

Prob. 8.1 The maximum strain criterion is formed by drawing a box around the four measured strengths: X, X' Y and Y'. Interactions among failure modes are ignored. Can we rationalize the Tresca interaction, drawn on the left of the figure below? Why is it not admissible to have a concave inward failure envelope, shown on the right?

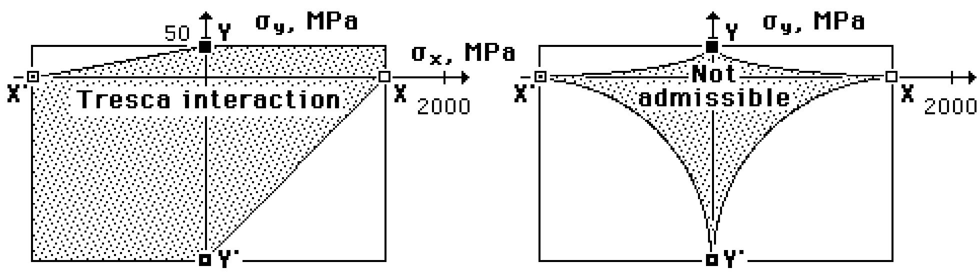

FIGURE 8.29 TRESCA INTERACTIONS AND CONCAVE ENVELOPES USING T300/5208 DATA

Prob. 8.2 How can the quadratic failure criterion be extended from 2- to 3-dimension. How many strength parameters would there be, from six for 2-dimension to what in 3-dimension?

Prob. 8.3 The quadratic failure criterion is limited to the strength of a ply within a laminate. It is an intralaminar failure criterion. How would you extend the quadratic criterion to a interlaminar criterion? The criterion can be based on the three out-of-plane components. How many strength parameters will there be? Can they be reduced by one if we use the quadratic invariant formed by the two out-of-plane shear components?

Prob. 8.4 In the quadratic criterion, each combined state of stress and the corresponding state of strain has a unique strength ratio. It can be applied in any reference axes, on or off the symmetry axes. The maximum stress or strain criterion can only be applied to the material axes. More importantly, strength ratio R is a scalar quantity, and is related to safety factor. It has a numeric value that remains the same for all coordinate systems. How can a similar measurement be defined for the maximum stress or strain criterion?

Prob. 8.5 If the [0] envelope in strain space is shown in the figure below, how would one derive graphically (not numerically) the envelopes for [90], [45] and [-45] in the same three views?

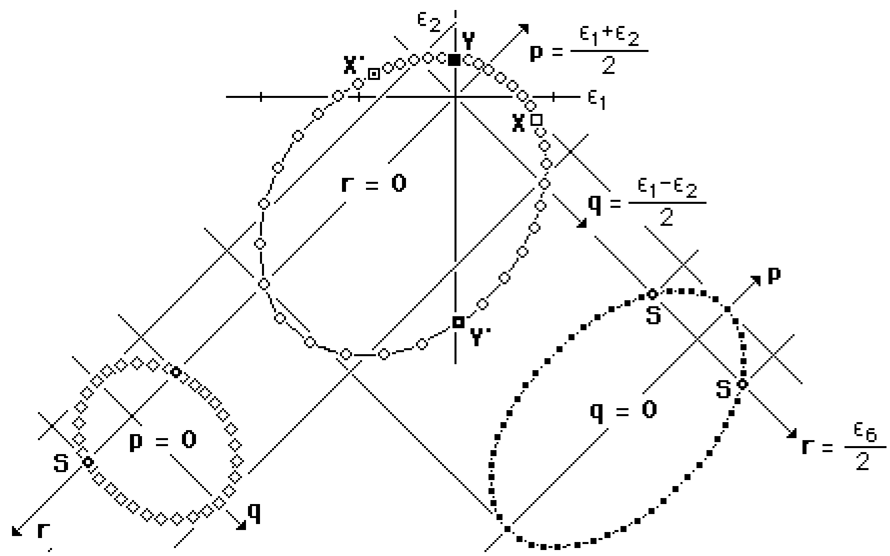

FIGURE 8.30 THREE VIEWS OF THE FAILURE ENVELOPE OF [0] T300/5208, WHERE THE LINEAR COMBINATIONS OF THE STRAINS COMPONENTS ARE DEFINED IN TABLE 2.15 ON PAGE 2-19

Prob. 8.6 When tensile and compressive strengths are different, as is the case for most composite materials, the envelope for constant R and k are different from that for constant K The difference is shown in the following figures. The values for R and 1/k are linearly related to the safety factor; the K value, however, is not. The former is expands like rays radiating from the origin; the latter forms confocal ellipses with reducing size.

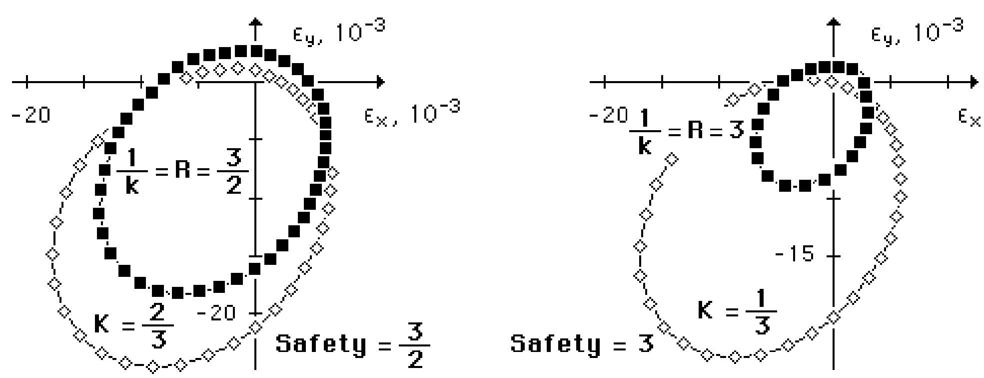

FIGURE 8.31 COMPARISON BETWEEN STRENGTH RATIO R, FAILURE INDEX k AND FEA INDEX K

Explain why constant FEA index envelope is the same as constant shear strength in the quadratic envelope, shown below.

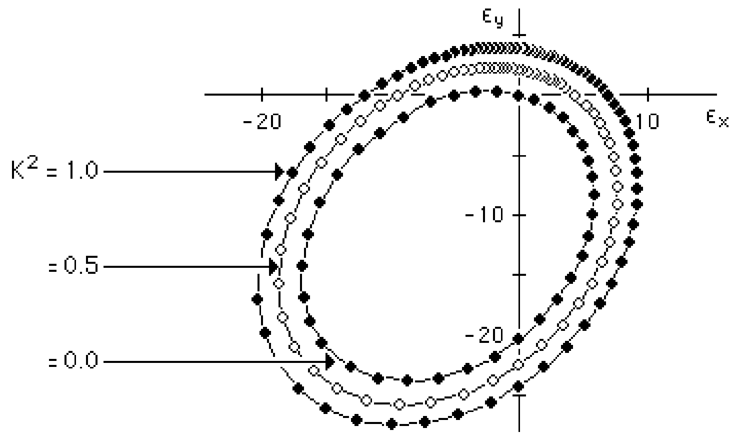

FIGURE 8.31 LOCI OF CONSTANT FEA INDEX IN STRAIN SPACE FOR T300/5208

Section 9

STRENGTHS OF LAMINATES

Strength of a laminate is often defined by the first ply failure (FPF), which is simply the inner envelope of all plies. When external loading reaches the FPF, micro cracking or fiber failure can begin. To claim additional load-carrying capability of the laminate, plies that have reached the FPF must be degraded by an iterative procedure until the ultimate strength of the laminate is reached. A ply-by-ply progressive failure scenario can be modeled. Rules are defined to assess the extent and sequence of degradation processes. A simple model based on simultaneous failure gives good results as compared with those from the progressive model when the state of stress is homogeneous. For non-homogeneous stress, however, a progressive degradation is recommended.

Other features of this section include the effect of hygrothermal expansions resulting from multidirectional lamination which can be calculated using classical linear thermoelastic theory. In many practical materials, curing stresses can be relieved by moisture absorption. Also included in this section is the recommendation of the use of failure index instead of the strength ratio, when the flexural strength of a laminate is in question.

9.1 FIRST PLY FAILURE ENVELOPES

The strength of a laminate is a function of the applied load, and the ply materials and layups in the laminate. As we have explained in the previous section, failure envelopes in strain space are invariant; i.e., their shapes remain the same independent of the presence of other plies. Thus, the failure envelope for a [0/90] laminate is formed simply by superimposing [0] and [90] plies. The inner envelope is the first-ply-failure (FPF). In principle, we can load, unload, and reload a laminate and experience no damage as long as we do not go beyond the FPF envelope. The FPF describes the maximum capability of the intact plies.

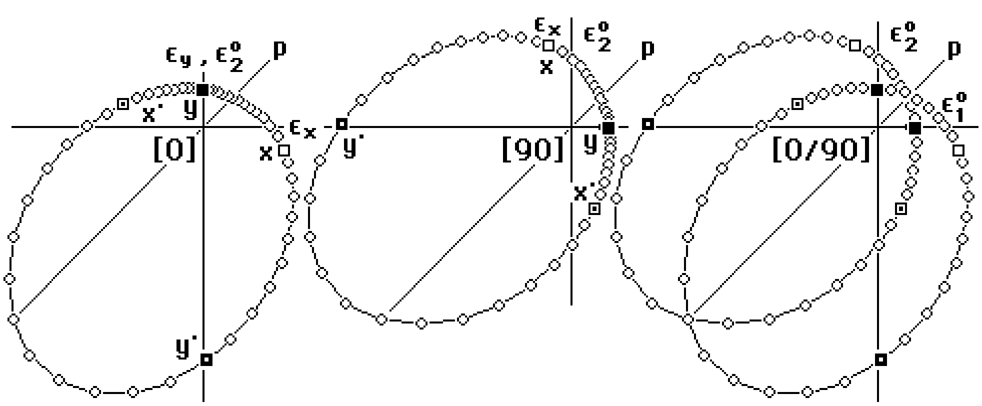

FIGURE 9.1 QUADRATIC FAILURE ENVELOPES OF [0], [90], AND [0/90] IN STRAIN SPACE

In Figure 9.1, a [90] ply can be generated from a [0] ply by a rotation about the p-axis, the bisector in the 1st and 3rd quadrants. This invariant **p** was defined in Table 2.15 on p. 2-19. The cross-ply laminate is simply generated by sliding one ply over the other. The material is T300/5208.

We show in the following figure the FPF of [π/4] laminates for T300/5208 and E-glass/epoxy composite materials. In these laminates, the initial failure in the normal strain plane is controlled by the [0] and [90] plies. The [45] and [-45] plies do not control the FPF in this plane. The [45] and [-45] plies, however, can control the FPF envelope when shear is present.

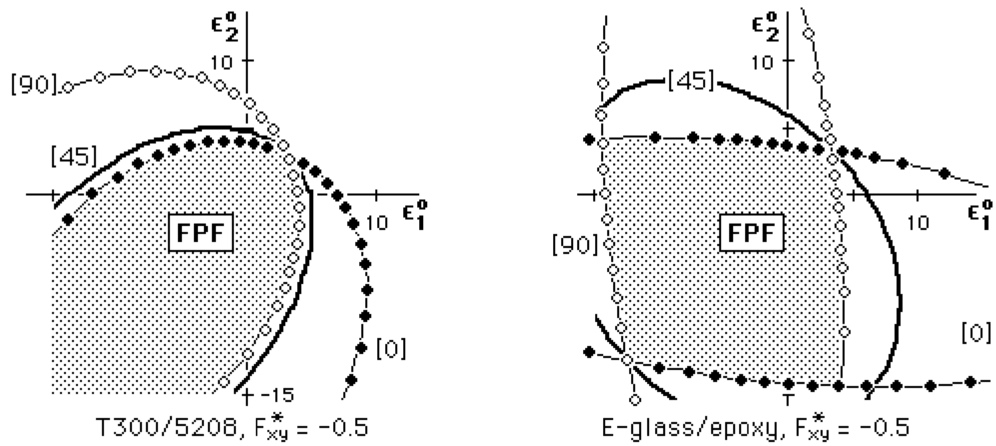

FIGURE 9.2 THE FIRST PLY FAILURE ENVELOPES FOR TWO COMMON COMPOSITES

STRESS-SPACE FAILURE ENVELOPES

As we have seen, the strain space representation of the FPF is simple to generate from individual plies. Stress space representation of the same laminate, on the other hand, cannot be generated by superimposing individual envelopes of plies. Failure envelope in stress space is controlled by [H] and {H}, vector products of the strength parameters [G] and {G}, and the laminate compliance, shown in the following equation. As the laminate layup changes, its compliance will change; so will the resulting failure envelope.

In-plane stress-strain relation: $\boldsymbol{\epsilon_i^o = a_{ij}^*\sigma_j^o}$

Quadratic failure criterion in strain space: $\boldsymbol{G_{ij}\epsilon_i^o\epsilon_j^o + G_i\epsilon_i^o = 1}$

Combining the above: $\boldsymbol{H_{ij}\sigma_i^o\sigma_j^o + H_i\sigma_i^o = 1}$, where $H_{ij} = G_{kl}a_{ki}^*a_{lj}^*$, $H_i = G_j a_{ji}^*$ (9.1)

The strain- and stress-space formulations are compared in the flow diagrams below. The strain space formulation is independent of the ply layup and, therefore, has one less step in strength analysis than the stress formulation. Implicit in the analysis is the linearity of the composite materials up the ultimate strength. For each state of stress there is a unique state of strain. Thus the formulations are completely interchangeable for the FPF envelope. For laminates with micro cracks, stress and strain envelopes will in general be different.

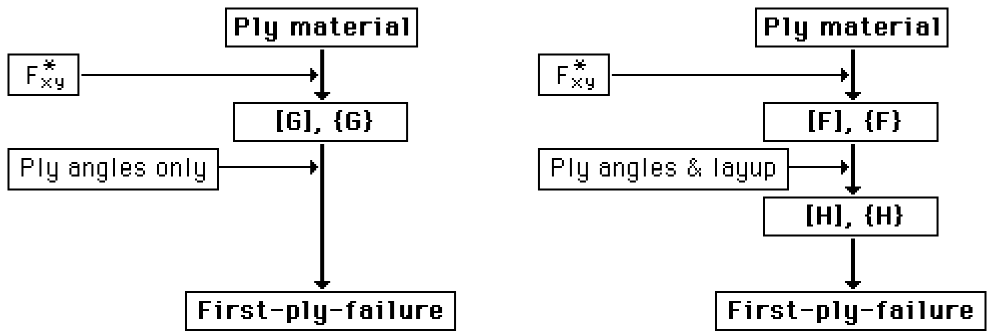

FIGURE 9.3 THE FPF FORMULATIONS IN STRAIN- AND STRESS-SPACE

$$
\left.
\begin{aligned}
&H_{11}^{(0)} = G_{xx}a_{11}^{*2}+2G_{xy}a_{11}^{*}a_{12}^{*}+G_{yy}a_{12}^{*2}, \quad H_{22}^{(0)} = G_{xx}a_{12}^{*2}+2G_{xy}a_{12}^{*}a_{22}^{*}+G_{yy}a_{22}^{*2} \\
&H_{12}^{(0)} = G_{xx}a_{11}^{*}a_{12}^{*}+2G_{xy}(a_{11}^{*}a_{22}^{*}+a_{12}^{*2})+G_{yy}a_{12}^{*}a_{22}^{*}, \quad H_{66}^{(0)} = G_{ss}a_{66}^{*2} \\
&H_{1}^{(0)} = G_{x}a_{11}^{*}+G_{y}a_{12}^{*}, \quad H_{2}^{(0)} = G_{x}a_{12}^{*}+G_{y}a_{22}^{*}
\end{aligned}
\right| \qquad (9.2)
$$

The laminate strength parameters [H] and {H} for the [0] ply in a [0/90] cross-ply laminate are shown in the equation above. For the [90] ply in the same cross-ply laminate, indices 1 and 2 are interchanged. As the layup changes, the compliance changes resulting in a shape changes of the laminate envelope.

In Figure 9.4, we show in stress space the FPF envelopes for two T300/5208 cross-ply laminated composites. As the layup changes, the shape changes as well. The envelopes in Figures 9.2, however, do not change with layup because they are represented in strain space.

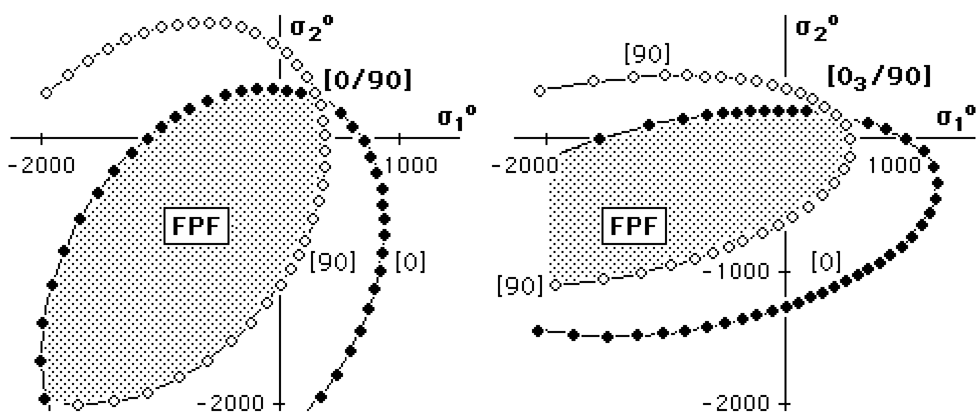

FIGURE 9.4 THE FPF ENVELOPES IN STRESS SPACE OF TWO CROSS-PLY LAMINATES

In Figure 9.5, we show in stress space two FPF envelopes for E-glass/epoxy cross-ply laminated composites. As the layup changes, the shape also changes.

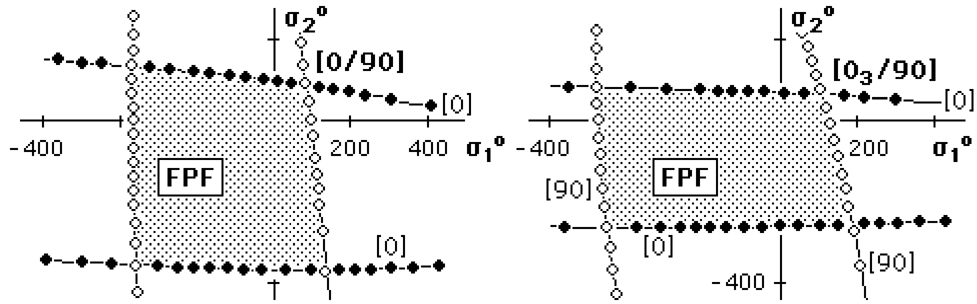

FIGURE 9.5 THE FPF IN STRESS SPACE OF TWO CROSS-PLY LAMINATES OF E-GLASS/EPOXY

9.2 PLY-BY-PLY STRESS, AND FPF STRENGTH ANALYSIS

Laminated plate theory provides a basis for a ply-by-ply stress analysis. The method was applied earlier in this book; e.g., in Sections 4 and 5, In-Plane and Flexural Stiffness, respectively. Ply-by-ply strength analysis is simply the application of a failure criterion to the state of combined stresses or strains to determine whether failure is about to or has already occurred in each ply.

Applied load, MN/m	N_1	**1.00**	Laminate layup		θ_1	θ_2	θ_3
	N_2	**-1.00**	**$[0_2/45/-45]_{9S}$**	[θ]	**0**	**45**	**-45**
	N_6	**2.00**		[#/grp]	**2.0**	**1.0**	**1.0**
Laminate stress, MPa	σ_1^o	110	Laminate-axis ply stress, MPa	σ_1	309.	262.	-440.
	σ_2^o	-110		σ_2	-41.	172.	-530.
	σ_6^o	220		σ_6	59.	265.	497.
Laminate strain, 10^{-3}	ϵ_1^o	1.77	Ply-axis ply stress, MPa	σ_x	309.	482.	-982.
	ϵ_2^o	-4.48		σ_y	-41.	-48.	13.
	ϵ_6^o	8.18		σ_s	59.	-45.	45.
				R	1.47	1.70	1.00

FIGURE 9.6 PLY-BY-PLY STRESS ANALYSIS AND STRENGTH RATIOS

The laminate in the last figure is 72 plies thick, and the load applied is {1,-1,2} MN/m. The FPF stress is reached at this applied load. Note in the last row in the figure above that the strength ratio **R** is unity for the [-45]. The others plies have 1.47 for [0], and 1.70 for [45]. These numbers are scalars and represent factors of safety. If the load is reduced by one half, the corresponding strength ratios will double. If the number of layers is doubled, by having 18 repeated sub-laminates, the strength ratios will also double. The linear relations of load, laminate thickness, and strength ratio make design easy.

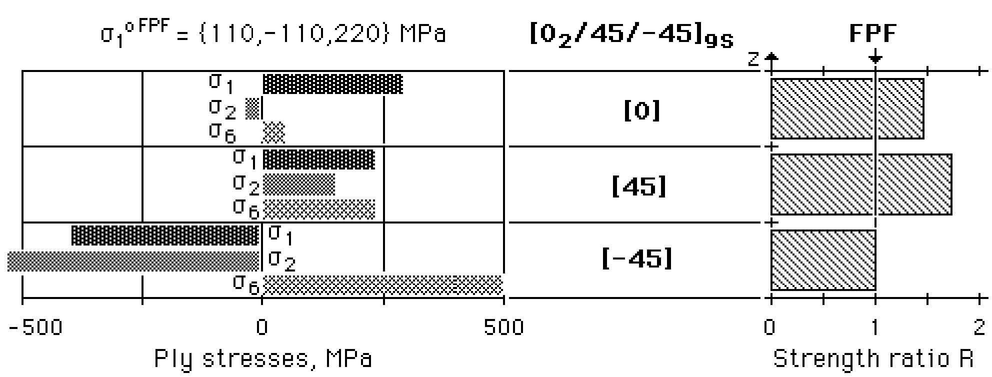

FIGURE 9.7 PLY-BY-PLY STRESS ANALYSIS AND CORRESPONDING STRENGTH RATIOS

Ply stresses, shown on the left of the figure above, have three components for each set, and are dependent upon coordinate axes. It is hopeless to try to make a judgment on the state of stress, good or bad, or larger or smaller than a reference value. The significance of strain components are similarly elusive. That is why we resort to invariants and scalars, the value of which can be judged larger or smaller than another number. Our quadratic failure criteria, in Equation 8.1 on page 8-3, are scalar products, and are easier to use than the values of stress or strain components.

When a symmetric laminate is subjected to bending, laminated plate theory assumes that the strain is linear across the thickness, and the ply stress distribution is piece-wise linear. The strength ratio, as discussed in the last section, is a hyperbolic function of the z-axis, which is the ply position. Since ply angles vary in a laminate, the hyperbolic functions will be piece-wise hyperbolic. This is shown in the figure below, where a cross-ply laminate is subjected to a single bending moment. The flexural strength at the FPF is 785 MPa, which corresponds to a strength ratio of unity. The controlling ply is located at the top surface of the outer [90] ply. This strength ratio is lower than that at the outer surface of the [0] ply, which is equal to 1.24.

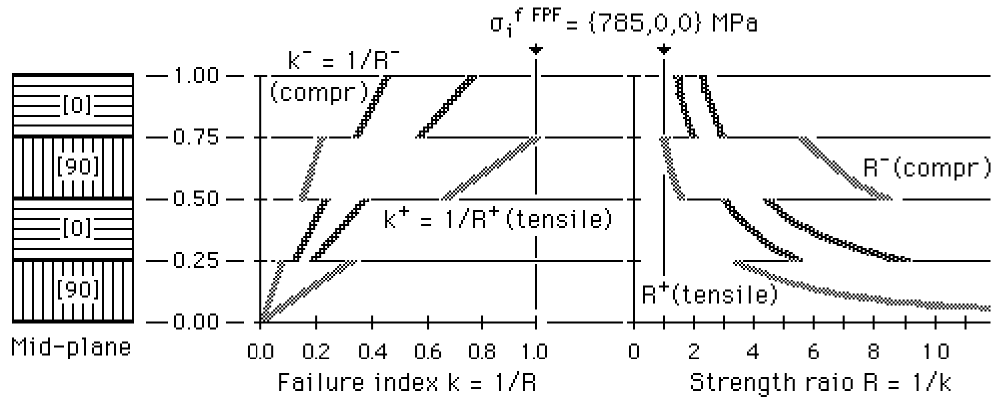

FIGURE 9.8 PIECE-WISE LINEAR AND HYPERBOLIC DISTRIBUTIONS OF FAILURE INDEX AND STRENGTH RATIOS TOWARD THE FPF VALUE OF UNITY

As we presented in Figure 8.26 on page 8-20, failure index is linear when a laminate is subjected to bending. We also show this distribution in the figure above. The FPF condition is reached at the top of the [90] ply. Throughout the thickness of this ply, or any other [90] in the laminate, we only need to draw a straight line from the origin. The compressive stress of the [90] ply, located opposite the middle plane, will have a different failure index. However, it remains linear. The same linear relations apply to [0] ply in tension and compression.

We have covered only the first ply failure of laminates subjected to combined in-plane, and simple bending loadings. The FPF loads do not necessarily mean the ultimate load. Plies that have not failed at the FPF may continue to carry load beyond FPF. This post-FPF behavior will be discussed in the sub-section 9.5 on page 9-8.

9.3 UNIAXIAL STRENGTHS OF ANGLE-PLY LAMINATES

Angle-plies are laminates with [±**ø**]. When they are subjected to normal stresses (without shear), they are unique because plus and minus oriented plies will fail simultaneously. Thus the first ply failure is also the last-ply-failure. Suffice to say that unidirectional plies by themselves will also fail completely. Therefore the first and last failures are the same. For this reason, we can discuss these special laminate failures before considering the post-FPF behavior.

We will show in the next two figures the uniaxial tensile and compressive strengths of angle-ply laminates with the lamination angle varying from 0 to 90. As a comparison, we repeat the off-axis unidirectional ply with the same variation of ply angle from 0 to 90. The ply material for the first figure is T300/5208, and the second is E-glass/epoxy.

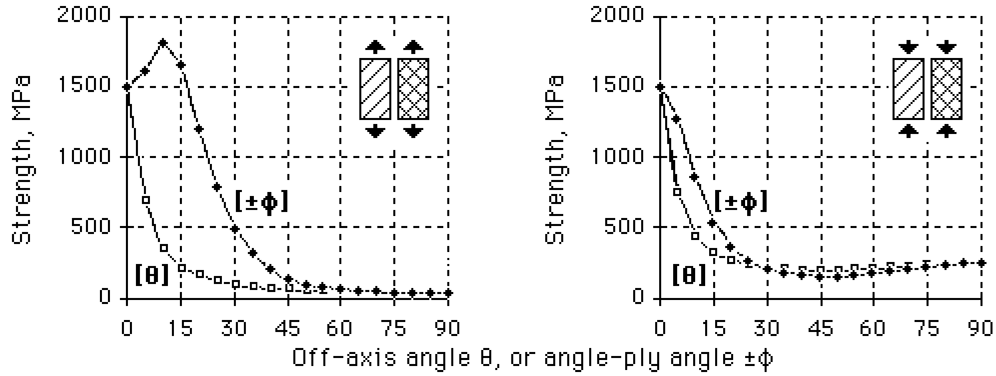

FIGURE 9.9 UNIAXIAL TENSILE AND COMPRESSIVE STRENGTHS OF ANGLE-PLY LAMINATES AND OFF-AXIS UNIDIRECTIONAL PLY OF T300/5208

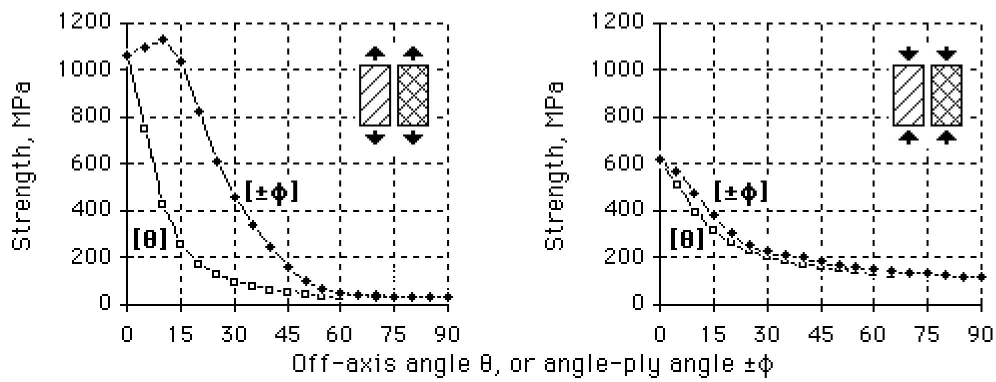

FIGURE 9.10 UNIAXIAL TENSILE AND COMPRESSIVE STRENGTHS OF ANGLE-PLY LAMINATES AND OFF-AXIS UNIDIRECTIONAL PLY OF E-GLASS/EPOXY

Both composite materials exhibit the same behavior qualitatively. There is a significant difference between the uniaxial tensile strength of the angle-ply laminate and the off-axis unidirectional ply. The difference between the compressive strengths, on the other hand, is almost negligible.

In Figure 4.18 on page 4-13, we showed the use of off-axis plies and angle-ply laminates to back-calculate the longitudinal shear modulus of the basic ply. Using the same specimens, we can back-calculate the shear strength from the uniaxial strengths following the relations shown in the last two figures.

9.4 HYGROTHERMAL STRESSES

When multidirectional laminates are cured and cooled to room temperature, residual stresses will exist because thermal contraction of each ply is anisotropic. When moisture is subsequently absorbed, hygro expansion is also anisotropic. It reduces thermal stresses, an analogous stress relief. In this section we wish to develop the effect on the quadratic failure criterion when hygrothermal stresses are included.

We will now define strength ratios for our failure criterion as we have done in the previous section. We prefer to use strain space over stress space. We can have strength ratios defined by the total strain, or split the total strain into two parts: one mechanical, and the other residual. The definitions of strength ratios are shown below:

$$\left.\begin{aligned} \epsilon_i^{max} &= R^{total}(\epsilon_i)^{total} = R^{total}(\epsilon_i^m+\epsilon_i^r) = R^{total}(\epsilon_i^m+\epsilon_i^n-e_i) \\ \epsilon_i^{max} &= R^m\epsilon_i^m+R^r\epsilon_i^r = R^m\epsilon_i^m+R^r(\epsilon_i^n-e_i) \end{aligned}\right] \quad (9.3)$$

We prefer splitting strength ratios into mechanical and residual parts on the basis that each part of the strain can act independently. Residual strains are functions of the cure temperature, and moisture content. For a given hygrothermal combination, the strains are fixed. When we apply mechanical loads to the laminate, we want to know the maximum load that the laminate can sustain. The mechanical part of the strength ratio gives that information. We therefore prefer having two strength ratios.

By substituting strength ratios and strains into the failure criterion in strain space, we have:

$$G_{ij}(R^m\epsilon_i{}^m+R^r\epsilon_i{}^r)(R^m\epsilon_j{}^m+R^r\epsilon_j{}^r)+G_i(R^m\epsilon_i{}^m+R^r\epsilon_i{}^r)-1 = 0 \tag{9.4}$$

If we are interested in the mechanical strength ratio, we can solve for it by letting the residual strength ratio equal unity. The results of the quadratic equation are shown below:

$$a(R^m)^2+bR^m+c = 0,\ \ R^m = [(b/2a)^2-c/a]^{1/2}-(b/2a)$$

$$\text{where}\ \ a = a^m,\ \ b = b^{sum} = b^m+b^{mix},\ \ c = -1+a^r+b^r \tag{9.5}$$

The coefficients of the quadratic equation are defined as follows:

$$a^m = G_{xx}(\epsilon_x{}^m)^2+2G_{xy}\epsilon_x{}^m\epsilon_y{}^m+G_{yy}(\epsilon_y{}^m)^2+G_{ss}(\epsilon_s{}^m)^2$$

$$a^r = G_{xx}(\epsilon_x{}^r)^2+2G_{xy}\epsilon_x{}^r\epsilon_y{}^r+G_{yy}(\epsilon_y{}^r)^2+G_{ss}(\epsilon_s{}^r)^2$$

$$b^m = G_x\epsilon_x{}^m+G_y\epsilon_y{}^m+G_s\epsilon_s{}^m,\ \ b^r = G_x\epsilon_x{}^r+G_y\epsilon_y{}^r+G_s\epsilon_s{}^r$$

$$b^{mix} = 2\left[G_{xx}\epsilon_x{}^m\epsilon_x{}^r+G_{xy}\epsilon_x{}^m\epsilon_y{}^r+G_{xy}\epsilon_y{}^m\epsilon_x{}^r+G_{yy}\epsilon_y{}^m\epsilon_y{}^r+G_{ss}\epsilon_s{}^m\epsilon_s{}^r\right] \tag{9.6}$$

If we are interested in the residual strength ratio, we can solve for it as follows. The answer gives the maximum combination of temperature difference and moisture content that causes first ply failure in the laminate, with or without mechanical loads.

$$a(R^r)^2+bR^r+c = 0,\ \ R^r = [(b/2a)^2-c/a]^{1/2}-(b/2a)$$

$$\text{where}\ \ a = a^r,\ \ b = b^{sum} = b^r+b^{mix},\ \ c = -1+a^m+b^m \tag{9.7}$$

In this formulation we assume that temperature and moisture change proportionally. If we wish to find the self-destruct temperature or moisture content, we must fix either the moisture content or temperature difference.

In the next two figures, laminates under three hygrothermal combinations are compared:

- First, we assume that there are no residual stresses which corresponds to a room temperature cure and the composite does not absorb moisture.
- The second case is for a newly cured laminate which has only the temperature difference between room temperature and the cure temperature. Moisture content is zero because there is no time to absorb moisture.
- The third case is called long term: it has both temperature difference and saturation level of moisture of 0.005 or 0.5 percent.

Figure 9.11 shows the uniaxial tensile strength of [π/4] laminate for three hygrothermal combinations. The first-ply-failure for each combination is highlighted. The newly cured case, shown in the middle, has a low FPF due to the curing stresses. As moisture is absorbed, which is very common among organic matrices, a stress relief takes place. At 0.5 percent moisture content, the FPF strength is nearly equal to the case where hygrothermal stresses are ignored. The offsetting temperature and moisture effects provide designers a short cut. If a composite is to be used in space where humidity is zero, we have to accept a low FPF resulting from the temperature difference.

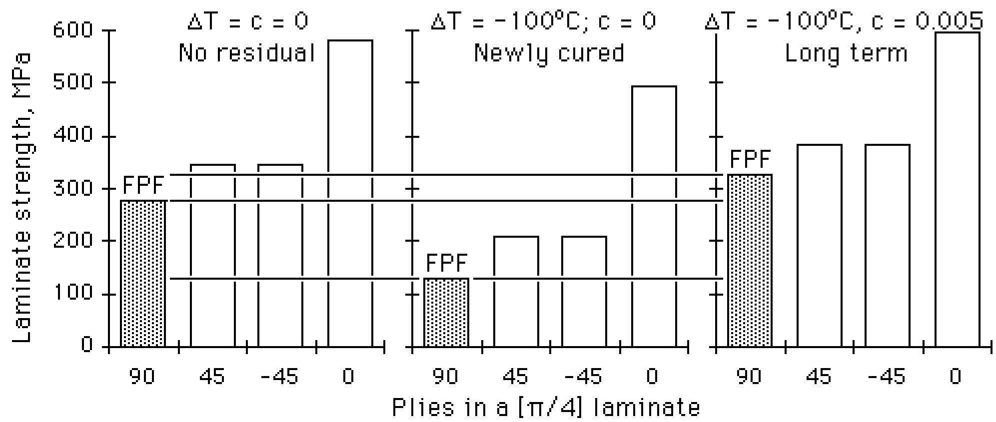

FIGURE 9.11 TENSILE STRENGTH BASED ON FPF FOR VARIOUS CONDITIONS

The figure below shows the same case except uniaxial compressive strength is also shown. The same comments can be made about the importance of residual stresses. The ply that controls the FPF strength is [0] for this laminate.

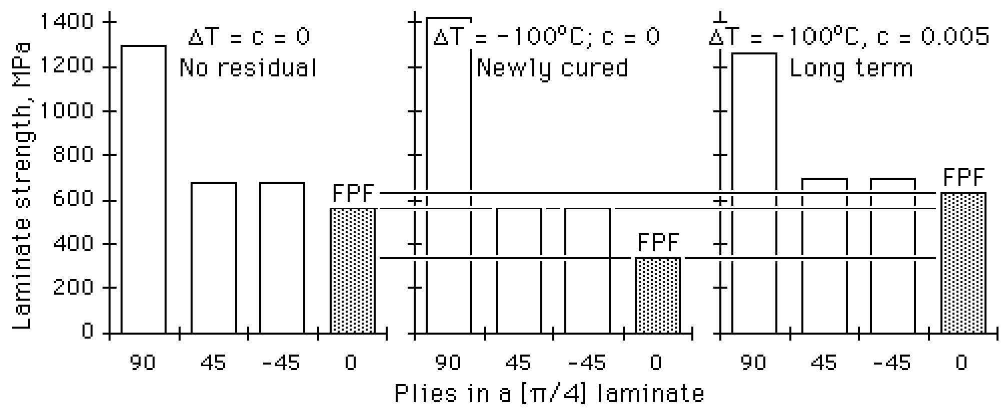

FIGURE 9.12 COMPRESSIVE STRENGTH BASED ON FPF FOR VARIOUS HYGROTHERMAL CONDITIONS

Hygrothermal stresses exist in composite materials, and should be factored in design. The linear theory, presented here, is easy to implement. As composite materials are subjected to higher and lower temperatures than before, hygrothermal stresses can no longer be ignored.

9.5 STRENGTH AFTER FIRST PLY FAILURE

We have seen earlier in this section the FPF envelope formed by the innermost segment of plies in a laminate. Can the laminate carry additional load beyond the FPF? In the figure below, we show two possible envelopes derived from a cross-ply laminate [0/90] made of T300-5208 composite materials. The inner envelope is the FPF, shown on the left. Is the last ply failure (LPF, shown on the right) simply the outermost envelope of the original intact plies? Once the FPF is reached, we assume that one or more plies become degraded by the formation of micro cracks, or by catastrophic fiber break or buckling. Thus, the determination of the LPF requires analysis of progressively degraded plies. It will not be an extension of the intact plies.

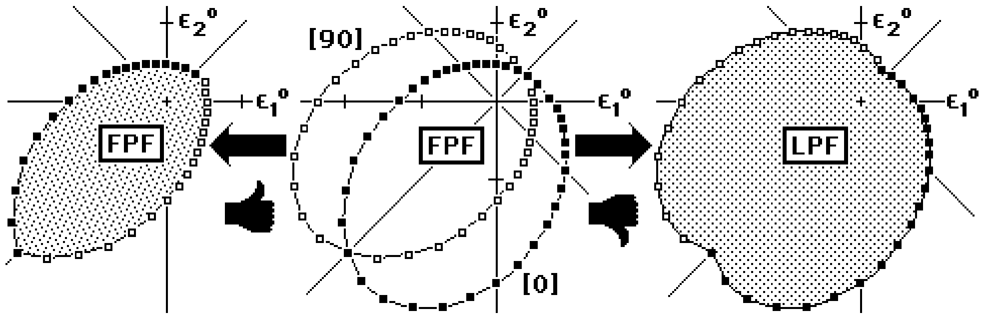

FIGURE 9.13 POSSIBLE FAILURE ENVELOPES OF A [0/90] OF T300/5208

In Section 7, Micromechanics, we showed a method of calculating the reduced ply transverse and shear moduli due the presence of micro cracks; the results are shown in Table 7.5 on page 7-11. We also showed the dependence of longitudinal compressive strength on longitudinal shear modulus, shown in Figure 7.17 on page 7-15. Using the stiffness and strength of plies degraded by micro cracks, or fiber failure, we can now determine the nature of the post-FPF strength.

In the next figure, we show the micro cracks in a cross-ply laminate of graphite/epoxy composite materials. The stacking sequence is $[0/90]_{2S}$. Note the aspect ratio cited in Figure 7.9 remains the same for the one- and two-ply [90].

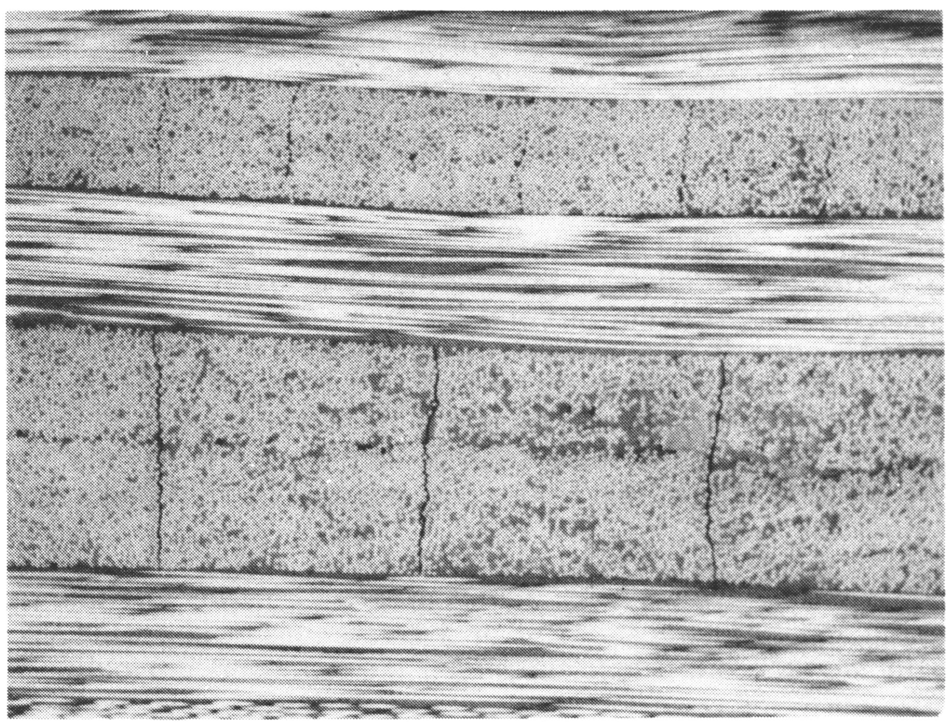

FIGURE 9.14 PHOTOMICROGRAPHS OF MICRO CRACKS IN A CROSS-PLY LAMINATE SUBJECTED TO A UNIAXIAL TENSILE LOAD

PROGRESSIVE FAILURES

The first ply failure of a laminate is easily determined by superposition. Materials within the FPF are intact, linear, and independent of load history. The FPF in stress space is precisely the same as in strain space. Laminate behavior beyond the FPF is based on degraded plies. Laminates are no longer linear, and their behavior is load dependent.

A progressive failure model based on a ply-by-ply strength analysis will be used for the prediction of the post-FPF strength. A flow diagram for the traditional criterion and its extension to include degradation is shown below. The ultimate strength is reached after all plies are degraded progressively.

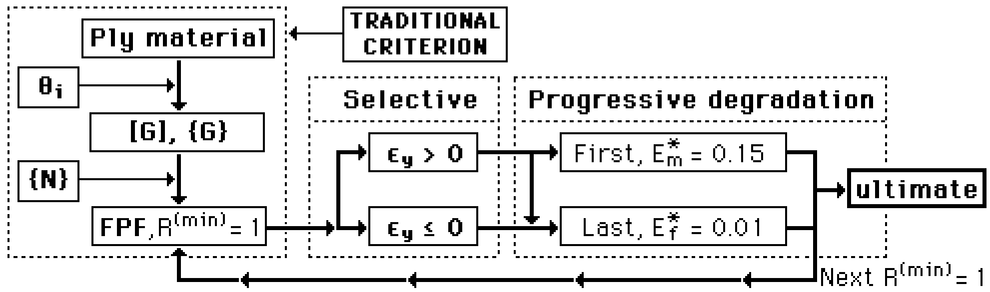

FIGURE 9.15 FLOW DIAGRAM FOR FPF, SELECTIVE AND PROGRESSIVE PLY-BY-PLY DEGRADATION

The traditional application of failure criteria does not allow matrix and fiber degradations. When plies are loaded beyond the FPF, they will have reduced stiffnesses to reflect the presence of micro cracks and fiber failure. In the figure above, two modes of degradation are possible, to be selected by the transverse ply strain:

1) If the transverse ply strain is positive, plies can degrade twice: first, by micro cracks where matrix stiffness is reduced but fiber stiffness is retained; secondly, by fiber failure where all ply moduli are reduced to near zero.

2) If the transverse ply strain is zero or negative, plies can degrade only once. Since matrix degradation is not permitted, the only mode is fiber failure.

Progressive degradation begins with the ply that reaches a unity strength ratio first. This ply will be tested for the mode of degradation depending on the on-axis ply strain. When the correct degradation is applied to the ply, the laminate is analyzed again to find the next ply failure. The latter ply will be degraded. The process continues until all plies have failed.

In Table 9.1 below, the stiffness and strength of intact and degraded plies are shown. For plies having matrix degradation, a factor of 0.15 is used. Using the formulas of micromechanics, we determine the loss of transverse and shear moduli, as we have done in Figure 7.11 on page 7-10. In addition, we reduce the Poisson's ratio and the interaction term in the failure criterion by the same 0.15 factor. The exponent **n** used in the loss of longitudinal compressive strength is 0.1, as in Equation 7.17 on page 7-15. All other ply strengths remain intact. The degraded ply is modeled by the loss of stiffness without loss of strength, as shown in Figure 7.10 on page 7-9. The failure strain is greatly increased.

For fiber degradation, we apply a factor of 0.01 to both the matrix and fiber moduli, as well as Poisson's ratio and the interaction term. In this degradation, strengths are also retained while stiffnesses are reduced. The failure strains are increased 100 fold.

Degradation of plies that have partially or completely failed is a critical component in our attempt to predict the stiffness and strength beyond the FPF. As plies fail progressively, strain energy of all plies must be redistributed. In homogeneous stress, the intact plies absorb the energy from the degraded plies. In non-homogeneous stress, the redistribution takes place not only among adjacent plies but also among neighboring regions and elements. The degradation process will depend on the boundary conditions.

TABLE 9.1 COMPARISON BETWEEN INTACT AND DEGRADED PLY DATA FOR T300/5208

	Intact	Matrix degradation			Fiber degradation		
	Baseline	Modified	Mod/B		Modified	Mod/B	
Efx	259	259	1.000		2.590	0.010	← E_f^*
Em	3.40	0.51	0.150	← E_m^*	0.034	0.010	← E_f^*
Ex	181.00	181.000	1.000		1.810	0.010	← E_f^*
Ey	10.30	2.507	0.243		0.186	0.018	
nu/x	0.28	0.042	0.150	← E_m^*	0.003	0.010	← E_f^*
Es	7.17	1.479	0.206		0.105	0.015	
X	1500	1500	1.00		1500	1.00	
X'	1500	1281	0.85	← n = 0.1	983	0.66	← n = 0.1
Y	40	40	1.00		40	1.00	
Y'	246	246	1.00		246	1.00	
S	68	68	1.00		68	1.00	
Fxy*	-0.50	-0.08	0.15	← E_m^*	-0.01	0.01	← E_f^*

INTACT AND DEGRADED PLIES

There is no additional assumption necessary to plot a degraded ply using the quadratic failure criterion. From the data of intact and matrix degraded plies, listed in Table 9.1, we can plot the resulting failure envelopes. They are shown in Figure 9.16 below. On the left is the intact [0] envelope in strain space. In the middle is the matrix degraded [0] envelope. The degradation factor used in this case is 0.15. We superimpose the intact and degraded plies, and the result is shown on the right.

In the third quadrant the degraded ply has a lower strength than the intact ply, and this segment of the degraded [0] is shown as a dashed line. Since matrix degradation occurs only after the FPF, not before, the degraded [0] exists only beyond the intact [0]. This is shown in a solid line on the right of Figure 9.16. The degraded envelope is anchored by the longitudinal tensile strength X. In the limit when the matrix degradation factor goes to zero, the degraded envelope becomes two parallel lines, similar to the prediction of the maximum strain criterion. The other anchor is the longitudinal compressive strength. However, its value changes because of the reduced shear modulus according to Equation 7.11 on page 7-14.

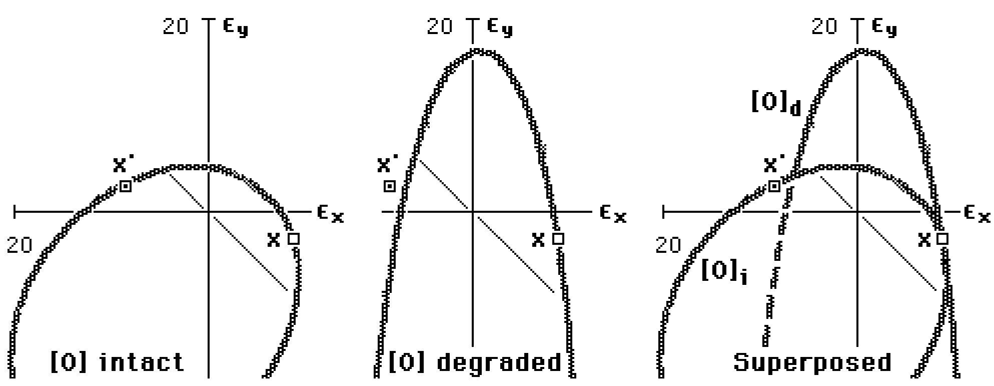

FIGURE 9.16 INTACT AND MATRIX DEGRADED ENVELOPES OF [0] T300/5208

SELECTIVE DEGRADATION BY MICRO CRACKING

Selective degradation is determined by the sign of the transverse ply strain. It truncates the total degraded envelopes in Figures 9.15 and 9.16. On the left of the figure below, the total degradation is shown for [0] and [90]. In the previous figure, only [0] degradation was shown. When we impose the selective degradation, the resulting degraded [0] and [90] plies are truncated, and shown on the right of Figure 9.17:

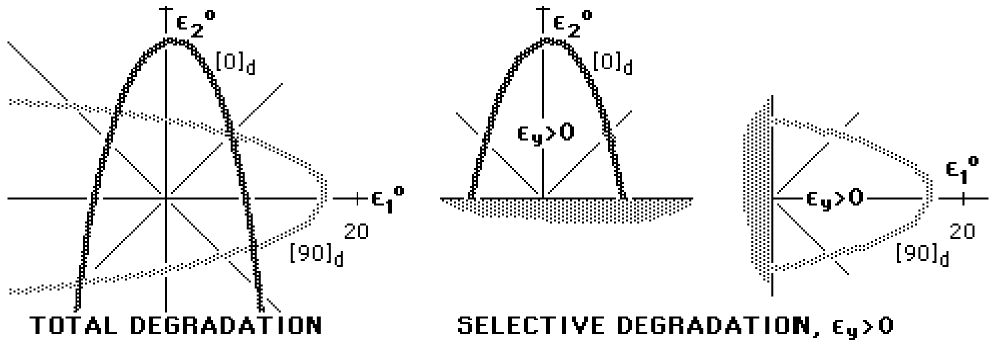

FIGURE 9.17 SELECTIVELY DEGRADED PLIES OF [0] AND [90], BY A FACTOR OF 0.15

When we combine the results of the last two figures, we have the following degraded [0] and [90]. The crossed areas represent the increase in strain capability after FPF.

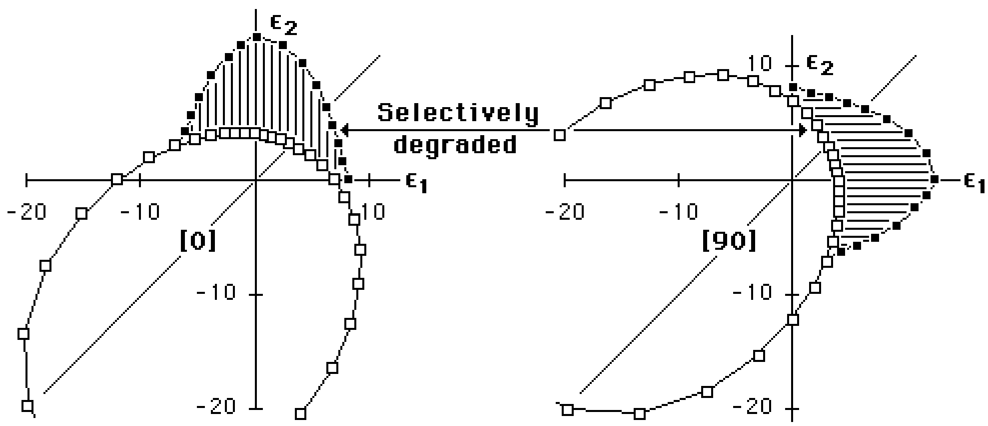

FIGURE 9.18 SELECTIVELY DEGRADED [0] AND [90] FOR T300/5208

PROGRESSIVE FAILURES OF A [0/90] LAMINATE

In order to illustrate how progressive failure is implemented, we will examine four straining paths for the failure envelope discussed above, repeated again in the figure below.

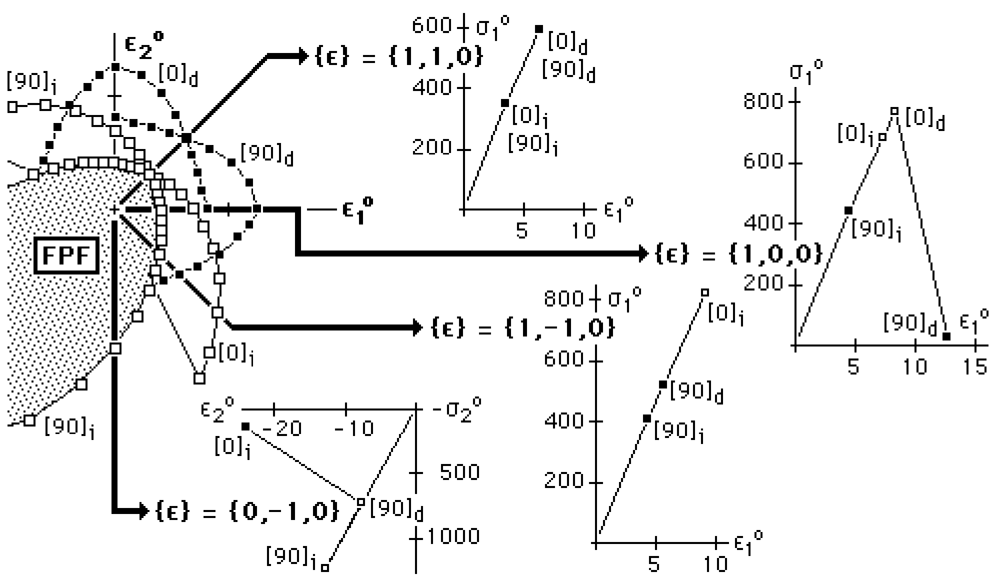

FIGURE 9.19 FOUR STRAINING PATHS AND THE RESULTING STRESS-STRAIN CURVES WITH THE SEQUENCE OF PLY FAILURES INDICATED

On the left of Figure 9.19, the intact and degraded plies of [0/90] are shown, in open and filled squares respectively. Four straining paths are also shown:

(1) A hydrostatic strain along the +45 degree or a combined strain path of {1,1,0},

(2) A uniaxial strain along the zero degree or a strain path of {1,0,0},

(3) A combined strains along -45 degree or a strain path of {1,-1,0}, and

(4) A uniaxial compression strain along 90 degree or a strain path of {0,-1,0}.

For the hydrostatic strain or stress, both plies act the same and simultaneously. The initial failure occurs at the intact ply where the two envelopes join in the first quadrant. Beyond the FPF, the laminate continues to carry load until the ultimate pressure is reached. The ultimate pressure is a function of the degradation factor.

In the following figure, we show the sensitivity of the pressure associated with each matrix degradation factor. When there is no degradation, the factor is unity, and it is the FPF pressure at 360 MPa. If there is no saturation level for the micro cracks, the degradation factor would approach zero, for which case the ultimate pressure would be 750 MPa, which is precisely one half of the longitudinal strength of 1500 MPa. When we determine that a saturation level is reached at a degradation factor between 0.1 and 0.2, we have bounded the ultimate hydrostatic pressure. In the figure below, we show that for the case of a 0.2 degradation factor, the ultimate pressure is 600 MPa. Both [0] and [90] plies would fail simultaneously at this pressure.

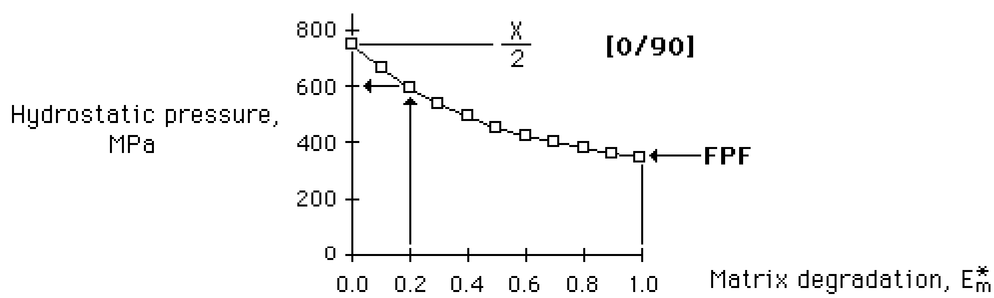

FIGURE 9.20 ULTIMATE PRESSURE AS A FUNCTION OF MATRIX DEGRADATION FACTOR FOR A [0/90] LAMINATE OF T300/5208

Thus, there is life after the FPF for this loading. To take advantage of the additional load-carrying capability in a pressure vessel, a liner is normally installed to prevent leakage of fluid with the presence of micro cracks in the vessel wall, as described in Subsection 7.7.

Under uniaxial straining, shown as the second stress-strain curve in Figure 9.18, the value of the matrix degradation factor is also significant. In Figure 9.19, five stress-strain curves of uniaxial straining are shown with different matrix degradation factors. When the factor is unity, the failure of the laminate is controlled by the [90] ply, and it is the FPF stress. This stress is independent of the degradation factor. It is applied to the ply stiffness after FPF, as shown by the horizontal line that runs through all five curves.

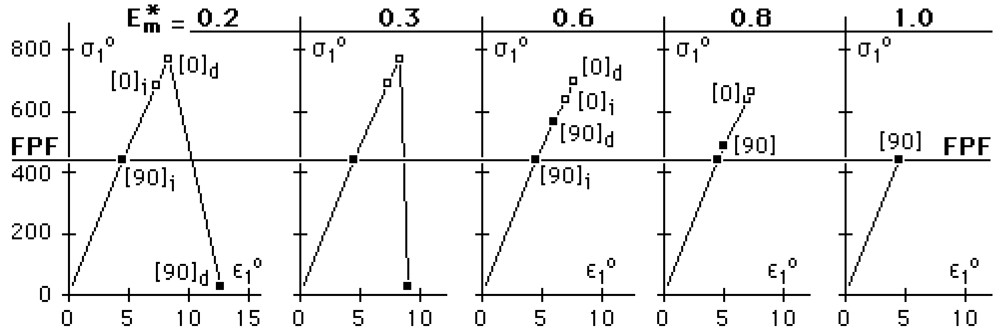

FIGURE 9.21 STRESS-STRAIN CURVES FOR UNIAXIAL STRAINING FOR VARYING VALUES OF THE MATRIX DEGRADATION FACTOR FOR A [0/90]

If we examine the curves above from right to left, we see that as micro cracks increase, the [0] ply begins to take additional stress. When the degradation factor is 0.8 or 0.6, both [0] and [90] are degraded twice when the ultimate is reached. When matrix degradation factor is 0.3, 0.2, or lower, [90] is degraded once when the ultimate strength is reached. For a homogeneous state of stress, the second [90] degradation is of no interest. But for a non-homogeneous state, the post ultimate behavior, such as the second degradation of [90], cannot be ignored.

In the third stress-strain curve in Figure 9.19, the combined strains are {1,-1,0}. The [90] is degraded twice, while the [0] is only degraded once because the transverse strain is negative. The stress level where the degraded [90] fails is again a function of the matrix degradation factor. It has no effect on the ultimate strength.

Finally, if we apply uniaxial compressive strain along the [90] ply to the same [0/90] laminate, the [90] ply will fail first. Since transverse ply strain is positive, the degraded [90] will have a lower longitudinal compressive strength than that of the intact [90]. The stiffness loss is in the transverse direction. We can see in the following figure that the compressive strength decreases. After the second or fiber degradation, the [0] has very low stiffness and strength. Since the intact [90] controls the laminate strength by stability, the matrix degradation factor has no effect. There is no post-FPF strength. That is seen in the ultimate surface of the [0/90] in the third, and part of the second and fourth quadrants in Figure 9.19.

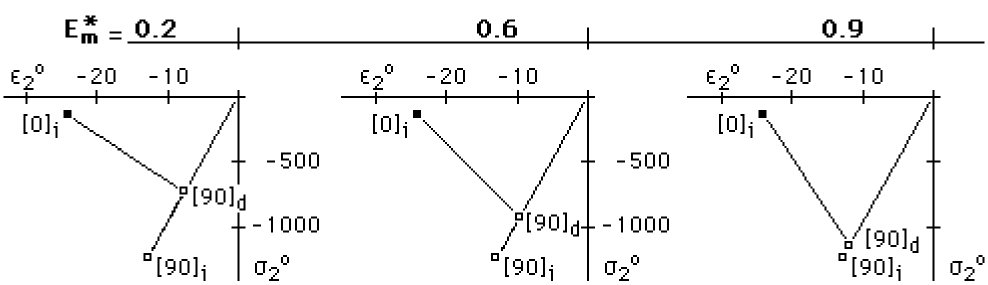

FIGURE 9.22 UNIAXIAL COMPRESSIVE STRAIN FOR THREE DEGRADATION FACTORS

ULTIMATE FAILURE ENVELOPES

We have seen that the behavior of a laminate beyond the FPF requires a system of degradation and rules governing the progression of failures on a ply-by-ply basis. A simple extension of the FPF without degradation would result in an envelope shown on the right of Figure 9.13 on page 9-8. We will show in the figures below the failure envelopes of T300/5208 and E-glass/epoxy in stress and strain spaces. The strain space representations have extended regions resulting from the degraded ply stiffnesses. In all cases, the criterion for the ultimate strength is based on the maximum value of a stress invariant, which appears more useful than the maximum of a strain invariant.

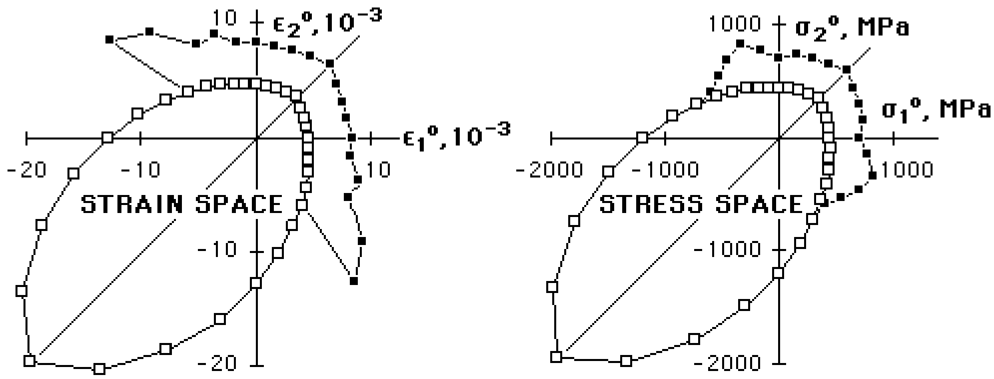

FIGURE 9.23 THE FPF AND ULTIMATE ENVELOPES FOR [0/90] LAMINATE OF T300/5208

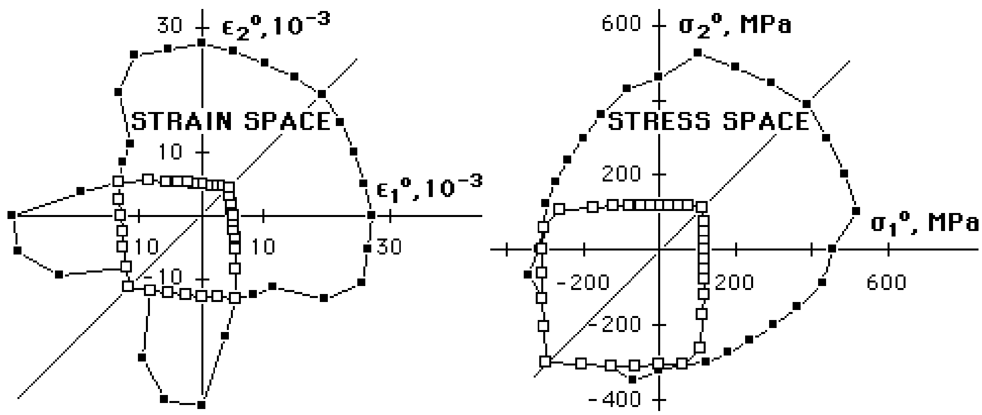

FIGURE 9.24 THE FPF AND ULTIMATE ENVELOPES FOR [0/90] OF E-GLASS/EPOXY

9.6 PROGRESSIVE VERSUS SIMULTANEOUS DEGRADATION

Progressive degradation, shown in Figure 9.15 on page 9-9 is more general than the simultaneous degradation in Figure 9.25 above for post-FPF behavior. The former is an iterative, time-consuming process. The latter is simplified by degrading all plies after the FPF is reached. The ultimate is reached by the ply having the lowest strength ratio among all degraded plies. Only matrix degradation is used. The once-through process of simultaneous degradation is shown below, where selective degradation is retained.

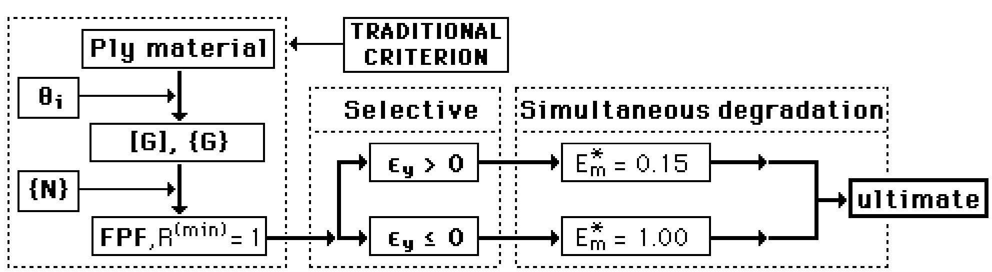

FIGURE 9.25 THE FLOW DIAGRAM FOR A SIMULTANEOUS DEGRADATION MODEL

Comparisons of the two degradation models are made in the following figures with three different stress loading paths. The laminates are [/4] of T300/5208 material. In each figure, two stress-strain curves are shown. On the left is the result of the progressive degradation; on the right, the simultaneous degradation. The stress axis is the magnitude of the applied stress in the 1-direction. The resulting strains in 1- and 2-directions are also shown. For uniaxial stress, the second strain is the Poisson strain. For biaxial stresses, both strains contain the Poisson coupling automatically. Poisson strain does not appear separately.

There is no difference in the prediction of the FPF between the two models. The difference between the two degradation models is in the post-FPF behavior. For the progressive degradation, plies can continue to degrade after the ultimate is reached. For the simultaneous degradation, only matrix degradation is imposed on all plies after the FPF. There is no capability after the total degradation.

In the first figure below where uniaxial tension is compared, both models give the same FPF as expected, but also the same ultimate. The [±45] degradation does not appear in the simultaneous model because it is not controlling. The controlling ply is the intact [0] ply. This ply does not have micro cracks because the transverse ply strain is the Poisson contraction strain of the laminate.

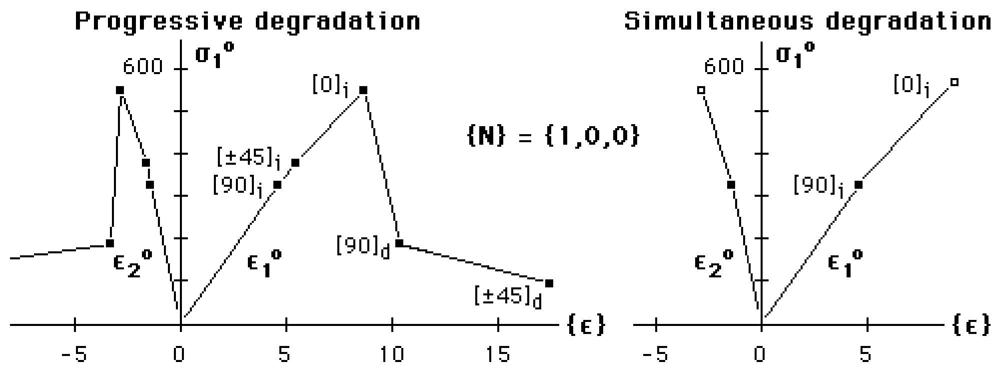

FIGURE 9.26 UNIAXIAL TENSION UNDER PROGRESSIVE AND SIMULTANEOUS DEGRADATIONS

The next case is a biaxial tension-compression stress state. The FPF stress is the same for both models. Although the difference in the predicted ultimate stress is small, the controlling ply is different. The progressive degradation identifies the [90] ply as controlling; the simultaneous degradation identifies the [±45] ply.

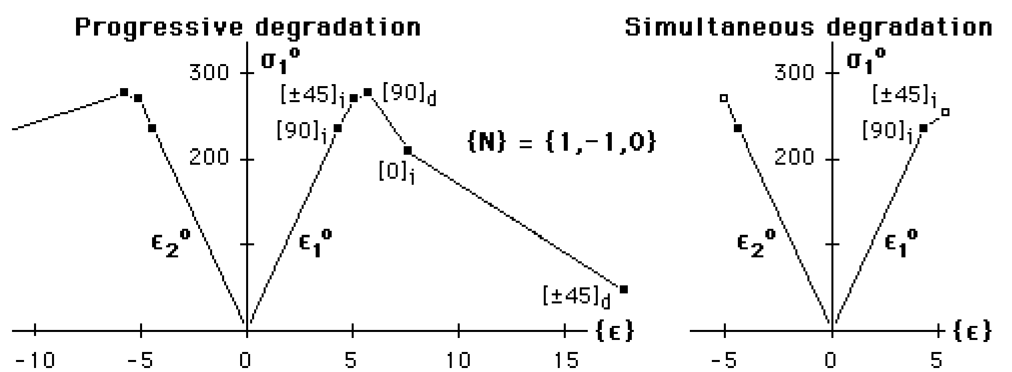

FIGURE 9.27 BIAXIAL TENSION-COMPRESSION UNDER PROGRESSIVE AND SIMULTANEOUS DEGRADATIONS

In the figure below, we show a biaxial tension case which occurs in a pressure vessel. The stress or internal pressure at the FPF is the same for both models. So is the ultimate stress or pressure for both models.

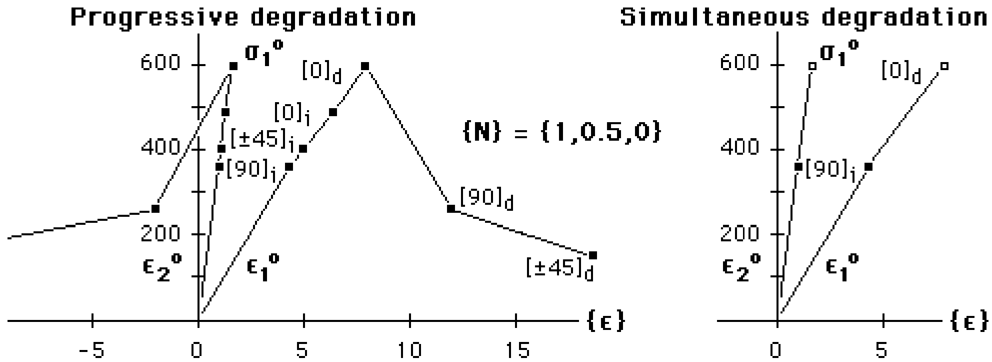

FIGURE 9.28 BIAXIAL TENSION-TENSION UNDER PROGRESSIVE AND SIMULTANEOUS DEGRADATIONS

Based on the comparisons made in these cases, we believe that simultaneous degradation is a viable shortcut for homogeneous stress states. For a non-homogeneous stress state, such as a laminate with an opening, simultaneous degradation is not likely to be accurate. It may be applied on an element-by-element basis. But we would expect that the redistribution of strain energy or ply stresses by the simultaneous degradation would be significantly different from the progressive degradation. Our recommendation is to use the simultaneous degradation model for homogeneous stress only, and use caution in applying it for non-homogenous stress.

9.7 CONCLUSIONS

A systematic and internally consistent criterion for defining design failure envelopes has been demonstrated. The envelopes are easy to generate and provide designers with a pictorial view of the performance of a family of laminates. For the FPF envelope, strain space representation has many convenient features. But an applied load, which would appear as a vector in this space, will rotate as the lay-up of the laminate changes. In stress space, the applied load vector is unique and not affected by the laminate lay-up.

When a laminate is loaded beyond the FPF, additional load-carrying capability may be possible if micro cracks are allowed to form. This is allowed if the transverse ply strain is tensile. The degraded ply continues to carry load until fiber failure occurs. If the transverse ply strain is zero or compressive, the ply will fail by fiber mode only. It will be catastrophic. Thus each ply can fail at most twice.

The additional load-carrying capability is shown, for example, in Figures 9.22 and 9.23 on page 9-14. In filament wound pressure vessels, liners are used to take advantage of the additional pressure beyond the FPF level. For the glass/epoxy composite material in Figure 9.23, this additional pressure is several times the FPF envelope shown in the first quadrant of the figure. Setting the FPF as a design limit is conservative. The post-FPF strength, however, can be used to provide a margin of safety so the design limit can be increased to the FPF level.

Degradation factors are applied when the strength ratio of a ply reaches unity. A matrix degradation factor between 0.1 and 0.2 is recommended to simulate a degraded ply with micro cracks that have reached a saturation level. The fiber degradation factor of 0.01 is recommended to simulate complete breakdown of the ply.

For the strength of a laminate on a local or element level, we recommend a ply-by-ply degradation. Each laminate would fail progressively. As plies fail, new stiffness of the degraded laminate is computed until all plies have failed. For homogeneous state of stress ply failures after the peak stress is of little interest. Simultaneous ply failure is a simpler model than the progressive model. The iterative process is not required. For a non-homogeneous state, degradation of all plies may have to be considered until a global failure occurs. Simultaneous ply failure may not be adequate. A fully progressive analysis is a better method for determining strength beyond the FPF.

9.8 PROBLEMS

Prob. 9.1 Stress space representation of failure envelope is good to visualize simple and complex states of stresses. In the clock shown on the left of the figure below, a 3 o'clock stress vector is the uniaxial tensile stress along the 1-axis; and a 6 o'clock vector, a transverse compressive stress. In strain space, stress vectors are no longer as simple as a clock. Laminate compliance is involved. What distortion of the clock face is necessary. Locate all 12 Roman numerals in the figure on the right. The laminate is T300/5208 material, and [0_3/90] cross-plied.

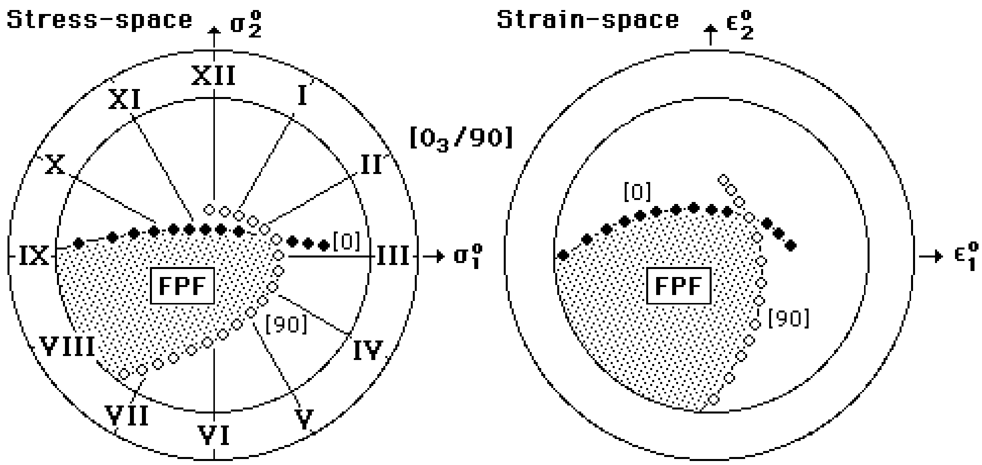

FIGURE 9.29 FPF ENVELOPES OF [0_3/90] LAMINATE IN STRESS AND STRAIN SPACES

Prob. 9.2 Does principal stress design lead to the strongest laminate? This is accomplished by orienting a cross-ply laminate along the principal stress axes. How would multiple loading conditions affect this approach?

Prob. 9.3 Is it possible to have simultaneous ply failures for [0/90], [±ø], and [ø/ø']? Is there any limit on the applied load? Is the laminate the strongest when simultaneous failures occur?

Prob. 9.4 Maximum strain criterion is constructed by drawing boxes from the four measured strengths X, X', Y, and Y'. On the left of the figure below, boxes are drawn for [0] and [90] in strain space. The FPF would be the overlapped area. The LPF and ultimate can be constructed by drawing a box through the longitudinal tensile and compressive strengths as anchors points. Is this process correct? How does one explain the additional area claimed by [0/90] that is outside the domain of either [0] or [90]? The annexed area is shaded in the figure on the right.

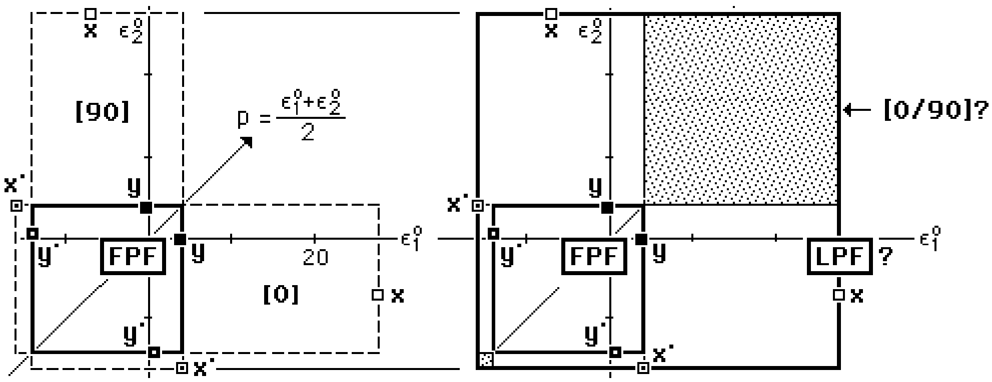

FIGURE 9.30 MAXIMUM STRAIN CRITERION OF [0/90] E-GLASS/EPOXY COMPOSITE

Prob. 9.5 Maximum strain or stress criterion has the distinction of simple identification of failure modes. This is easily accomplished for E-glass/epoxy composite materials, shown on the left of the figure below. Matrix enveloped is within the fiber envelope. If the same process of drawing boxes is applied to T300/5208, shown on the right, the matrix and fiber envelopes overlap. The FPF is easy to define for this material. How does one define the ultimate?

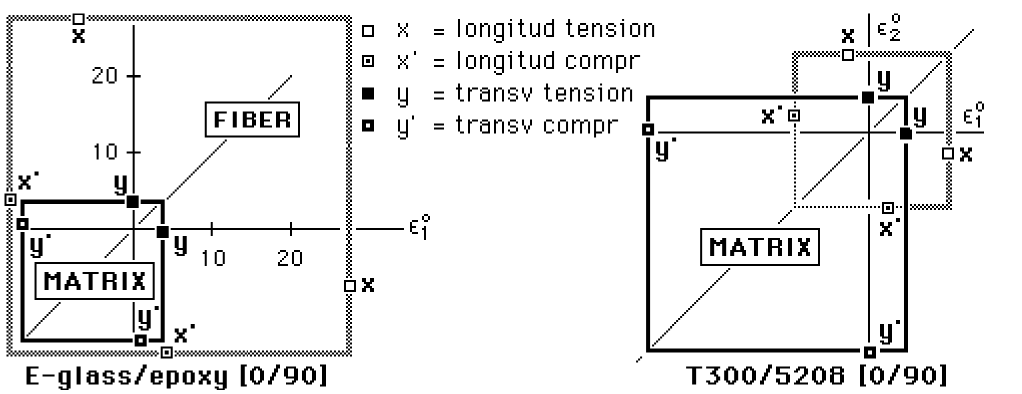

FIGURE 9.31 FAILURE MODE IDENTIFICATION BY MAXIMUM STRAIN CRITERION

Prob. 9.6 The FPF envelopes for various values of the interaction terms are listed in the figure below. When the values are larger than 1, and smaller than -1, are the envelopes admissible? It is obvious that the surface on the left is not admissible for having infinite strength in some combined strains. The figure on the right is closed. Is this admissible?

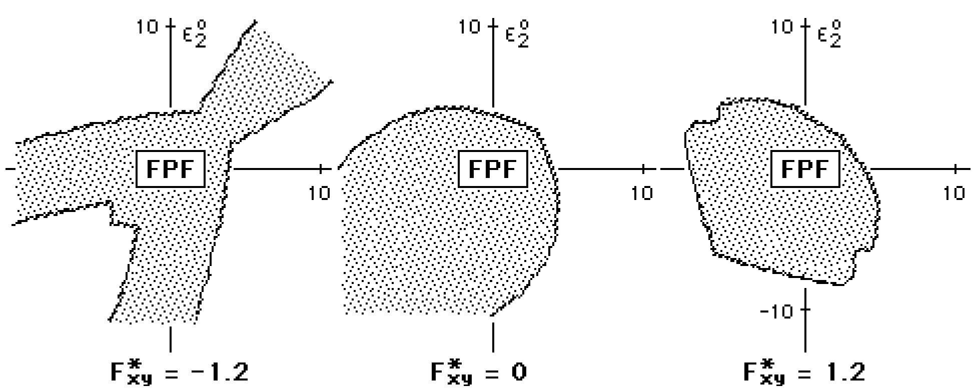

FIGURE 9.32 FPF OF [PI/4] LAMINATES FOR VARIOUS INTERACTION TERMS (T300/5208)

Section 10

MIC-MAC^{Lite}

A key for successful applications of the theory of composites design to practical problem solving is the ability to carry out calculations. One powerful tool is the spreadsheet-based Mic-Mac or Micro-Macromechanics analysis. A special version, Mic-Mac^*Lite*, will be made an integral part of this book. This section explains the design and operation of this program which encompasses the salient features of the method outlined in the book. The method is easy to learn and to use and gives instant answers for which guess work should not be attempted.

10.1 OVERALL DESIGN

Spreadsheet had its beginning in VisiCalc first developed by graduate students at two better known institutions of higher learning in Cambridge, Massacusetts, in the early 1980's. Even in its early days, the power and utility were astonishing. The success of Apple II could be attributed the spreadsheet. In fact it was VisiCalc that made Apple and later IBM PC, not the other way around.

Spreadsheet is a sheet made of cells that contain data, calculations with logical decisions. Calculations are performed simultaneously when a new set of data are initiated. It is different from conventional programs which follow predetermined sequences. Mic-Mac stands for Micro-Macromechanics analysis. The lite version is a minimal format but is capable of illustrating the some of the power of spreadsheet.

The Mic-Mac is constructed in accordance with several distinct panels or modules shown in Figure 10.1. On the upper left corner of the spread sheet is the Control Module which displays cells for inputs and cells for resulting calculations. Below Control Module are ply data for some typical composite materials. The next module is the Ply Stiffness and Strength which are expressed in formats useful for laminated plate theory and failure criteria. The third module is for the calculation of Laminate Stiffness, compliance and engineering constants. The fourth is the Stress Analysis which converts imposed loads and the resulting strains. The fifth and final module is Strength Analysis using five different failure criteria.

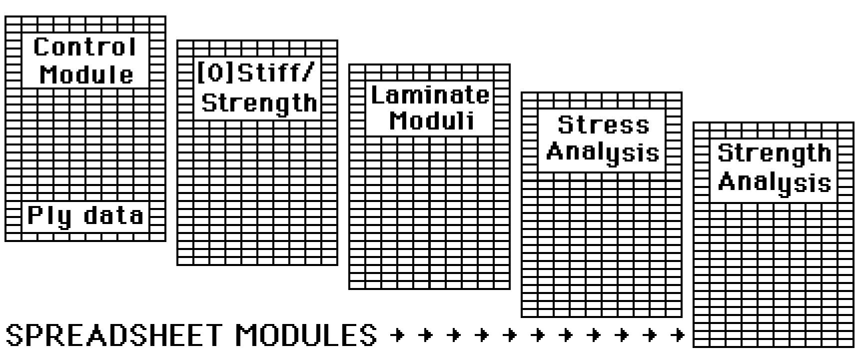

FIGURE 10.1 CONTROL MODULE AND OTHERS IN MIC-MAC^ LITE

10.2 CONTROL MODULE

The opening window of Mic-Mac is the control module which defines that input cells in BOLD letters, and outputs in plain ones. This Mic-Mac is restricted to in-plane behavior of a symmetric laminate. There are five sets of input required. The overall layout of the Control Module, shown in Figure 10.2, has in the top row the name of this Mic-Mac; i.e., Laminated Plate Theory (LPT) for in-plane behavior having stress resultants (sigma's) as inputs. Other may have in-plane strains as inputs. Ply materials is also shown. In this case it is T300/N5208 or T3/N52 for short. In this module, most commonly used inputs and outputs are shown and be elaborated.

		A	B	C	D	E	F	
Control module	**1**	LPT: in-plane/sig				Ply mat	T3/N52[	Ply name
	2	[angle]	**0**	**90**	**45**	**-45**		
	3	[ply#]	**1**	**1**	**1**	**1**		
	4	[Rotate	R/FPF	k/FPF	[repeat]	h, #	h, E-3	
	5	**0**	0.55	1.81	**10**	80	10	
	6		{E^o}	nu21,61	{N}MN/m	<sig^o>	<eps^o>	
	7	1	70	0.30	**1**	100	0.6	
	8	2	70	0.00	**2**	200	2.4	
	9	6	27	0.00	**3**	300	11.2	
	10							
FPF	**11**	Failure	TW/-0.5	TW/0.0	Hashin	max sig	max eps	
	12	R/FPF	0.55	0.60	0.64	0.65	0.55	
	13	R*/FPF	1.00	1.08	1.16	1.18	0.99	

FIGURE 10.2 CONTROL MODULE LAYOUT AND ABSOLUTE AND RELATIVE FPF

The top section of the Control Module contains the following inputs and outputs.

1) Ply angle and number of layers per angle, shown in cells [B2-E3] in Figure 10.2. Ply angles in degrees can have from 1 to 4 angles. The number of layers in each ply group can be 0 or any positive integers and/or fractions. Fractions are only meaningful as a percentage plies in a laminate.

2) Rotation of laminate in cell A5. This is a rigid body rotation of the laminated defined by the data in the last item. The angle is measured in degrees and can assume any positive or negative value.

3) Repeating index of sub-laminates in cell D5. The laminate defined in item 1 above can be treated as a sub-laminate. The repeating index simply multiply the sub-laminate to form the total laminate. The use of repeating sub-laminates is recommended for both design and manufacturing. To ensure lamiante toughness, sub-laminates should be kept to the smallest possible number. The more sub-laminates that exist in a total laminate, higher resistance to delamination can be expected.

	A	B	C	D	E	F
2	[angle]	0	90	45	-45	
3	[ply#]	1	1	1	1	

Specify up to four ply angles and number of plies for each angle from zero and up, in integer or fraction

4	[Rotate	R/FPF	k/FPF	[repeat]	h, #	h, E-3
5	0	0.55	1.81	10	80	10

Specify rigid body rotation of laminate, and number of repeating sub-laminates (Figure 5.11); e.g., $[\pi/4]_{10S}$.

Outputs are strength ratio R based on First-ply-failure, FPF, (Figures 9.1 - 9.7); failure index k (= 1/R in Equation 8.13); total number of plies of a symmetric laminate (4x10x2 = 80); total laminate thickness h in mm or mil.

FIGURE 10.3 INPUTS: PLY ANGLES AND NUMBERS, LAMINATE ROTATION AND REPEAT

The outputs in this Control Module includes strength ratio **R** calculated based on the first-ply-failure (FPF), failure index **k** which is a reciprocal of **R**, total number of plies (80 in this case), and the total thickness **h** of the laminate in cell F5. **R** and **k** are handy scaling factors as explained in Section 8.8.

The bottom section of the Control Module contains the following inputs and outputs, shown in Figure 10.4.

1) In-plane stress resultants {N} are the input in cells D7-9. Any finite values for the three components are admissible. Simple states of stress such as uniaxial tensile {1,0,0} or compressive {-1,0,0} resultants and pure shear {0,0,1} are particularly useful. The initial principal strengths of **X,X',Y,Y',S,** shown in Table 8.1 should be recovered, and equal in value to the corresponding strength ratio **R**.

2) The outputs include three elastic moduli in 1,2, 6 (shear) directions in cells B7-9, and three coupling coefficients: one Poisson ratio and two shear coupling in cells C7-9.

3) The effective in-plane stress, stress resultants **{N}** divided by laminate thickness **h** in cells E7-9; and the resulting in-plane strrains in cell F7-9.

	A	B	C	D	E	F
6		{E^o}	nu21,61	{N}MN/m	<sig^o>	<eps^o>
7	1	70	0.30	1	100	0.6
8	2	70	0.00	2	200	2.4
9	6	27	0.00	3	300	11.2

Specify in-plane loads; i.e., {1,2,3} in MN/m or kip/in.

Outputs include engineering constants E_1^o, E_2^o, E_6^o; $nu_{21}^o, nu_{61}^o, nu_{62}^o$; effective in-plane stress and strain (Equation 4.3).

11	Failure	TW/-0.5	TW/0.0	Hashin	max sig	max eps
12	R/FPF	0.55	0.60	0.64	0.65	0.55
13	R*/FPF	1.00	1.08	1.16	1.18	0.99

Strength ratio/FPF (Equations 8.10-12) for five criteria: Tsai-Wu/-0.5, Tsai-Wu/0, Hashin, max stress and max strain; R values in absolute and normalized with respect to TW/-0.5.

FIGURE 10.4 INPUT: APPLIED STRESS RESULTANTS AND OUTPUTS: LAMINATE ENGINEERING CONSTANTS, IN-PLANE STRESS AND STRAIN, AND STRENGTH RATIOS

In rows 12 in Figure 10.4, strength ratios **R** based on first-ply-failures (FPF) are calcualted for five failure criteria: Tsai-Wu/-0.5, Tsai-Wu/0.0, Hashin, max stress and max strain. They will have the same value when uniaxial stresses or pure shear are applied to a unidirectional ply. As we stated earlier, the principal strengths listed in Table 8.1 will be recovered.

If multidirectional laminates and/or more complex stresses are the inputs, strength ratios for different failure criteria will be different. In row 13, we show all ratios in row 12 are divided by the case of Tsai-Wu/-0.5, in cell B12. These are normalized strength ratios and are easy to compare the differences among all five failure criteria.

10.3 PLY DATABASE

Ply data are stored in certain blocks, in accordance to a fixed format. Cell locations of ply data are defined in cells [A16-E18]. Stiffness components are given in GPa or msi; strength components in MPa or ksi; ply thickness in mm or mil, respectively.

• The first row contains four engineering constants from Table 3.2 and stored in cells B20-E20, following the name of a ply in cell A16. The ply in place now is T300/N5208[SI], or T3/N52[SI] for short.

• The second row contains the five principal strengths (**X,X',Y,Y',S**) from Table 8.1 and stored in cells A21-E21.

• The final row contains the normalized interaction term for Tsai-Wu failure criteria (between -1/2 and 0), unit ply thickness, fiber volume fraction and specific gravity (Table 3.2).

The data block that is active in the program is defined by cells [A20-E22].

Three ply materials are shown in three blocks for database. Each block can be "copied & paste" onto the active block for use by the program.

		A	B	C	D	E
Data format	15	Ply data definitions:				
	16	NAME	Ex,GPa	Ey,GPa	nu/x	Es,GPa
	17	X,MPa	X',MPa	Y,MPa	Y',MPa	S,MPa
	18	Fxy*	ho, mm	Vf	rho/ply	
Ply data	19	Ply data block used in program:				
	20	T3/N52	181	10.3	0.28	7.17
	21	1500	1500	40	246	68
	22	-0.5	0.125	0.7	1.6	
	23	Ply database (copy & paste onto block A20):				
Ply #1	24	T3/N52	181	10.3	0.28	7.17
	25	1500	1500	40	246	68
	26	-0.5	0.125	0.7	1.6	
Ply #2	27	E-glass	38.6	8.27	0.26	4.14
	28	1062	610	31	118	72
	29	-0.5	0.125	0.45	1.8	
Ply #3	30	AS/350	138	8.96	0.3	7.1
	31	1447	1447	52	206	93
	32	-0.5	0.125	0.66	1.6	

FIGURE 10.5 PLY DATA FORMAT, LOCATION AND DATABASE

If English units are preferred, database should have appropriate units in msi for stiffness, ksi for strength, mil for ply thickness. Others are dimensionless. Stiffness and strength properties in English can be found in Appendix C, Tables C.2 and C.4.

10.4 PLY DATA FOR LAMINATES

Ply data for laminates can be calculated from engineering constants and principal strengths. From engineering constants in cells H3-6, unit ply thickness in cell H7, fiber volume fraction in cell H8, we can calculate plane stress stiffness components **[Q]** in cells H10-13, linear combinations in **U**s in cells H15-19, and quasi-isotropic constants in cells H21-22. The relevant formulas are indicated on the left side of Figures 10.6.

From principal strengths, both the parameters in stress space in **F**s and strain space in **G**s are calculated for failure criteria shown in three columns in Figure 10.6: Tsai-Wu/-0.5, Tsai-Wu/0.0, and Hashin with column headings in cells J2-L2, respectively.

10.5 LAMINATE STIFFNESS

In this module the laminate in-plane stiffness and compliance, and effective engineering constants are calculated for a symmetric laminate. This is shown in Figures 10.7.

The position and thickness of each ply group and the total thickness of the laminate **h** in cell R12 are determined. The thickness of each ply group is shown in cells N11-Q11. Ply stiffness for each ply group is calculated using Equation 3.12 and shown in cells N15-20 for the first fly group, and so on. Laminate stiffness, compliance and engineering constants are then calculated and shown in this figure. The stiffness of the sub-laminate [A]o is in cells R15-20; that of the laminate based on repeated sub-laminate 10 times (**r** in cell R5) is in cells S15-20; finally, the normalized laminate stiffness **[A*] (=[A]/h)** is in cells S23-28.

		G	H	I	J	K	L	
	1	PLY DAT	T3/N52[SI]					
Table 3.2	2	Stiffnes	Baseline		TW/-0.5	TW/0.0	Hashin	
	3	Ex	181.00	Ply & consti strengths MPa or ksi				Table 8.1
	4	Ey	10.30	X	1500	1500	1.0E+07	
	5	nu/x	0.28	X'	1500	1500	1.0E+07	
	6	Es	7.17	Y	40	40	40	
	7	ho, mm	0.125	Y'	246	246	246	
	8	vol/f	0.70	S	68	68	68	
Eq. 3.1	9	Plane stress stiff		[Fxy*]	-0.50	0.00	0.00	Table 8.2
	10	Qxx	181.81	Strength parameters, E-6				Eq. 8.2
	11	Qyy	10.35	Fxx	0.44	0.44	0.00	
	12	Qxy	2.90	Fyy	101.63	101.63	101.63	
	13	Qss	7.17	Fxy	-3.36	0.00	0.00	
Table 3.1	14	Linear combinati		Fss	216.26	216.26	216.26	
	15	U1	76.4	Fx,E-3	0.00	0.00	0.00	
	16	U2	85.7	Fy,E-3	20.93	20.93	20.93	
	17	U3	19.7	Gxx	12004	15544	853	Eq. 8.7
	18	U4	22.6	Gyy	10681	10882	10878	
	19	U5=G^iso	26.9	Gxy	-3069	3280	3046	
Eq. 3.13	20	Quasi-isotropic		Gss	11118	11118	11118	
	21	E^iso	69.7	Gx	61	61	61	
	22	nu^iso	0.30	Gy	217	217	217	

FIGURE 10.6 PLY ELASTIC MODULI AND STRENGTHS

		M	N	O	P	Q	R	S
	1	LAMINATE MODULUS MODULE - elastic constants						
	2	Laminate code: {[theta/#, . . .]r/zc}s						
	3	Angle	theta/1	theta/2	theta/3	theta/4		
θ_i	4	[theta]	0	90	45	-45	[r]	
n_i	5	[#/grp]	1	1	1	1	10	
2θ	6	2X,rad	0.00	3.14	1.57	-1.57	unit,#ply	h/2,#ply
4θ	7	4X,rad	0.00	6.28	3.14	-3.14	4	40.0
	8						u	
Eq. 4.6	9	Top z*	1.000	0.975	0.950	0.925	5E-07	
	10	Bott z*	0.975	0.950	0.925	0.900		
	11	del(z*)	0.025	0.025	0.025	0.025	h	
	12						0.010	
Equation 3.12	14	Stiff	[Q]/1	[Q]/2	[Q]/3	[Q]/4	[A]o	[A]
	15	11	181.81	10.35	56.66	56.66	0.038	0.764
	16	22	10.35	181.81	56.66	56.66	0.038	0.764
	17	21=12	2.90	2.90	42.32	42.32	0.011	0.226
	18	66	7.17	7.17	46.59	46.59	0.013	0.269
	19	61=16	0.00	0.00	42.87	-42.87	0.000	0.000
	20	62=26	0.00	0.00	42.87	-42.87	0.000	0.000
Equation 4.4	22	Compl	[a]		[a*]	Equation 4.5	Ei o	[A*],GPa
	23	11	1E+00		1E-02		69.68	76.37
	24	22	1E+00		1E-02		69.68	76.37
	25	21=12	-4E-01		-4E-03		0.30	22.61
	26	66	4E+00		4E-02		26.88	26.88
	27	61=16	4E-17		4E-19		0.00	0.00
	28	62=26	-1E-16		-1E-18		0.00	0.00

FIGURE 10.7 IN-PLANE STIFFNESS, COMPLIANCE AND ENGINEERING CONSTANTS OF A LAMINATE

10.6 STRESS ANALYSIS MODULE

This is an analysis of the in-plane behavior of a symmetric laminate. The applied stress resultants are selected in cells D7-9 in Control Module cells and transfered to cells V8-10 in this stress analysis module. The resulting in-plane strains in cells X8-10 are obtained from the stress-strain relations in Equation 4.3 or Figure 4.3.

		U	V	W	X	Y	Z	AA	
	1	STRESS ANALYSIS MODULE							
θ_i	2	theta	0	90	45	-45	[r]		
n_i	3	#/group	1	1	1	1	10		
2θ	4	2Xtheta	0.00	3.14	1.57	-1.57	h	1E-02	
	5	top z	0.005	0.005	0.005	0.005	h^2/6	2E-05	
	6	Laminate loads & strains							
Eq. 4.3	7		{N}		eps o		(p,q,r)ep	In-plane	Table 2.15
	8	1	1		0.59		p o	1.52	
	9	2	2		2.45		q o	-0.93	
	10	6	3		11.16		r o	5.58	
	11								
Fig. 2.12	12	On-axis epsilons							
	13	epsx o	0.59	2.45	7.10	-4.06			
	14	epsy o	2.45	0.59	-4.06	7.10			
	15	epss o	11.16	-11.16	1.86	-1.86			

FIGURE 10.8 LAMINATE AND ON-AXIS PLY STRAINS RESULTING FROM APPLIED STRESSES

From the laminate strains eps o in cells X8-10, on-axis or ply-axis strains for each ply group can be obtained from one of several strain transformation relations. We have chosen the multiple angle formation shown in Figure 10.9 below. The strain transformation is shown on the right of this figure. The definition of **p,q,r** are shown in Table 2.15 are related to the Mohr's circle. The on-axis strain for the first ply gourp is in cells V13-15, and so on for the other three ply groups.

$$\begin{Bmatrix}\sigma_1'\\ \sigma_2'\\ \sigma_6'\end{Bmatrix} = \begin{bmatrix}1 & \cos 2\theta & \sin 2\theta\\ 1 & -\cos 2\theta & \sin 2\theta\\ & -\sin 2\theta & \cos 2\theta\end{bmatrix}\begin{Bmatrix}p\\ q\\ r\end{Bmatrix}_{\sigma} \qquad \begin{Bmatrix}\epsilon_1'\\ \epsilon_2'\\ \epsilon_6'\end{Bmatrix} = \begin{bmatrix}1 & \cos 2\theta & \sin 2\theta\\ 1 & -\cos 2\theta & \sin 2\theta\\ & -\sin 2\theta & \cos 2\theta\end{bmatrix}\begin{Bmatrix}p\\ q\\ r\end{Bmatrix}_{\epsilon}$$

FIGURE 10.9 STRESS AND STRAIN TRANSFORMATION IN TERMS OF THEIR LINEAR COMBINATIONS OF COMPONENTS

10.7 PLY-BY-PLY ON-AXIS STRESS

Shown in Figure 10.10 is a simple application of stress-strain relation for the calculation of on-axis stress from on-axis strain using Equation 3.5. The stress for the first ply group is in cells V27-29.

Also shown in this figure are the maximum strains in tension in cells Z20-22 and in compression in cells AA20-22. The corresponding tensile strengths are in cells Z27-29 and compressive in cells AA27-29.

Tensile and compressive strains at failure and strengths are taken directly from Table 8.3. The failure strain for each failure mode is the corresponding strength divided by the Young's or shear modulus. For unidirectional plies, positive and negative shears have the same shear strength. It is assumed that all stress-strain relations are linear to failure. These relations are shown in Equation 10.1 in Section 10.8. For most composites, this assumption is reasonal for tensile and pure shear strengths. For compressive strengths it is difficult to separate material failure from fiber buckling as we have stated in Section 8.

		U	V	W	X	Y	Z	AA	
	1	STRESS ANALYSIS MODULE							
θ_i	2	theta	0	90	45	-45			
n_i	3	#/group	1	1	1	1			
Fig. 2.12	19	On-axis strains					eps*+	eps*-	Table 8.3
	20	eps x	0.59	2.45	7.10	-4.06	8.29	8.29	
	21	eps y	2.45	0.59	-4.06	7.10	3.88	23.88	
	22	eps s	11.16	-11.16	1.86	-1.86	9.48	9.48	
	23								
	24						Ulti	Ulti	
	25						Tens	Compr	
Eq. 3.5	26	On-axis mech stresses					sig*+	sig*-	Table 8.3
	27	sig x	114	446	1278	-718	1500	1500	
	28	sig y	27	13	-21	62	40	246	
	29	sig s	80	-80	13	-13	68	68	

FIGURE 10.10 ON-AXIS STRAINS AND STRESSES AND ULTIMATE STRENGTH VALUES

10.8 MAXIMUM STRESS AND MAXIMUM STRAIN CRITERIA

Shown in Figure 10.11 are the applications of maximum stress and maximum strain failure criteria. The on-axis strains shown in Figure 10.10 are compared with the corresponding ultimate strains. Their ratio is the strength ratio **R**. Each on-axis strain is compared with the appropriate tensile or compressive ultimate strains. The resulting strength ratio is listed in cells AC20-21 for the first ply group. The lowest strength ratio for each ply group is listed in row AC24-AF24. The failure mode for the first ply group is 0.85 due to a shear failure shown in cell AC22. Same for the second group at 90 degree. The third ply group at 45 degree, failure is at 1.17 due to fiber shown in cell AE20; the the fourth ply group at -45 degree, due to transverse failure at 0.55 in cell AF21.

		Z	AA	AB	AC	AD	AE	AF	AG
	1			STRENGTH ANALYSIS					
θ_i	2			theta	0	90	45	-45	
n_i	3			#/group	1	1	1	1	
Fig.8.25	19	eps*+	eps*-	R/strains				Hashin (max eps)	
	20	8.29	8.29	eps x	14.15	3.39	1.17	2.04	1.17
	21	3.88	23.88	eps y	1.59	6.63	5.88	0.55	
	22	9.48	9.48	eps s	0.85	0.85	5.10	5.10	
	23							R/max strain	
	24	Ulti Tens	Ulti Compr	R/min	0.85	0.85	1.17	0.55	0.55
	25								
Fig.8.25	26	sig*+	sig*-	R/stresses				Hashin (max sig)	
	27	1500	1500	sig x	13.21	3.36	1.17	2.09	1.17
	28	40	246	sig y	1.48	3.04	11.44	0.65	
	29	68	68	sig s	0.85	0.85	5.10	5.10	
	30							R/max stress	
	31			R/min	0.85	0.85	1.17	0.65	0.65

FIGURE 10.11 STRENGTH RATIOS BASED ON MAX STRAIN AND MAX STRESS CRITERIA

A identical analysis can be made using the maximum stress failure criteion. The resulrs are shown in cells [AC27-AE29].

For Hashin criterion, maximum strain or stress criterion is applied to the fiber direction in tension and compression. Using maximum strain, the controlling strength ratio is shown in cell AG21; for maximum stress in cell AG26. It is fortuitous that the two strength ratios are equal. They are in general different which can be seen if AC20 is compared with AC27, and so on.

The inequalities for the calculation of strength ratios based on maximum strain criterion are shown in Equation 10.1: those based on maximum stress criterion are shown in Equation 10.2:

$$R_x = \epsilon_x{}^*/\epsilon_x \text{ if } \epsilon_x > 0, \text{ or } R_x' = \epsilon_x{}^{*'}/|\epsilon_x| \text{ if } \epsilon_x < 0$$

$$R_y = \epsilon_y{}^*/\epsilon_y \text{ if } \epsilon_y > 0, \text{ or } R_y' = \epsilon_y{}^{*'}/|\epsilon_y| \text{ if } \epsilon_y < 0$$

$$R_s = \epsilon_s{}^*/|\epsilon_s|, \ \epsilon_s{}^* = S/E_s$$

$$\text{where} \quad \epsilon_x{}^* = X/E_x, \ \epsilon_x{}^{*'} = X'/E_x, \ \epsilon_y{}^* = Y/E_y, \ \epsilon_y{}^{*'} = Y'/E_y,$$

$$\epsilon_x{}^{*'} = X'/E_x, \ \epsilon_y{}^{*'} = Y'/E_y, \ \epsilon_s{}^* = S/E_s \tag{10.1}$$

$$R_x = X/\sigma_x \text{ if } \sigma_x > 0, \text{ or } R_x' = X'/|\sigma_x| \text{ if } \sigma_x < 0$$

$$R_y = Y/\sigma_y \text{ if } \sigma_y > 0, \text{ or } R_y' = Y'/|\sigma_y| \text{ if } \sigma_y < 0$$

$$R_s = S/|\sigma_s| \tag{10.2}$$

10.9 QUADRATIC FAILURE CRITERIA

In Figure 10.12 and 10.13, two Tsai-Wu quadratic criteria are applied; with -0.5 and 0.0 for the normalized interaction terms, respectively. The resulting strength ratios for ply groups are shown in row AC12-AF12 and AI12-AL12, respectively. The first-ply-failure or FPF values are shown in AG14 for TW/-0.5, and AM14 for TW/0.0, respectively.

		AB	AC	AD	AE	AF	AG	
	1	STRENGTH ANALYSIS (Tsai-Wu/-0.5) -						
θ_i	2	theta	0	90	45	-45		
n_i	3	#/group	1	1	1	1		
2θ	4	2Xtheta	0.00	3.14	1.57	-1.57		
Fxy*	5	Fxy*=-0.5						
Equation 8.12	6	a	1.44	1.45	1.00	0.95		
	7	b	0.57	0.28	-0.45	1.29		
	8	b/2a	0.20	0.09	-0.23	0.68		
	12	R	0.66	0.74	1.25	0.55	TW/-0.5	Quadratic
	13						FPF	
	14						0.55	R/TW/-0.5

FIGURE 10.12 STRENGTH RATIOS BASED ON TSAI-WU/-0.5 INTERACTION TERM

		AH	AI	AJ	AK	AL	AM	
	1	STRENGTH ANALYSIS (Tsai-Wu/0.0) -						
θ_i	2	theta	0	90	45	-45		
n_i	3	#/group	1	1	1	1		
2θ	4	2Xtheta	0.00	3.14	1.57	-1.57		
Fxy*	5	Fxy*=0						
Equation 8.12	6	a	1.46	1.49	0.81	0.65		
	7	b	0.57	0.28	-0.45	1.29		
	8	b/2a	0.19	0.09	-0.28	0.99		
	12	R	0.66	0.73	1.42	0.60	TW/0.0	Quadratic
	13						FPF	
	14						0.60	R/TW/0.0

FIGURE 10.13 STRENGTH RATIOS BASED ON TSAI-WU/0.0 INTERACTION TERM

		AN	AO	AP	AQ	AR	
	1	STRENGTH ANALYSIS (Hashin) -					
θ_i	2	theta	0.0	90.0	45.0	-45.0	
n_i	3	#/group	1.0	1.0	1.0	1.0	
2θ	4	2Xtheta	0.0	3.1	1.6	-1.6	
Fxy*	5	Fxy*=0	X,X' = inf				
Eq 8.12	6	a	1.46	1.40	0.09	0.42	
	7	b	0.57	0.28	-0.45	1.29	
	8	b/2a	0.19	0.10	-2.63	1.52	
	12	R	0.66	0.75	6.95	0.64	Quadratic
$[0]^+,[0]^-$	16	R/X,X'	13.21	3.36	1.17	2.09	Max stress
	17	R/min	0.66	0.75	1.17	0.64	
	18			Hashin	FPF	0.64	R/Hashin

FIGURE 10.14 STRENGTH RATIOS BASED ON HASHIN FAILURE CRITERION

10.10 SAMPLE PROBLEMS

Practice makes perfect - this is true today as ever. Some users of Mic-Mac have claimed that there is no better tool for designing composites. We therefore urge potential users to go through the sample problems recommended here.

The program will run as data are entered. The response is instantaneous. There are only four sets of input data (all in bold face numerals) required; i.e.,

1) Lamination by selecting up to the angle and ply number for each ply group up to four;

2) Repeating index for sub-laminates in cell D5;

3) Rigid body rotation of laminate in cell A5.

Outputs are user defined. We have selected the most useful data in our opinion to be displayed in the Control Module. They are the engineering constants, laminate stresses and strains, and strength ratios from five failure criteria. Other equally important data can be the laminate stiffness matrixces**[A]** and **[A*]**, compliance **[a]** and **[a*]**, ply stresses, ply strains, and ply-by-ply strength ratios. These data can be found in various cells as explained in the previous sections. For example, **[A]** and **[A*]** are located cells S16-20 and S23-28, respectively. Engineering constants which we have shown in the Control Module are located in cells R23-28. Thus it is a choice by the user which data need to be displayed at what cells. This is easily done with spreadsheels.

RECOVERING PLY DATA

To enhance confidence in this program, the first step is to recover the original ply data.

The following excercises are recommended.

1) Select laminate: [0]; {N} = {1,0,0} in cells D7-9, Rotation 0 in cell A5; Repeat 10 in cell D5: outputs: R/FPF = 3.75 in cell B5; h # = 20 in cell E5; h = 2.5 mm in cell F5; {E} = 181 . . . in cells B7-9; sig = 400 . . . in cells E7-9; eps = 2.21 . . . in cells F7-9. The ply engineering constants are recovered in cells B7-9 and C7-9. Poisson's ratio is also recovered if the ratio of the negative value of transverse strain in cell F8 is divided by the axial strain in cell F7; i.e., 0.62/2.21 = 0.28.

2) Increase {N} by strength ratio 3.75; i.e., {3.75,0,0} in cells D7-9, outputs: R = k = 1 in cells B5 and C5, X = 1500 MPa in cell E7 and x = 8.29 in cell F7 are recovered. Strength ratios of all criteria agree as expected. R is therefore a convenient scaling factor for applied load.

3) Change uniaxial tensile to compressive, output X' in a negative stress value of 1500 MOPa is recovered incell E7.

4) Select rotation of 90 degree in cell A5, the longitudinal and transvserse stiffness are interchanged; R in cell B5 is also changed. If uniaxial stress is multiplied by the R value (0.1), the transverse tensile strength Y (= 40) is recovered in cell E7, and R is now 1. If uniaxial compressive is imposed, R = 0.62. If the stress is changed to -0.62, Y' of 246 is recovered, and R is now 1.

5) Select {N} = {0,1,0} which is uniaxial tension along the 2-axis, the same results as those in (1) above will appear. Conversely if the angle of rotation is made zero, the results are those for unaxial loading along the 2-axis, then the results in (4) will appear.

6) Another way of changing angle for uniplies would be the angle in cell B2. While either B2 or rotation in A5 can be used for studying uniplies, for lamiantes the use of angles in row B2-E2 is different from rotation of entire laminate in cell A5.

7) Failure index k is also a handy scaling factor for lamiante thickness. In the case of (1) of uniaixial tensile on [0], k is 0.27. Which means that the number of plies can be reduced to 27 percent or a repeat index of 2.7 in cell D5, the R value will be unity. The number of plies will be aproximately 5.4 and thickness 0.7 mm.

OFF-AXIS PROPERTIES OF [0]

Off-axis stiffness and strength can be easily obtained from changing the values in cell B2 or A5.

1) If a rotation of 45 degree is placed in cell A5, the eingeering constants are now: [17,17,9,0.17,-0.77,-0.77] starting with cell C7.

2) If ply angle in B2 is changed to -45, this will cancel the rigid body rotation of +45, the resulting engineering contants should be the on-axis constants of [181,10.3, 7, 0.28,0,0], as expected.

3) If the rotation angle is zero, we will have the engineering constants for a [-45] ply in which case the constants are the same as those in (1) except the shear coupling coefficients are now positive in cells C8 and C9.

4) At [10], a ply angle of 10 degrees, which is an ASTM recommended off-axis test coupon, the stiffness matrix is now fully populated; i.e., there are nonzero shear coupling coefficients in cells C8 and C9. The stiffness along the 1-axis dropped from 181 to 108 GPa. R is now 1.37 which translate to an ultimate stress level of 548 MPa. This is also considerably lower than the original1500 value for X.

5) In all four cases cited above, the number of ples in cell B3 and the repeating index in cell D5 have impact on the laminate stresses and strains and the strength ratios but not on the engineering constants. The former are related to laminate thickness; the latter are normalized by lamiante thickness and will not be affected by the thickness. Try to chang the values in cell B2 and D5 and see what change and what remain constant.

6) For an off-axis coupon, say, [45], shear coupling is an importnat factor in its stress-strain relation. Let the roation be 45 in cell A5, the induced strains in cells E7-9 from a uniaxial stress of {1,0,0} are {23.9,-4.0,-18.3}. A significant shear strain is induced. This behavior is attibuted to the shear coupling coefficient of -0.77 in cell C8 which is equal to -18.3/23.9, the ratio of the induced shear over axial strains.

Unlike Young's modulus and Poisson's ratio, the shear coupling coefficient is odd, not even; i.e., it changes signs from [45] to [-45]. If [-45] is used in the rotation, both the shear coupling in cell C7 and the induced shear strain in cell F9 are now positive. Similarly, if the applied load is changed to negative, the induced axial and shear strains will also change sign.

7) If a pure shear {0,0,1} in cells D7-9 is imposed on [45] plate, the induced strains in cells F7-9 are {-18,-18,42}. There will be a positive shear strain as expected. But because of shear coupling of
-0.77 in cell C8-9, there will be a contraction in normal strains. The ratio of the normal to shear strains is equal to -18/42 = -0.43. This is precisely the value of -0.77 corrected by the ratio of Young's modulus and shear modulus of 9/17 in cells B9 and B7; i.e., -0.77x0/17 = -0.43. This is one of the reciprocal relations shown on the last line of Equation 3.11.

CROSS-PLY LAMINATES

This class of laminates consists of a family of [0/90]. The ratios of the two orthogonal ply angles may be different.

1) The simplest is [0/90] having equal plies of the two angles. The angles and ply numbers are [0] in cell B2, unity in cell B3; [90] in cell C2 and unity in cell C3. The lamiante rotation is zero in cell A5 and repeating index is 10 in cell D5. The resulting laminate engineering constants are [96,96,7,0.03,0,0] starting with cell C7. This is a square symmetric laminate having equal stiffness in the 1- and 2-axis. It is nearly exactly 1/2 of the longitudinal stiffness of the ply. This rule-of-mixtures rule is true for highly anisotropic ply like typical CFRP.

This relation is less true for GFRP which is less anistropic. This can be shown by copying the GFRP ply data in block [A27-E29] and pasting them in the active data block [A20-E22]. The engineering constant along the 1-axis is 39 GPa and that of the [0/90] laminate is 24 GPa, which is much higher than 1/2 of 39.

2) The shear modulus is the same as that of the ply. So the laminate is not isotropic. Laminate Poisson's ratio in cell C7 is very small. Shear coupling coefficients in cells C8 and C9 are zero as expected for an square symmetric or orthotropic laminate.

3) A [0/90] is square symmetric which one can easily show by rotating it 90 degree (put this value in cell A5). The engineering constants in cells B7 et al do not change. The laminate is not isotropic which can be shown if the rotation angle is different from 0 or 90. Try a value of 38 in cell A5. Every engineering constant will change.

4) Returning to T300/5208 CFRP and under unaxial tensile stress resultants of {1,0,0}, the strength ratio of FPF is 1.87 in cell B5. All five faillure criteria yield the the same strength ratio as seen in cells B13-F13. To find the stress and strain levels at the FPF load, multiply the imposed unit load by the strength ratio or a new laod of {1.87,0,0}, the resulting strength ratio is now unity. The effective stress is 374 MPa in cell E7 and the FPF strain is 3.9 E-3 in cell F7. This strain is often referred to as the level for micro cracking in the [90] plies emerges

The number of plies that can sustain the FPF load can be found by changing repeating index of 10 in cell D5 by multiplying strength index k of 0.54 in cell C5. We now have a new repeating index of 5.4, the strength ratio is unity in cell B5, the ply number is 21.6 in cell E5, and total laminate thickness is 2.7 mm. For real laminate, ply numbers must be integer and even. Thus one round off can be achieved by using a repeat index of 5.5 in cell D5 which would result in a ply number of 22 in cell E5.

5) Now investigate another cross-ply laminate [0_2/90] where the cross-ply ratio is 2. This is done by putting 2 in cell B3. The resulting engineering constants are [125,67,7,0.04,0,0]. The rule-of-mixtures for the stiffness ccomponents along the 1- and 2-axis. The mixtures rule would have predicted 120 and 40 GPa, instead of the correct values from laminated plate theory are 167 and 67 GPa, respectively.

6) The FPF stress would be obtained by increasing the uniaxial load by a factor of 3.64, the strength ratio in cell B5. The results of an applied load of {3.64,0,0} in cells D7-D9 yields a laminte stress of 485 MPa in cell E7, and strain of 3.9 E-3 in cell F7. This failure strain is the same as the [0/90] laminate in (2) above. The number of plies required to sustain the FPF load is obtained by chaning the repeating index of 10 in cell D5 to that of 10 x 0.27 in cell C5 or a new repeating index of 2.7. The number of plies for the laminate is 16.2 plies.

The sub-laminate for this laminate requires a minimum of 3 plies (two [0] and one [90]) a round off value for the lamiante would be 18 plies. This can be achieved by changing the repeating index to 3 that would lead to 18 plies and a total thickness of 2.3 mm. The actual strength ratio of this rounded lamiante would be 1.09 shown in cell B5. The maximum stress at FPF would be 484 MPa which is obtained by changing the imposed stress to 1.09 in cell D7. The strain at FPF remains 3.9 E-3 in cell F7.

Note also that the same strength values are obtained for all five failure criteria, shown in cells B13-F13.

7) If we rotate 45 degree (in cell A5) of the [0/90] we will have a [±45]. The resulting engineering constants in cells A7 et al are [25,25,47,0.75,0,0]. The remarkable effect is that the Young's modlus in the 1- and 2-axis dropped to 7 fold from 181 to 25, and the shear modulus increased 7 fold from 7 to 47.

Poisson's ratio is 0.75, higher the usual upper limit of 0.5 for isotropic material. This can be seen also in the strains induced by uniaxial stress. The axial extension is 8 E-3 and the lateral contraction is 6 shown in cells F12 and F13, respectively.

8) The solution of Problem 4.5, illustrated in Figure 4.35, can be solved numerically with this example. The shear modulus of the ply (T300/5208) can be found to be the ratio of the appied shear stress divided by 2 or 100 MPa in cellE7 and the difference of the two normal strains in cells F12 and F13. The resulting is 14 E-3. Thus 100/14 = 7.1 GPa which is the shear modulus of the ply.

9) The tensile strength of [±45] is very low. This can be found by imposing a uniaxial load of {0.62,0,0} in cell D7-9. The effective stress is then 124 MPa shown in cell E7. The reuslting failure strains are 4.9 E-3 and -3.7 in cells F7-8.

If a uniaxial compressive load is applied; i.e., {-1,0,0} in cells D7-9, the strength ratio will be 0.74. With a new load of {-0.74,0,0}, the strength ratio is not unity and the failure stress is -148 Mpa, slightly higher than the tensile stress of 124.

10) If we wish to know about the laminate shear strength, we first impose a pure shear load of {0,0,1} in cells D7-9, the strength ratio is now 1.76 shown in cell B5. A new load of {0,0,1.76} in cells D7-9 will produce a shear strength of 352 MPa in cell E9, and the strength ratio for this stress is unity in cell B5. This is a five fold increase over the ply shear strength of 68 MPa.

BIAXIAL LOADING

Biaxial stresses are encountered in cylindrical and shperical shells subjected to internal and/or external pressures. The Mic-Mac can help to understand how the strength of laminates can be determined, and the difference in the predicted strength ratios among various failure criteria.

1) Find the strength of [0] under hydrostatic tension and compression. First select loading {1,1,0} , adn the resulting strength ratio in cell B5 is 0.10 in cell B5. The tensile failure strength would be obtained when load is changed to {0.1,0.1,0}. The ultimate pressure is 40 MPa and the failure strain transverse to the fiber is 3.8 E-3 which is aproximately a value of 40 MPa for Y and 3.88 E-3 for y in Table 8.3, respectively. The strength ratio is unity in cell B5. All five failure criteria predict strength ratios within 2 percent.

2) Conversely, the transverse compressive strength can be obtained by selecting a load of {-1,-1,0}, the resulting strength ratio is 0.65. The apply a load of {-0.65,-0.65,0}, the ultimate comrpessive strength is now 260 MPa in cells E7-8, and the transverse compressive strain of 24.8 in cell F8. This is 6 percent higher than the Y' value of 246 MPa and 4 percent larger than the value of 23.88 in y' in Table 8.3. The strength ratio is unity in cell B5. Tsai-Wu/-0.5 predicts 5 percent higher strength ratios as the other four criteria.

3) With either hydrostatic tensile or compressive stresses imposed on [0], what will happen when the ply is rotated? Place any value for laminate rotation in cell A5. Strength ratio remains invariant. Ply stresses also remain constant. But engineering constants will change according to the effect of coordinate transformation. The resulting strains will change because the sitffness has changed. Variation in strength ratios by different failure criteria, but it is less than 2 percent.

4) If a membrane load for pressure vessels of {1,2,0} is imposed, the strength ratio is 0.05. We can now impose {0.5,1.0,0} on the [0], we have lamiante stresses of {20,40,0} and strains of {0.0,3.9,0}. The transverse streaa and strain are practically the same as Y at 40 MPa and y at 3.88 E-3 listed in Table 8.3. All five failure criteria predict the same strength ratio.

5) If a membrane compression for pressure vessels of {-1,-2,0} is imposed, the strength ratio is now 0.32. If a new load of {-0.32,-0.64,0} is imposed, the strength ratio nearly unity, the transverse stress is 256 MPa (as compared with 246 in Y') and the transverse strain is 24.7 (as compared with 23.88 as y'). All five failure criteria predict strength ratios within 3 percent.

6) If a unit hydrostatic tensile load is applied to [0/90], the strength ratio is 1.51, from which the ultimate stress is 302 MPa and strain is 3.1 E-3. The only surprising output is the strength ratio predicted by maximum strain criteion in cell F12-13, having a 27 percent higher value than most of the others.

7) If a unit hydrostatic compressive load is applied to [0/90], the strength ratio is 9.8, from which the ultimate pressure is 1,960 MPa and the failure strain is -19.8 E-3. There is a huge disparity in the strength ratios predicted by various criteria. Both Tsai-Wu crieria have higher strength ratios than the other three. The difference is caused by the

8) Rigid-body rotation of the laminate does not change the strength ratios or laminate strains.

10.11 CONCLUSIONS

We have tried to show the power of Mic-Mac not only as a learning tool but for actual design. There is no way that guesswork should play a part in seeking an understanding how plies interact in a laminate. For sure, parallel springs would not be adequate. Plies are two dimensional. There is no simple model that can descirbe their behavrior. Matrix inversion can trick simple minded explanation.

It is equally dangerous to assume the roles of fibers, the matrix and the interface. Again it is safe to say that the interaction is complex. Simple models that would lead to common expressions of fiber or matrix domination is very subjective. Mic-Mac can help in resolving contraversies.

There are of course plenty of limitations. Mic-Mac is based on linear theory and classical laminated plate theory. Out-of-plane behavior such as delmination and stacking sequence effect cannot be solved. While it is attractive to cite nonlinear phenomenon as a catch-all of the limitations of linear theory, practical solutions need not depend on nonlinear theory. To gain confidence in composites design, it is often useful to use the linear prediction as a guideline for empirical approach. Many useful results for design can be obtained.

Like any emerging technology, composite materials and structures are exciting and present many challenges. It is particularly suited for the young mind not burdened with metals background. A can-do attitude can bring new applications not possible with traditional materials and processes. Plesae think composites!